DEPARTAMENTO DE QUÍMICA ANÁLITICA

DESARROLLO DE APLICACIONES CUANTITATIVAS DE LA ESPECTROMETRÍA VIBRACIONAL PARA EL CONTROL DE CALIDAD

SERGIO ARMENTA ESTRELA

UNIVERSITAT DE VALENCIA
Servei de Publicacions
2007

Aquesta Tesi Doctoral va ser presentada a Valencia el dia 3 de Novembre de 2006 davant un tribunal format per:

- D. Frederic Cadet
- D. José Manuel Andrade Garda
- D. Marcelo Blanco Romia
- D. Constantinos Georgiou
- D ª. María José Medina Hernández

Va ser dirigida per:
D. Miguel de la Guardia Cirugeda
D. Salvador Garrigues Mateo

Depòsit legal:
I.S.B.N.:978-84-370-6758-2
Edita: Universitat de València
Servei de Publicacions
C/ Artes Gráficas, 13 bajo
46010 València
Spain
Telèfon: 963864115

TESIS DOCTORAL
QUÍMICA ANALÍTICA

Desarrollo de aplicaciones cuantitativas de la espectrometría vibracional para el control de calidad

SERGIO ARMENTA ESTRELA

UNIVERSITAT DE VALÈNCIA
València 2006

Universitat de Valencia
Departamento de Química Analítica
Campus de Burjassot
46100 Burjassot, España.

El Dr. D. MIGUEL DE LA GUARDIA CIRUGEDA, Catedrático de Universidad y el Dr. D. SALVADOR GARRIGUES MATEO, Profesor Titular de Universidad, del Departamento de Química Analítica de la Universitat de València (Estudi General),

CERTIFICAN

Que D. Sergio Armenta Estrela ha realizado la presente Tesis Doctoral titulada **"Desarrollo de aplicaciones cuantitativas de la espectrometría vibracional para el control de calidad"** bajo su dirección en el Departamento de Química Analítica de la Universidad de Valencia y autorizan su presentación para optar al Grado de Doctor en Química.

Y para que así conste, a los efectos oportunos,
firman la presente en Valencia, Febrero de 2006.

Dr. D. Miguel de la Guardia Cirugeda Dr. D. Salvador Garrigues Mateo

Llegados a este momento es hora de expresar mi más sincero agradecimiento a todas las personas que han hecho posible o han facilitado, en mayor o menor medida, la realización de esta Tesis Doctoral.

Deseo agradecer a mis directores, Salvador Garrigues Mateo y Miguel de la Guardia Cirugeda no sólo el asesoramiento científico, aclaraciones y observaciones críticas sino también su apoyo y colaboración durante este tiempo. Me gustaría hacer extensibles estos agradecimientos al resto de profesores del grupo de investigación, Agustín Pastor, Ángel Morales y Marisa Cervera, quienes también han estado dispuestos a echarme una mano cuando la he necesitado.

Me siento afortunado de haber compartido parte de esta experiencia con los profesores Bernhard Lendl, de la Universidad Técnica de Viena y Philippe Rondeau y Emmanuel Bourdon de la Universidad de la Reunión. Gracias por haberme hecho sentir como en casa tan lejos de ella.

No puedo olvidarme de mis compañeros de laboratorio Xavi, Paco, Eva, Bela, Josep y todos aquellos que, aunque han cambiado de aires, han pasado algún tiempo con nosotros Guillermo, Jesús, Asun, Rafa, Carmen, Mari Paz,... con los que he compartido momentos inolvidables y espero no perder el contacto.

Mención especial merecen mis padres, quienes, en su día, me infundieron la ética y el rigor que marcan mi transitar por la vida y para quienes no hay palabras suficientes. A Jasmina me gustaría reconocerle su comprensión y paciencia durante todo este tiempo, gracias por haber estado siempre a mi lado y soportarme cada vez que me convierto en un caso perdido. Como no podía ser de otra forma, agradecer a mi hermano Oscar su apoyo inagotable. A mi familia, a mi tío Salvador, mi tía Amparo, mi tía Maruja, mis primos y sobrinos, gracias por vuestros ánimos. No quiero olvidarme de José y Blanca, quienes siempre me han tratado con mucho cariño.

En último lugar, pero no por ello menos importante, ya que sin esta ayuda hubiera sido mucho más complicado realizar esta Tesis Doctoral, me gustaría agradecer el soporte económico del Ministerio de Educación y Ciencia (Ref. AP2002-1874) y la financiación recibida de los proyectos de la Generalitat Valenciana GVO1-249, GVO4B/247 y Grupos C3-118 y de la Universitat de València proyecto UV-AE-20050203.

Todos somos científicos cuando somos
niños, pero al crecer,
sólo algunos conservan un poco de esa curiosidad
que es la madre de la ciencia.

Juan Aguilar M.
Biólogo teórico

ÍNDICE

1. OBJETIVOS

2. INTRODUCCIÓN

1.1. Evolución histórica de la espectroscopia vibracional
1.2. Espectroscopia IR en el análisis cuantitativo
  i. Medidas de transmisión
  ii. Medidas de reflectancia total atenuada
  iii. Medidas de reflectancia difusa
  iv. Medidas fotoacústicas en el IR
1.3. Espectroscopia Raman en el análisis cuantitativo
1.4. Espectroscopia vibracional en el control de calidad

3. RESUMEN

a. Medidas de transmisión
b. Medidas de reflectancia total atenuada
c. Medidas de reflectancia difusa
d. Medidas fotoacústicas en la región del infrarrojo Medio
e. Medidas de emisión Raman

4. RESULTADOS Y DISCUSIÓN

a. Transmission spectroscopy
  1. Solid Sampling Fourier transform infrared determination of Mancozeb in pesticide formulations
  2. Fourier transform infrared spectrometric strategies for the determination of Buprofezin in pesticide formulations
  3. FTIR approaches for Diuron determination in commercial pesticide formulations
  4. A validated and fast procedure for FTIR determination of Cypermethrin and Chlorpyrifos
  5. FTIR determination of Aspartame and Acesulfame-K in tabletop sweeteners
  6. Optimization of transmission near infrared spectrometry procedures for quality control in pesticide formulations
  7. Automated Fourier transform near infrared determination of buprofezin in pesticide formulations
b. Atenuatted total reflectance
  1. Attenuated total reflection-Fourier transform infrared analysis of the fermentation process of pineapple
c. Diffuse reflectance spectroscopy
  1. Quality control of agrochemical formulations by diffuse reflectance near infrared spectrometry

OBJETIVOS

1. OBJETIVOS

Una de las principales preocupaciones de la Química Analítica actual es el desarrollo de métodos de análisis que sean medioambientalmente sostenibles. Procedimientos que, sin sacrificar características analíticas como precisión y exactitud, reduzcan la cantidad de residuos generados en los laboratorios, para que de esta forma puedan aplicarse como análisis de rutina en el control de calidad, para los que otras características como rapidez y consumo de reactivos son tan importantes como las anteriores. Estos métodos analíticos que disminuyen, o incluso eliminan, la cantidad de residuos generados proporcionan una serie de ventajas como son un ahorro en el coste de reactivos, una mejora de las condiciones de seguridad e higiene en el trabajo y una reducción en los costes de gestión y tratamiento de los residuos.

Esta Tesis Doctoral se enmarca dentro del proyecto de investigación "**Análisis cuantitativo, ambientalmente sostenible, por espectrometría vibracional"** financiado por la Oficina de Ciència i Tecnologia de la Generalitat Valenciana**,** y persigue los siguientes objetivos específicos:

- ***El desarrollo de herramientas analíticas basadas en el empleo de técnicas vibracionales que permitan el control de productos manufacturados*** con diferentes características físico-químicas (composición, concentración y naturaleza de sustancia activa, tipo de presentación,…). Las muestras analizadas durante la realización de esta Tesis Doctoral se pueden dividir en dos grupos: el primero esta formado por pesticidas comerciales, en los que el ingrediente activo esta en concentraciones del orden de porcentaje, mientras que el segundo agrupa muestras alimentarias, como edulcorantes de mesa, néctar de fruta y bebidas energéticas, en los que los analitos están presentes en concentraciones tanto a niveles de porcentaje como en partes por millón.

- ***Diseño y puesta a punto de procedimientos sencillos basados en medidas directas y no destructivas de muestras sólidas***, eliminando así por completo el uso de disolventes y reactivos y minimizando el tratamiento previo de la muestra que, por otra parte puede ser almacenada para posteriores análisis o comprobaciones.

- Cuando el análisis directo no sea viable, se buscará la ***reducción de la cantidad de disolventes*** utilizados en el proceso de extracción del analito así como el empleo de disolventes menos tóxicos. Se evaluará la posibilidad del empleo de disolventes no halogenados para medidas de transmisión en el infrarrojo medio, para reducir de esta forma la toxicidad y el efecto sobre el medio ambiente de este tipo de disolventes. De la misma forma se desarrollarán métodos automatizados basados en medidas en línea (*flow injection analysis,* FIA), pudiendo incluir también etapas de preparación de la muestra y/o extracción de los analitos, de modo que se favorezca la reducción del consumo de disolventes y a la vez se minimice el contacto del operador con sustancias tóxicas.

- ***Mejorar la productividad incrementando la frecuencia de análisis.***

- Así mismo, se desarrollarán procedimientos basados en espectrometría vibracional que permitan ***la determinación simultánea de más de un ingrediente activo***.

- ***Demostrar la utilidad de la espectrometría vibracional para la monitorización de reacciones*** donde es necesario un control de los parámetros de calidad tanto de las materias primas y de los productos finales así como de las etapas intermedias del proceso, de forma que se puedan corregir errores prácticamente en tiempo real minimizando las pérdidas económicas.

En definitiva, el propósito de esta Tesis es demostrar las ventajas y, por tanto, la utilidad de la espectrometría vibracional para realizar el control de calidad de productos manufacturados en sectores industriales tan importantes como son el agroquímico y el alimentario. Con este fin, se han desarrollado, validado y evaluado, en términos de exactitud, precisión y limites de detección y/o cuantificación, métodos de análisis basados en el empleo de técnicas vibracionales (espectrometría infrarroja, en la región próxima y media, y Raman) utilizando, en cada caso, diferentes modos de medida (transmisión, reflectancia total atenuada, reflectancia difusa, espectroscopia fotoacústica y *back scattering*).

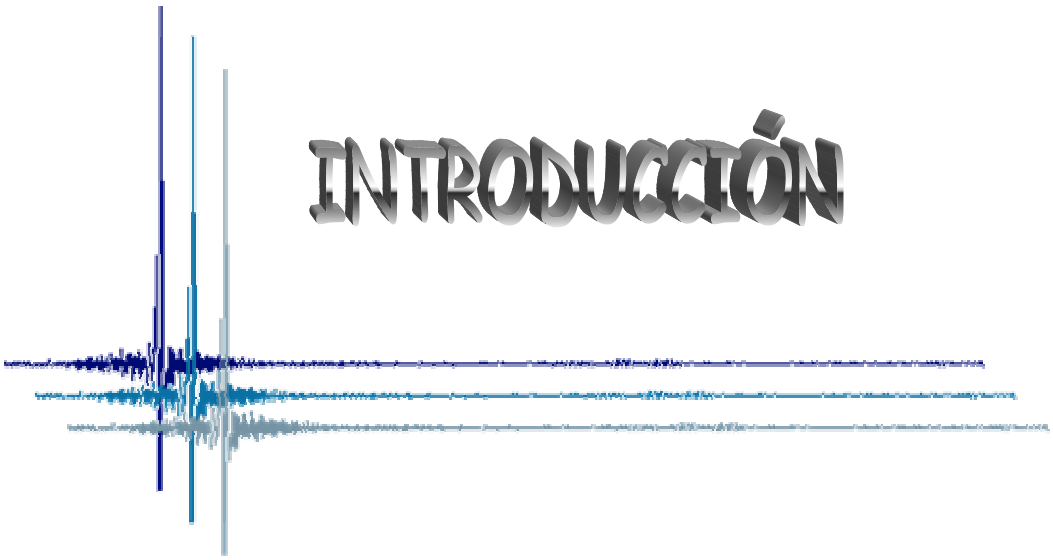

INTRODUCCIÓN

2. INTRODUCCIÓN

Se conoce como espectroscopia vibracional al conjunto de metodologías analíticas que dan como resultado espectros que son reflejo de los modos de vibración de la muestra y, por tanto, son característicos de su estructura molecular. La información presente en dichos espectros puede ser usada tanto para el análisis cualitativo (posición de las bandas) como para el cuantitativo (intensidad de las mismas). Podemos dividir estas metodologías en dos grandes grupos: la espectroscopia infrarroja (IR) y la espectroscopia Raman. La diferencia se debe a las distintas reglas de selección mecano-cuánticas en que están basadas, ya que para obtener un espectro infrarrojo es necesario un cambio en el momento dipolar mientras que en el caso de la espectroscopia Raman es necesario un cambio en la polarizabilidad de la molécula [*Skoog et al.*, 2003].

La absorción IR provoca una transición de la molécula a un nivel vibracional excitado y ésta sólo se produce cuando hay un cambio en el momento dipolar de la molécula como consecuencia de su vibración. Cabe reseñar que las bandas de absorción en la zona del IR cercano (NIR) se deben a sobretonos o combinaciones de las bandas vibracionales fundamentales que se producen en la región del infrarrojo medio (MIR) [*Blanco et al.,* 1998]. Por tanto, la información contenida en un espectro NIR será reflejo de la propia de un espectro MIR, pero las bandas suelen estar solapadas y ser de menor intensidad que las propias del MIR. Esta intensidad será menor cuanto mayor sea el orden del sobretono.

Por otra parte, para que se produzca actividad Raman, la polarizabilidad de un enlace tiene que variar en función de la distancia entre los núcleos de los átomos que lo forman. Debido a estos requisitos, los espectros IR y Raman no son idénticos, sino complementarios.

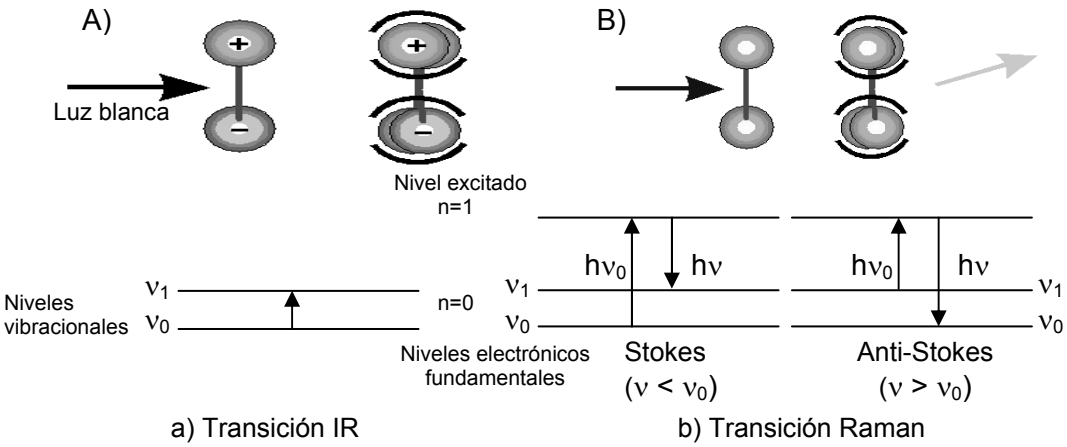

Figura 1. A) Principios en los que están basadas la espectrometría de absorción en el IR (A) y de emisión Raman (B).

1.1. Evolución histórica de la espectroscopia vibracional

El descubrimiento de la radiación IR tuvo lugar en 1800 cuando W. Herschel [*Herschel*, 1800], un astrónomo inglés de origen alemán, midió la temperatura en las distintas regiones del espectro visible, comprobando que la temperatura variaba al pasar de la parte azul a la roja. Colocó el termómetro un poco más allá, en una región donde no había luz visible, y descubrió que la temperatura era todavía más alta, concluyendo que existía otro tipo de luz más allá del rojo, a la que llamó radiación *infrarroja*, capaz de proporcionar un mayor calentamiento.

Fue necesario el paso de un siglo hasta que en 1900 W. Coblentz construyó un espectrómetro IR con un prisma de roca salina y un detector térmico conectado a un galvanómetro. Coblentz descubrió, con ayuda de su espectrómetro, que cada compuesto tenía un espectro IR diferente y característico y que gracias a esta huella dactilar podía diferenciar unos compuestos de otros.

Sin embargo, los primeros equipos comerciales para la obtención de espectros en el IR no aparecieron hasta mediados del siglo XX. Pero no fue hasta la década de 1980 cuando se introdujeron en el mercado los espectrómetros de transformada de Fourier (FT) que amplían en gran

medida las posibilidades de esta técnica. Con los espectrómetros IR convencionales dispersivos con monocromador era difícil acceder a la región de 10 a 400 cm^{-1} (IR lejano (FIR)), por eso los primeros espectrómetros de transformada de Fourier se diseñaron especialmente para esa región. De cualquier modo, este empleo de sistemas interferométricos y de transformada de Fourier se ha extendido hoy en día a instrumentos que permiten barrer toda la región IR, prácticamente, desplazando del mercado, a los espectrofotómetros dispersivos con monocromador y redes de difracción. La mayor sensibilidad de los equipos FT, la mejor relación señal/ruido, su mejor precisión y exactitud en la medida de la frecuencia y su mayor velocidad de adquisición, que permite la posibilidad de obtener un espectro a partir de la acumulación de un gran número de barridos del sistema interferométrico, ha permitido disponer de una herramienta analítica que ofrece una importante selectividad y una adecuada sensibilidad para la determinación de un gran número de analitos en diferentes tipos de muestras.

Por otra parte, el efecto Raman fue descubierto en 1928 por el físico hindú *C.V. Raman* [*Raman y Krishnan*, 1928]. En un proceso de colisión inelástico entre un fotón y moléculas pertenecientes a una muestra, el fotón pierde energía al excitar vibraciones típicas de las moléculas. La pérdida de energía de los fotones incidentes se analiza con un espectrómetro óptico, obteniéndose de este modo un espectro Raman, que es único para cada tipo de material y sirve como una "huella digital" para identificarlo.

Este efecto se mantuvo como una curiosidad científica hasta la invención de los LASER ("*light amplification by stimulated emission of radiation*") (fuentes comerciales vendidas a principio de la década de 1970) y los detectores de acoplamiento de carga (CCD) de estado sólido (desarrollados a finales de la década de 1980 [*Wang y McCreery,* 1989]).

En el cronograma de la Figura 2 se indican los principales hitos que han constituido al avance y desarrollo de las diferentes técnicas de espectrometría vibracional.

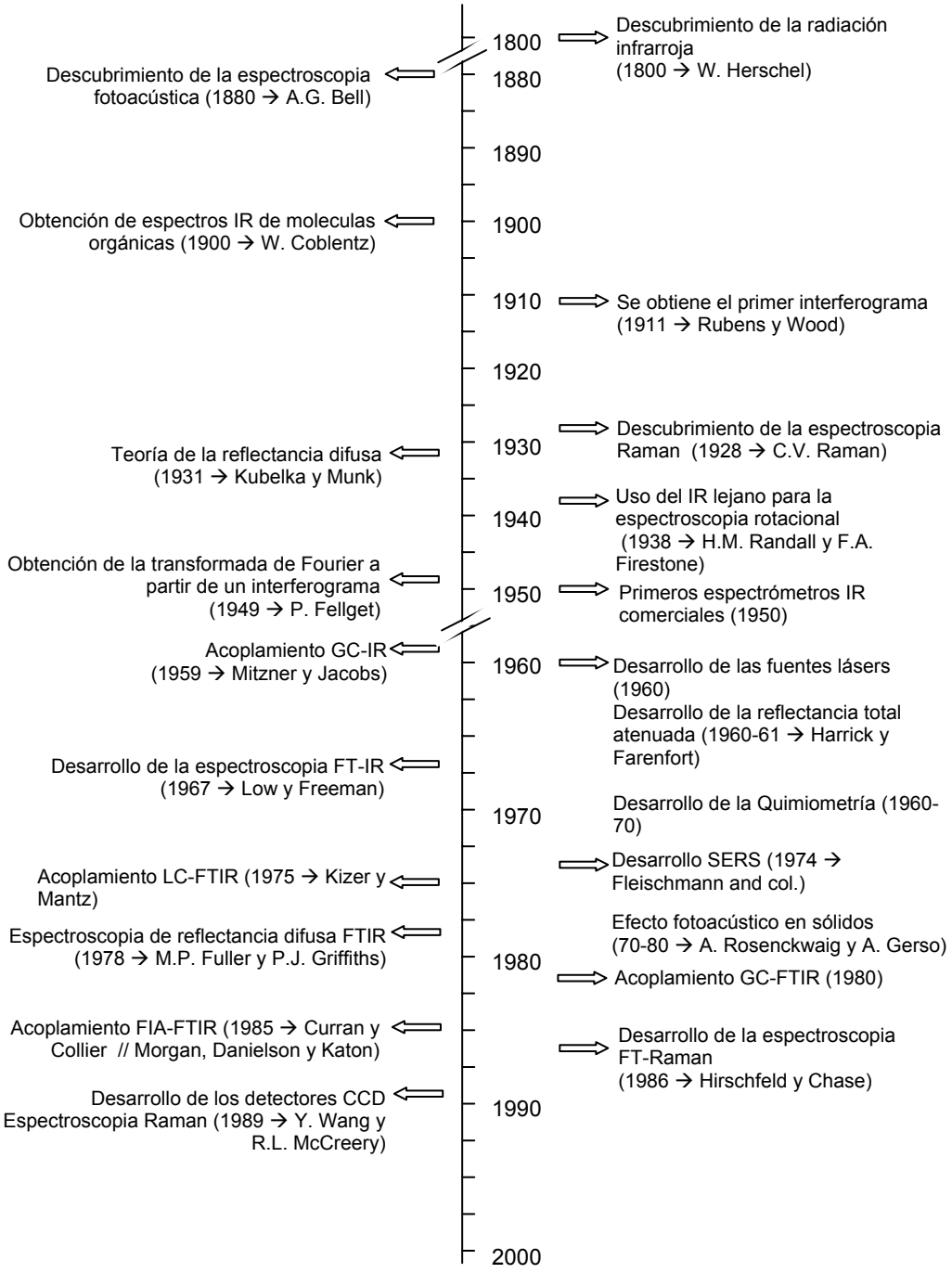

Figura 2. Cronología de los desarrollos esenciales de la espectrometría vibracional.

1.2. Espectroscopia IR en el análisis cuantitativo

La región infrarroja del espectro electromagnético corresponde a la radiación con números de onda comprendidos entre 12800 y 10 cm^{-1}. El espectro IR se divide en tres regiones denominadas infrarrojo cercano, medio y lejano. El infrarrojo cercano está formado por la radiación con números de onda entre 12800 y 4000 cm^{-1}, el infrarrojo medio abarca entre los 4000 a 200 cm^{-1} y finalmente la región comprendida entre 200 y 10 cm^{-1} es la conocida como infrarrojo lejano.

A pesar del uso sistemático de la espectrometría IR para el análisis cualitativo, su empleo para llevar a cabo determinaciones cuantitativas no ha sido tan generalizado como el de otras espectrometrías. Ello se ha debido básicamente a limitaciones en términos de sensibilidad y a una falta de transparencia en el MIR de los disolventes y materiales habitualmente empleados [*Cadet y de la Guardia,* 2000].

La espectroscopia IR es una técnica adecuada para el análisis de una gran variedad de materiales, desde polvos hasta polímeros, pasando por líquidos viscosos, disoluciones acuosas u orgánicas y gases. Existen diferentes modos de registrar el espectro en la región IR entre los que destacan las medidas de absorción, de reflectancia total atenuada, de reflectancia difusa y fotoacústicas. Seleccionar el modo de medida más adecuado para la obtención del espectro IR de una determinada muestra depende de varios factores entre los que cabe destacar el estado físico de la muestra, la información que se está buscando (análisis de superficie, de profundidad o multicapas,…), cantidad de muestra necesaria y, por último pero no por ello menos importante, del tiempo disponible y coste asumible para la obtención de los espectros (preparación de la muestra, reactivos necesarios, residuos generados,…) [*Hannah,* 2002].

Las ventajas e inconvenientes de la espectroscopia IR en el análisis cuantitativo están ligadas, en gran medida, al modo de medida, esto es, de obtención del espectro. En este sentido vamos a comentar los

fundamentos y principales aplicaciones de los distintos modos de registro en el IR.

I. Medidas de transmisión

El principio en el que se basa el análisis cuantitativo utilizando medidas de transmisión en la región IR es que la absorción de radiación por parte de la muestra está directamente relacionada con la concentración de los constituyentes de ésta. Esta relación viene marcada por la ley de Lambert-Beer y puede describirse como:

$$A = \varepsilon\, b\, c \qquad \text{Ec. 1}$$

donde **A** es la absorbancia, **ε** el coeficiente de extinción molar a una determinada frecuencia o número de onda, **b** el paso óptico de la celda o camino recorrido por el haz de radiación dentro de la muestra y **c** la concentración en la que se encuentra presente el analito.

Por tanto, una de las características necesarias que este tipo de medidas deben cumplir, para poder llevar a cabo análisis cuantitativos, es la obtención de pasos ópticos constantes y reproducibles. Este requisito es fácil de conseguir en el caso de análisis de líquidos, disoluciones y gases contenidos en el interior de celdas de medida con pasos ópticos constantes, pero no es tan sencillo en el caso de sólidos o películas delgadas.

La obtención del espectro MIR de muestras líquidas o en disolución tiene ciertas limitaciones como son la utilización de celdas especiales para líquidos (con pasos ópticos, por lo general, del orden de 1 mm o fracciones del mismo), y la selección adecuada del disolvente y del material empleado en las ventanas de la celda de medida. En la Figura 3, se indican los disolventes más comunes utilizados en los estudios espectroscópicos en la región MIR, detallando el intervalo en el que ofrecen una transparencia adecuada para permitir su empleo. Es evidente que no existe un compuesto que sea transparente en todo el intervalo MIR y para seleccionar el más adecuado hay que tener en cuenta otras características propias del disolvente, como son su

toxicidad o su temperatura de ebullición, así como la compatibilidad con los otros elementos utilizados para la obtención del espectro, como es el caso del material de las celdas de medida. Los disolventes más empleados, por su relativa baja absorción en el MIR, son el diclorometano (CH_2Cl_2), el cloroformo ($CHCl_3$), el tetracloruro de carbono (CCl_4) y otros organohalogenados. Todos estos disolventes se caracterizan por ser tóxicos y dañinos para la capa de ozono, además de ser muy volátiles, con puntos de ebullición entre 40 y 76 ºC [*Merck*, 2001], lo que dificulta el trabajo con ellos y supone un impacto negativo no sólo para el personal del laboratorio que los maneja sino también sobre el medio ambiente [*ONU,* 1999].

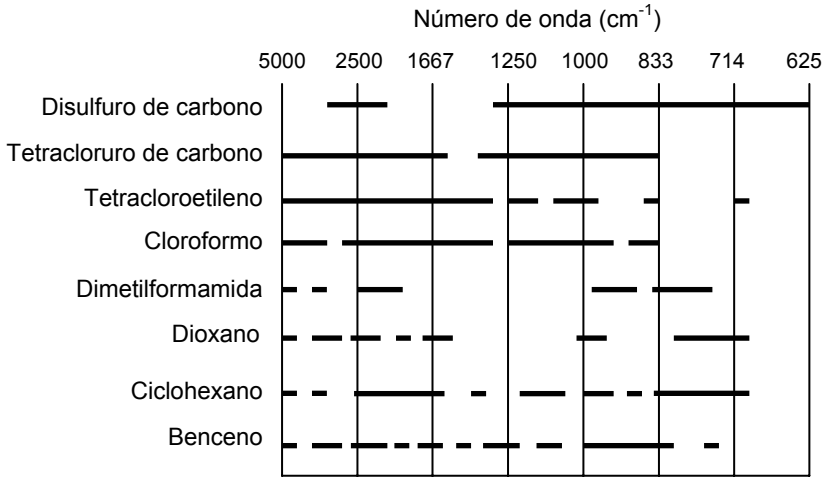

Figura 3. Transparencia de los disolventes habitualmente utilizados en la región del infrarrojo medio. Las líneas horizontales indican las regiones utiles.

Por otra parte, el agua y los alcoholes son menos utilizados debido a su intensa absorción en esta región del espectro electromagnético (falta de transparencia), que hace que para trabajar con disoluciones acuosas y/o alcohólicas sea necesario reducir el paso óptico de la celda de medida hasta un espesor de unas pocas micras (<25 μm) [*Lendl et al.*, 1997]. Otro problema de las disoluciones acuosas es que atacan a los haluros de metales alcalinos, que son los materiales más

utilizados en la construcción de las ventanas de las cubetas, por lo que se requiere el empleo de otros materiales como el BaF_2, CaF_2 o ZnSe (entre otros).

Para obtener el espectro MIR de una sustancia en fase sólida, es necesaria la dispersión de ésta en una matriz líquida o sólida [*Hannah,* 2002]. En esta técnica el sólido debe estar finamente pulverizado, hasta conseguir que el tamaño de partícula sea menor que la longitud de onda de la radiación, evitando así la dispersión de ésta. Una de las formas más populares de manipulación de muestras sólidas es la dispersión en pastillas de KBr, aunque presenta la dificultad de la preparación de las muestras y la necesidad de añadir un patrón interno a la mezcla muestra/KBr para poder cuantificar el analito como consecuencia de la no obtención de pasos ópticos (espesores de pastilla) constantes y/o reproducibles. El espesor de la pastilla de KBr no debe ser muy grande para evitar el efecto de la dispersión de la radiación que provocará un desplazamiento de la línea base.

Para la obtención de espectros de sustancias gaseosas o fácilmente volátiles se usan celdas especiales con un paso óptico que varía entre unos centímetros y varios metros, los pasos ópticos largos se obtienen recubriendo la superficie de la celda con un material reflectante y empleando el paso múltiple de la radiación a través de la celda.

Por otra parte, los espectros de absorción del NIR para muestras líquidas se obtienen de forma similar a los de la región del ultravioleta y del visible (UV/vis), es decir, utilizando cubetas de cuarzo o vidrio óptico con una longitud variable entre 0.1 y varios centímetros, siendo lo más habitual el trabajo con celdas de 1 cm. Los disolventes más utilizados en esta región, como puede verse en la Figura 4, son aquellos que no contienen grupos O-H y N-H, estos enlaces presentan gran absorción en el NIR. Debido a que las bandas de absorción en la zona del infrarrojo próximo son sobretonos o bandas de combinación, sus absortividades molares son pequeñas y, en consecuencia, los límites de detección que pueden obtenerse son más grandes que los

equivalentes en la región MIR a pesar de trabajar con pasos ópticos mayores.

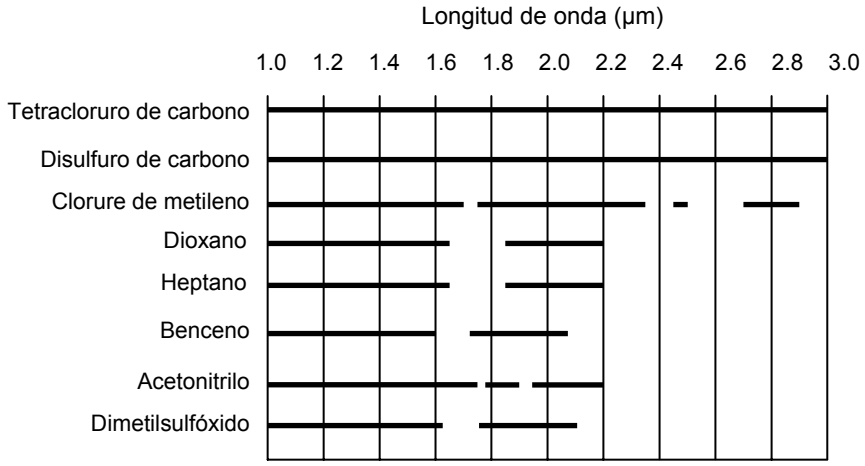

Figura 4. Transparencia de los disolventes habitualmente utilizados en la región del infrarrojo cercano. Las líneas continuas indican una transparencia satisfactoria para emplearlos con cubetas de 1 cm.

Uno de los problemas que se presenta en el registro de transmisión del espectro de una muestra líquida o en disolución, particularmente acuosa, en esta región del NIR es que las medidas son bastante sensibles a la temperatura, por lo que se hace necesario introducir la celda en un recipiente termostatizado, para evitar cambios espectrales debidos a variaciones de la temperatura y calentamientos en la muestra [*Ozaki y Berry,* 2002].

El espectro de transmisión NIR de una muestra sólida, en forma de polvo o partículas de mayor o menor tamaño, también se puede obtener introduciendo ésta en una celda de paso óptico constante. Debido a la influencia de parámetros físicos (tamaño y forma de las partículas y estado de la superficie) en el espectro NIR, es importante obtener un tamaño de partícula homogéneo, por lo que es necesario un tratamiento previo de la muestra.

Recientemente se han desarrollado instrumentos para la obtención de espectros de transmitancia en el NIR de pastillas o tabletas sólidas sin la necesidad de manipulación previa [*Corti et al.,* 1999]. En este caso, no se puede decir que se cumpla estrictamente la ley de Beer, ya que por efecto de la dispersión una parte importante de la radiación puede sufrir reflectancia difusa (que no cumple la ley de Beer). Aunque este efecto está presente, los instrumentos empleados para medidas de transmisión directamente sobre muestras sólidas están diseñados para minimizar la componente de reflectancia difusa y que la señal analítica dependa fundamentalmente de la absorbancia producida por la muestra.

II. Medidas de reflectancia total atenuada

La espectroscopia de reflectancia total atenuada (ATR), desarrollada de forma independiente por Harrick [*Harrick*, 1960] y Farenfort [*Farenfort*, 1961], es un tipo de espectroscopia de reflexión en la cual la muestra se coloca en contacto con un elemento de reflexión interna (IRE) con un alto índice de refracción. La radiación IR se enfoca y se hace incidir sobre uno de los extremos del borde del IRE, de modo que el haz se transmite a través y mediante reflexión en las caras internas del IRE, hasta que sale por el otro extremo de éste y se dirige a un detector apropiado. Aunque la reflexión interna tiene lugar en la interfase entre la muestra y el IRE, la radiación penetra una pequeña distancia en la muestra $\boldsymbol{d_p}$, pudiendo ser absorbida por ella (ondas evanescentes). El grado de penetración de la onda evanescente en la muestra depende de una serie de parámetros, entre ellos la longitud de onda de la radiación **(λ)**, el ángulo de incidencia de ésta **(θ)** y de los índices de refracción del material del IRE **(n1)** y de la muestra **(n2)** [*Mirabella,* 2002].

$$d_p = \frac{\lambda}{2\pi n_1 \sqrt{\sin^2 \theta - \left(\frac{n_2}{n_1}\right)^2}} \qquad \text{Ec. 2}$$

En el caso de que la muestra absorba radiación, la onda incidente se atenuará y su reflectancia podrá expresarse de la siguiente forma:

$$R = 1 - \alpha d_e \qquad \text{Ec. 3}$$

donde $\mathbf{d_e}$ es el espesor de capa efectivo y **α** el coeficiente de absorción de la capa. La pérdida energética en la radiación se conoce como reflectancia total atenuada. Para múltiples reflexiones (N), la reflectancia total se expresa como:

$$R^N = (1 - \alpha d_e)^N \qquad \text{Ec. 4}$$

El espesor de capa efectivo es una medida de la longitud de la interacción de la radiación con la muestra y se define como la longitud necesaria en medidas de transmisión para obtener la misma absorbancia que la obtenida con una única reflexión en el límite de fase de un medio.

$$d_e = a / \alpha \qquad \text{Ec. 5}$$

donde el parámetro de absorción **a** se define como la pérdida de intensidad por reflexión:

$$a = (100 - R)\ \% \qquad \text{Ec. 6}$$

Por tanto, son varios los factores que van a influir en las medidas por reflectancia total atenuada:

La longitud de onda de la radiación infrarroja afecta a la profundidad en que ésta penetra en la muestra, de forma que se obtiene una mayor penetración a medida que aumenta la longitud de onda. Este efecto puede ser corregido mediante funciones matemáticas llamadas correcciones ATR.

El ángulo de incidencia, que se refiere al ángulo con el cual se refleja la radiación IR dentro del cristal por primera vez. Los ángulos de incidencia utilizados habitualmente son de 40º, 45º ó 60º (al incrementar el ángulo de incidencia se aumenta la distancia de penetración pero se reduce el número de reflexiones disminuyendo de forma global la sensibilidad de las medidas).

El número total de reflexiones, que puede aumentarse utilizando un cristal más delgado o largo [*Smith*, 1979]. Este número total de reflexiones **(N)** puede calcularse a partir de la expresión:

$$N=\frac{L}{t}\cot\alpha \qquad \text{Ec. 7}$$

donde **L** es la longitud del IRE, **t** el espesor, **α** el ángulo de incidencia. Al aumentar el número de reflexiones se consigue un aumento en la sensibilidad de la medida, pero también una mayor señal del disolvente. Además se produce una disminución de la señal del haz de radiación, con lo que aumenta el ruido de fondo.

Un contacto efectivo entre la muestra y el cristal. En el caso de líquidos esto es fácil de conseguir, pero cuando se trabaja con sólidos es necesario realizar una presión para conseguir un buen contacto entre ambos materiales [*Smith*, 1996]. En este último caso tiene también mucha importancia el tamaño de partícula.

Las mayores ventajas que aporta la espectroscopia de reflectancia total atenuada es la posibilidad de obtener espectros en la región MIR de disoluciones que absorban fuertemente, como es el caso de las acuosas. Estos registros, que equivalen a los que se obtendrían utilizando celdas de transmisión con pasos ópticos del orden de micras, son posibles debido a la pequeña penetración de la radiación en la muestra. La reproducibilidad de las medidas es posible debido a la propiedad que tienen los espectros de ser independientes del espesor de la muestra siempre que éste sea superior al espesor de capa efectivo.

En cuanto a la geometría de los accesorios ATR cabe destacar los diferentes diseños de las celdas de medida [*Hind et al.,* 2001]. La más ampliamente utilizada es el accesorio en posición horizontal, que como puede verse en la Figura 5, consiste en colocar el IRE de forma horizontal dejando una pequeña depresión en la parte superior para colocar la muestra en estudio.

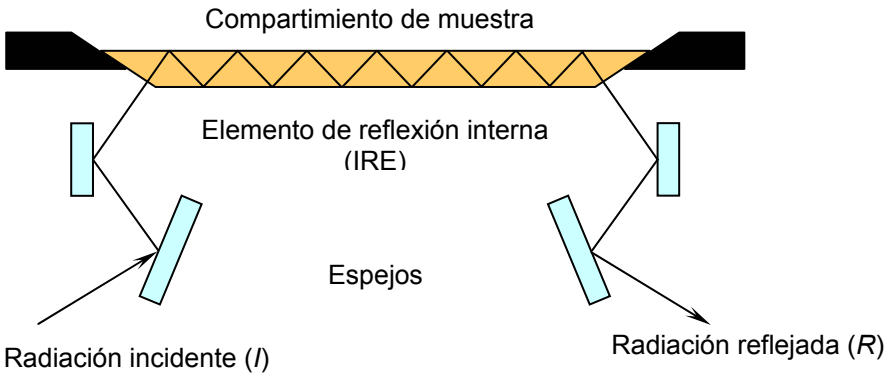

Figura 5. Diagrama esquemático de una típica celda ATR horizontal.

Las razones de ser la geometría más empleada las encontramos en su asequible precio y disponibilidad. Son celdas relativamente simples en diseño, fáciles de usar y mantener, con una limpieza sencilla y elevada robustez. Otra ventaja de las celdas horizontales es la facilidad para convertirse en celdas de flujo.

Otra geometría habitualmente usada es el diseño en forma de cámara, ya sea en posición horizontal o vertical. El diseño de ambas celdas está basado en la ubicación del IRE en el interior de una cámara que lo rodea. Un diseño habitual es el mostrado en la Figura 6, el cual utiliza un cilindro horizontal. Una ventaja de este tipo de celdas horizontales es la facilidad de acoplarlos a un sistema FIA, sin embargo, las desventajas que presentan son la dificultad de limpieza y la imposibilidad de obtener una buena reproducibilidad en soluciones con partículas en suspensión.

Otro tipo de accesorios, mucho menos utilizados que los anteriores, son las llamadas sondas de inmersión. Ésto es debido a que su diseño sólo permite una o dos reflexiones, lo que limita enormemente la sensibilidad que pueda obtenerse en comparación con los diseños

comentados anteriormente. La limpieza de estas sondas es también sencilla y son particularmente útiles en procesos industriales *on-line* o *at-line*, donde se requiere una medida y limpieza rápida.

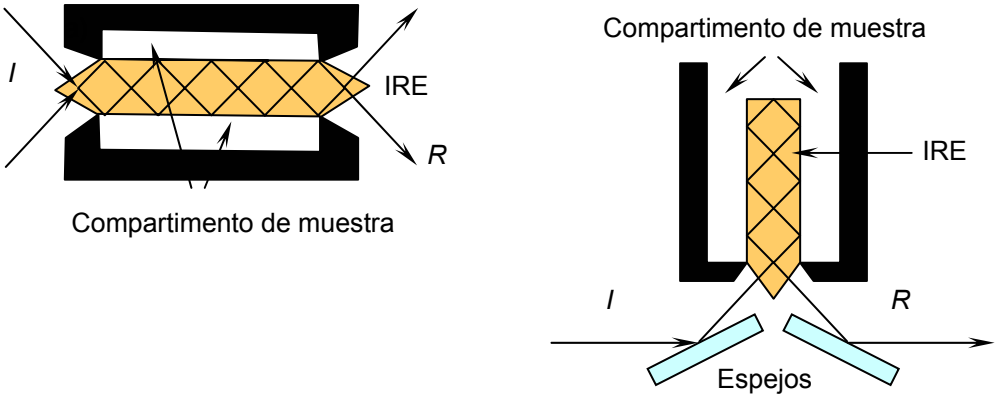

Figura 6. Diagrama esquemático de una típica celda ATR en forma de cámara con el IRE en posición a) horizontal y b) vertical.

En lo que respecta a los materiales comercializados para ser utilizados como IREs hay que destacar la gran variedad que actualmente existe en el mercado. Los más comunes son el seleniuro de zinc, el germanio, el sulfuro de zinc, el silicio y el diamante [*Fitzpatrick y Reffner,* 2002]. Para elegir el material IRE más adecuado se han de tener en cuenta diferentes factores, entre ellos el intervalo espectral de interés, la compatibilidad del sistema IRE/analito de interés, la naturaleza del disolvente que se va a emplear, el pH del sistema, las propiedades físicas y químicas del IRE y su coste de adquisición. En la Tabla 1 se indican las propiedades de los materiales mas utilizados como IRE [*Thermo Spectra-Tech*, 2001].

Tabla 1. Características físico-químicas de los materiales utilizados habitualmente como IREs.

Material IRE	n	Dureza (Knoop)	Densidad (g/cm^3)	Punto de fusión (ºC)	Rango de transmisión (cm^{-1})	Comentarios
AMTIR	2.5	170	4.40	300	11000-1000	Relativamente duro y frágil. Resistente a ác. Atacado por bases fuertes.
CdTe	2.7	56	6.20	1040	10000-500	Muy frágil. Atacado por oxidantes y ác. Poco soluble en ác.
Diamante	2.4	7000	3.5	3500	4500-2500 1667-33	Muy duro. Resistente a la corrosión y a P elevadas. Atacado por el $Cr_2O_7^{2-}$ y H_2SO_4.
Ge	4.0	550	5.32	936	5000-900	Duro, frágil. Pérdidas por reflexión. Atacado por H_2SO_4 caliente y agua regia.
Cuarzo	1.4	174	2.6	1610	25000-2200 250-FIR	Usado en el UV-vis y NIR. Atacado por HF.
Zafiro	1.7	1370	4.00	2030	33000-2800	Muy duro e inerte. Atacado por ác. conc. y bases.
Si	3.4	1150	2.33	1420	9500-1500 350-FIR	Duro, frágil. Resistente a golpes térmicos y mecánicos. Atacado por HF y HNO_3.
KRS-5	2.4	40	7.45	415	14000-400	Deformable a P elevada.Tóxico. Soluble en bases. Atacado por agentes complejantes.
ZnSe	2.4	137	5.27	1520	20000-700	Duro. Fácilmente rompible. Bajas pérdidas por reflexión. Atacado por ác. y bases fuertes. Tóxico.
ZnS	2.2	178	4.08	1830	14000-1000	Resistente a golpes térmicos y mecánicos. Atacado por ác. y oxidantes fuertes.

n=índice de refracción

III. Medidas de reflectancia difusa

La reflectancia difusa es una forma eficaz de obtener espectros IR directamente de un sólido con una mínima preparación de la muestra. Es una alternativa a la técnica de preparación de pastillas de KBr para la obtención de espectros MIR de polvos o sustancias sólidas con una superficie rugosa (papel, carbón, tejidos (tela),…).

El principio en que se basa esta técnica es que cualquier radiación enfocada sobre una superficie puede ser, dependiendo de las características de la superficie, absorbida, directamente reflejada (reflexión especular), internamente reflejada o difundida en todas direcciones tras penetrar en alguna molécula y ser absorbida en parte por ésta. Este último efecto es la base de la espectroscopia de reflectancia difusa [*Griffiths y Olinger,* 2002].

La reflectancia difusa, desarrollada por primera vez por Kubelka y Munk [*Kubelka y Munk,* 1931], es la consecuencia de la entrada de radiación en una o más partículas de muestra y su difusión en la misma en todas direcciones. Este componente de la radiación contiene datos relativos a las propiedades de la muestra, sin embargo la reflectancia difusa no puede separarse de la reflexión especular, aunque la contribución de ésta al espectro final se minimiza controlando la posición del detector con respecto a la muestra. Posteriormente, la radiación dispersada en todas direcciones junto con la reflejada es dirigida hacia el detector [*Blanco et al*., 1998].

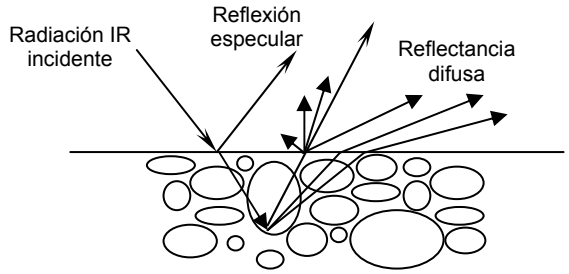

Figura 7. Representación esquemática de la interacción de la radiación infrarroja con un sólido para generar un espectro de reflectancia difusa.

Desde el punto de visto cuantitativo, no existe una relación lineal entre la intensidad de las bandas y la concentración de la muestra, y el análisis cuantitativo se hace bastante complicado. La ley de Lambert-Beer, usada normalmente en transmisión, no es directamente aplicable para las medidas de reflectancia difusa, sin embargo, se obtiene una expresión similar con la utilización de la ecuación de Kubelka-Munk. Esta teoría asume que la radiación que incide en un medio dispersante sufre simultáneamente un proceso de absorción y dispersión, de forma que la radiación reflejada, en el caso de muestras opacas y de espesor infinito, puede describirse como:

$$F=\frac{(1\ \ R)^2}{2R}=\frac{k}{s} \qquad \text{Ec. 8}$$

donde, **k** es el coeficiente de absorción (2.303*ε*c), **s** el coeficiente de dispersión, **R** el índice de reflexión definido como espectro de muestra en polvo/espectro de dilución de polvo, de forma que si **s** es constante (propiedad intrínseca de un material y que depende solamente del tamaño de partícula), a una frecuencia determinada la función de Kubelka-Munk depende directamente de la concentración.

Una de las propiedades que deben cumplir las muestras para que se le pueda aplicar la Ecuación 8 es tener un grosor semi-infinito, es decir, que la distancia de penetración media de la radiación (ya que cada fotón recorre un camino distinto) atraviese la suficiente distancia en la muestra como para considerarla semi-infinita (en la práctica varios milímetros es más que suficiente para satisfacer esta condición) [*Milosevic y Berets,* 2002]. Cuando se cumple esta condición, la distancia de penetración , $\mathbf{d_p}$, está relacionada con el coeficiente de absorción, **k**, mediante las ecuaciones 9 y 10.

$$d_p=1/\alpha \qquad \text{Ec. 9}$$

donde **α** es un parámetro que viene definido por:

$$\alpha=\sqrt{k(k+2s)} \qquad \text{Ec. 10}$$

De forma que la distancia de penetración será mayor cuanto menor sea dicho coeficiente, por lo que la sensibilidad aumenta cuando disminuye **k** debido al aumento de la distancia de penetración [*Milosevic y Berets,* 2002].

En la práctica, se utiliza la reflectancia relativa que es la relación de las intensidades de luz reflejadas por la muestra y por un estándar. Se suele utilizar como estándares materiales estables, y con una elevada y relativamente constante reflectancia absoluta en la región espectral de interés, tales como el teflón, sulfato de bario, óxido de magnesio o placas cerámicas de alúmina de alta pureza.

Los espectros de reflectancia difusa no son idénticos a los espectros de absorción ordinarios. En general, se observan los mismos picos pero las intensidades relativas son distintas. El formato final en el que se suelen presentar los espectros de reflectancia difusa es % reflectancia o bien log 1/R: el porcentaje de reflectancia sería equivalente al % de transmitancia y el log de 1/R a la absorbancia. Otra forma de expresar los espectros obtenidos es mediante las unidades de Kubelka-Munk. Estas unidades eliminan cualquier efecto dependiente de la longitud de onda de la radiación incidente [*Eilert y Wetzel*, 2002].

Las propiedades específicas de un material que afectan a la calidad de un espectro de reflectancia difusa son las siguientes [*Armaroli et al.* 2004]:

- Índice de refracción de la muestra. Si éste es muy elevado la contribución de la reflexión especular será mayor.
- Tamaño de partícula. Una forma de disminuir la contribución debida a la reflexión especular de las partículas de gran tamaño, es triturar la muestra hasta conseguir un tamaño de partícula homogéneo, menor de 10 μm. Si la muestra presenta una elevada absorción, ésta debe ser diluida en un diluyente adecuado (cloruro o bromuro potásico). Por norma general, la dilución garantiza una profunda penetración de la radiación y una menor reflexión especular de la superficie de la muestra, de ese modo se incrementa la contribución al espectro de la

parte de la radiación que contiene datos relativos a las propiedades de la muestra, aumentando, de esta forma, la sensibilidad.

- Grado de compactación.
- Homogeneidad. Asegurando la homogeneidad de las muestras se consigue una mejor linealidad entre la señal y la concentración.
- Concentración. Una concentración elevada de analito provocará una mayor reflexión especular.
- Coeficiente de absorción.

Debido a las características intrínsecas de este modo de medida, las ventajas que ofrece la reflectancia difusa son las siguientes:

- tratamiento previo de la muestra inexistente o mínimo,
- capacidad para analizar muestras no transparentes y/o heterogéneas,
- se evita el empleo de reactivos y/o disolventes y se minimiza la generación de residuos,
- y, por último, es un método no destructivo, de forma que la muestra puede conservarse para posteriores análisis.

Los principales inconvenientes que presenta esta técnica de la reflectancia difusa es la dificultad de calibración, debido principalmente a que propiedades físicas de la muestra, como por ejemplo el tamaño de partícula, afectan enormemente al espectro registrado, siendo necesario el empleo de métodos multivariantes de calibración para llevar a cabo determinaciones cuantitativas. Esta desventaja ha sido subsanada gracias a los grandes avances producidos en la Quimiometría en las últimas décadas [*Blanco et al.,* 1998].

A pesar de los inconvenientes citados y al mayor peso de sus ventajas, la espectroscopia de reflectancia difusa se ha convertido en una de las herramientas más importantes para la determinación cuantitativa de muestras sólidas, sobre todo en sectores industriales tan importantes como el farmacéutico [*Blanco et al.,* 1998].

IV. Espectroscopia fotoacústica

La espectroscopia fotoacústica u optoacústica (PAS), se desarrolló a principios de la década de 1970 y proporciona un medio válido para obtener espectros en la región ultravioleta, visible e infrarrojo de sólidos, semisólidos y líquidos turbios sin la necesidad de realizar un tratamiento previo de éstos.

La espectroscopia PAS se basa en el efecto de absorción de radiación que fue investigado por A.G. Bell en 1881 [*Bell*, 1881]. Este efecto se observa cuando un gas, que se encuentra cerrado en el interior de una cámara, es irradiado con un haz de radiación intermitente de una longitud de onda tal que es absorbido por el gas. La radiación absorbida por el gas provoca calentamientos que causan cambios regulares en la presión en el interior de la cámara. Dichos cambios de presión pueden detectarse con un micrófono sensible [*Michaelian,* 2003].

En el caso de sólidos tenemos un efecto similar al comentado para gases [*Rosencwaig et al*., 1976], es decir, la relajación no radiante del sólido absorbente provoca un flujo de calor periódico desde el sólido hacia el gas que le rodea (que no debe ser absorbente de la radiacion, por lo que suele utilizarse nitrógeno o helio); las fluctuaciones de presión resultantes en el gas son detectadas en el micrófono. Las ondas térmicas, que se propagan hacia la superficie de la muestra, decaen rápidamente. Por tanto, esta disminución limita la profundidad en la cual la generación de señal tiene lugar. Esta profundidad, **L**, disminuye cuando aumenta la frecuencia de modulación, ***f:***

$$L = \sqrt{\frac{D}{\pi f}} \qquad \text{Ec. 11}$$

donde **D** es la difusividad térmica de la muestra. Por tanto, la profundidad **L** puede variarse ajustando la frecuencia de modulación. Esta propiedad la hace muy útil para estudios de materiales

heterogéneos, donde variando la frecuencia de modulación es posible detectar variaciones en la composición de la muestra en función de la profundidad de la medida [*McClelland et al.*, 2002]. Además del citado efecto de decaimiento de las ondas térmicas, también encontramos otro efecto significativo como es la reflexión en la superficie de la muestra hacia el interior. Este efecto provoca una disminución de la relación señal/ruido.

El rango espectral de un detector fotoacústico depende solamente de la transparencia del material utilizado en la ventana de la cámara de muestra. Habitualmente, se utilizan ventanas de KBr (región UV-MIR), cuarzo (UV-NIR), CsI (UV-200 cm^{-1}), ZnSe (NIR y MIR hasta 560 cm^{-1}) y polietileno (FIR).

En los estudios fotoacústicos, la muestra sólida o líquida se coloca en un receptáculo de unos pocos mm de diámetro, dentro de una cámara cerrada, que se purga con helio o cualquier otro gas no absorbente, y un micrófono sensible que actúa como detector (el helio aumenta la sensibilidad en un factor de 2 a 3, permite operar con frecuencias más elevadas y elimina las interferencias de dióxido de carbono y vapor de agua presentes en el aire normal).

La forma más habitual de expresar los espectros obtenidos mediante este modo de medida es utilizar unidades fotoacústicas (PAS). Los espectros son normalizados frente al espectro de un material negro absorbente (normalmente *carbon black powder, glassy carbon,* grafito o *carbon-black filled rubber*) para corregir posibles variaciones de la fuente, la óptica o la respuesta del detector. Dichos valores a una frecuencia determinada vienen definidos por la ecuación:

$$PAS = 100(IS/IB) \qquad \text{Ec. 12}$$

donde **IS** es la intensidad de energía emitida en forma de ondas térmicas por la muestra y **IB** corresponde a la intensidad de energía emitida por el material de referencia. Numéricamente este valor es idéntico al % de transmitancia [*Termo Nicolet Corp.,* 2002].

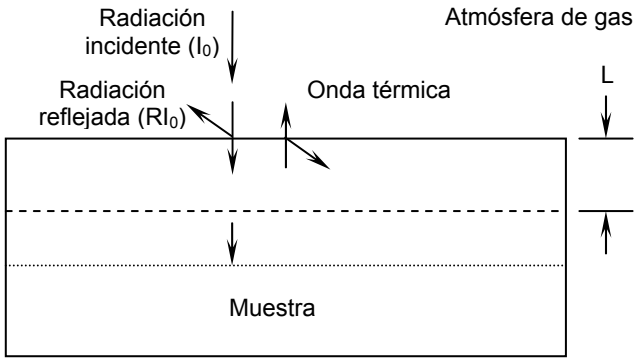

Figura 8. Mecanismos de generación de un espectro FTIR-PAS de una muestra sólida.

La característica más relevante de esta metodología es que la radiación reflejada o dispersada por la muestra no tiene ningún efecto en el micrófono y por tanto no interfiere.

Se pueden obtener espectros fotoacústicos en la región MIR empleando diferentes modos de medida en función de la incidencia de la radiación IR sobre la muestra y la posición relativa de esta última respecto de la cámara de gas y el micrófono: absorbancia fotoacústica, reflectancia difusa y transmitancia (Figura 9).

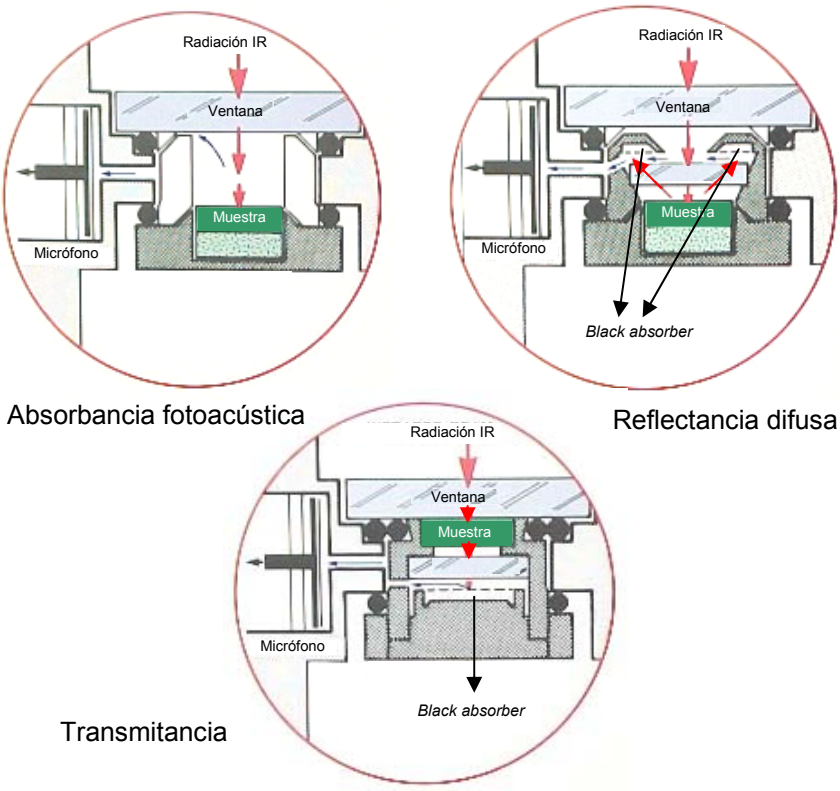

Figura 9. Diferentes modos de medida empleados habitualmente para obtener espectros fotoacústicos.

Los accesorios para obtener los espectros de reflectancia difusa y transmitancia mediante medidas fotoacústicas están dotados de superficies recubiertas con material absorbente (*black absorber)*, donde la radiación reflejada o transmitida, respectivamente, es absorbida y se genera, de esta forma, la señal fotoacústica. La distancia entre la muestra y la superficie absorbente debe ser muy pequeña para que la generación fotoacústica sea eficiente. Por el contrario, el accesorio de absorbancia fotoacústica se basa en la generación de señal convencional proveniente directamente de la muestra. De esta forma se puede obtener el espectro que mejor se ajuste a las características del analito que se pretende analizar [*MTEC,* 2005].

1.3. Espectroscopia Raman en el análisis cuantitativo

El principio en el que se basa la espectroscopia Raman consiste en irradiar una sustancia con una fuente monocromática generada por un láser y registrar el espectro de la radiación dispersada a un cierto ángulo (generalmente a 90 ó 180 grados). La radiación dispersada puede ser de tres tipos, que se denominan Stokes, anti-Stokes y Rayleigh. Esta última, la más intensa, coincide en longitud de onda con la de la fuente de excitación y no debe incidir sobre el detector.

En los espectros Raman la abscisa corresponde al desplazamiento de los números de onda, que se define como la diferencia de energia expresada como números de onda, entre la radiación observada y la de la fuente de emisión [*Bell et al.,* 2002].

Cabe destacar que las líneas Stokes se encuentran a números de onda inferiores respecto al pico Rayleigh, mientras que los picos anti-Stokes aparecen a números de onda superiores al de la fuente. Las líneas anti-Stokes suelen ser menos intensas que las correspondientes líneas Stokes, es por ello que sólo se utiliza la parte Stokes del espectro.

Hasta principios de la década de 1980, los espectrómetros Raman tenían diseños semejantes a los instrumentos dispersivos UV/vis clásicos, es decir, sistemas de doble red de difracción para minimizar la radiación no deseable y fotomultiplicadores como sistema de detección. Los espectrómetros Raman dispersivos emplean habitualmente como fuente de radiación un láser con longitud de onda entre 782-830 (láser de diodos) y 514.5-488.0 nm (láser argón). Una ventaja de los láseres de longitud de onda corta (región visible) es el aumento de la señal Raman, debido a que la eficiencia de la dispersión Raman es proporcional a $1/\lambda^4$, así que el aumento de la eficiencia será mayor a medida que la longitud de onda sea menor. Sin embargo, es común en este tipo de instrumentos la aparición de interferencias debidas a la fluorescencia de algún componente de la muestra en los espectros Raman. La fluorescencia es el proceso por el cual una molécula irradiada emite un fotón desde el estado singulete excitado hasta el estado singulete fundamental, de forma que cuanto mayor sea la energía del láser (menor longitud de onda), mayor será la

probabilidad de que tenga lugar el fenómeno de la fluorescencia, que oculta la señal Raman.

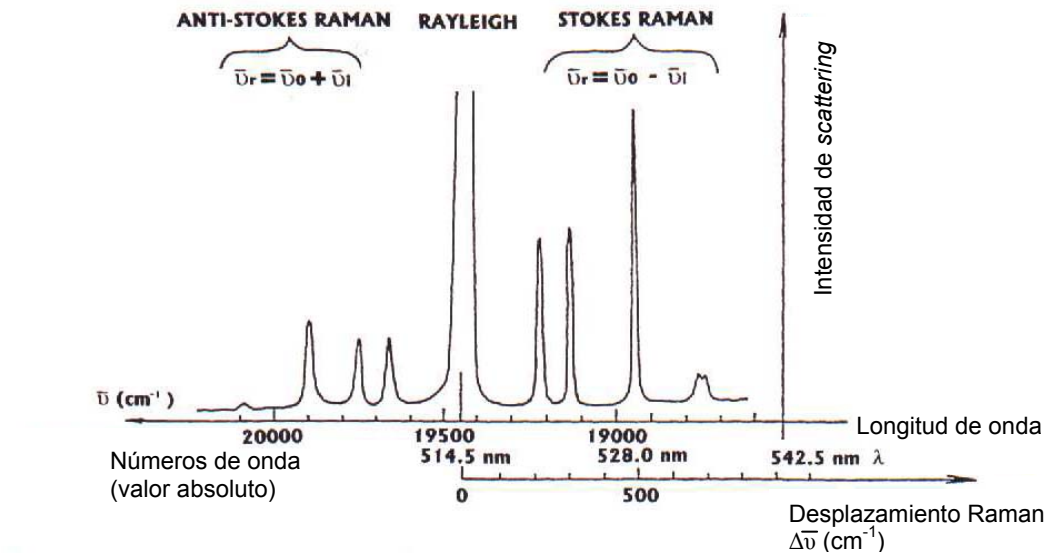

Figura 10. Representación esquemática de un espectro Raman excitado con láser de argón (λ=514.5 nm).

En la actualidad los equipos Raman comerciales pueden dividirse en dos categorías: FT-Raman o instrumentos multicanal con dispositivos de acoplamiento de carga (CCD). Los dispositivos con detectores CCD son sensibles a la radiación de 782 nm producida por láseres de diodo, que provocan la excitación Raman de muchos compuestos sin generar una fluorescencia apreciable. Por otro lado, la espectrometría Raman por transformada de Fourier evita los problemas presentes en los equipos dispersivos, eliminando la fluorescencia de fondo y haciendo posible el uso de una fuente láser mucho menos intensa, como la del láser de *Neodimium:Yttrium Aluminum Garnet* (Nd:YAG) que emite radiación sólo en el IR cercano a 1064 nm. Esta radiación no es lo suficientemente energética como para producir la excitación electrónica de la mayoría de las moléculas impidiendo así la fluorescencia.

Las mayores ventajas que presenta la espectroscopia Raman son las siguientes:

- No se requiere un tratamiento previo de la muestra, ya que puede ser irradiada directamente por la fuente láser.
- Muestras húmedas e incluso disoluciones acuosas pueden ser analizadas.
- El espectro Raman puede ser obtenido a través de plástico [*Skoulika y Geourgiou,* 2003] o vidrio [*Nordon et al.,* 2005], facilitando el análisis de las muestras directamente en el interior de su envase.
- Se pueden acoplar fibras ópticas de vidrio para análisis a distancia.
- Las bandas Raman son usualmente más estrechas que las obtenidas en el IR, existiendo de este modo menos solapamientos espectrales.

Sin embargo, el mayor inconveniente que presenta la espectroscopia Raman, además del efecto mencionado anteriormente de la fluorescencia, es la baja sensibilidad, incluso menor que la obtenida en espectroscopia IR. Con el fin de aumentar la sensibilidad de esta técnica, se desarrolló la *espectroscopia Raman de superficie aumentada* (SERS) [*Fleischmann et al.,* 1974], donde la muestra es adsorbida por la superficie de partículas metálicas coloidales o bien sobre superficies rugosas de dichos metales. La sensibilidad aumenta de esta forma, entre 3 y 6 órdenes de magnitud, aunque posteriores estudios han conseguido mejoras en la sensibilidad con factores de 10^{13} a 10^{15} [*Zeisel et al.,* 1998]. Existen diferentes técnicas de manipulación de la muestra en la espectroscopia SERS. En una de ellas, se suspenden partículas de oro o plata coloidal en una disolución de la muestra (normalmente acuosa) y se hace fluir a través de un tubo fino de vidrio que es irradiado por el láser. Otro de los métodos está basado en el depósito de una delgada película de partículas metálicas coloidales sobre una placa de vidrio al que se le añaden unas gotas de disolución de la muestra. Alternativamente, se puede depositar la muestra sobre un electródo metálico rugoso, que a continuación se retira de la disolución y se expone a la fuente láser. Una desventaja de la espectroscopia SERS es que la posición de una molécula con respecto al substrato metálico es muy

difícil de controlar y por lo tanto de mantener por lo que las medidas son poco reproducibles, dificultando cualquier tratamiento cuantitativo de los mismos.

1.4. Espectroscopia vibracional en el control de calidad

En las últimas décadas, con la popularización de los instrumentos basados en la transformada de Fourier, ha aumentado de forma considerable el interés de la industria por el uso de métodos basados en espectrometría vibracional para el control de calidad de productos manufacturados o materias primas. Unido a este hecho, el tremendo desarrollo de la Quimiometría [*Geladi*, 2003] y de los métodos automatizados [*Garrigues y de la Guardia*, 2002], ha incrementado las posibilidades de la espectrometría vibracional para procesar muestras relativamente complejas, sin la necesidad de realizar largos tratamientos previos, obteniendo unas excelentes frecuencias de análisis y reduciendo el consumo tanto de reactivos como de disolventes.

Con el fin de conocer la evolución de la literatura científica relativa al análisis cuantitativo mediante espectroscopia infrarroja por transformada de Fourier en las regiones del infrarrojo medio (FT-MIR) y próximo (FT-NIR) la espectroscopia fotoacústica y Raman, se ha considerado el número de referencias aparecidas en el Analytical Abstracts desde 1980 hasta el año 2005.

Como puede apreciarse en la Figura 11, el 70.0 % de los estudios publicados corresponde al empleo de la espectroscopia FTIR, el 14.0% a métodos basados en medidas NIR, el 12.6% utilizan la espectroscopia Raman y sólo el 3.3% emplean técnicas fotoacústicas.

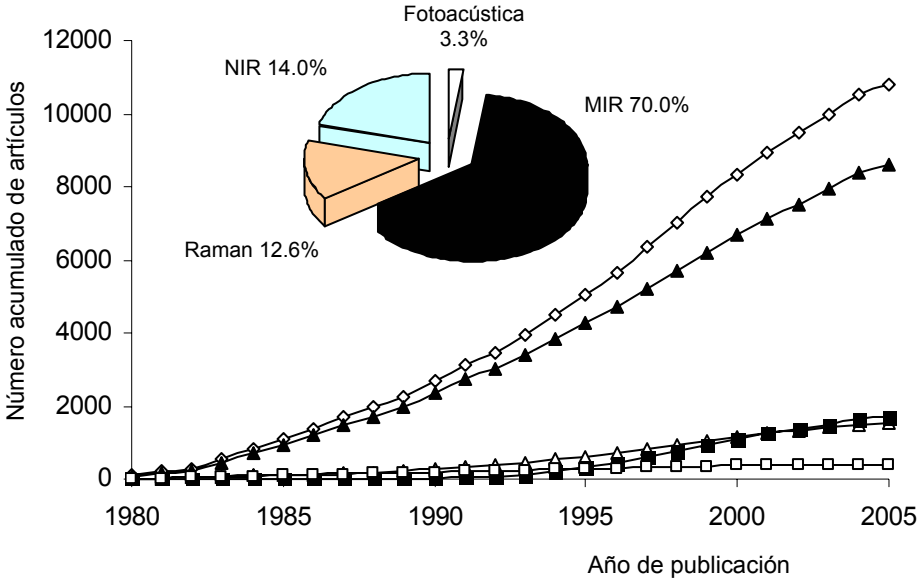

Figura 11. Evolución de la literatura científica que emplea la espectrometría vibracional en el análisis cuantitativo: 10808 artículos publicados. Detalle: Distribución de la literatura científica en función de la técnica empleada (*fuente:* Analytical Abstracts: 1980-2005).

Como se ha comentado con anterioridad, el desarrollo de la Quimiometría es una de las principales razones para el despegue definitivo de los métodos cuantitativos basados en el empleo de técnicas vibracionales. Si se comparan la Figura 12 con la anterior puede apreciarse un efecto sinérgico entre la evolución de los métodos quimiométricos y el aumento de las aplicaciones cuantitativas de la espectrometría vibracional.

Las herramientas quimiométricas más empleadas para el análisis de los datos obtenidos mediante técnicas vibracionales son el análisis de componentes principales (PCA) [*Mark,* 1989], mínimos cuadrados parciales (PLS) [*Martens y Naes,* 1991] y las redes neuronales (NN) [*Haykin*, 1999]. Estas herramientas han sido utilizadas tanto para la evaluación de la composición como para el análisis de las propiedades físicas.

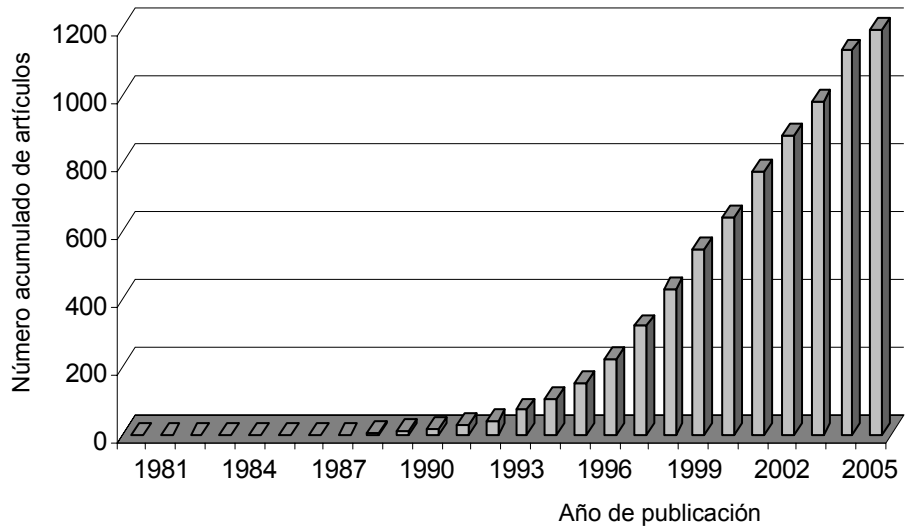

Figura 12. Evolución de la literatura publicada basada en estudios quimiométricos empleando la espectroscopia vibracional.

Gracias a estos avances en el campo de la Quimiometría, el número de aplicaciones NIR en los diferentes campos ha crecido enormemente en los últimos años [*McClure,* 1994].

Por otra parte, las ventajas aportadas por la combinación de análisis en flujo con técnicas vibracionales, como son la rápida monitorización del rango espectral elegido, posibilidad de análisis simultáneo de varios compuestos, reducción de reactivos y disolventes, menor contacto del operario con sustancias tóxicas,… hacen que este tipo de sistemas sean particularmente útiles para el control de calidad de productos manufacturados [*Garrigues y de la Guardia,* 2002].

En relación a los diferentes campos de aplicación de los métodos vibracionales, en la Figura 13 puede verse claramente que los sectores alimentario, industrial-farmacéutico y medioambiental son aquellos en los que más ampliamente se han aplicado las técnicas vibracionales como métodos para el control de calidad [*Olinga y Siesler*, 2000]. Este hecho no es sorprendente ya que la falta de sensibilidad de estas metodologías las

hace apropiadas para este tipo de análisis en los que el analito es un componente mayoritario. Por otra parte, la combinación de métodos quimiométricos y vibracionales constituye una potente herramienta en la determinación simultánea de diferentes parámetros físicos y químicos en productos alimentarios [*Downey,* 1998, *Reeves y Zapf*, 1998, *Wilson y Tapp*, 1999] o industriales [*Estienne et al., 2000*, *Hidajat y Chong,* 2000].

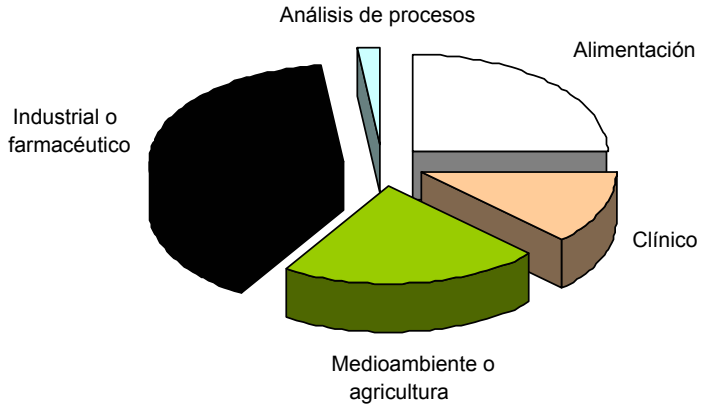

Figura 13. Distribución de la literatura publicada sobre los métodos cuantitativos basados en el empleo de técnicas vibracionales en función del campo de aplicación.

Recientemente, se ha generalizado el empleo de métodos vibracionales en el control de calidad de productos tan ampliamente utilizados como son los pesticidas y productos fitosanitarios. Debido a sus características físico-químicas y a la concentración de la mayoría de ellos en las formulaciones comerciales, la espectrometría vibracional es una técnica adecuada para su análisis cuantitativo, reduciendo el tiempo de análisis y consumo de disolventes en comparación con los métodos convencionales basados en separaciones cromatográficas [*Armenta et al.,* 2005].

En este sentido, los precedentes que existen en la bibliografía del análisis de pesticidas en formulados por espectrometría vibracional están basados en la medida del área o la altura de una banda de absorción en la región del infrarrojo medio (ver Tabla 2) o de una banda de emisión del espectro Raman (ver Tabla 3) tras la extracción del principio activo con un

disolvente apropiado que, en la mayoría de los casos, es de tipo organoclorado o bien la medida directa directa sobre muestras líquidas.

Tabla 2. Artículos publicados en los últimos años basados en determinaciones cuantitativas de pesticidas en formulaciones comerciales mediante espectrometría FT-MIR.

Analito	LOD	% Recuperación	% RSD	Frecuencia de análisis (h^{-1})	Disolvente	Generación de residuos	Referencia
Artemisinin		97.66	0.98		CCl_4		Liu et al., 1994
Carbaril	1.6 µg ml^{-1}			53	CH_2Cl_2		Gallignani et al., 1993
Clorpirifos-etil					TMP[a] Solvesso 100[b1] Solvesso 150[b2]		Almond y Knowles, 1999
Clorsulfuron	6 µg g^{-1}		0.3	60	$CHCl_3$		Quintás et al., 2003(a)
Cipermetrina		90-97			$CHCl_3$		Sharma et al., 1997
Deltametrina		90-97			$CHCl_3$		Sharma et al., 1997
Endosulfan	150 µg g^{-1}	101 ± 1	1.4	60	$CHCl_3$	2.7 ml	Quintás et al., 2005
Fenoxicarb	14 µg g^{-1}		0.12		$CHCl_3$		Quintás et al., 2003(b)
Fenvalerato		93-99			$CHCl_3$		Gupta et al., 1996
Fluometuron	6.5 µg g^{-1}	99 ± 2	1.6		$CHCl_3$	7 ml	Quintás et al., 2002
Folpet	17 µg g^{-1} 17 µg g^{-1}	100 ± 1	1.1 2.0	60	$CHCl_3$ $CHCl_3$	2.7 ml	Quintás et al., 2003(c)
Imidacloprid	9 µg g^{-1} 6 µg g^{-1}		0.3 0.6	60	$CHCl_3$ $CHCl_3$	2.5 ml	Quintás et al., 2004(a)
Malation	12 µg ml^{-1}		0.4		$CHCl_3$	2 ml	Quintás et al., 2004(b)
Metalaxil	16 µg g^{-1} 16 µg g^{-1}	100 ± 1	1.9 2.6	60	$CHCl_3$ $CHCl_3$	2.7 ml	Quintás et al., 2003(c)
Pirimicarb	13 µg g^{-1}	100 ± 1	0.2	60	$CHCl_3$	2.7 ml	Quintás et al., 2005
Tiram	785 µg		2.5				Cassella et al., 2000
Ziram	400 µg		6.4				Cassella et al., 2000
Ziram	55 µg	103 ± 2	6	17			Cassella et al., 2001

[a]. TMP: Trimetilpentano, [b] Disolventes aromáticos: [1] contenido de aromaticos > 98% (v/v), [2] contenido de aromaticos > 99% (v/v).

Tabla 3. Artículos publicados en los últimos años basados en determinaciones cuantitativas de pesticidas en formulaciones comerciales mediante espectrometría FT-Raman.

Analito	LOD	% RSD	Frecuencia de análisis (h^{-1})	Disolvente	Referencia
Clorpirifos-etil				TMP[a] Solvesso 100[b1] Solvesso 150[b2]	Almond y Knowles, 1999
Diazinon	0.1-0.4 M	0.1-7.8	-	xileno	Skoulika et al., 2000(a)
Fention	0.14 - 0.36 M	0.4 - 6.8	-	xileno	Skoulika et al., 1999
Malation	1.8 %p/p	4.5	18	$CHCl_3$	Quintás et al., 2003(d)
Metil-paration		0.1-6.8	-	xileno	Skoulika y Georgiou, 2000(b)
Metil-paration	1 ppm	4.1 1.4		metanol	Sato-Berru et al., 2004
Mepiquat	0.3 %p/p	2.7	40	agua	Quintás et al., 2004(c)

Como puede apreciarse en dichas tablas, la contribución de nuestro grupo de investigación al desarrollo de métodos simples, rápidos y medioambientalmente sostenibles para la determinación de ingredientes activos en formulaciones comerciales de pesticidas por espectrometría

vibracional ha sido considerable. Por otra parte, de los resultados de esta revisión bibliográfica se puede afirmar que no existen precedentes de determinaciones cuantitativas de pesticidas en formulados comerciales empleando técnicas vibracionales y medida directa sobre muestras sólidas, sin la necesidad de extraer el principio activo de la matriz mediante disolventes. Este tipo de medidas reducirían la manipulación de la muestra, el efecto negativo de los disolventes orgánicos sobre el medio ambiente y la generación de residuos, además las muestras podrían ser almacenadas para posteriores análisis. Estos métodos analíticos directos, sin tratamiento previo de las muestras, proporcionan una serie de ventajas como son un ahorro en el coste de reactivos, una mejora de las condiciones de seguridad e higiene en el trabajo y una reducción en los costes de gestión y tratamiento de los residuos.

RESUMEN

2. RESUMEN

La industria necesita disponer de procedimientos analíticos rápidos y fiables para controlar de forma eficiente los productos manufacturados, métodos que permitan la obtención de resultados de forma más rápida y económica, reduciendo la manipulación de la muestra, el consumo de reactivos y la generación de residuos, minimizando, de esta forma, el impacto negativo sobre el medioambiente. La mayoría de los Métodos Oficiales empleados habitualmente en el control de calidad de productos manufacturados están basados en separaciones cromatográficas. Estos procedimientos implican un elevado consumo de disolvente y una gran generación de residuos, así como una dilución previa de aquellas muestras en las que el analito se encuentra a niveles de porcentaje, implicando también un incremento del tiempo de análisis. En este sentido, la presente Tesis Doctoral propone diferentes aplicaciones de la espectrometría vibracional para el control de calidad de muestras comerciales de distintos sectores industriales (pesticidas y productos fitosanitarios, suplementos alimenticios o bebidas), como alternativa al uso de procedimientos cromatográficos.

Los productos analizados durante este trabajo presentan características físico-químicas muy diferentes: distinta composición, niveles de concentración de sustancia activa, tamaño de partícula, presentación del producto final,…

Con la intención de generalizar el uso de la espectrometría vibracional como herramienta analítica para el control de calidad en la industria se han propuesto métodos basados en diferentes modos de medida en los que se busca la reducción del tiempo de análisis, eliminación o reducción del consumo de reactivos y la generación de residuos y la facilidad para poder llevar a cabo una automatización. Estos modos de medida han sido seleccionados en función de sus propiedades intrínsecas y de las características físico-químicas de las muestras analizadas. En este sentido podemos dividir esta memoria de Tesis en los siguientes apartados:

a. Medidas de transmisión
b. Medidas de reflectancia total atenuada
c. Medidas de reflectancia difusa
d. Medidas fotoacústicas en el infrarrojo medio
e. Medidas de emisión Raman

3.a Medidas de transmisión

Los distintos métodos que se han propuesto para la determinación de analitos mediante medidas de transmisión pueden clasificarse en dos grupos, atendiendo a la manipulación que se requiere realizar sobre la muestra:

- Los basados en medidas directas sobre muestras sólidas empleando la técnica de pastillas de KBr en la región MIR.

- Los que contemplan la extracción del analito con un disolvente adecuado y posterior medida del extracto. En este sentido se ha considerado la etapa de extracción *off-line* o en continuo, pudiendo realizarse el registro de los espectros en régimen estricto (*batch*, flujo parado) o en flujo continuo.

En la Tabla 4 se enumeran las aplicaciones que se integran en este apartado, indicando sus principales características.

Tabla 4. Resumen de los diferentes métodos propuestos para la determinación de analitos mediante medidas de transmisión en la región del infrarrojo.

		Analito	Comentario
Medidas directas			
MIR Fase sólida		Mancozeb	Pastillas de KBr
Extracción con disolvente			
MIR			
Determinación individual	*Batch*	Buprofezin, Diuron	Extracción con cloroformo, medida del espectro en flujo parado
	On-line	Buprofezin, Diuron	Extracción con cloroformo, medida del espectro en continuo
Determinación simultánea	*Batch*	Cypermethrin y clorpirifos	Extracción con cloroformo, medida del espectro en flujo parado
	On-line	Aspartamo y acesulfamo	Extracción secuencial con diferentes disolventes
NIR			
Determinación individual	*Batch*	Iprodione	Extracción con acetonitrilo, medida del espectro en flujo parado
	On-line	Buprofezin	Extracción con acetonitrilo, medida del espectro en continuo

La instrumentación utilizada en el caso de las determinaciones cuantitativas en el MIR fue un espectrómetro FT-MIR Nicolet Magna 750, un Bruker Tensor 27 y un Mattson Research RS1 equipados con un detector de sulfato de triglicina deuterada (DTGS) y sulfato de triglicina deuterada dopado con lantano (Bruker Tensor 27), un divisor de haz de KBr o Ge/KBr (Mattson Research RS1) y una celda de flujo con ventanas de seleniuro de zinc (ZnSe) para el caso de medidas en disolución. Para aquellos procedimientos que utilizan la región NIR se utilizó un espectrómetro FT-NIR Bruker MPA equipado con un detector de arseniuro de Indio y Galio (InGaAs), un divisor de haz de cuarzo y una celda del mismo material de 5 mm de paso óptico.

Las medidas directas sobre muestras sólidas fueron aplicadas a la determinación de mancozeb en formulaciones comerciales. Este pesticida sintético, de la familia de los ditiocarbamatos, es insoluble en la mayoría de disolventes orgánicos e inorgánicos, de forma que es imposible realizar una extracción o disolución sin su destrucción. Por tanto, se hace necesario una estrategia de medida en fase sólida. Debido a que con la técnica de pastillas de KBr se obtienen espesores de pastilla (esto es, pasos ópticos) muy poco reproducibles es necesario emplear un patrón interno para realizar análisis cuantitativos. Se han considerado diferentes opciones para seleccionar el compuesto que va a ser utilizado como estándar interno. La primera de ellas consiste en la adición a la muestra de tiocianato potásico para ser utilizado como patrón interno, ya que este compuesto presenta un reducido número de bandas de absorción, evitando así la interferencia con las propias del analito. En la segunda opción se ha considerado la utilización de un compuesto presente en la muestra, ferrocianuro férrico, como referencia interna, y el empleo del método de adición estándar como estrategia de calibración. De esta forma se evita añadir un compuesto sobre la muestra que pueda alterar las características de ésta, pero sería necesario realizar una adición estándar para el análisis de cada una de las formulaciones comerciales.

La última opción considerada, que puede aplicarse en aquellos casos en los que el mancozeb esté acompañado por otro ingrediente activo que

sea fácilmente determinable, plantea el empleo de este otro componente de la muestra como patrón interno. Para nuestro caso, se analizará previamente en la muestra el contenido de este segundo componente mediante una extracción con cloroformo y posterior medida IR de la disolución. La estrategia aplicada está basada en la utilización de una calibración multivariada (mínimos cuadrados parciales, PLS) y emplea un set de calibración formado por pastillas de KBr con diferentes relaciones entre mancozeb, cimoxanilo (el segundo componente activo de la muestra que va a ser utilizado como patrón interno) y caolín (un coadyuvante típico en este tipo de formulaciones sólidas). Para predecir la concentración del primero en la muestra problema se utiliza el cociente entre las bandas propias del mancozeb y las del cimoxanilo.

Esta metodología, a pesar de reducir el empleo de reactivos y la generación de residuos, incluso el tiempo de análisis con respecto a otros métodos para el análisis de mancozeb [*Lo et al.,* 1996], plantea problemas derivados del tedioso y complicado tratamiento de la muestra. La preparación de las pastillas de KBr y las dificultades en la calibración hacen que la utilidad de esta metodología sea muy reducida, siendo aplicable solo en casos extremos donde la extracción del analito no sea posible.

Para reducir dicho tratamiento de la muestra, y por tanto mejorar la repetibilidad de las medidas y aumentar la productividad en el laboratorio, se desarrollaron métodos basados en la extracción del analito para posterior medida en disolución. El desarrollo y puesta a punto de estos procedimientos, fácilmente automatizables, implica en su estudio la realización de varias etapas:

- *Selección de las condiciones más adecuadas de extracción.*

  En el caso de realizar una extracción *off-line* los parámetros estudiados para trabajar con las condiciones más adecuadas han sido el modo (mecánica o por ultrasonidos) y el tiempo de agitación. Para ello, se ha determinado el grado de recuperación de los diferentes analitos de las muestras en función de estos factores.

A modo de ejemplo, en la Figura 14, se indican los resultados obtenidos para la comparación de ambos modos de agitación en la extracción de buprofezin, un pesticida formulado como polvo mojable. Como puede apreciarse, la agitación por ultrasonidos es más efectiva proporcionando una mayor extracción en un menor tiempo. En la figura se observa una disminución en el porcentaje de recuperación del buprofezin cuando el tiempo de agitación por ultrasonidos es superior a 10 minutos, probablemente debido a que la generación de radicales libres en el sistema pueda afectar a la estabilidad del pesticida. Es por ello que, para este tipo de muestra, se seleccionaron 10 minutos como tiempo de agitación.

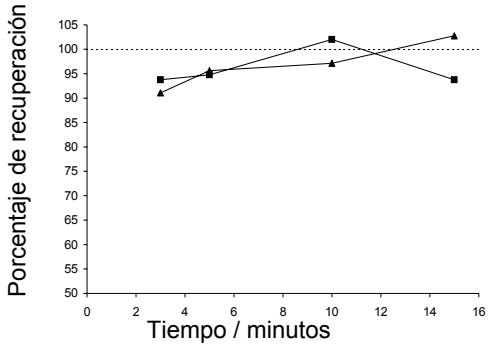

Figura 14. Porcentaje de recuperación del pesticida buprofezin en función del tiempo y del modo de agitación, para 30 mg de muestra que contiene un 25 % p/p de Buprofezin y empleando cloroformo como disolvente. (-▲-, agitación mecánica, -■- agitación por ultrasonidos). (Fuente: Analytica Chimica Acta, **468** (2002) 81-90).

Por otra parte, también se han estudiado extracciones en línea que, además de reducir el contacto del operador con productos tóxicos, incrementan el grado de automatización del procedimiento y reducen el consumo de reactivos. Se han utilizado diferentes montajes experimentales dependiendo del tipo de presentación del formulado comercial, las características físico-químicas del analito y del tratamiento al que deben someterse las muestras.

En la Figura 15 pueden verse, a modo de ejemplo, dos de los montajes empleados para el análisis de pesticidas por espectrometría vibracional en la región NIR y MIR, en los que se integra una unidad de extracción y una unidad de filtración. De esta forma se logra una

reducción de la manipulación de la muestra y del contacto del operador con sustancia tóxicas ya que el disolvente o el extracto de la muestra es introducido en el sistema con la ayuda de bombas peristálticas. Estos sistemas pueden ser utilizados para la medida en modo de flujo parado, o en flujo continuo, introduciendo de forma secuencial patrones y muestras en la celda de medida y registrando los correspondientes espectros en flujo parado para mejorar la repetibilidad de las medidas.

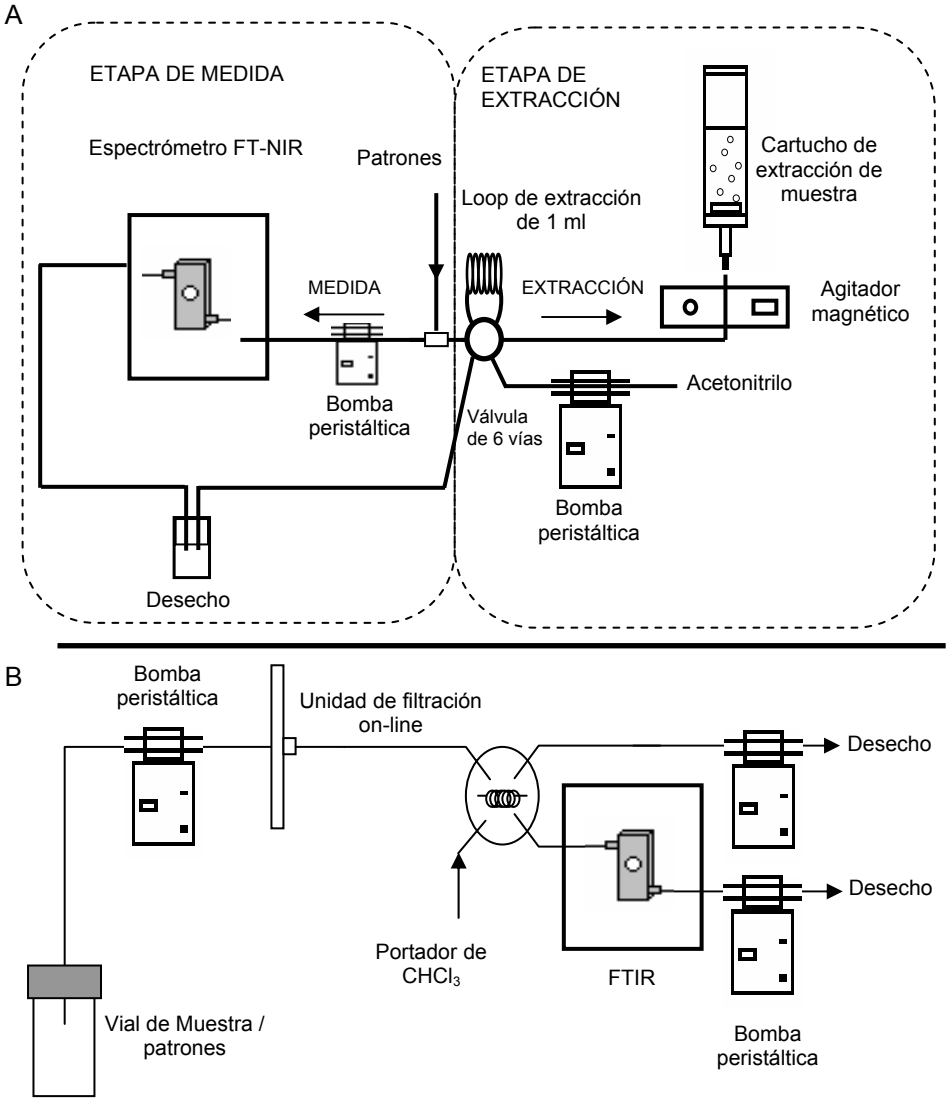

Figura 15. Montajes utilizados para la extracción *on-line* en a) la determinación de buprofezin en pesticidas comerciales mediante espectrometría NIR y b) la determinación de diuron en formulaciones mediante espectroscopia MIR. (Fuente: a) Journal of near infrared spectroscopy, **13** (2005) 161-168, y b) Journal of agricultural and food chemistry, **53** (2005) 5842-5847).

Además se diseñó un sistema para el análisis en flujo de varios analitos extraídos de forma secuencial mediante el empleo de diferentes disolventes y/o mezclas de ellos. Estas estrategias de extracción *on-line* se compararon con los resultados obtenidos cuando el tratamiento de la muestra se realizaba *off-line*. Los distintos enfoques para el tratamiento de la muestra que se indican en la Figura 16, proporcionaron extracciones cuantitativas permitiendo la determinación simultánea de aspartamo y acesulfamo-K en edulcorantes de mesa, minimizando la manipulación de la muestra y el tiempo de análisis y, lo más importante, debido a la extracción secuencial se reducen las interferencias espectrales mutuas entre ambos analitos.

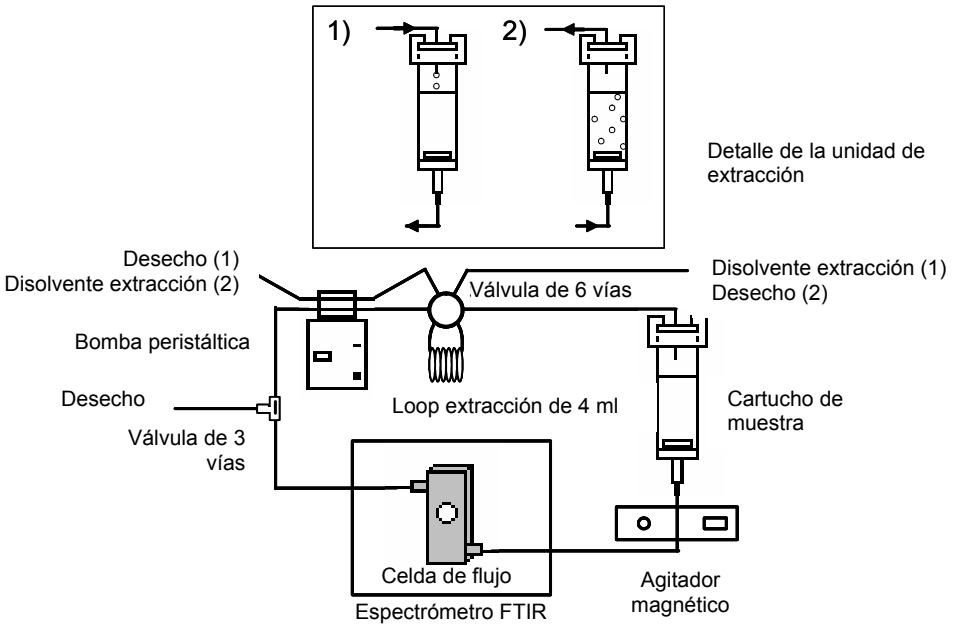

Figura 16. Sistema de extracción en línea diseñado para la determinación de aspartamo y acesulfamo-K en edulcorantes de mesa mediante espectrometría MIR. Detalle: Diferentes estrategias de extracción del analito basadas en la circulación del disolvente

a través del sistema o bien en la introducción del disolvente en el cartucho de extracción y recirculación de aire para favorecer el proceso de extracción (Fuente: Journal of Agricultural and Food Chemistry, 52 (2004) 7799).

- *Estudio de los parámetros instrumentales.*

La calidad de los espectrómetros IR por transformada de Fourier está fuertemente influenciada por variables instrumentales como la resolución nominal, el número de barridos acumulados por espectro, la velocidad del espejo y el factor de *zero filling* (que establece el número de puntos en el espectro final).

La resolución nominal afecta a la definición de las bandas de absorción, es decir, una mejor resolución nominal nos va a permitir diferenciar bandas que estén muy próximas lo que, en definitiva, mejora la selectividad de las medidas. Sin embargo esto implica un aumento del ruido y del tiempo necesario para la adquisición del espectro. Debido a limitaciones instrumentales, los valores de resolución nominal se encuentran restringidos a un determinado intervalo que depende del equipo empleado.

El aumento del número acumulado de barridos del interferómetro que se promedian para la obtención del espectro final mejora la relación señal/ruido, permitiendo una mayor precisión de las medidas. Sin embargo, el aumento del número de barridos acumulados implica también un incremento del tiempo de adquisición del espectro, con lo que se reduce la frecuencia de medida. Si este no es un factor especialmente significativo cuando se considera el tiempo total requerido para la realización de un análisis, incluyendo las etapas de preparación de la muestra, si que es especialmente importante en el caso de medidas *on-line* en las que la velocidad de adquisición de los espectros es un factor decisivo.

La velocidad del espejo móvil del interferómetro es otro de los parámetros que afectan a la calidad del espectro. Una mayor velocidad permite obtener un mayor número de barridos en un tiempo determinado pero supone un incremento del ruido del espectro, de

forma que el valor más adecuado viene determinado por el tipo de detector utilizado.

Otro factor que puede mejorar la calidad espectral es la aplicación de la función de *zero filling*. Esta función determina el número de puntos de relleno que son introducidos entre los datos medidos antes de realizar la transformada de Fourier y consigue una mejora de la definición del espectro sin modificar la resolución nominal verdadera con la que se efectuó la adquisición de las medidas. Sin embargo, la aplicación de esta función implica un mayor tiempo durante el cálculo de la transformada, lo que afecta al tiempo de adquisición.

Para obtener, en cada caso, las condiciones instrumentales más adecuadas para las determinaciones cuantitativas, tanto en el MIR como en el NIR, se ha estudiado el efecto de la resolución nominal y el número de barridos acumulados por espectro sobre el espectro IR.

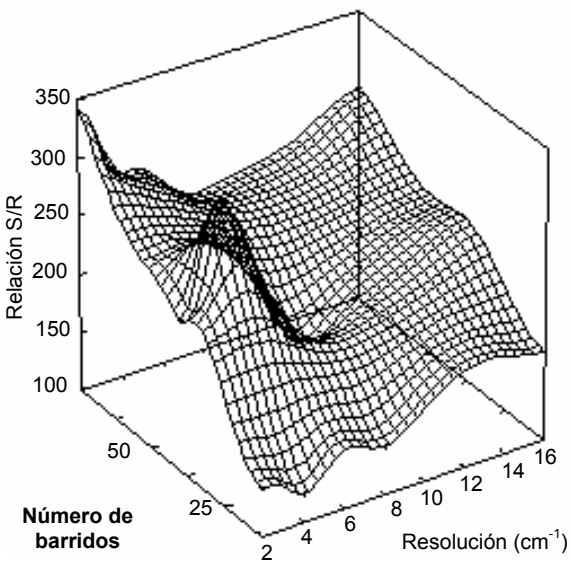

Figura 17. Efecto de la resolución nominal y el número acumulado de scans sobre la relación señal ruido de un espectro de patrón de Clorpirifos de 5.18 mg g^{-1} de concentración.

Las condiciones más adecuadas para los análisis por espectrometría MIR fueron 4 cm^{-1} de resolución nominal y 25 barridos acumulados por

espectro (ver Figura 17), que permitían una sensibilidad y una frecuencia de medida aceptables.

Adicionalmente se realizó, en la región NIR, un estudio más detallado de cómo afectan todas las variables instrumentales comentadas a las características analíticas del método desarrollado. Para ello se trabajó con un programa comercial de tratamiento estadístico Minitab Release 14 y mediante un diseño experimental basado en una primera etapa de *screening* mediante un diseño factorial fraccionado y una segunda etapa de búsqueda del valor óptimo mediante un diseño de compuesto central (*central composite design*) y definiendo una función de optimización en la que se le asignará distinto peso específico a propiedades analíticas tales como precisión, exactitud, sensibilidad, productividad,… Como puede verse en la Figura 18 los parámetros que afectan significativamente dependen de la función escogida como respuesta, por tanto, para seleccionar unos valores óptimos de resolución nominal, número de barridos, velocidad del espejo móvil y zero filling es necesario estudiar cuál es la función respuesta mas apropiada a nuestras exigencias.

Una de las conclusiones más destacables de este estudio de optimización es que las condiciones instrumentales más adecuadas son completamente diferentes de aquellas obtenidas en los estudios para el MIR. Un número de barridos relativamente bajo significa un aumento de la frecuencia de análisis debido a la reducción en el tiempo de medida, aunque se obtiene una relación señal ruido más pobre. Una resolución nominal de 16 cm^{-1} aumenta la frecuencia de análisis y la relación señal ruido sin reducir excesivamente la sensibilidad del método, debido a que en esta región las bandas de absorción son relativamente anchas y no se ven tan afectadas por la definición espectral. El factor de zero filling no afecta considerablemente a la mayoría de características analíticas del procedimiento y la velocidad del espejo interesa que sea relativamente elevada ya que logrará reducir el tiempo de análisis sin afectar de forma significativa en otros parámetros como sensibilidad, exactitud o límite de detección.

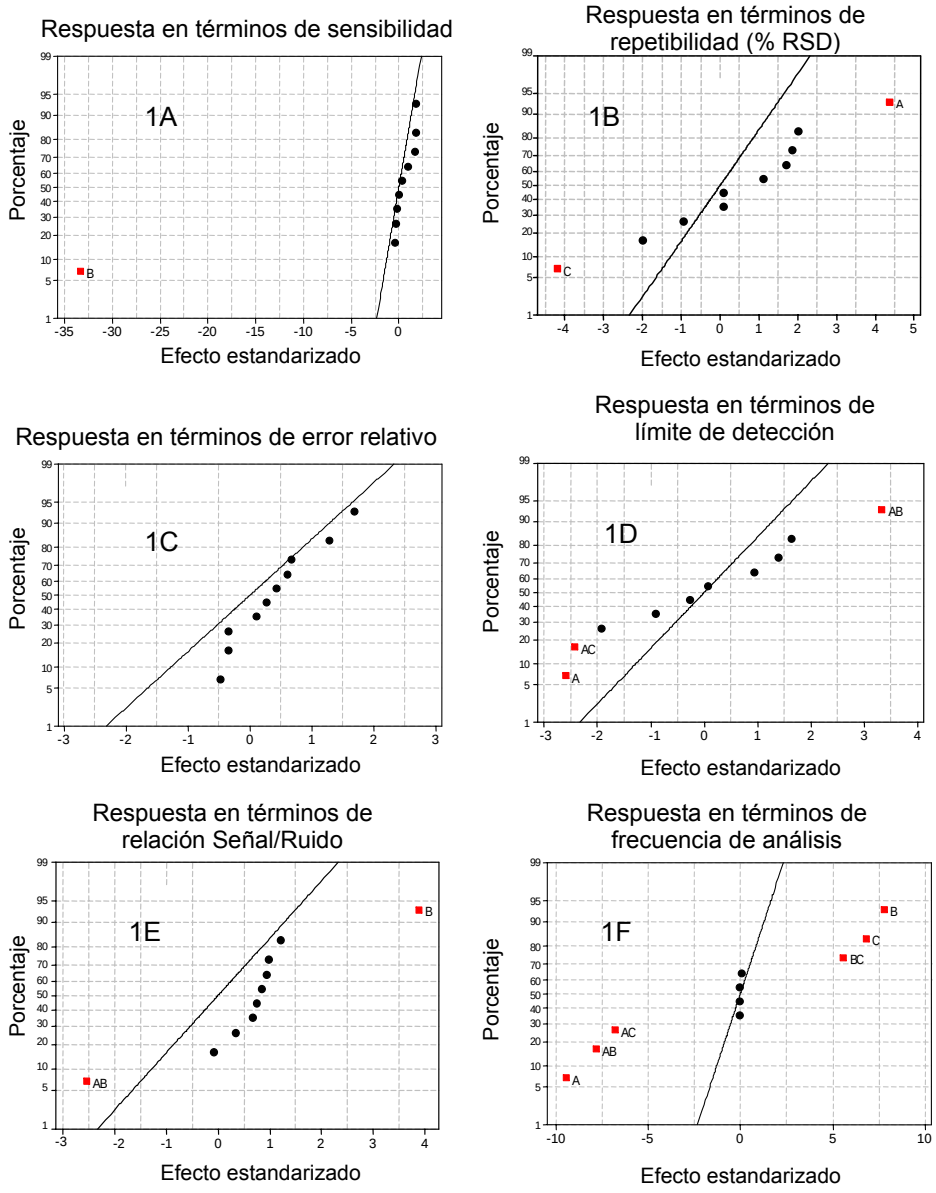

Figura 18. Gráfica de probabilidad normal para el diseño factorial completo 2^4 en el studio de diferentes funciones respuesta para la determinación de FT-NIR de iprodiona en formulados comerciales. □, efecto significativo; •, efecto no significativo. Factores: A= número acumulado de barridos, B= resolución nominal, C= velocidad del espejo móvil del interferómetro, D= factor de *zero filling*.

- *Estudio de las condiciones de medida.*

Otro aspecto a tener en cuenta en la puesta a punto de un método basado en técnicas vibracionales son las condiciones seleccionadas para la medida en los espectros, de forma que proporcionen características analíticas adecuadas para la determinación cuantitativa. Se ha estudiado el empleo de medidas de altura y/o área de las bandas de absorción características de los analitos objeto de estudio, empleando distintas correcciones de línea base con el objeto de corregir posibles desplazamientos del espectro o solapamientos espectrales debido a la interferencia de otros compuestos o sustancias presentes. En la Tabla 5 se muestra, a modo de ejemplo, los resultados obtenidos en el estudio llevado a cabo para la determinación simultánea de cipermetrina y clorpirifos en el IR medio utilizando cloroformo como disolvente.

Tabla 5. Características analíticas de la determinación FT-MIR de cipermetrina y clorpirifos utilizando diferentes bandas y criterios de línea base.

Modo de medida	**Longitud de onda (cm^{-1})**	Corrección de línea base	$a \pm s_a$	$b \pm s_b$	R^2	% R.S.D.	L.O.D. (% p/p)
Cipermetrina:			curva de calibración (y=a+b C (mg g-1))				
Altura	1742	2000	0.0002 ± 0.0001	0.00953 ± 0.00004	0.9993	0.3	0.6
Área	1747-1737	2000	0.0017 ± 0.0008	0.1007 ± 0.0008	0.9998	0.4	0.7
Altura	1587	1650	0.00031 ± 0.00009	0.00926 ± 0.00003	0.9999	0.9	0.3
Área	1592-1982	1650	0.002 ± 0.001	0.082 ± 0.001	0.9997	0.8	0.5
Altura	1488	1530	0.0003 ± 0.0002	0.01514 ± 0.00005	0.9998	1.0	0.3
Área	1493-1483	1530	0.000 ± 0.002	0.147 ± 0.002	0.9995	1.1	0.6
Altura	1076	1097-1061	0.0003 ± 0.0002	0.00558 ± 0.00008	0.997	1.2	1.4
Área	1081-1071	1097-1061	0.000 ± 0.002	0.070 ± 0.002	0.998	0.9	1.0
Clorpirifos:			curva de calibración (y=a+b C (mg g-1))				
Área	**1554-1544**	1650	0.002 ± 0.001	0.0527 ± 0.0004	0.9993	0.10	0.2
Altura	**1549**	1650	0.0009 ± 0.0002	0.00639 ± 0.00007	0.9993	0.2	0.4
Altura	**1549**	1650-1527	0.0004 ± 0.0002	0.00600 ± 0.00004	0.9992	0.2	0.5
Altura	1412	2000	0.0006 ± 0.0004	0.0290 ± 0.0001	0.9996	0.3	0.2
Área	1417-1407	2000	0.009 ± 0.005	0.270 ± 0.002	0.9995	0.4	0.9
Altura	968	2000	0.0008 ± 0.0003	0.01839 ± 0.00009	0.9996	0.4	0.9
Área	973-963	2000	0.007 ± 0.004	0.207 ± 0.002	0.9994	0.6	0.8

La selección de las condiciones de medida más adecuadas se establece en términos de sensibilidad, límite de detección y precisión, obviamente sin dejar de lado la exactitud. Para la cipermetrina se trabajó con la medida del área de la banda de absorción entre 1747 y 1737 cm^{-1} corregida con una línea base a 2000 cm^{-1}, que proporcionaba una sensibilidad y un límite de detección adecuados y una excelente repetibilidad. Para el caso del clorpirifos se seleccionó la medida de la altura de la banda de absorción situada en 1549 cm^{-1}, corregida en este caso con una línea base situada en 1650 cm^{-1} que evitaba solapamientos con las bandas de absorción típicas de la cipermetrina y que proporcionaba características analíticas adecuadas para su determinación en formulados comerciales.

- *Validación de los procedimientos desarrollados.*

El último de los pasos realizados en todos los procedimientos desarrollados fue la validación de los mismos en términos de exactitud, precisión y límites de detección y determinación.

La exactitud se comprobó mediante comparación de los resultados obtenidos por las técnicas vibracionales con los obtenidos mediante el empleo de métodos de referencia basados, en la mayoría de los casos, en separaciones cromatográficas. Estos métodos de referencia han sido los recomendados por organismos internacionales [CIPAC Methods, AOAC]. Cuando no existían métodos de referencia, se han desarrollado a partir de la información de procedimientos empleados por otros autores para el análisis de estas moléculas en muestras de una naturaleza lo más similar posible. Como puede observarse en la Tabla 6, todos los métodos proporcionaron resultados estadísticamente comparables con los obtenidos por el método de referencia y que cumpliría con las especificaciones legales para este tipo de productos.

Otra forma para determinar la exactitud de los procedimientos ha sido mediante ensayos de recuperación y la aplicación del método de la adición estándar, que se ha utilizado para calcular el porcentaje de recuperación de un analito adicionado sobre la muestra. Se recomienda utilizar este

procedimiento siempre que no sea posible reproducir la matriz en la que se encuentra presente el analito. La recuperación media obtenida en todos los casos está dentro del intervalo recomendado por *CIPAC* [*CIPAC Guidelines*], para este tipo de análisis y que se indican a continuación.

% p/p analito	% recuperación
>10	98.0 – 102.0
1 – 10	97.0 – 103.0
>1	95.0 – 105.0

Tabla 6. Resumen de los resultados obtenidos en el análisis de formulaciones comerciales mediante procedimientos vibracionales comparados con los obtenidos mediante los métodos de referencia.

Analito	Estrategia	% p/p métodos vibracionales	Valores de referencia	% Error
Buprofezin	FIA-FT MIR	25.7 ± 0.5	25.0*	2.7
	MIR Flujo parado	25.5 ± 0.2	25.0*	2.0
Diuron	FIA-FT MIR	80.8 ± 0.8	82.7 ± 0.3	2.3
		84 ± 2	82.6 ± 0.4	1.7
		84 ± 2	83.0 ± 0.4	1.2
		42 ± 2	40.3 ± 0.5	4.2
		20.9 ± 0.4	20.5 ± 0.6	2.0
	MIR Flujo parado	83.1 ± 0.3	82.7 ± 0.3	0.5
		82.6 ± 0.5	82.6 ± 0.4	0.0
		83.0 ± 0.7	83.0 ± 0.4	0.0
		40.1 ± 0.6	40.3 ± 0.5	-0.5
		20.8 ± 0.5	20.5 ± 0.6	1.5
Cipermetrina	MIR Flujo parado	12.2 ± 0.1	12.1 ± 0.1	0.82
		2.08 ± 0.07	2.10 ± 0.05	-0.9
		4.32 ± 0.05	4.35 ± 0.04	-0.69
Clorpirifos	MIR Flujo parado	46.4 ± 0.8	46.2 ± 0.2	0.4
		50.3 ± 0.5	50.2 ± 0.1	0.20
		37.6 ± 0.8	37.2 ± 0.5	1.08
		45.1 ± 0.2	45.3 ± 0.3	-0.44
Aspartamo	FIA-FT MIR	11.83 ± 0.08	11.88 ± 0.02	-0.4
		38.4 ± 0.2	38.5 ± 0.2	-0.3
		38.70 ± 0.10	38.7 ± 0.2	-0.03
Acesulfamo-K	FIA-FT MIR	11.74 ± 0.14	11.71 ± 0.02	0.3
Buprofezin	FIA-FT NIR	26.80 ± 0.07	26.72 ± 0.16	0.3
		26.79 ± 0.05	26.86 ± 0.06	-0.3
		26.78 ± 0.04	26.70 ± 0.16	0.3
		25.41 ± 0.07	25.50 ± 0.10	-0.4

* Valores suministrados por el fabricante.

La incertidumbre de los resultados analíticos, expresada como desviación estándar relativa, ha sido comparada con los límites máximos que, según *CIPAC* [*CIPAC Guidelines*], deben reflejar los resultados analíticos de un procedimiento desarrollado para el análisis de

formulaciones de pesticidas, y que se calcula mediante la ecuación de Horwitz.

$$RSD < 2^{(1-0.5\ \log C)}\ 0.67$$

Así, para aceptar un método analítico la desviación estándar relativa en la medida de cinco muestras, debe ser menor que la calculada con dicha ecuación. Debido a la reducción del tratamiento previo de la muestra y el elevado grado de automatización, la reproducibilidad obtenida fue en todos los casos, menor que la exigida, cumpliendo con la normativa dictada por este organismo.

Los límites de detección fueron evaluados según el método descrito por la IUPAC [*Corley*, 2003], por el cual:

$$LOD = \frac{k \quad s_b}{\text{pendiente}}$$

donde k=3, proporcionando un nivel de probabilidad del 99.86 %, y s_b es la desviación estándar de cinco medidas de un blanco. Para el límite de cuantificación se aplica el mismo criterio pero considerando k=10.

La Tabla 7 muestra los límites de detección y cuantificación obtenidos en los métodos desarrollados, siendo en todos los casos aceptables para el orden de concentración en el que se encontraba el analito.

Tabla 7. Resumen de los límites de detección obtenidos en los métodos desarrollados utilizando el criterio de la IUPAC.

Analito	Estrategia	LOD (% p/p)	LOQ (% p/p)	% p/p analito
Buprofezin	FIA-FT MIR	0.12	0.4	~25
	MIR Flujo parado	<0.1	0.3	
Diuron	FIA-FT MIR	0.7	2	20-80
	MIR Flujo parado	0.8	3	
Cipermetrrina	MIR Flujo parado	0.7	2	2-12
Clorpirifos	MIR Flujo parado	0.4	1.3	37-50
Aspartamo	FIA-FT MIR	0.09	0.3	1139
Acesulfamo-K	FIA-FT MIR	0.9	3	~11
Buprofezin	FIA-FT NIR	0.012	0.04	~25

Con lo comentado anteriormente, puede concluirse diciendo que los métodos basados en la extracción del analito mediante el uso de un disolvente apropiado, o mezcla de ellos, y posterior medida del extracto en

la región MIR o NIR reduce la cantidad de disolvente empleado (menos de 3 ml de disolvente orgánico; cloroformo en el caso del MIR y acetonitrilo en el NIR). La frecuencia de análisis se incrementa de forma significativa frente a los métodos de referencia basados en separaciones cromatográficas. El único inconveniente que presentan estas metodologías para este tipo de análisis es el uso de disolventes orgánicos para extraer al principio activo. En unos casos el analito es insoluble en agua y en otros, el empleo de este disolvente no es compatible con el paso óptico utilizado en las celdas de medida. Teniendo en cuenta estas limitaciones y la dificultad observada en el desarrollo de métodos de análisis directos sobre sustancias sólidas mediante medidas de transmisión, se han desarrollados procedimientos basados en otras técnicas de medida para el análisis de disoluciones acuosas y muestras sólidas sin tratamientos previos (reduciendo de esta forma el impacto ambiental y los costes derivados del tratamiento de residuos y adquisición de reactivos).

3.b Medidas de reflectancia total atenuada

Como se ha comentado en la introducción, la espectroscopia vibracional es una técnica muy útil en la monitorización de reacciones donde es necesario un control de los parámetros de calidad tanto de los productos de partida utilizados como materia prima, de los productos finales, así como de las etapas intermedias del proceso. Un claro ejemplo es el caso de procesos biológicos en los que intervienen enzimas, para la producción de productos de interés como alcoholes, aminoácidos, antibióticos,… En estos casos una monitorización continua de la reacción controla de forma efectiva la calidad de los productos finales y permite corregir errores en tiempo real, alcanzándose el máximo rendimiento y efectividad, de forma que se minimicen las pérdidas económicas. En este sentido, en la fermentación de productos azucarados, la determinación *on-line* del alcohol generado proporciona un modo de controlar este tipo de reacción.

Se van a estudiar las condiciones que permitan, mediante el empleo de la espectrometría vibracional, controlar la evolución del proceso de fermentación del néctar de piña. Para ello, se seguirá el cambio que

experimenta la concentración de etanol y de los azúcares mayoritarios presentes en el medio. Debido a que el análisis de disoluciones acuosas en la región MIR mediante medidas de transmitancia requiere el uso de celdas con pasos ópticos muy reducidos (inferiores a 25 μm) la estrategia seleccionada para realizar este estudio se basa en el empleo de medidas de reflectancia total atenuada.

La instrumentación utilizada para realizar esta monitorización ha sido un espectrómetro FT-MIR Nicolet 460 Protege equipado con un detector DTGS, un divisor de haz de KBr y una celda ATR horizontal con un cristal de germanio (Ge).

Como primer paso en el desarrollo de este procedimiento de medidas ATR se llevó a cabo el estudio del efecto de los parámetros instrumentales sobre la relación señal ruido del espectro.

Como puede observarse en la Figura 19, la relación señal/ruido aumenta al incrementar la resolución nominal, pero de la misma forma aumenta también la desviación estándar de las medidas y se produce una pérdida de información espectral debido a la menor definición de las bandas, lo que afectará a la selectividad y, por ende, a la exactitud.

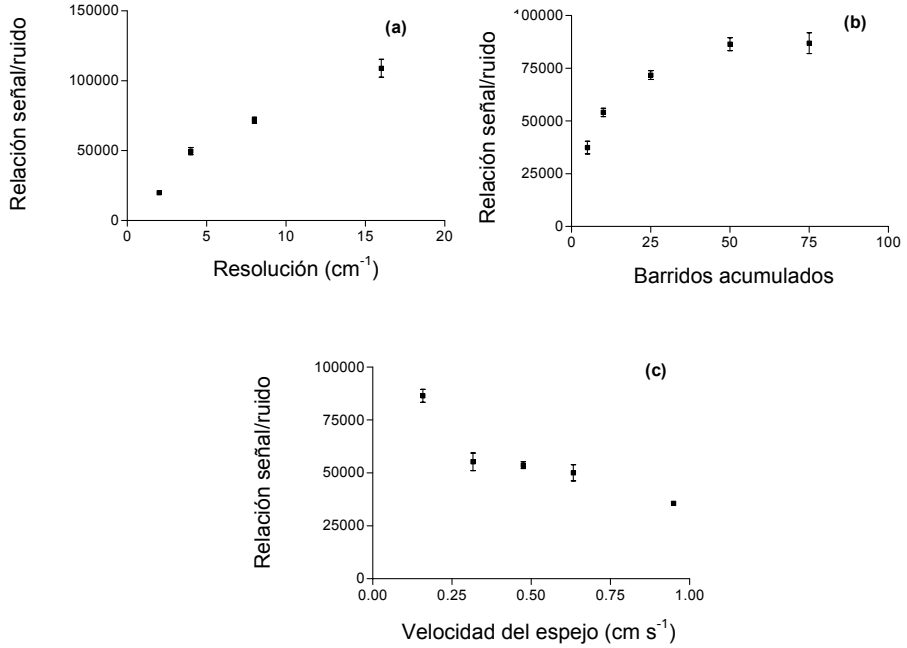

Figura 19. Efecto de las condiciones instrumentales sobre el espectro ATR de una disolución que contiene 8.6, 9.0, 11.2 y 16.3 % p/p de glucosa, fructosa, sacarosa y etanol respectivamente.

En el caso del número acumulado de barridos puede verse que se mejora la relación señal/ruido acumulando un número elevado de *scans,* pero de la misma forma se incrementa el tiempo de adquisición del espectro, pudiendo provocar la deposición de la materia sólida en suspensión (p.e. pulpa) presente en el zumo de piña fermentado. Por último, el aumento de la velocidad del espejo móvil implica una fuerte disminución de la relación señal ruido empeorando la calidad de los espectros.

En conclusión, de las experiencias realizadas y para la ejecución del resto del estudio se escogieron como valores adecuados una resolución nominal de 8 cm^{-1}, la acumulación de 50 *scans* por espectro y una velocidad del espejo móvil del interferómetro de 0.1581 cm s^{-1}.

Por otra parte, como puede apreciarse en la comparación de los espectros ATR de los analitos implicados en este estudio (Figura 20), existen fuertes solapamientos en las bandas de absorción, en la región comprendida entre 1100 y 900 cm^{-1} debidas a los enlaces C-O-C y C-O-H presentes en la molécula de los azúcares y del etanol. Debido a esto, la

determinación simultánea basada en el empleo de la calibración univariante a partir de patrones individuales de cada uno de los compuestos estudiados se hace inviable.

Dada la imposibilidad de realizar una calibración univariante que proporcione buenos resultados, se ensayaron diferentes estrategias basadas en la calibración multivariada por mínimos cuadrados parciales, (PLS), aplicándola a los espectros sin tratar y a la primera derivada de los mismos. El set de calibración esta basado en un diseño clásico de 4^2 estándares para los cuatro analitos de interés (glucosa, fructosa, sacarosa y etanol), a dos niveles de concentración.

Los mejores resultados obtenidos se muestran en la Tabla 8. Como puede observarse el empleo de la primera derivada mejora la selectividad lo que se traduce en una mejor capacidad predictiva del modelo.

Tabla 8. Estadísticos obtenidos para el modelo de calibración PLS, establecido mediante el empleo de la primera derivada de los espectros ATR-FTIR, y utilizado para en la monitorización del proceso de fermentación del néctar de piña.

Región	Línea base	Compuesto	Factores[a]	$R^{2,b}$	RMSEC[c]	Error promedio de validación[d] (%)
1531 - 907	-	Glucosa	7	0.9998	0.040	2.9
		Fructosa	8	0.9996	0.021	2.1
		Sacarosa	5	0.9999	0.063	2.6
		Etanol	6	0.9997	0.074	3.6

[a]. Número de variables latentes elegidas de forma que se obtiene el mínimo valor de *PRESS*.
[b]. Coeficiente de regresión.
[c]. *Root mean square* error de calibración para una validación cruzada.
[d]. Error relativo (%) promedio obtenido en la validación sin considerar el signo.

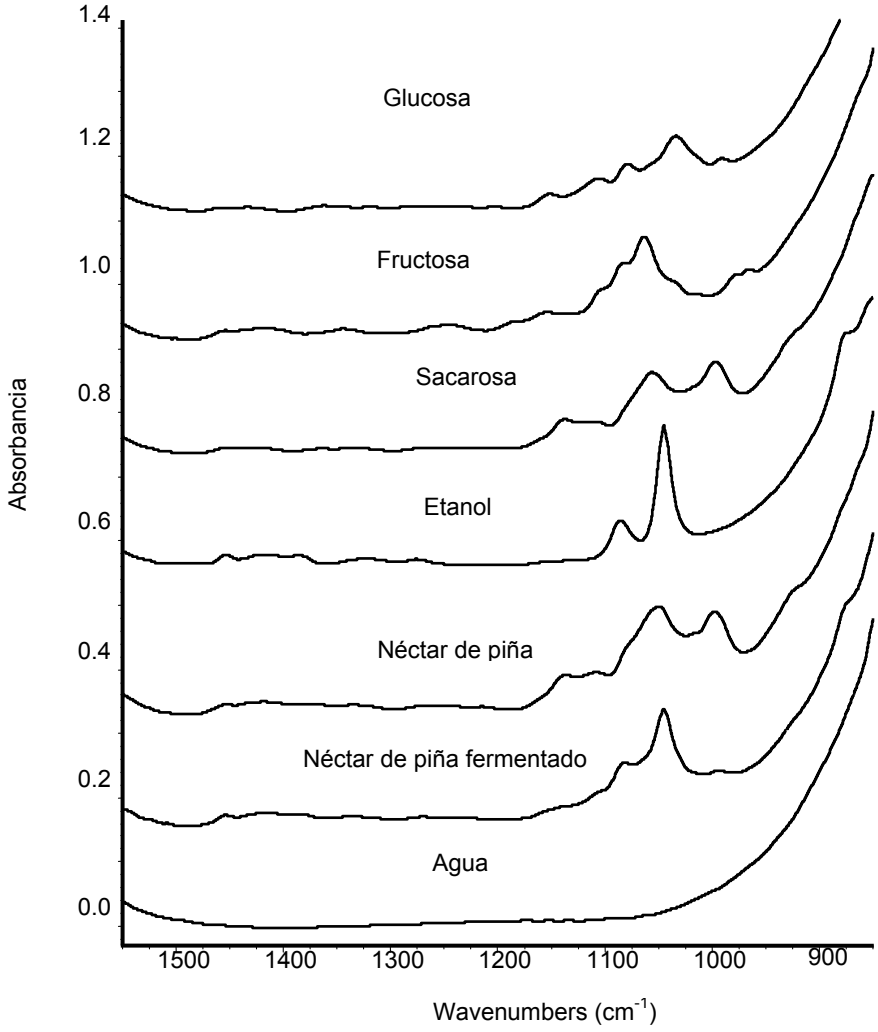

Figura 20. Espectros de reflectancia total atenuada de disoluciones de glucosa (6.0 %p/p), fructosa (8.0 % p/p), sacarosa (7.0 % p/p) y etanol (8.1 % p/p) y de néctar de piña antes y después de la fermentación. Los espectros se obtuvieron acumulando 50 *scans* y con una resolución nominal de 8 cm^{-1} empleando como referencia la celda vacía (Fuente: Analytica Chimica Acta 545 (2005) 102).

Adicionalmente, se evaluó la interferencia que provoca el alcohol producido durante la fermentación en la determinación de la glucosa, fructosa y sacarosa. De dicho estudio se concluye, tal como puede verse en la Figura 21, que el porcentaje de recuperación obtenido para los distintos azúcares analizados permanece en torno al 100% para concentraciones de etanol en la muestra (comprendidos entre el 0 y el 5 % p/p).

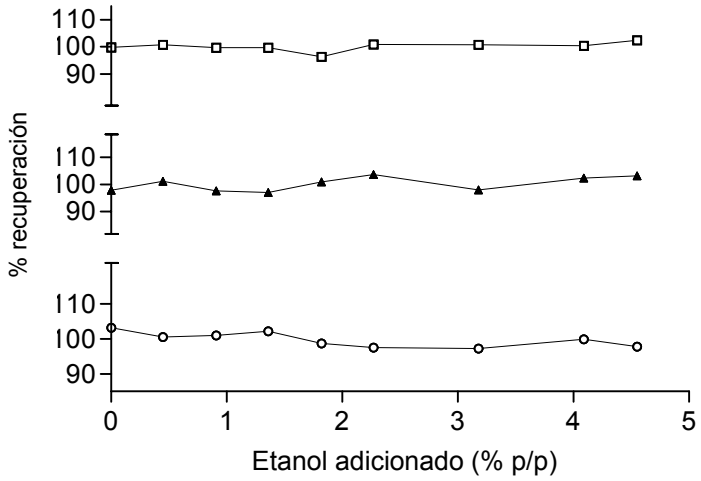

Figura 21. Efecto de la concentración del etanol sobre el porcentaje de recuperación de (▲) glucosa, (○) fructosa y (□) sacarosa, empleando la calibración PLS.

Por último, para evaluar la exactitud del procedimiento desarrollado, se compararon los resultados obtenidos para la determinación del alcohol generado en la fermentación de un néctar de piña esterilizado y uno sin tratar con los obtenidos mediante un método de referencia basado en la reacción del etanol con dicromato y posterior medida espectrofotométrica [*Fletcher y Van Staden*, 2003]. La Figura 22 muestra como para el néctar esterilizado la concentración de los cuatro analitos permanece invariable mientras que en el néctar que no ha sido tratado la concentración de etanol aumenta de forma significativa mientras que el porcentaje de sacarosa (el azúcar mayoritario inicialmente en el néctar) se reduce drásticamente. La concentración de glucosa y fructosa en un principio se reduce hasta

prácticamente cero para aumentar ligeramente debido a la hidrólisis de la sacarosa.

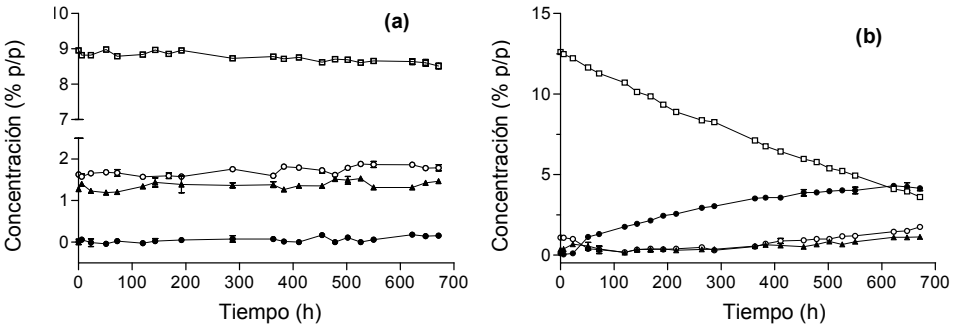

Figura 22. Monitorización mediante espectrometría ATR FTIR de la reacción de fermentación del néctar de piña esterilizado (a) y uno sin esterilizar (b). (▲) glucosa, (○) fructosa, (□) sacarosa, y (●) etanol.

El método desarrollado proporcionó resultados comparables con los obtenidos mediante el método de referencia para la determinación de etanol. Además, los valores de glucosa obtenidos se compararon con un método de referencia basado en ensayos enzimáticos [*Huggett y Nixon,* 1957], obteniéndose, también resultados comparables.

De este modo se verifica que la espectroscopia FTIR basada en medidas de reflectancia total atenuada, en combinación con la Quimiometría, resulta ser una herramienta muy útil para la monitorización de este tipo de procesos de fermentación.

Las ventajas que aporta el método desarrollado son su rapidez y su sencillez, ya que no requiere ningún tratamiento previo de la muestra. Además, el procedimiento puede ser fácilmente automatizado, con la posibilidad de realizar medidas *on-line*. Adicionalmente, no necesita reactivos de forma que también se elimina la generación de residuos, ofreciendo una alternativa medioambientalmente sostenible a los métodos tradicionales aportando soluciones al problema de la fuerte absorción del agua en la región MIR del espectro electromagnético.

3.c Medidas de reflectancia difusa

Ya se ha comentado que, las principales ventajas de la espectroscopia de reflectancia difusa se basan en su naturaleza no destructiva, en su capacidad de analizar productos en tiempo real, el bajo coste de mantenimiento de la instrumentación y la posibilidad de realizar medidas directas sobre muestras sólidas, reduciendo la generación de residuos y permitiendo que las muestras sean almacenadas para su posterior comprobación. Sin embargo, el principal inconveniente de este tipo de medidas es que las bandas del espectro están fuertemente influenciadas por un elevado número de parámetros químicos, físicos y estructurales, por lo que la utilización de métodos quimiométricos para extraer información relevante de los espectros se hace imprescindible. Para la calibración, es obligatorio incorporar la variabilidad tanto química como física atribuible al tipo de productos que se van a analizar, para ello, en la mayoría de los casos, como set de calibración se utilizan muestras sintéticas o previamente analizadas por otros procedimientos.

La intención del siguiente estudio es desarrollar un método directo, rápido y preciso, basado en medidas de reflectancia difusa en la región NIR, para el control de calidad de diferentes pesticidas comerciales que minimice la generación de residuos, de forma que sea un procedimiento “limpio” y, por tanto, reduzca los costes de los análisis. Para ello se seleccionaron distintos pesticidas como moléculas testigo (ver figura 23).

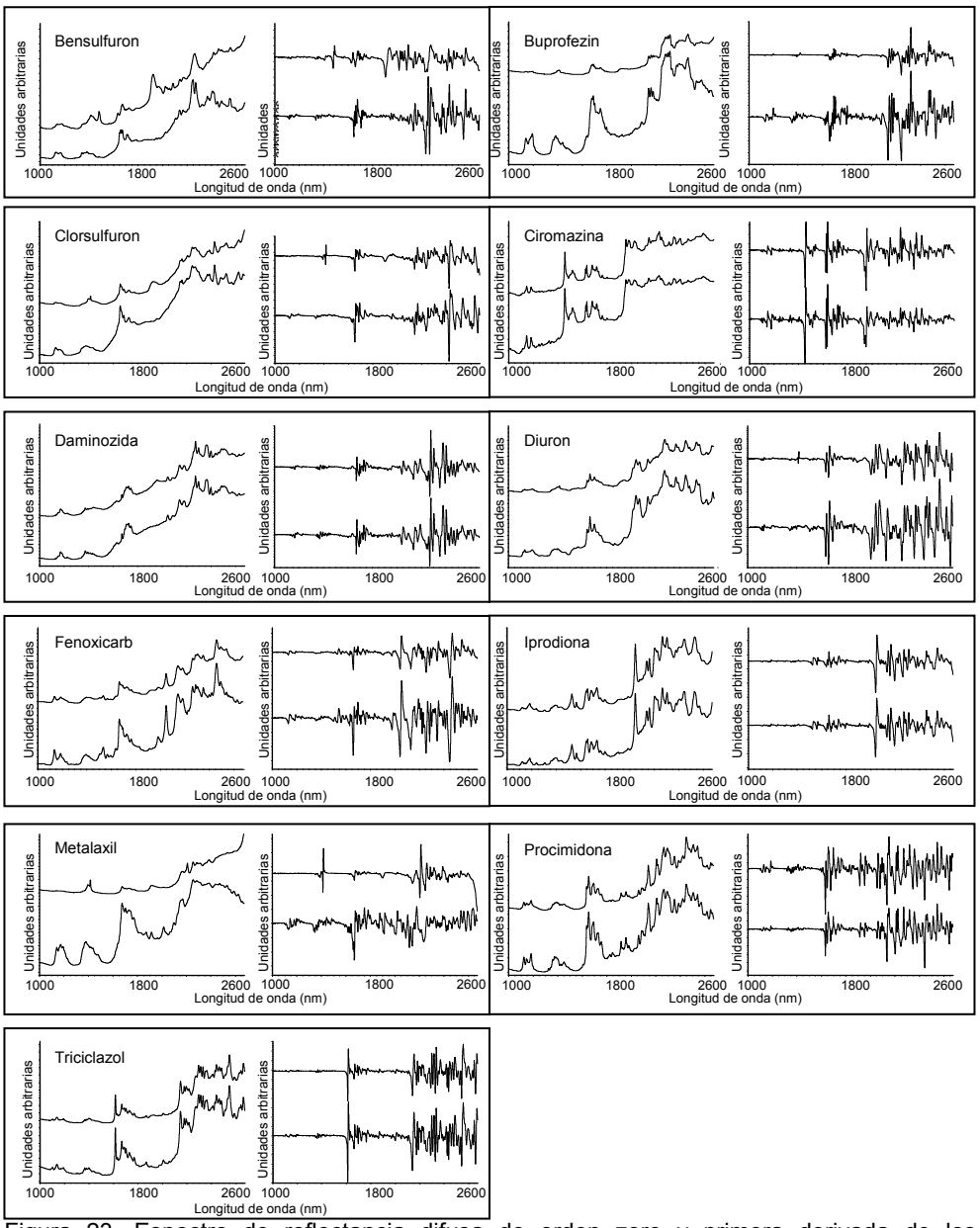

Figura 23. Espectro de reflectancia difusa de orden zero y primera derivada de los pesticides seleccionados para el estudio y de muestras comerciales que los contienen. Bensulfuron, Buprofezin, Clorsulfuron, Ciromazina, Daminozida, Diuron, Fenoxicarb, Iprodiona, Metalaxil, Procimidona y Triciclazol. Nota: Espectros de patrones y muestras de formulaciones comerciales (60% p/p Bensulfuron, 25% p/p Buprofezin, 75% p/p Clorsulfuron, 75% p/p Ciromazina, 85% p/p Daminozida, 80% p/p Diuron, 25% p/p Fenoxicarb, 50% p/p Iprodiona, 25% p/p Metalaxil, 50% p/p Procimidona y 75% p/p Triciclazol) obtenidos para los productos sólidos colocados en viales de vidrio de 10 mm de diámetro interno en la base.

Para llevar a cabo la determinación a partir de los espectros NIR de reflectancia difusa obtenidos directamente de las muestras contenidas en viales de vidrio, se ensayó un modelo PLS basado en el uso de 11 muestras comerciales como set de calibración. Se estudiaron diferentes regiones espectrales, para distintos criterios de corrección de línea base, tanto a partir de los espectros directos como de la primera derivada de los mismos.

El modelo inicial para la calibración PLS utiliza una muestra comercial de cada pesticida y 10 blancos formados por el resto de muestras comerciales.

Posteriormente, este modelo se mejoró mediante la inclusión al set de calibración de 22 muestras adicionadas (11 por encima y 11 por debajo de la concentración teórica), con lo que se consigue mejorar la capacidad predictiva.

Por último, se estudió el efecto del número de factores utilizados en el modelo sobre la capacidad predictiva del modelo, utilizando para ello como estadísticos el valor del *predicted residual error sum of squares* (PRESS) y el error promedio de la determinación. El elevado número de factores necesarios para la determinación de dichos principios activos en formulaciones comerciales (ver Tabla 9) probablemente sea debido al número de blancos introducidos (el resto de pesticidas) con diferente contribución espectral y a diferencias en las propiedades físicas de las matrices de las muestras.

Tabla 9. Características analíticas del método PLS/NIR para la determinación de pesticidas en formulaciones comerciales.

Región (cm^{-1})	Tratamiento previo	Pesticida	Factores[a]	$R^{2,b}$	RMSEC (% p/p)[c]	Error promedio[d] (%)	% Recuperación	
							UD*	OD*
1618-2630	Primera derivada	Bensulfuron	18	0.9998	0.388	1.2	100.9 ± 0.3	99.1 ± 1.0
	-	Buprofezin	22	0.9993	0.310	0.8	99.3 ± 0.6	100.8 ± 0.2
		Clorsulfuron	13	0.998	1.30	0.7	98.7 ± 0.7	99.0 ± 0.3
		Ciromazina	23	0.9993	0.800	2.0	101.4 ± 0.3	99.7 ± 0.3
		Daminozida	16	0.998	1.30	1.1	102.6 ± 0.1	98.5 ± 0.8
		Diuron	22	0.9998	0.441	3.1	100.6 ± 0.9	102.8 ± 0.6
	Primera derivada	Fenoxicarb	16	0.998	0.648	1.4	102.6 ± 0.8	100.1 ± 0.3
	-	Iprodiona	16	0.995	1.60	2.7	103.9 ± 0.4	98.2 ± 0.2
	Primera derivada	Metalaxil	17	0.9996	0.259	0.3	102.8 ± 0.4	101.6 ± 0.2
		Procimidona	19	0.9998	0.345	3.1	100.1 ± 0.9	101.5 ± 0.3
		Triciclazole	19	0.9998	0.338	0.5	100.8 ± 0.5	99.3 ± 0.4

[a]. Número de factores seleccionados para obtener el mínimo valor de PRESS.
[b]. R^2 es el coeficiente de correlación obtenido para la regresión entre los valores encontrados y los actuales para el set de calibración.
[c]. *Root mean square calibration error* para una validación cruzada.
[d]. Error promedio (%) encontrado para la comparación con los resultados obtenidos por HPLC.
**UD:* muestras *under-dosed. OD:* muestras *over-dosed.*
En todos los casos se realizó como criterio de línea base (linear removed).

Finalmente, en la Tabla 10 se comparan los resultados obtenidos mediante el método de referencia (HPLC) y el procedimiento desarrollado por reflectancia difusa. Como puede verse, en todos los casos se obtienen resultados comparables, con errores relativos inferiores al 4%.

Estudios adicionales pusieron de manifiesto que las recuperaciones obtenidas para muestras adicionadas con analito y diluidas con coadyuvante (Tabla 9) son en la mayoría de los casos aceptables, obteniéndose solo en algunos pocos casos recuperaciones superiores al 102%.

Tabla 10. Resultados obtenidos por reflectancia difusa NIR y HPLC para las diferentes muestras comerciales estudiadas.

Pesticida	Muestra	HPLC (% p/p)	NIR (% p/p)	Error relativo %
Bensulfuron	1	61.7 ± 0.6	60.6 ± 0.4	1.8
	2	60.9 ± 0.3	60.8 ± 0.5	0.5
Buprofezin	3	26.86 ± 0.06	27.2 ± 0.2	1.3
	4	26.70 ± 0.16	26.8 ± 0.2	0.4
Clorsulfuron	5	76.4 ± 0.2	76.48 ± 0.07	0.10
	6	76.4 ± 0.2	77.41 ± 0.2	1.3
Ciromazina	7	76.8 ± 0.3	77.4 ± 0.8	0.8
	8	75.4 ± 0.2	73.0 ± 1.1	3.2
Daminozida	9	85.47 ± 0.03	85.60 ± 0.11	0.11
	10	85.3 ± 0.3	83.5 ± 0.2	2.1
Diuron	11	82.6 ± 0.4	80.3 ± 0.9	2.8
	12	83.0 ± 0.4	80.2 ± 0.8	3.3
Fenoxicarb	13	23.50 ± 0.10	23.9 ± 0.4	1.6
	14	24.00 ± 0.06	24.3 ± 0.2	1.2
Iprodiona	15	48.94 ± 0.03	50.3 ± 0.2	2.8
	16	49.04 ± 0.03	50.2 ± 0.3	2.6
Metalaxil	17	25.44 ± 0.11	25.33 ± 0.12	0.3
	18	25.16 ± 0.05	25.1 ± 0.2	0.3
Procimidona	19	51.6 ± 0.2	48.6 ± 1.1	3.7
	20	50.5 ± 0.3	50.3 ± 0.5	2.4
Triciclazol	21	75.5 ± 0.2	74.9 ± 0.8	0.8
	22	75.5 ± 0.1	75.4 ± 1.5	0.14

Esta aplicación pone de manifiesto el gran potencial de la reflectancia difusa en la región NIR combinada con métodos quimiométricos para el control de calidad de pesticidas comerciales en el sector agroalimentario. A pesar de las dificultades de la calibración (necesidad de calibrar con muestras previamente analizadas en las que se tenga en cuenta la variabilidad física a la vez que la diferente concentración de analito), pero considerando que el número de muestras requerido para el calibrado es bajo, el procedimiento reduce el tiempo de análisis, elimina el consumo de disolventes y el tratamiento previo de las muestras sin sacrificar exactitud y precisión.

3.d Medidas fotoacústicas en la región del infrarrojo medio

Otra alternativa vibracional para el análisis directo de muestras sólidas es el empleo de la espectroscopia fotoacústica. Los métodos basados en este tipo de medidas se caracterizan por su capacidad para analizar directamente muestras sólidas sin necesidad de un tratamiento complejo de las mismas, una mínima cantidad de muestra necesaria y por ser un método no destructivo, por lo que puede almacenarse la muestra tras su análisis. A diferencia de la espectroscopia de reflectancia difusa, donde la composición de la muestra afecta enormemente la señal analítica, en este caso se pueden utilizar patrones sintéticos en el set de calibración.

Esta técnica se ha aplicado a la determinación directa del pesticida mancozeb en formulaciones agroquímicas, todos ellos en presentación en forma de polvo mojable.

De igual forma que para los anteriores modos de medida, se realizó un estudio del efecto de las variables instrumentales que más puedan influir (la resolución nominal, la velocidad del espejo móvil y el número acumulado de barridos) en la obtención de los espectros PAS-FT-MIR. Las condiciones más adecuadas fueron 4 cm^{-1} de resolución nominal, que proporciona una relación señal ruido adecuada, una velocidad del espejo móvil de 2.2 kHz, con la que se obtiene la mejor relación señal ruido y un tiempo de adquisición aceptable y 25 barridos por espectro, como compromiso entre sensibilidad y frecuencia de análisis.

Considerando la existencia en el mercado de formulados comerciales conteniendo mancozeb con muy diferente composición química, se procedió a realizar un análisis jerárquico para clasificar las muestras a partir de las diferencias en su espectro PAS-FT-MIR. Como puede verse en la Figura 24, se obtuvieron 4 grupos diferentes que correspondían a muestras en las que el mancozeb estaba co-formulado con diferentes principios activos.

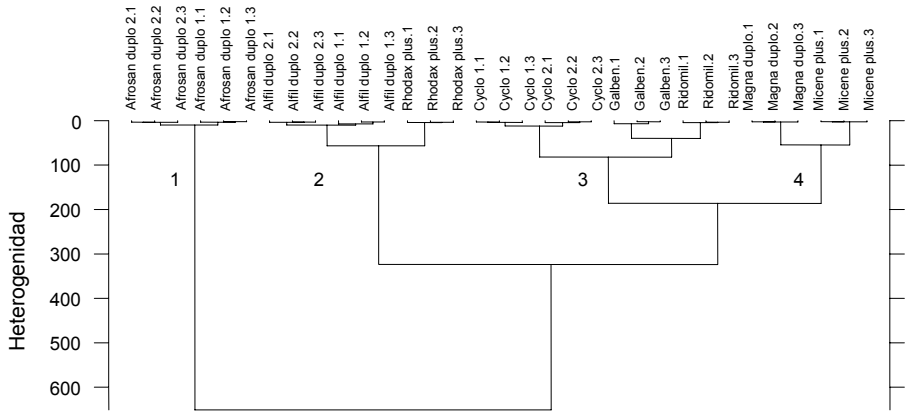

Figura 24. Clasificación dendográfica de muestras comerciales utilizando la distancia Euclídea del espectro PAS-FT-MIR y aplicando el método de unión de Ward. Nota: Para el análisis jerárquico se utilizó la región del espectro comprendida entre 3550 y 706 cm^{-1} sin preprocesado.

Debido a que la calibración externa monoparamétrica proporcionó una linealidad muy pobre y errores promedios para la exactitud muy elevados se ensayó un modelo basado en calibración multivariante. Para ello se empleó un set de calibración compuesto por diferentes estándares de mancozeb diluido en caolín (un coadyuvante típico en este tipo de formulaciones). Las diferencias en la composición y, por tanto, en el espectro provocaron que un modelo único para el análisis de todos los grupos resultara ineficaz, por tanto se ensayaron diferentes modelos para cada uno de los grupos, usando diferentes regiones y correcciones de línea base, tal como se indica en la Figura 25.

En la Tabla 11 se indican las diferentes regiones empleadas, el RMSEC obtenido en la calibración y el error promedio para el análisis de muestras comerciales.

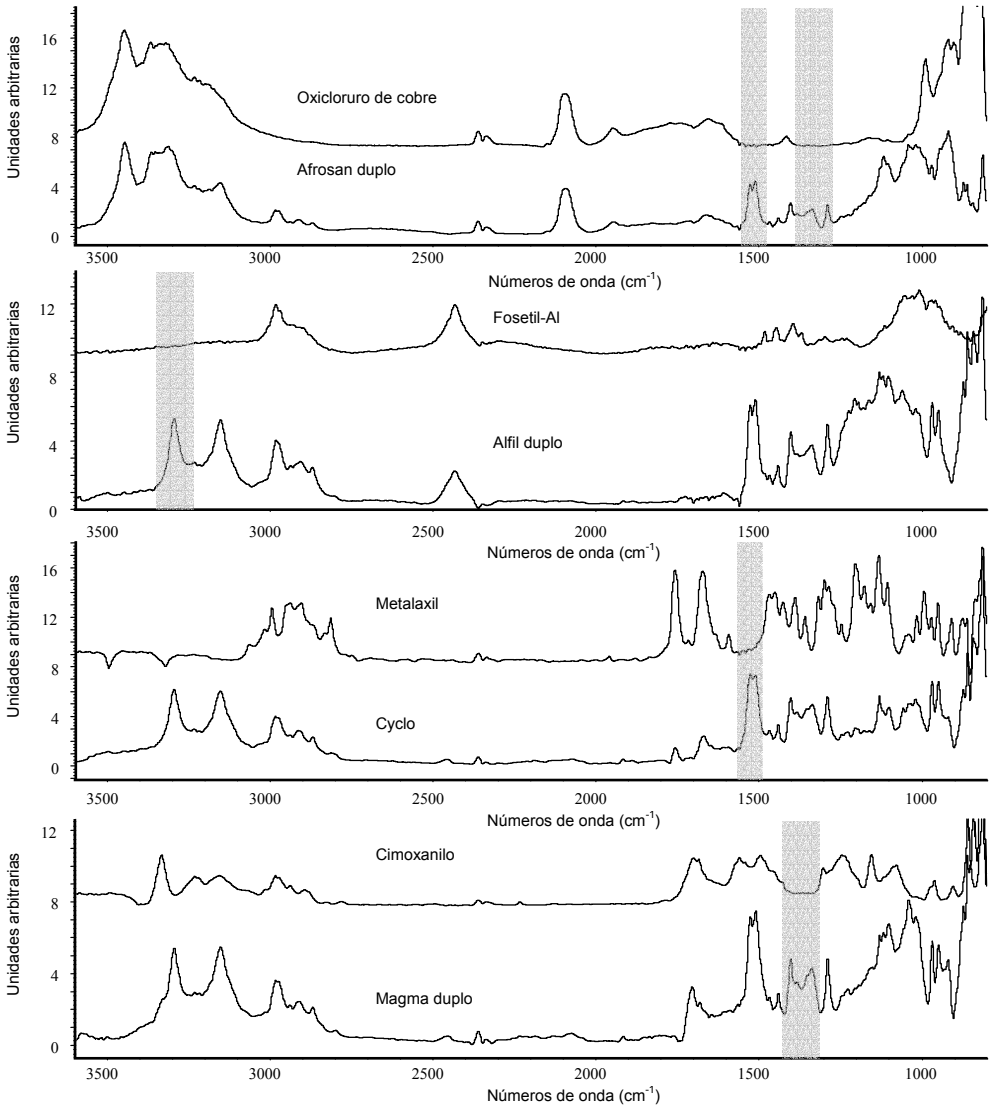

Figura 25. Espectros PAS-FTIR de cada grupo de muestras y del principio activo co-formulado con el mancozeb en cada caso. Nota: Las zonas sombreadas corresponden a las regiones escogidas para la calibración PLS en cada uno de los modelos considerados.

Tabla 11. Características analíticas de la determinación PAS-FTIR de mancozeb en formulaciones comerciales.

Región (cm^{-1})	Línea base (cm^{-1})	R^2 [a]	Número de Factores[b]	RMSEC (% p/p)[c]	E_r (%)[d]
Grupo 1					
1390-1269	-	0.9992	3	1.1	3.1
1543-1474	-				
Grupo 2					
3334-3211	3055	0.997	2	2.1	2.1
Grupo 3					
1543-1474	-	0.9991	2	1.3	2.5
Grupo 4					
1456-1306	-	0.9996	3	0.812	4.4

[a]. R^2 es el coeficiente de correlación entre los valores actuales y los predichos para la concentración de analito en el set de calibración.
[b]. Número de factores seleccionados para obtener el mínimo valor de PRESS.
[c]. *Root mean square calibration* error para una validación cruzada.
[d]. Error promedio relativo (%) obtenido de la comparación con los resultados obtenidos por HPLC.

La comparación de los resultados obtenidos por el método desarrollado y un método de referencia basado en una separación cromatográfica con derivatización previa, proporcionó la siguiente ecuación $C_{PAS\ FTIR}=(-0.6 \pm 1.4) + (1.00 \pm 0.03)C_{HPLC}$ con un valor de r=0.997, donde la pendiente y la ordenada en el origen son estadísticamente comparables a 1 y a 0, respectivamente, para un nivel de probabilidad del 95%.

Por tanto, el método desarrollado es simple, rápido, no-destructivo, aporta las ventajas de los métodos directos, como es el caso de la espectroscopia de reflectancia difusa y no es necesario disponer de una gran cantidad de muestras que varíen en sus propiedades físicas y químicas para construir el set de calibración, ya que éste puede estar compuesto por un número reducido de patrones sintéticos.

3.e Medidas de emisión Raman

Dentro de esta línea de investigación para el desarrollo de métodos directos, simples, rápidos y medioambientalmente sostenibles, la siguiente estrategia desarrollada para el control de calidad de productos manufacturados está basada en medidas de emisión Raman de muestras sólidas contenidas en viales de vidrio. Estos métodos Raman se compararon con procedimientos de referencia cromatográficos y de transmitancia en el infrarrojo medio.

Para el registro de los espectros Raman se utilizó un espectrómetro por transformada de Fourier Bruker RFS100/S equipado con un detector de germanio refrigerado con nitrogeno líquido y un láser de *Neodymium:yttrium-aluminum-garnet* (Nd:YAG) que emite a 1064 nm, y con una potencia máxima de 2 W. Como celda de medida se usaron viales estándar de vidrio, de los utilizados habitualmente para cromatografía con unas dimensiones de 12 x 32 mm y un volumen aproximado de 2 ml.

En primer lugar se realizó un estudio de las variables instrumentales que afectan al espectro Raman. Como puede verse en la Figura 26, el número acumulado de barridos y la resolución nominal producen un efecto similar al producido en el caso de medidas de transmisión en el MIR.

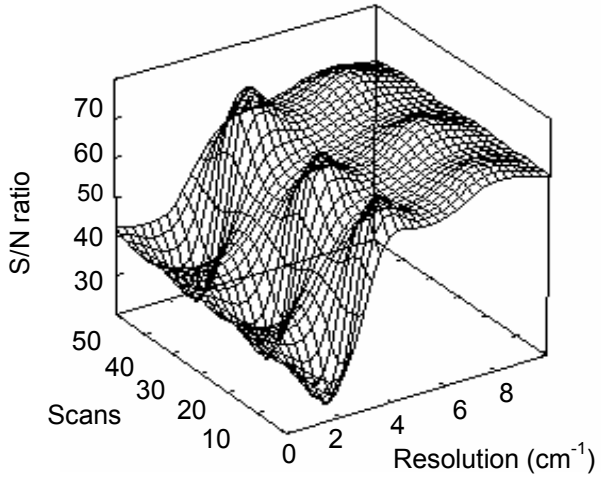

Figura 26. Efecto del número acumulado de barridos y de la resolución nominal sobre la relación señal/ruido del espectro FT-Raman de un patrón de ciromacina de concentración 55.4 % p/p utilizando cloruro sódico como diluyente.

Por otra parte, un aumento en la potencia del láser provoca un incremento de la señal Raman (Figura 27), sin embargo, si la potencia de excitación es demasiado elevada puede calentar la muestra excesivamente, pudiéndose descomponer ésta u observarse fenómenos de desplazamiento de la línea base del espectro. Por tanto, se escogió un valor intermedio para realizar los análisis.

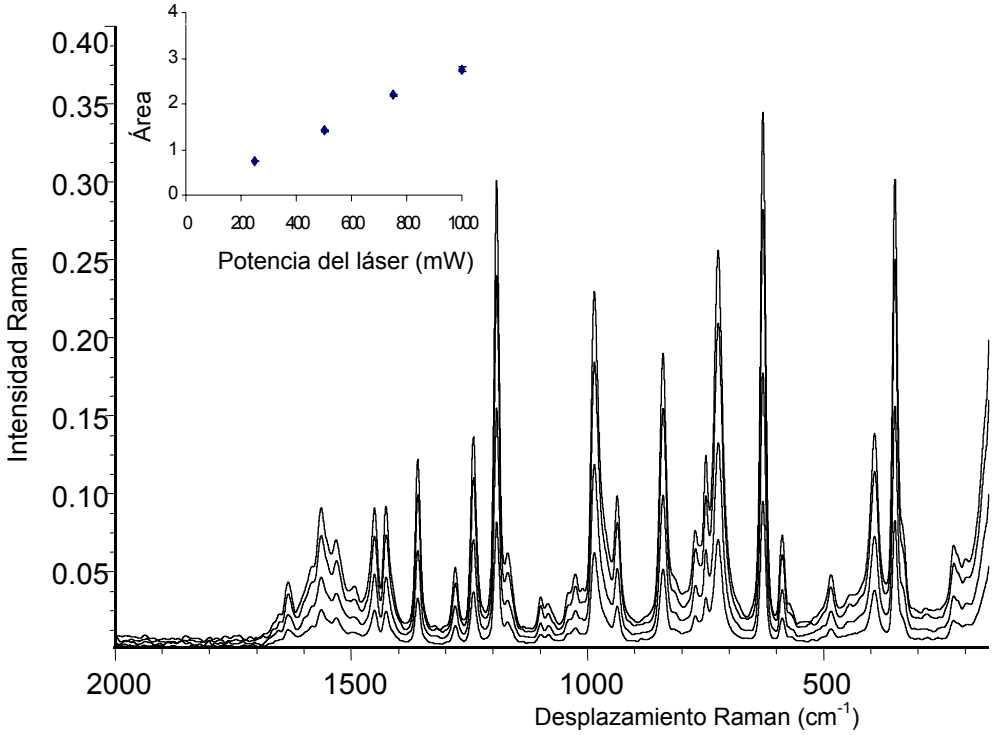

Figura 27. Efecto de la potencia del láser en la determinación de ciromacina mediante espectrometría FT-Raman. Detalle: Relación entre el área y la potencia de láser, para medidas entre 633 y 623 cm^{-1} de un patrón de ciromacina del 55.4 % p/p, acumulando en todos los casos 25 *scans* por espectro y trabajando a una resolución de 4 cm^{-1}.

Otros parámetros estudiados pero que resultaron afectar de forma menos significativa a la relación señal/ruido, han sido el factor de *zero filling* y la velocidad del espejo móvil del interferómetro.

Adicionalmente, se evaluó el efecto del uso de diferentes viales y del cambio de la posición de un mismo vial sobre la repetibilidad de las medidas, obteniéndose valores adecuados para la determinación cuantitativa de los diferentes analitos teniendo en cuenta la concentración en la que se encontraban en las muestras (RSD inferiores a 5.9%).

Se evaluaron diferentes regiones, criterios de línea base y modos de medida para obtener unas características analíticas adecuadas para la determinación de pesticidas en formulados comerciales (Tabla 12).

Tabla 12. Características analíticas de la determinación FT-Raman de ciromacina, usando diferentes bandas, criterios de corrección de línea base y modos de medida.

Modo de medida	Desplazamiento Raman (cm^{-1})	Corrección de línea base (cm^{-1})	ecuación del calibrado		R^2	% RSD	LOD (% p/p)
			$a \pm s_a$	$b \pm s_b$			
Altura	1359	1388-1331	-0.0008 ± 0.0003	0.0894 ± 0.0006	0.9995	0.8	1.4
Área	1364-1354		-0.006 ± 0.002	0.724 ± 0.004	0.9997	0.5	1.9
Altura	1241	1262-1216	-0.0010 ± 0.0005	0.0967 ± 0.0009	0.9991	1.6	1.1
Área	1246-1236		-0.006 ± 0.003	0.783 ± 0.006	0.9994	0.9	1.0
Altura	1193	1215-1176	-0.0009 ± 0.0007	0.219 ± 0.001	0.9997	0.4	0.1
Área	1198-1188		-0.009 ± 0.004	1.675 ± 0.008	0.9998	0.8	0.9
Altura	986	1006-900	-0.0005 ± 0.0007	0.159 ± 0.001	0.9994	0.8	0.2
Área	991-981		-0.003 ± 0.007	1.58 ± 0.01	0.9994	0.6	0.02
Altura	839	873-796	-0.0018 ± 0.0009	0.138 ± 0.002	0.999	1.9	0.4
Área	844-834		-0.016 ± 0.008	1.18 ± 0.01	0.999	1.5	0.2
Altura	725	789-659	-0.002 ± 0.001	0.186 ± 0.002	0.999	0.6	0.1
Área	730-720		-0.017 ± 0.009	1.62 ± 0.02	0.999	0.4	0.3
Altura	628	663-601	-0.0002 ± 0.0009	0.281 ± 0.002	0.9996	0.7	1.2
Área	633-623		0.000 ± 0.007	2.23 ± 0.01	0.9997	0.4	0.8
Altura	350	369-311	-0.005 ± 0.002	0.241 ± 0.004	0.997	1.0	0.1
Área	355-345		-0.03 ± 0.01	1.73 ± 0.03	0.998	0.9	0.7

Esta selección de condiciones de medida y región espectral se realizó teniendo en cuenta, además, las posibles interferencias debidas a

coadyuvantes presentes en la formulación o a posibles principios activos co-formulados con el analito de interés, es decir, en términos de exactitud.

Este procedimiento no solo se aplicó al análisis de pesticidas en formulados sino también a la determinación de la composición de edulcorantes sólidos.

En el caso de la determinación simultánea de sacarina y ciclamato sódico en el que existen interferencias entre los analitos a determinar y otros componentes de la muestra (glucosa monohidrato), la calibración univariada no es viable y se obtienen errores relativos excesivamente grandes, por tanto, se ensayó el empleo de la calibración multivariada basada en el uso del PLS, estudiándose diferentes estrategias para llevar a cabo la determinación de forma exacta y precisa. La primera de ellas utilizaba como set de calibración un conjunto de patrones con diferentes concentraciones de sacarina y ciclamato sódico. La segunda introducía también en el set de calibración la glucosa monohidrato, un compuesto presente en este tipo de formulaciones. Los errores relativos obtenidos fueron mejores en el segundo caso (1.1 y 1.9% para sacarina y ciclamato, respectivamente).

Posteriormente, se estudió la estabilidad de las muestras y los patrones almacenados a temperatura ambiente en el interior de los viales de vidrio. Los resultados obtenidos tres meses después fueron estadísticamente comparables a los anteriores y a los obtenidos para el análisis de los mismas muestras por un método de referencia (HPLC) y uno basado en medidas de transmitancia FTIR, para un nivel de probabilidad del 95%, poniendo de manifiesto la exactitud del procedimiento

Por otra parte, la repetibilidad obtenida como desviación estándar relativa fue menor del 1 %.

En resumen, con esta metodología FT-Raman se consigue eliminar el tratamiento previo de las muestras y se evita la generación de residuos. Los métodos propuestos resultan sencillos y simples, evitando las dificultades de calibración de los procedimientos anteriores (FT-NIR, fotoacústica) basados en medidas directas sobre muestras sólidas. El

inconveniente fundamental que presentan estos procedimientos es el elevado coste de adquisición del instrumental necesario y el pobre límite de detección obtenido, consecuencia de la baja sensibilidad de las medidas. Todo esto limita el campo de aplicación de las medidas directas por espectrometría Raman al análisis de componentes que se encuentran en concentración del orden de porcentaje.

Debido a esta última desventaja, se desarrolló un método de preconcentración *on-line* del analito sobre una fase sólida adecuada y posterior medida del mismo directamente sobre la fase sólida. Este procedimiento se ha aplicado a la determinación de cafeína en bebidas energéticas y constituye el primer antecedente de espectrometría FT-Raman en fase sólida.

El procedimiento consiste en hacer pasar un volumen de la muestra líquida a través de un tubo de vidrio relleno con la fase sólida apropiada para la retención del analito (en el caso en estudio, C18). La colocación previamente de una fase diferente a la C18 permite retener otros componentes presentes en la muestra y que pueden suponer una interferencia o incluso provocar fenómenos de fluorescencia a la hora de efectuar la medida FT-Raman. Para el caso particular del análisis de cafeína, este relleno anterior fue de tipo LC-SAX, de forma que se retenía gran parte de los compuestos iónicos presentes en la muestra.

Como puede verse en las Figuras 28 y 29, se estudió cual era la capacidad de retención máxima de la C18, así como la distribución espacial, esto es, como quedaba retenido el analito en la fase. De los resultados obtenidos se comprobó que 300 mg de C18 eran capaces de retener cuantitativamente hasta 7 mg de cafeína lo que supone una concentración del 2.3 % p/p en la fase sólida y que la máxima señal se obtiene entre los 7.5 y 12.5 mm a contar desde la parte superior de la fase.

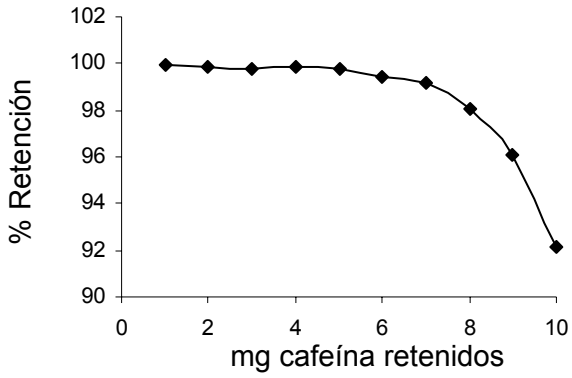

Figura 28. Capacidad de retención de 300 mg de fase sólida C18.

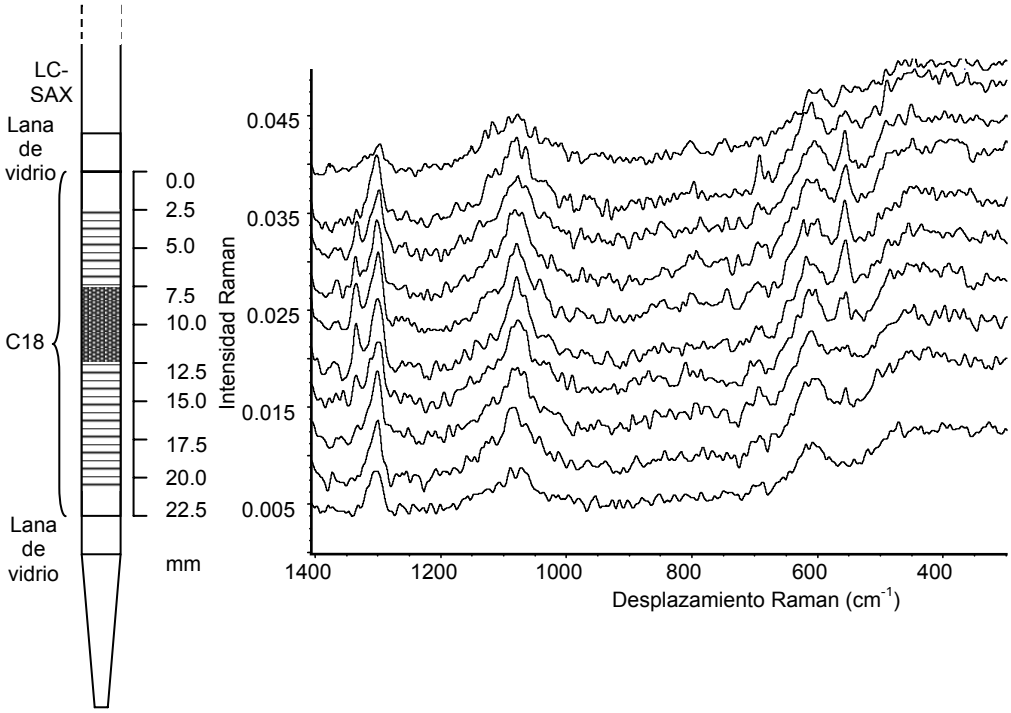

Figura 29. Distribución de cafeína a través de la fase sólida tipo C18 contenida en el interior de un tubo de vidrio de 5 mm de diámetro interno. Los espectros FT-Raman se corresponden con las medidas realizadas a los valores de posición (en mm) señalados para un patrón conteniendo 400 mg l^{-1} de cafeína.

Por otra parte se obtuvo una repetibilidad, calculada como desviación estándar relativa, del 1.4 % para medidas sobre el mismo cartucho y del 5.0 % para medidas sobre diferentes cartuchos.

Se evaluaron, también otras variables experimentales, como la velocidad de carga de la fase estacionaria, obteniéndose que para 10 ml de muestra conteniendo 200 mg l^{-1} de cafeína la retención era cuantitativa dentro del intervalo 1.62 - 7.50 ml min^{-1}, por tanto se escogió este último valor para la retención de cafeína en la C18, de forma que se reduce al máximo el tiempo de análisis.

Para la cuantificación de la cafeína, se ensayaron distintos tipos de calibración univariada, escogiendo para ello diferentes bandas típicas de la cafeína (entre 556 y 1335 cm^{-1}). El empleo de medidas de área entre 573 y 542 cm^{-1}, utilizando una corrección de línea base entre 580 y 540 cm^{-1}, proporcionó una sensibilidad adecuada, un límite de detección de 18 mg l^{-1} y una repetibilidad del 3 %, siendo apropiada para la determinación de cafeína en bebidas energéticas.

Como puede verse en la Tabla 13, se realizó una validación del método propuesto en términos de exactitud, comparando los resultados obtenidos para el análisis de 12 muestras comerciales por el procedimiento desarrollado y por un método de referencia basado en una separación cromatográfica. Los resultados obtenidos fueron estadísticamente comparables entre sí, aunque la precisión para las medidas Raman fue sensiblemente inferior, aunque en la mayoría de los casos por debajo del 5%.

Tabla 13. Resultados obtenidos para el análisis de diferentes muestras comerciales de bebidas energéticas mediante espectrocopia Raman y por un método de referencia cromatográfico.

Muestra	HPLC-UV (Cafeína mg l^{-1})	SP-FT-Raman (Cafeína mg l^{-1})	t_{exp}
Burn	225.6 ± 0.5	221 ± 7	1.466
Burn (Sin azúcar)	224.8 ± 0.6	230 ± 8	1.444
Red Bull	235.5 ± 1.0	235 ± 6	0.180
Red Bull (Sin azúcar)	240.7 ± 0.3	238 ± 6	1.005
Mountain Dew	308.7 ± 1.5	305 ± 6	1.338
Hacendado	106.4 ± 0.9	108 ± 6	0.590
Carrefour	243.7 ± 0.2	247 ± 6	1.229
Big Puma	241.0 ± 1.4	239 ± 4	1.055
Non stop (naranja)	111.4 ± 0.5	110 ± 4	0.780
Non stop (limón)	109.4 ± 0.5	106 ± 5	1.513
Locura	197.2 ± 0.5	198 ± 7	0.255
Locura (Sin azúcar)	213.91 ± 0.06	218 ± 6	1.370

t_{tab} = 1.812, para un nivel de probabilidad del 95 % y 10 grados de libertad.
Los valores de concentración son el promedio de dos análisis independientes medidos por triplicado ± la desviación estándar de los 6 valores encontrados.

Como ha quedado patente, la combinación de la espectrometría FT-Raman y la retención en fase sólida proporciona un claro aumento de la sensibilidad con respecto a las medidas Raman directas en disolución. Además, pueden evitarse los problemas derivados de la fluorescencia en las muestras por retención previa de compuestos en una fase sólida aniónica, permitiendo llevar a cabo, en un solo paso, la pre-concentración y el *clean-up* del analito.

En resumen, los procedimientos vibracionales desarrollados durante esta Tesis Doctoral son válidos para la determinación de analitos en una gran variedad de productos manufacturados con distintas propiedades físicas y químicas. La elección de la metodología más adecuada, en cada

caso, deberá realizarse en función de las características intrínsecas del analito, de la matriz y, por supuesto, de las exigencias de la determinación.

Los trabajos que se integran en esta Tesis Doctoral forman parte de los proyectos I+D de la Generalitat Valenciana **GVO1-249**, **GVO4B/247** y **Grupos C3-118** y de la Universitat de València proyecto **UV-AE-20050203** y constituyen una de las líneas de investigación dentro de la actividad que ha venido realizando el grupo **SOLINQUIANA** en el Departamento de Química Analítica de la Universitat de València (Estudi General).

RESULTADOS Y DISCUSIÓN

TRANSMISSION SPECTROSCOPY

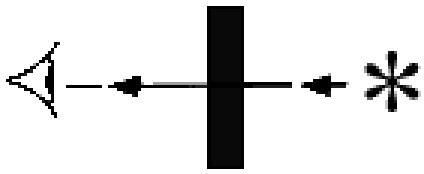

Solid Sampling Fourier transform infrared determination of Mancozeb in pesticide formulations

Sergio Armenta, Salvador Garrigues and Miguel de la Guardia
Department of Analytical Chemistry, Universitat de València. Edifici Jeroni Muñoz, 50th Dr Moliner, 46100 Burjassot, Valencia, Spain.

Talanta 65 (2005) 971-979.

Impact factor of this journal (2004): 2.532
Source: Journal citation reports ISI Web of Knowledge, 2004.

Available online at www.sciencedirect.com
SCIENCE DIRECT®
Talanta 65 (2005) 971–979
Talanta
www.elsevier.com/locate/talanta

Solid sampling Fourier transform infrared determination of Mancozeb in pesticide formulations

Sergio Armenta, Salvador Garrigues*, Miguel de la Guardia

Department of Analytical Chemistry, University of Valencia, Edifici Jeroni Muñoz, 50th Dr. Moliner, 46100 Burjassot, Valencia, Spain

Received 11 March 2004; received in revised form 24 July 2004; accepted 23 August 2004
Available online 27 September 2004

Abstract

A series of approaches have been assayed for FTIR determination of Mancozeb in several solid commercial fungicides using different calibration strategies. The simplest procedure was based on the use of the ratio between the absorbance of a characteristic band of Mancozeb and that of a KSCN internal standard measured in the FTIR spectra obtained from KBr pellets. It was employed the quotient between peak height absorbance values at 1525 cm^{-1} for Mancozeb and 2070 cm^{-1} for KSCN. In these conditions a precision as relative standard deviation (RSD) of 0.6% and a relative accuracy error of 0.8% (w/w) were found. For complex formulations, containing other compounds with characteristic absorption bands at different wavenumbers than Mancozeb, one of them was used as internal reference being employed the standard addition approach. In this case, the Mancozeb bands at 1525 cm^{-1} or at 1289 cm^{-1} were employed, being used the ferrocyanide band at 2075 cm^{-1} as internal reference. RSD values between 0.7–1.4% and a relative accuracy error of 3% (w/w) were found. A third strategy was based on the use of partial least squares (PLS) calibration. A reference set was prepared mixing Mancozeb, Kaolin, Cymoxanil and KBr, being predicted the Mancozeb concentration in pesticide formulations by using the quotient between absorbance bands of Mancozeb and those of Cymoxanil. In these conditions a relative accuracy error of 0.6% (w/w) and a relative standard deviation of 1.3% were found.

Keywords: Mancozeb; FTIR determination; Pesticide formulations; Internal standardization; Solid sampling; KBr pellets; PLS

1. Introduction

In the infrared literature it can be found a series of models for the quantitative analysis of samples based on the use of bands quotients between different components. These strategies avoid problems arising from the lack of information about the thickness of solid pellets or liquid sample drops deposited between two crystals. The aforementioned studies have been applied to the determination of the average condensation degree of surfactants [1,2] or the proportion between two active principles in a pharmaceutical formulation [3,4]. In recent years, new studies were developed to provide robust models based on the use of quotients between absorbance bands of two [5,6] or more components [7] present in the sample to avoid problems related with the election of internal standard and the compatibility with the sample components could appear [8,9].

Mancozeb, a [[1,2-etilenbisditiocarbamate](2-)] of manganese and zinc mixture, is a synthetic pesticide, which has been used since 1967 as a fungicide to prevent the growth of moulds and to protect plants and crops against damage caused by fungi. Mancozeb needs to be sprayed on surfaces of leaves and crops for protection against moulds. Fortunately the toxicity of Mancozeb is very low, with LD_{50} values of the order of several g kg^{-1} [10]. It is available in commercial formulations as dusts, water-dispersible granules, wettable powders, and ready-to-use formulations. It is commonly found in combination with other pesticides like Cymoxanil, Metalaxyl, Fosetyl-Al or copper oxychloride [11].

* Corresponding author. Tel.: +34 963543158; fax: +34 963544838.
E-mail address: salvador.garrigues@uv.es (S. Garrigues).

0039-9140/$ – see front matter © 2004 Elsevier B.V. All rights reserved.
doi:10.1016/j.talanta.2004.08.029

The analysis of alkylenebis (dithiocarbamates) of some divalent metal ions is hampered by their low solubility, low stability, and polymeric structure. Indirect methods include spectrophotometry [12,13], gas chromatography (GC) [14], or reversed phase ion-pair chromatography [15] determination of the reaction products liberated after reduction, in an acidic medium, to carbon disulfide. It is important to note that these methods are typically unable to distinguish among various dithiocarbamates since most of them can be degraded to CS_2. Other methods for determination of ethylenebisdithiocarbamates rely on the measurement of the metallic portion of the compounds, and therefore, many of these methods are similar to those for detection of inorganic manganese or zinc [16]. However, these methodologies assure the content of metal but cannot evaluate the possible degradation of pesticide molecules.

As it has been suggested by the CIPAC, chromatographic methods, based on both, gas and liquid chromatography, are currently employed for routine analysis of pesticide formulations [17]. However, recent studies have evidenced the ability of infrared spectrometry methods as an adequate alternative technique for the resolution of this analytical demand. Pyrethroids, such as cyperthrind and deltamethrin, have been analysed in emulsifiable concentrate formulations by FTIR spectrometry after separation by thin layer chromatography and re-dissolution in CCl_4 [18]. Iprodione has been determined in wettable powder after extracting with CH_2Cl_2 and measurement at 3355 cm^{-1} [19]. Attenuated total reflectance (ATR) infrared spectrometry combined with principal components regression (PCR) analysis has been applied to the determination of chlorpyrifos-ethyl in agrochemical formulations [20].

The improvement of FTIR determinations through the use of flow injection analysis has been applied to solve problems related to the determination of Carbaryl [21] and Buprofezin [22] and the simultaneous determination of active ingredients in commercial pesticide formulations [23], also including, in some cases, the sample treatment step, as for Malathion on-line determination [24].

Dithiocarbamate pesticides, such as Ziram and Thiram can be directly analyzed from solid formulations using chloroform as a solvent [25]. Ziram has been also determined after acid decomposition and the CS_2 generated measured by vapour phase FTIR [26].

Due to the extremely low solubility of Mancozeb in common organic solvents employed for FTIR spectrometry, also including polar ones such as alcohol or water, this pesticide can not be easy analyzed in dissolution and it is necessary to obtain the infrared spectra directly from the solid sample using diffuse reflectance (DR), attenuated total reflectance (ATR), photoacoustic or absorbance measurements in KBr pellets.

The aim of this study has been the development of simple strategies which could be used for routine determination of Mancozeb in commercial formulated fungicides based on the use of FTIR transmittance measurements in KBr pellets and thus, a series of direct measurements of the quotient between absorbance bands of Mancozeb and those of selected internal reference were suggested for the analysis of different pesticide formulations.

The use of the quotient between the absorbance of Mancozeb and that of a reference compound was employed on using: (i) external calibration, (ii) standard addition approach, and (iii) partial least squares calibration; thus offering a series of alternatives to solve the problem of the direct analysis of solid samples by transmittance FTIR without a previous dissolution.

2. Experimental

2.1. Apparatus and reagents

A Mattson Research RS1 Fourier transform infrared spectrometer (Madison, WI, USA) equipped with a temperature-stabilized DGTS detector with a Ge/KBr beamsplitter and precise digital signal processing (DSP) was employed for all the IR spectral measurements with a nominal resolution of 4 cm^{-1} and accumulating 25 scans.

For the mass measurements it was used a Mettler Toledo AG285 (Columbus, OH, USA) balance with a precision of ±0.01 mg.

PLS data treatment was carried out using Omnic Quant IR (version 1.2) software from Nicolet (Madison, WI, USA).

Mancozeb (88.1% (w/w)), Cymoxanil (98.0% (w/w)) and Kaolin, technical products were supplied by Laboratorios Afrasa S.A. and commercial formulations were obtained from the Spanish market. All the disks were prepared using KBr, spectroscopy IR grade, from Panreac (Barcelona, Spain). Analytical reagent grade potassium thiocyanate from Panreac (Barcelona, Spain) was employed as internal standard.

2.2. Recommended procedure

2.2.1. External calibration in the presence of an added internal standard

An accurately weighted amount of 1.50 mg (±0.01 mg) KSCN was added to 2.00 mg (±0.01 mg) sample and 500.0 mg (±0.1 mg) KBr. The mixture was grounded and homogenized for 5 min in an agate mortar. The mixture was pressed at 10 tones in a 13 mm diameter evacuable pellet die and the FTIR spectrum of the resultant KBr disk recorded in the range from 4000 to 400 cm^{-1}, at 4 cm^{-1} resolution and accumulating 25 scans for spectrum. The background spectrum was established, under identical instrumental conditions, from the air.

An external calibration curve was established with KBr disks containing different amounts of Mancozeb in the presence of KSCN as internal standard, using the quotient between the bands at 1525 cm^{-1}, with a baseline established between 1556 and 1430 cm^{-1} for Mancozeb and that of KSCN

of 2070 cm^{-1}, with a baseline established between 2233 and 1930 cm^{-1}.

2.2.2. Standard addition in the presence of a well known sample component

An accurate weight of the order of 25 mg of a commercial formulation which contains also ferric ferrocyanide and copper oxychloride, was mixed with 300 mg KBr. On the other hand a stock mixture of pure Mancozeb and KBr (20 mg Mancozeb in 250 mg KBr) was prepared. From mixtures of the diluted sample and the stock powder, it was prepared a series of standards with a constant concentration of ferric ferrocyanide and different added amounts of Mancozeb.

Solid mixtures were pressed and the FTIR spectra of the KBr disks recorded using the aforementioned instrumental conditions. Peak area and peak height measurements corresponding to Mancozeb bands were divided by data corresponding to the 2075 cm^{-1} ferrocyanide band, using a baseline between 1986 and 2158 cm^{-1}, and Mancozeb determined using the standard addition aproach from absorbance quotient data as a function of added mg of the pesticide, being selected the peak height data at 1289 cm^{-1} for Mancozeb corrected with a baseline located at 1272 cm^{-1}.

2.2.3. Partial least squares calibration in the presence of an internal standard

About 4 mg Cymoxanil and different quantities of Mancozeb, from 40 to 55 mg, and Kaolin (a coadyuvant present in the formulations), from 41 to 56 mg, were mixed with KBr in order to prepare a calibration set. Two milligrams of sample were diluted with 250 mg KBr and the FTIR spectra of the KBr pellets were recorded. Absorbance data corresponding to Mancozeb were divided by those corresponding to Cymoxanil, employed as internal standard, and from these data a PLS model was established on using the calibration set, being predicted Mancozeb concentration in commercially available samples by using a three factors model and the spectral range between 1579 and 1269 cm^{-1} corrected with a two points baseline situated between 1581 and 1269 cm^{-1} for Mancozeb and the measurement of peak height at 1705 cm^{-1} corrected with a baseline established between 1786 and 1689 cm^{-1} for the internal reference of Cymoxanil.

2.3. Mathematical treatments assayed

The determination of Mancozeb, from its characteristic bands obtained in solid KBr pellets, can be carried out by using an internal standard in order to avoid the problems related to establish quantitative data in conditions for which it is difficult to fix the bandpass.

Three alternatives were assayed in the present study.

2.3.1. External calibration by using an added internal standard

The quotient between the absorbance at two characteristic bands of each compound, A_M and A_K, respectively, in a series of standards containing the same amount of component K, provides a regression line of A_M/A_K versus $[M]/[K]$ which pass through the origin, being independent on the optical pathlength because for each KBr pellet disk the bandpass is the same for both compounds. So, the regression line $A_M/A_K = \varepsilon_M/\varepsilon_K \times [M]/[K]$, in which ε_M and ε_K are the absorption coefficients of M and K at the corresponding bands considered, could be used to obtain the concentration of the analyte in unknown samples to which the internal standard was added.

2.3.2. Standard addition analysis using an internal reference

For samples containing mixtures of different compounds, which present their characteristics absorption bands at different wavenumbers, it can be established a relationship between the absorbance at two wavenumbers (each of one corresponding to each compound), considered for a same spectrum, which will be independent on the bandpass and will depend on the proportion between the concentrations of the two compounds.

The addition of different amounts of the analyte to be determined to a series of fixed aliquots of the sample to be analysed provides a typical standard addition expression

$$\frac{A_M}{A_K} = \frac{\varepsilon_M}{\varepsilon_K} \times \frac{M_{\text{sample(mg)}}}{K_{\text{(mg)}}} + \frac{\varepsilon_M}{\varepsilon_K} \times \frac{M_{\text{standard(mg)}}}{K_{\text{(mg)}}}$$

being ε_M and ε_K the absorption coefficient of the analyte, (M), and the reference compound, (K), at the considered wavenumbers. From the quotient between the intercept, $\varepsilon_M/\varepsilon_K \times [M]_{\text{sample}}/[K]$ and the slope $\varepsilon_M/\varepsilon_K \times [K]$, it can be obtained the mass in mg of the analyte in the aliquot taken from the sample.

2.3.3. Partial least squares using internal reference

For the determination of Mancozeb in samples containing a second active ingredient which affects the Mancozeb signal but can be easy and accurately analysed, thus latter compound can be used as an internal reference and a PLS treatment of relative absorbance values could be used. It can be prepared a series of matched standards containing well known amounts of the reference and the analyte in order to develop a calibration model in which absorbance band quotients, instead of pure absorbance data at fixed wavenumbers, will be used.

An appropriate data adjustment of the calibration set could be useful for obtaining the concentration of the analyte in an unknown solid sample in which the reference compound has been previously determined after leaching it with an appropriate solvent. So, absorbance bands quotient data and reference concentration can be used for prediction of the insoluble analyte.

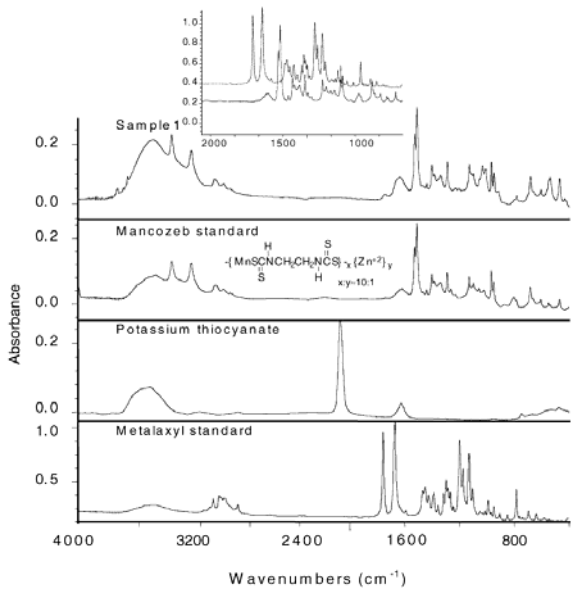

Fig. 1. FTIR spectra of KBr disks of a commercial fungicide sample which contains Mancozeb and Metalaxyl (Sample 1), Mancozeb, KSCN and Metalaxyl standards. Inset: FTIR spectra of a Mancozeb standard of 0.4 mg g^{-1} (bottom) and a Metalaxyl standard of 0.4 mg g^{-1} (top). All the spectra were recorded between 4000 and 400 cm^{-1}, at 4 cm^{-1} resolution, accumulating 25 scans for spectrum and the background was established, under identical conditions, from air.

3. Results and discussion

3.1. Determination of Mancozeb by addition of a reference compound

3.1.1. FTIR absorbance spectra

Fig. 1 shows the FTIR spectra of KBr disks of a Mancozeb standard, a commercial fungicide (Sample 1) containing 64% (w/w) Mancozeb and 8% (w/w) Metalaxyl, a Metalaxyl standard, and potassium thiocyanate, which will be employed as added reference compound for internal standardization.

Metalaxyl, methyl-*N*-(2,6-dimethylphenyl)-*N*-(2-xylyl)-DL-alaninate, is a systemic benzenoid fungicide used in mixtures as a foliar spray for tropical and subtropical crops, as a soil treatment for control of soil-borne pathogens, and as a seed treatment to control downy mildews.

As can be seen in the spectrum of Sample 1 are present the characteristic bands of Mancozeb, the most intense of these being those at 1525 and 1510 cm^{-1} which correspond to amide II band in CSNHR structures [27].

On the other hand, the thiocyanate stretching band at 2070 cm^{-1} could be used as reference to process absorbance band quotients between Mancozeb and KSCN in both, samples and standards, due to the absence of absorption at this wavenumber by all the compounds present in the sample.

3.1.2. Selection of the appropriate bands for the FTIR measurement of Mancozeb

As depicted in the inset of Fig. 1 the Mancozeb bands at 1525 and 1510 cm^{-1} do not overlap with any Metalaxyl band. So these bands are appropriate for Mancozeb determination in pesticide formulations containing Metalaxyl.

A series of Mancozeb standards, also containing KSCN as internal reference, with a Mancozeb/KSCN ratio between 5 and 1 were prepared according the recommended procedure for the external calibration. From the FTIR spectra of the aforementioned standards, and in order to choose the best analytical performance for the Mancozeb determination, different bands, measurement modes and baseline criteria were evaluated as can be seen in Table 1. This table shows the equations of the calibration lines, precision and accuracy values obtained for each band considered. The sensitivity of FTIR determination of Mancozeb varies from slope values of 0.109–0.60, being peak height based calibrations more sensitive than those obtained employing peak area measurements.

Table 1 evidences low correlation coefficients for calibrations established for area measurements, due to the appearance of a deformation of the thiocyanate band as a function of the relationship between Mancozeb and KSCN, as can be seen in Fig. 2. This deformation is probably due to the substitution of K^+ in KSCN by the Zn^{2+} of Mancozeb. So,

Table 1
Selection of IR bands for Mancozeb determination by using external calibration and KSCN as internal reference

Bands				Calibration line[a]		R^2	R.S.D.[b]	Mancozeb concentration[c] (% w/w) ± s	Er (%)[d]
Compound	Measurement mode	Wavenumber (cm^{-1})	Baseline (cm^{-1})	$a \pm s_a$	$b \pm s_b$				
Mancozeb	Height	1525	1556–1430	−0.06 ± 0.02	0.42 ± 0.01	0.998	0.2	64.5 ± 0.4	0.8
KSCN	Height	2070	2233–1930						
Mancozeb	Height	1510	1553–1428	−0.09 ± 0.04	0.60 ± 0.02	0.993	0.4	64.8 ± 0.4	1.2
KSCN	Height	2070	2233–1930						
Mancozeb	Area	1536–1518	1556–1451	−0.015 ± 0.006	0.109 ± 0.003	0.995	0.5	66.9 ± 0.3	5
KSCN	Area	2139–2013	2233–1930						
Mancozeb	Area	1519–1492	1553–1428	−0.02 ± 0.01	0.179 ± 0.007	0.993	1.0	68 ± 2	6
KSCN	Area	2139–2013	2233–1930						
Mancozeb	Area	1542–1485	1555–1427	−0.04 ± 0.02	0.30 ± 0.01	0.993	0.8	68 ± 2	6
KSCN	Area	2139–2013	2233–1930						

[a] Regression line: $A_{Mancozeb}/A_{KSCN} = a + b\,C_{Mancozeb}$ (mg)/C_{KSCN} (mg).
[b] R.S.D.: Relative standard deviation for a ratio Mancozeb/KSCN of 1.25 in KBr disk established from 5 different KBr pellets of a sample.
[c] Mancozeb concentration established in Sample 1, by using different criteria, in terms of % (w/w) ± S.D.
[d] Accuracy relative error, taking into account a reported concentration of 64% (w/w).

in this study, peak height data measurements of Mancozeb at 1525 cm^{-1} (corrected with a baseline established between 1556 and 1430 cm^{-1}) related to those of KSCN at 2070 cm^{-1} (with a baseline fixed between 2233 and 1930 cm^{-1}) will be recommended.

One commercial pesticide formulation containing Mancozeb and Metalaxyl was analyzed by the proposed procedure and as can be seen in Table 1 Mancozeb concentration found is comparable to that reported by the manufacturer. A relative error lower than 1% (w/w) and a repeatability of the 0.6% (expressed as a relative standard deviation) were obtained in the aforementioned conditions.

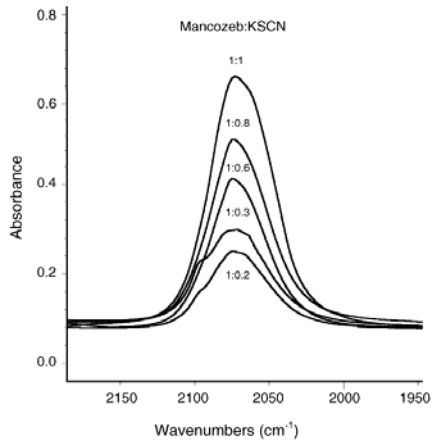

Fig. 2. Deformation on the thiocyanate band at 2070 cm^{-1} due to the presence of Mancozeb. Values indicated correspond to the Mancozeb:KSCN ratio in (w/w).

3.2. Determination of Mancozeb by standard addition analysis using an internal reference

3.2.1. FTIR absorbance spectra

FTIR spectra of KBr disks of a sample containing Mancozeb, ferric ferrocyanide and copper oxychloride and those of the different components considered can be seen in Fig. 3. The commercial sample (Sample 2) spectrum shows a higher number of bands than Mancozeb spectrum, due to the presence of ferric ferrocyanide and copper oxychloride in this product which avoid the use of KSCN as internal reference but provides another way for Mancozeb determination.

As can be seen in Fig. 3, the copper oxychloride (technical product) utilized in the manufacture of this commercial sample contains ferric ferrocyanide, evidenced by the presence of the band that appears at 2080 cm^{-1} due to –C≡N stretching [27]. The presence of ferrocyanide in oxychloride, which not affects the Mancozeb determination, was used as internal reference because the quantity of ferrocyanide belong constant in each sample and for the analysis of this kind of sample the strategy adopted was based on the use of the standard addition approach, being added increasing amounts of Mancozeb to constant sample aliquots.

3.2.2. Selection of the appropriate bands for the FTIR determination of Mancozeb by standard addition

As can be seen in the inset of Fig. 3 the FTIR spectrum of the commercial sample presents a series of characteristic bands of Mancozeb in the wavenumber range from 1550 to 1250 cm^{-1}. These bands do not overlap with bands of the other compounds present in the formulation. So, it is possible to process these data related to the absorbance at 2075 cm^{-1}. Table 2 shows the characteristic bands chosen for this study, processed with the previously defined standard addition model based on the use of the ratio between peak area or peak height of the selected absorbance bands. In all the cases, calibration lines were prepared as indicated in the

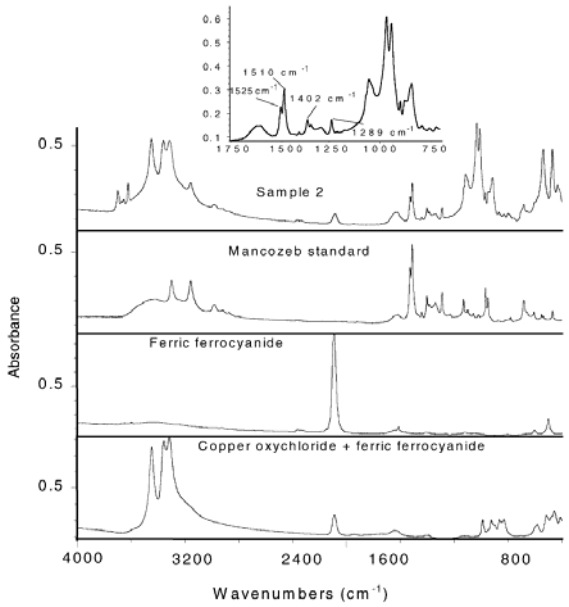

Fig. 3. FTIR spectra of KBr disks of a commercial fungicide which contains Mancozeb cooper oxychloride and ferric ferrocyanide (Sample 2), Mancozeb standard, ferric ferrocyanide and copper oxychloride with ferric ferrocyanide technical mixture. Inset: detailed spectrum of Sample 2 showing the bands selected for the determination of Mancozeb. All the spectra were recorded between 4000 and 400 cm^{-1}, at 4 cm^{-1} resolution, accumulating 25 scans for spectrum and the background was established, under identical conditions, from air.

Table 2
Selection of IR bands for determination of Mancozeb in a commercial sample using the standard addition method and ferrocyanide as internal reference

Bands				Calibration line[a]		R^2	R.S.D.[b]	Mancozeb concentration[c] (% w/w) ± s	Er (%)[d]
Compound	Measurement mode	Wavenumber (cm^{-1})	Baseline (cm^{-1})	$a \pm s_a$	$b \pm s_b$				
Mancozeb	Height	1525	735–1567	1.59 ± 0.17	3.27 ± 0.13	0.9967	1.4	18 ± 2	3
Ferrocyanide	Height	2075	1986–2158						
Mancozeb	Height	1510	1428–1554	2.4 ± 0.3	4.2 ± 0.2	0.9949	2	21 ± 3	20
Ferrocyanide	Height	2075	1986–2158						
Mancozeb	Height	1401	1425	0.74 ± 0.07	1.35 ± 0.06	0.996	0.9	20 ± 2	14
Ferrocyanide	Height	2075	1986–2158						
Mancozeb	Height	1289	1272	0.62 ± 0.05	1.31 ± 0.04	0.998	0.7	17 ± 1	−3
Ferrocyanide	Height	2075	1986–2158						
Mancozeb	Area	1557–1517	1557	0.97 ± 0.10	1.83 ± 0.08	0.9962	2	19 ± 2	8
Ferrocyanide	Area	2109–2050	2142–1994						
Mancozeb	Area	1517–1485	1554–1428	1.51 ± 0.18	2.68 ± 0.15	0.9938	2	20 ± 3	14
Ferrocyanide	Area	2109–2050	2142–1994						
Mancozeb	Area	1415–1391	1427	0.47 ± 0.06	0.73 ± 0.05	0.9923	1.5	23 ± 3	30
Ferrocyanide	Area	2109–2050	2142–1994						
Mancozeb	Area	1300–1279	1275	0.24 ± 0.03	0.50 ± 0.02	0.996	1.3	17 ± 2	−3
Ferrocyanide	Area	2109–2050	2142–1994						

[a] Regression line: $A_{Mancozeb}/A_{Ferrocyanide} = a + bC_{Mancozeb\ added}$ (mg).
[b] R.S.D.: Relative standard deviation for a sample with a 10 mg g^{-1} Mancozeb standard added (mg), established from 5 different KBr pellets of the sample.
[c] Mancozeb concentration established in Sample 2, by using different criteria, in terms of % (w/w) ± S.D.
[d] Accuracy relative error, taking into account a reported concentration of 17.5% (w/w).

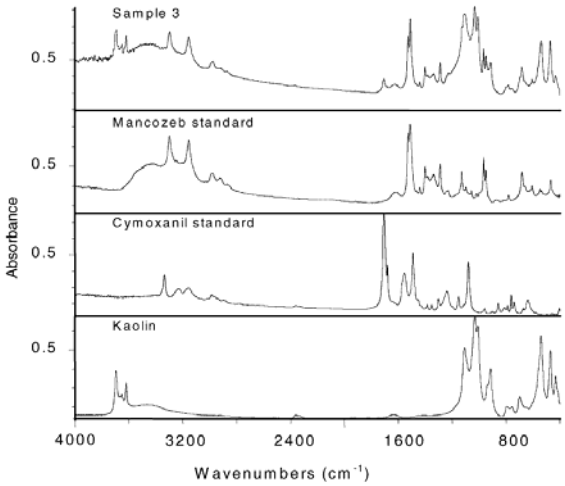

Fig. 4. FTIR spectra of KBr disks of a commercial fungicide containing Mancozeb, Kaolin and Cymoxanil (Sample 3), Mancozeb, Cymoxanil and Kaolin standards. All the spectra were recorded between 4000 and 400 cm^{-1}, at 4 cm^{-1} resolution, accumulating 25 scans for spectrum and the background was established, under identical conditions, from air.

Experimental section, by adding increasing amounts of Mancozeb to a fixed amount of sample.

The use of peak height ratio values provides a higher sensitivity than that obtained by the corresponding peak area measurements. The use of absorbance height data of Mancozeb at 1289 cm^{-1} and those of ferrocyanide at 2075 cm^{-1} provided the best regression coefficient and the best relative standard deviation. From the quotient between the intercept and the slope of the standard addition curve, a percentage of 17 ± 1% (w/w) of Mancozeb was obtained for the sample analyzed, that is a 3% lower than that indicated by the manufacturer.

3.3. Determination of Mancozeb by PLS–FTIR using an internal reference

3.3.1. FTIR absorbance spectras

Fig. 4 shows the FTIR spectra in KBr disk of Mancozeb, Cymoxanil and Kaolin standards, and that of a commercial fungicide sample containing 46.5% (w/w) Mancozeb and 4% (w/w) Cymoxanil.

Cymoxanil, 2-cyano-*N*-[(ethylamino)carbonyl]-2-(methoxyimino) acetamide, is an aliphatic nitrogen fungicide highly soluble in $CHCl_3$ [28], which can be determined by direct FTIR measurement at 1720 cm^{-1} after leaching with chloroform.

As can be seen, sample spectrum provides the typical bands corresponding to Mancozeb and the other compounds present in this formulation. Based on the fact that this formulation contains a 4% (w/w) Cymoxanil and this pesticide can be easily determined, it can be employed as internal reference, being possible to use the band at 1705 cm^{-1} to obtain absorbance data independent to the bandpass of each KBr disk measured.

3.3.2. PLS treatment of FTIR data

A calibration set integrated by 4 matched standards with a constant mass of Cymoxanil of 4 mg and quantities of Mancozeb from 40 to 55 mg, and Kaolin from 56 to 41 mg was used for PLS modelization. FTIR spectral data were mean centered after the appropriate selection of the spectral region in terms of both, wavenumber range and peak area or peak height. Additionally, in order to establish the best calibration model, different criteria to select the internal standard spectral data (see Table 3) and the number of factors were selected, taking into consideration the minimum value of the predicted residual error sum of squares (PRESS) for cross validation.

As can be seen in Table 3, when a wide spectral range was selected, it was obtained an excessively high standard deviation, which indicates that the calibration set for matched standards is unable to reproduce exactly the matrix of samples. The most accurate results were obtained for the region between 1579 and 1269 cm^{-1} (corrected with a baseline between 1581 and 1269 cm^{-1}), in which the most important bands of Mancozeb are present, and employing as internal standard the peak height of Cymoxanil at 1705 cm^{-1} (baseline established between 1786 and 1689 cm^{-1}). Under these conditions a root mean square error of calibration (RMSEC) of 0.10% (w/w), an accuracy relative error of 0.6% (w/w) and a precision, as relative standard deviation, of 1.3% were found for a sample con-

Table 3
Analytical features of the different regions employed in PLS calibration for Mancozeb determination in solid samples and using Cymoxanil as internal standard

Data employed					Analytical characteristics found			
Mancozeb		Internal standard			Factors[a]	Calibration error[b]	Mancozeb concentration[c]	E_r (%)[d]
Measurement region (cm^{-1})	Baseline (cm^{-1})	Measurement mode	Wavenumber (cm^{-1})	Baseline (cm^{-1})				
1581–399	1583	Height	1705	1786–1689	5	0.07	50 ± 30	8
1581–399	1583	Area	1713–1695	1786–1689	5	0.03	50 ± 30	8
1579–1269	1581–1269	Area	1713–1695	1786–1689	3	0.08	47.0 ± 1.5	1.2
1579–1269	1581–1269	Height	1705	1786–1689	3	0.10	46.8 ± 0.6	0.6
1581–1471	1583–1471	Height	1705	1786–1689	3	0.09	49 ± 2	5
1578–841	1578–841	Height	1705	1786–1689	3	0.11	48.6 ± 0.4	4
1577–1520	1577–1452	Height	1705	1786–1689	4	0.25	42 ± 7	−10

[a] The number of factors was chosen in order to obtain the minimum PRESS.
[b] Calibration mean error was found from the cross-validation for a set of standards with ratios between Mancozeb and Cymoxanil from 8.9 to 12.9.
[c] Results obtained for a Mancozeb concentration in terms of % (w/w) ± the corresponding standard deviation of 3 analysis.
[d] Accuracy error in % calculated for 3 independent determination of Mancozeb samples containing 46.5% (w/w).

taining 46.5% (w/w) Mancozeb and 4% (w/w) Cymoxanil.

4. Conclusions

The proposed calibration strategies for FTIR Mancozeb determination in different types of fungicide formulations, based on the use of KBr disks and absorbance bands ratio respect to different internal references, provide comparable results to those reported by the manufacturer with relative errors which varied from +0.8 to −3.0% (w/w). The methodologies developed are adequate for quality control of these fungicide formulations and provided the first precedent on the use of FTIR for the determination of Mancozeb.

The developed methods do not require any chemical pretreatment of samples. The use of reagents is reduced to the minimum because samples were processed without solvents, except in the case of PLS calibration with matched standards for prediction of Mancozeb concentration in samples containing Cymoxanil, in which case this latter compound, used as internal reference, must be determined separately by leaching with 3 ml $CHCl_3$.

On comparing the different strategies assayed, it can be concluded that the use of an internal standard, added to both, samples and standards, could be the simplest methodology but it requires the presence of a well defined and not interfered analyte band. However, it is clear from the examples provided through this study that for complex formulations it is not a good alternative.

The use of a sample component, as internal reference, involves the need of a separate determination of the concentrations of the reference compound. However, the use of the standard addition methodology avoids this problem, but increases the sample manipulation.

In this study we have presented different strategies for FTIR analysis of pesticides that can not be measured in solution and we let in the hands of the reader to choose the most appropriate strategy to be adopted as a function of sample composition and facilities to find an internal standard or to carry out additional determinations.

In fact, all the strategies commented here increase the applicability of traditional FTIR measurements on KBr disks from qualitative purposes to quantitative exploration of samples and offer a good alternative for the analysis of low soluble active ingredients like Mancozeb in pesticide formulations.

Acknowledgements

Authors acknowledge the financial support of the Generalitat Valenciana Project GV04B-247 and Grupos 03/118 to carry out this study. S. Armenta also acknowledges the FPU Grant of the Ministerio de Educación, Cultura y Deporte (Ref. AP2002-1874).

References

[1] M. de la Guardia-Cirugeda, J.L. Carrión-Dominguez, J. Medina-Escriche, Analyst 109 (1984) 457.
[2] J.L. Carrión-Dominguez, S. Sagrado, M. de la Guardia-Cirugeda, Anal. Chim. Acta 185 (1986) 101.
[3] Z.A. de Benzo, C. Gómez, S. Menéndez, M. de la Guardia-Cirugeda, A. Salvador, Microchem. J. 40 (1989) 271.
[4] J.V. de Julián-Ortiz, M. de la Guardia-Cirugeda, Can. J. Spectrosc. 25 (1990) 44.
[5] S. Garrigues, M. de la Guardia, Anal. Chim. Acta 242 (1991) 123.
[6] F. Bosch-Reig, J.V. Gimeno-Adelantado, M.C.M. Moya-Moreno, Talanta 58 (2002) 811.
[7] S. Garrigues, M. de la Guardia, Analyst 116 (1991) 1159.
[8] D.A. Cronin, K. MaKenzie, Food Chem. 35 (1990) 39.
[9] S. Haridoss, R. Tobazeon, J.P. Crine, Appl. Spectrosc. 42 (1988) 186.
[10] Environmental Protection Agency (USA). Health and environmental effects profile for Mancozeb, Report No. EPA/600/X-84/129.
[11] C. de Liñan, Vademecum de productos fitosanitarios y nutricionales, Ed. Agrotécnica S.L., Madrid, 2000.

[12] J.E. Woodrow, J.N. Seiber, D. Fitzell, J. Agric. Food Chem. 43 (1995) 1524.
[13] E.D. Caldas, M.H. Conceiçao, M.C.C. Miranda, L.C.K.R. de Souza, J.F. Lima, J. Agric. Food Chem. 49 (2001) 4521.
[14] A. Zena, P. Conte, A. Piccolo, Fresenius Environ. Bull. 8 (1999) 116.
[15] H. van-Lishaut, W. Schwack, J. AOAC. Int. 83 (2000) 720.
[16] C.C. Lo, M.H. Ho, M.D. Hung, J. Agric. Food Chem. 44 (1996) 2720.
[17] Collaborative International Pesticides Analytical Council (CIPAC) Handbook, CIPAC Ltd., Cambridge, UK, 1994.
[18] K.K. Sharma, S. Gupta, S.K. Handa, Talanta 44 (1997) 2075.
[19] A. Datta, M. Gopal, Bull. Environ. Contam. Toxicol. 62 (1999) 496.
[20] M.J. Almond, S.J. Knowles, Appl. Spectrosc. 53 (1999) 1128.
[21] M. Gallignani, S. Garrigues, A. Martinez-Vado, M. de la Guardia, Analyst 118 (1993) 1043.
[22] S. Armenta, G. Quintás, J. Moros, S. Garrigues, M. de la Guardia, Anal. Chim. Acta 468 (2002) 81.
[23] G. Quintas, S. Armenta, A. Morales-Noe, S. Garrigues, M. de la Guardia, Anal. Chim. Acta 480 (2003) 11.
[24] G. Quintás, A. Morales-Noe, S. Armenta, S. Garrigues, M. de la Guardia, Anal. Chim. Acta 502 (2004) 213.
[25] A.R. Cassella, R.J. Cassella, S. Garrigues, R.E. Santelli, R.C. de Campos, M. de la Guardia, Analyst 125 (2000) 1829.
[26] A.R. Cassella, S. Garrigues, R.C. de Campos, M. de la Guardia, Talanta 54 (2001) 1087.
[27] D. Lin-Vien, N.B. Colthup, W.G. Fateley, J.G. Grasselli, Infrared and Raman Characteristic Frequencies of Organic Molecules, Academic Press, London, 1991.
[28] United States Environmental Protection Agency. Office of Prevention, Pesticides and Toxic Substances (7501C), 1998.http://www.epa.gov/opprd001/factsheets/cymoxanil.pdf.

Fourier transform infrared spectrometric strategies for the determination of Buprofezin in pesticide formulations

Sergio Armenta, Guillermo Quintás, Javier Moros, Salvador Garrigues and Miguel de la Guardia
Department of Analytical Chemistry, Universitat de València. Edifici Jeroni Muñoz, 50th Dr Moliner, 46100 Burjassot, Valencia, Spain.

Analytica Chimica Acta 468 (2002) 81-90.

Impact factor of this journal (2004): 2.588
Source: Journal citation reports ISI Web of Knowledge, 2004.

ELSEVIER

Analytica Chimica Acta 468 (2002) 81–90

ANALYTICA CHIMICA ACTA

www.elsevier.com/locate/aca

Fourier transform infrared spectrometric strategies for the determination of Buprofezin in pesticide formulations

Sergio Armenta, Guillermo Quintás, Javier Moros, Salvador Garrigues*, Miguel de la Guardia

Department of Analytical Chemistry, University of Valencia, Edifici Jeroni Muñoz, 50 Dr. Moliner, 46100 Burjassot, Valencia, Spain

Received 19 March 2002; received in revised form 13 June 2002; accepted 9 July 2002

Abstract

Two different strategies for Buprofezin determination, an off-line extraction and stopped-flow determination and an automated procedure, based on the on-line extraction of Buprofezin samples with chloroform and flowing action analysis–fourier transform infrared (FIA–FT-IR) spectrometric measurement of the extracts, have been developed. For the treatment of the off-line extraction mode, data a three-factor partial least squares (PLSs) calibration was developed, using the region from 1465.7 to 1342.3 cm^{-1} with a single point baseline defined at 2051.9 cm^{-1} and based on the use of chloroform solutions of Buprofezin. The method provides a R.S.D. <0.1%, recoveries of the order of 100% and generates 25 ml of $CHCl_3$ waste for each sample.

On the other hand, the recommended FIA method provided a 3 s limit of detection of 20 $\mu g\,ml^{-1}$, which corresponds to 0.12% (w/w) in the solid sample, a repeatability of 0.8% as R.S.D., and a maximum sampling frequency for the whole procedure of 6 h^{-1}.

The waste generation, being lower than the off-line strategy, is only 3 ml of $CHCl_3$ per sample.

Keywords: Buprofezin; Fourier transform infrared spectrometry; Flow injection analysis; Stopped-flow; Partial least squares; Pesticide

1. Introduction

Buprofezin (2-*tert*-butylimino-3-isopropyl-5-phenyl-1,3,5-thiadiazinan-4-one) is an insecticide and acaricide with persistent parvicidal action against Homopterasome coleoptera and acarina, also effective against leafhoppers in rice and potatoes, whitefly in citrus plants, cotton and vegetables, coccidae, diaspididae (scale insects) and pseudococcidae (mealybugs) in citrus plants. It is also an insecticide with contact and stomach side effects [1].

Buprofezin is manufactured in several commercially available pesticide formulations as wetting powder in a concentration of 25% (w/w) or as emulsifiable concentrate with a concentration of 8% (w/w) and combined with methyl pirimiphos at 40% (w/w) [1]. Buprofezin determination can be carried out in different types of samples by liquid chromatography (LC) [2,3], and gas chromatography with electron capture detection [4], nitrogen–phosphorous detection [4,5] or mass spectrometric detection [6], but there is no specific procedure for Buprofezin quality control in pesticide formulations.

In spite of the fact that the main methods proposed in the literature for the determination of Buprofezin are based on chromatographic strategies, it is clear

* Corresponding author. Tel.: +34-96-3864838; fax: +34-96-3983158.
E-mail address: salvador.garrigues@uv.es (S. Garrigues).

0003-2670/02/$ – see front matter © 2002 Elsevier Science B.V. All rights reserved.
PII: S0003-2670(02)00656-6

that, for pesticide formulations, direct spectrometric measurements could be a good alternative. The presence of an aromatic ring in the structure of Buprofezin could be used to develop a simple UV–VIS spectrophotometric method. However, the presence of surfactant molecules in commercial formulations and the sensitivity of UV–VIS measurements, involve operational difficulties.

On the other hand, the Buprofezin absorption bands in the mid-infrared (IR) region, from 1850 to 950 cm^{-1}, as well as its concentration range in market samples, make Fourier transform (FT-IR) spectrometry an appropriate technique for the quantification of this analyte in commercial pesticide formulations. Despite this, there is no precedent of any method for the analysis of this kind of samples using FT-IR spectrometry.

The high solubility of Buprofezin in chloroform, and its transparency in the mid-IR region make this solvent suitable for FT-IR determination of Buprofezin. However, the use of chlorinated solvent must be reduced because of their ozone layer depleting action and thus, methodologies developed must reduce, as much as possible, the amount of $CHCl_3$ required. From the pioneering works of Morgan et al. [7] and Curran and Collier [8], the use of flow injection methodology, combined with IR detection, has contributed to the automation of FT-IR measurements [9], involving a strong reduction of the amounts of reagents consumed and waste generation [10]. It also reduces the handling of samples, and thus a mechanised flow procedure could be very convenient as has been previously shown [11–13].

The main objective of this work is the development of an FT-IR method for Buprofezin determination in pesticide formulation, and thus a comparison has been made between strategies in order to be able to carry out this determination in the best conditions from both aspects, the analytical figures of merit and the environmental side effects.

2. Experimental

2.1. Apparatus and reagents

A Nicolet Magna 750 FT-IR spectrometer (Madison, WI, USA), equipped with a temperature-stabilised deuterated tryglycine sulphate (DGTS) detector, was employed for spectral measurements, using a 0.11 mm pathlength micro-flow cell (Graseby-Specac, Orpington, UK) with ZnSe and CaF_2 windows.

Spectra treatment and data manipulation have been carried out using Omnic 2.1 and QuantIR 1.2 software from Nicolet.

To carry out the on-line extraction and flowing action analysis–fourier transform infrared (FIA–FT-IR) determination of Buprofezin, the manifold depicted in Fig. 1 was built up by employing two six-way Rheodyne 5041 injection valves (Cotati, CA) and two Gilson Minipuls 2 peristaltic pumps (Villiers-le-Bel, France) furnished with Viton (iso-versinic) tubes (1 mm i.d. and 3 mm o.d.). One of the pumps was employed to assure the carrier flow and sample or standard injection, and a second-one to made a closed-flow extraction unit in which the Buprofezin leaching with $CHCl_3$ could be carried out. A sample syringe and a mixing syringe provided an appropriate volume of the closed-flow system to assure sample stirring. The connecting tubes employed were made of PTFE of 0.8 and 1.5 mm i.d. The filtration unit incorporated a polyethylene filter. A debubbler was installed ahead of the measurement cell in order to avoid the presence of bubbles. The six-way valves were used to select sample and standard injection and to insert a selected volume of the extracted sample in to the carrier stream.

An ultrasonic water bath (J.P. Selecta, Barcelona, Spain) and a Vortex shaker (Velp Scientifica, Milano, Italy) were employed for shaking of samples during the off-line extraction.

Buprofezin standard (99.4% (w/w)) was supplied by Fluka (Buchs, Switzerland). Analytical grade chloroform stabilised with 150 mg l^{-1} of amylene (Scharlau, Barcelona, Spain), was employed for the preparation of samples and standards.

Buprofezin 25% (w/w) wetting powder commercial formulations were obtained from the Spanish market.

2.2. Off-line procedure

An amount of 30 mg of sample were dissolved in 25 ml of $CHCl_3$ by 10 min shaking in an ultrasonic water bath. This solution was passed through a 0.22 μm nylon filter and afterwards it was introduced in the measurement cell by a peristaltic pump. After a few seconds, the flow was stopped and the FT-IR spectra

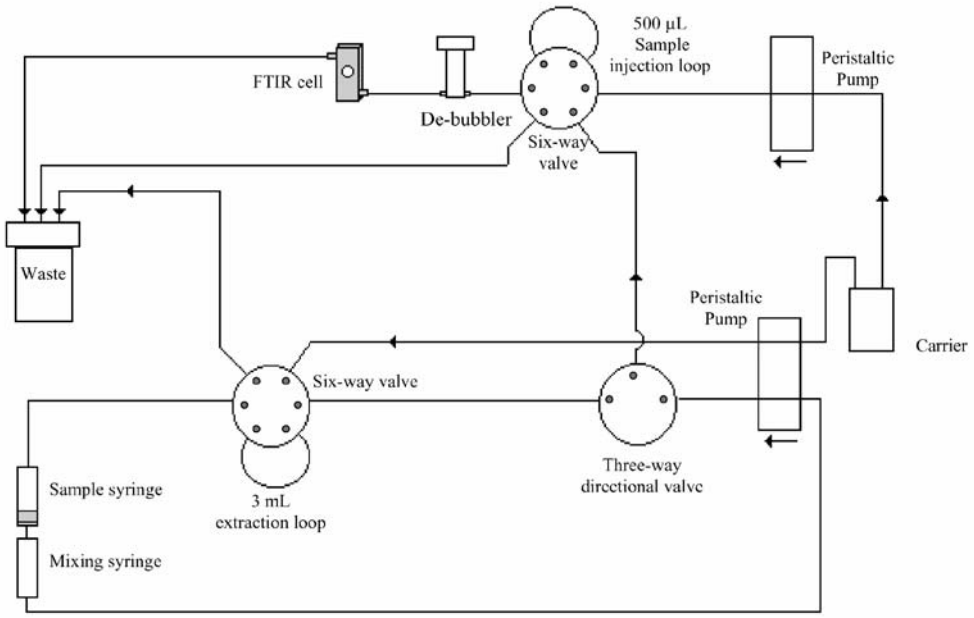

Fig. 1. Manifold employed for FIA–FT-IR Buprofezin determination in commercial pesticide samples.

were obtained from 4000 to 900 cm^{-1}, using a nominal resolution of 4 cm^{-1} and accumulating 25 scans, using a background spectrum of $CHCl_3$ measured under the same conditions.

The concentration of Buprofezin in samples was calculated by partial least squares (PLSs) using a calibration set made from pure solutions of Buprofezin in $CHCl_3$, being employed in the spectral range from 1466 to 1342 cm^{-1}, corrected with a single point baseline defined at 2052 cm^{-1}.

2.3. Flow injection (FI) procedure

An amount of 40 mg of sample was accurately weighted in a polypropylene syringe barrel of 3 ml internal volume placed between two polyethylene filters; 3 ml of chloroform was added. The polypropylene syringe barrel was placed in the FIA manifold (see Fig. 1) and $CHCl_3$ was circulated at 1.68 ml min^{-1} in a closed system for 6 min. After that, a 500 µl extract volume was sampled, by using the sample loop of an injection valve, and then injected into a chloroform carrier stream of 0.56 ml min^{-1}. The FT-IR spectra, between 4000 and 900 cm^{-1}, were continuously recorded as a function of time, using a nominal resolution of 4 cm^{-1} and accumulating two scans per point. Analytical measurements for Buprofezin were carried out as a function of time (chemigram) in the range 1415 to 1349 cm^{-1} with a baseline defined between 1417 and 1347 cm^{-1}. The chemigram peak height values obtained for samples were interpolated in an external calibration line established from the injection of 500 µl standard solutions of Buprofezin directly prepared in chloroform and measured under the same conditions as samples.

3. Results and discussion

3.1. FT-IR transmittance spectrum of Buprofezin

Fig. 2 shows the spectra, in the wavenumber range from 2100 to 1000 cm^{-1}, of a Buprofezin standard chloroformic solution of 0.67 mg g^{-1} and an

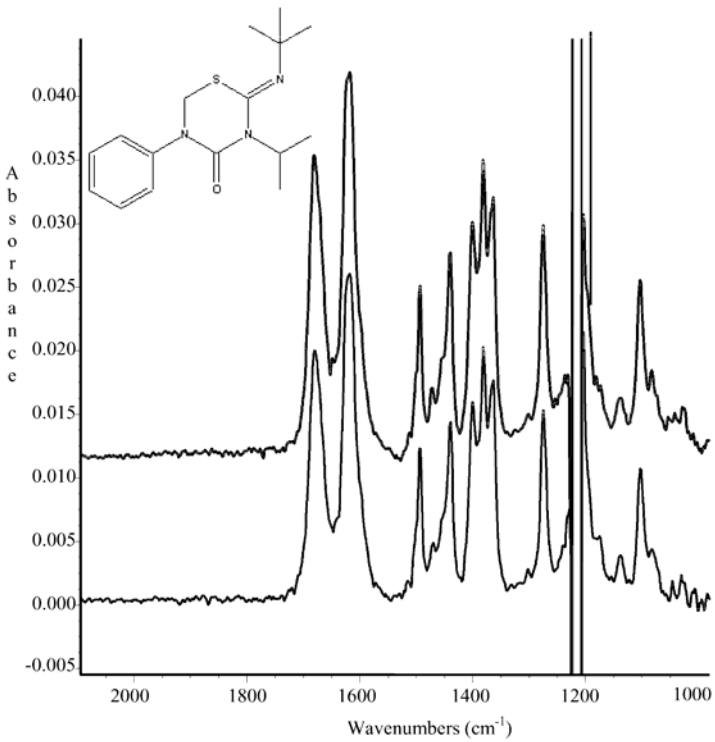

Fig. 2. FT-IR spectra of Buprofezin standard (bottom) and pesticide sample, extracted with $CHCl_3$ (top) as indicated in the recommended procedure. Buprofezin standard concentration: 0.67 mg g^{-1} and Buprofezin concentration of insecticide: 25% (w/w) equivalent to 0.80 mg g^{-1} in chloroform solution.

insecticide sample extract containing 0.80 mg g^{-1} Buprofezin. As can be seen the spectra of sample and standard are very similar and present the same bands. The more intense bands were the carbonyl band at 1681 cm^{-1}, that of 1620 cm^{-1} due to the stretching of the imine group, those at 1493, 1440 and 1400 cm^{-1}, corresponding to the benzene ring stretching, and the bands at 1381, 1364 and 1275 cm^{-1}, which correspond to *tert*-butyl stretching bands [14].

3.2. Effect of measurement conditions on Buprofezin determination

The effect of the number of accumulated scans and the nominal resolution employed for data acquisition was evaluated in order to improve the measurement conditions. The number of accumulated scans per spectrum was changed from 5 to 75, and the nominal resolution varied from 1 to 16 cm^{-1}.

As can be seen in Table 1, working with peak area values between 1415 and 1349 cm^{-1}, which include the three peaks at 1401, 1380 and 1364 cm^{-1}, the more intense signals were found for a 4 cm^{-1} nominal resolution these values also corresponding to the best repeatability. On the other hand, it can be seen that the most intense and precise results were those obtained when accumulating 75 scans with an acquisition time of 92 s, but in order to ensure a compromise between measurement frequency and precision values, 25 accumulated scans was selected that provide a three

Table 1
Effect of nominal resolution and number of accumulated scans

Nominal resolution (cm^{-1})[a]	Peak area ±S.D.	R.S.D. (%)	Data spacing (cm^{-1})	Number of scans[b]	Peak area ±S.D.	R.S.D. (%)	Time (s)
1	1.57 ± 0.02	1.3	0.482	5	1.49 ± 0.01	1.0	6
2	1.645 ± 0.007	0.5	0.964	10	1.46 ± 0.01	1.0	12
4	1.658 ± 0.001	0.1	1.928	25	1.53 ± 0.02	1.0	30
8	1.63 ± 0.01	0.7	3.857	50	1.485 ± 0.006	0.4	61
16	1.503 ± 0.007	0.4	7.714	75	1.552 ± 0.002	0.1	92

Peak area values from 1415 to 1349 cm^{-1} established using a baseline defined between 1417 and 1347 cm^{-1} obtained for a Buprofezin standard in $CHCl_3$.
[a] Data reported correspond to an accumulated number of 25 scans for a concentration of 1.67 mg g^{-1} Buprofezin.
[b] Data reported was found for a 4 cm^{-1} resolution and for a concentration of 1.55 mg g^{-1} Buprofezin.

times faster spectral recording than the accumulation of 75 scans.

3.3. Selection of FT-IR bands for Buprofezin determination

The purpose of this study was to find the peak or spectral region which provides the best sensitivity and repeatability for Buprofezin determination. Two different calibration strategies were tested, classical least squares and partial least squares. Table 2 shows the main figures of merit of different external calibration line obtained from the main Buprofezin bands in the region from 2000 to 1250 cm^{-1}. It can be seen from these equations that the use of peak area values provides the most sensitive procedures. On the other hand, it can be seen from the accuracy errors found in the analysis of a commercial sample containing 25% (w/w) Buprofezin that the use of area measurements is more accurate than measurements based on peak height.

Samples analysed contain calcium carbonate and propylene glycol monooleate, this latter compound being partially soluble in some organic solvents. The excess errors obtained in all cases for samples probably were due to the presence of the surfactant in the formulation composition.

In short, the use of the band between 1415 and 1349 cm^{-1} with a baseline fixed between 1417 and 1347 cm^{-1} gave a sensitivity of 0.94 area units mg^{-1} g

Table 2
Analytical features of different external calibration lines employed for the stopped-flow determination of Buprofezin

Band	Baseline	Calibration curve[a]		R^2	E_r[b] (%)	LOD[c]
		Intercept ± S.D.	Slope ± S.D.			
H[d]: 1682	1830	0.0004 ± 0.0002	0.0366 ± 0.0002	0.9998	8	0.0007
H: 1620	1830	−0.0001 ± 0.0001	0.0391 ± 0.0002	0.9992	6	0.01
H: 1401	1830	0.0004 ± 0.0002	0.0217 ± 0.0003	0.9998	28	0.006
H: 1364	1830	0.0000 ± 0.0001	0.0241 ± 0.0002	0.9994	15	0.007
H: 1275	1830	0.0001 ± 0.0002	0.0204 ± 0.0002	0.9994	26	0.008
A[e]: 1685–1675	1830	−0.004 ± 0.002	0.271 ± 0.003	0.999	3.2	0.008
A: 1415–1349	1417–1347	0.078 ± 0.007	0.940 ± 0.008	0.9994	2.0	0.005
A: 1624–1614	1830	0.002 ± 0.007	0.361 ± 0.009	0.993	6	0.003
A: 1406–1359	1420–1341	0.010 ± 0.003	0.953 ± 0.004	0.9999	8	0.003

[a] Calibration curve obtained for five standards of Buprofezin at concentrations from 0.33 to 1.34 mg g^{-1}.
[b] Accuracy error in% calculated for three independent determinations of a Buprofezin sample containing 25% (w/w).
[c] Limit of detection established for six independent measurements of a blank solution and a probability level of 99.6% ($k = 3$).
[d] Peak height values.
[e] Peak area values.

and accuracy errors of the order of +2%, thus, are of the same order as the precision expected for instrumental analysis, and a limit of detection of 5 $\mu g\,g^{-1}$, which corresponds to 0.4% (w/w) Buprofezin in pesticide formulations, for a sample mass of 40 mg which can be evaluated by carrying out the extraction of increasing amounts of sample.

Alternatively, the possibility of a PLS treatment of FT-IR data, was evaluated based on the use of a calibration set of $CHCl_3$ solutions of Buprofezin and evaluating the prediction capability of the system for the analysis of extracts from formulations.

In Table 3 are represented the main analytical features of the different wavenumbers ranges and baseline correction criteria employed for PLS calibration in the stopped-flow determination of Buprofezin. The accuracy relative errors were, in general, lower than those found previously for external calibration and with cross-validation mean calibration errors ranging from 0.0001 to 0.04 $mg\,g^{-1}$, having obtained standard variation values from 0.003 to 0.03 $mg\,g^{-1}$ for a pesticide sample solution of 0.789 $mg\,g^{-1}$ Buprofezin.

As can be seen, when the region selected was from 4000 to 1000 cm^{-1} both calibration and relative errors were higher than those obtained when the range selected was narrower. This fact is due to the presence of the window cell absorption bands and the incomplete transparency of $CHCl_3$. These problems could be avoided by eliminating the aforementioned regions, and thus results could be improved, as is shown in Table 3.

The best results were obtained when the region selected was from 1466 to 1342 cm^{-1}, corrected using a horizontal baseline defined at 2052 cm^{-1}, for which can be found an R.S.D., calibration error and accuracy relative error of 0.5%, 0.002 $mg\,g^{-1}$ and 2% respectively. In this case, the number of factors selected was 3, which evidences the absence of matrix or blank contributions found for the use of wide range wavenumber data.

Univariate calibration and PLS data treatment in all cases provide excess errors as compared with declared concentration. However, the relative error of +2%, obtained under best conditions, is compatible with the fact that in pesticide manufacture Buprofezin is added in excess in order to compensate possible degradation of this active principle during storage stage and to assure the nominal content in the final product.

3.4. Off-line extraction of Buprofezin

The extraction of Buprofezin in to $CHCl_3$ was carried out using two different shaking modes, ultrasonic and mechanical the shaking time needed to achieve a quantitative extraction of Buprofezin with 25 ml of $CHCl_3$ from 30 mg of sample being evaluated in every case. As depicted in Fig. 3, mechanical shaking

Table 3
Analytical features of different wavenumbers ranges employed for PLS calibration in the stopped-flow determination of Buprofezin

Data employed (cm^{-1})				Analytical characteristics found			
Region start	Region stop	Baseline start	Baseline stop	Factors[a]	S.D.[b]	Calibration error[c]	E_r[d] (%)
4000	1001	4000	1000	8	0.03	0.04	10
3113	1242	3237	993	9	0.002	0.0005	4
3217	1236	3217	–	11	0.006	0.0000	4
1707	1231	1894	–	5	0.003	0.001	4
1707	1578	1894	–	9	0.003	0.0000	4
1639	1574	1894	–	9	0.01	0.0001	4
1423	1350	2081	1009	3	0.003	0.006	4
1466	1342	2052	–	3	0.004	0.002	2
1508	1261	2081	1009	5	0.007	0.002	5
1506	1340	2081	1009	3	0.004	0.006	3

[a] The number of latent variables was chosen in order to obtain the minimum PRESS.
[b] S.D. ($mg\,g^{-1}$) calculated for the repeatability of results found for three independents determinations of a sample solution of 0.79 $mg\,g^{-1}$ Buprofezin.
[c] Absolute mean calibration error for a cross-validation.
[d] Relative error (%) found compared to those reported by the manufacturer.

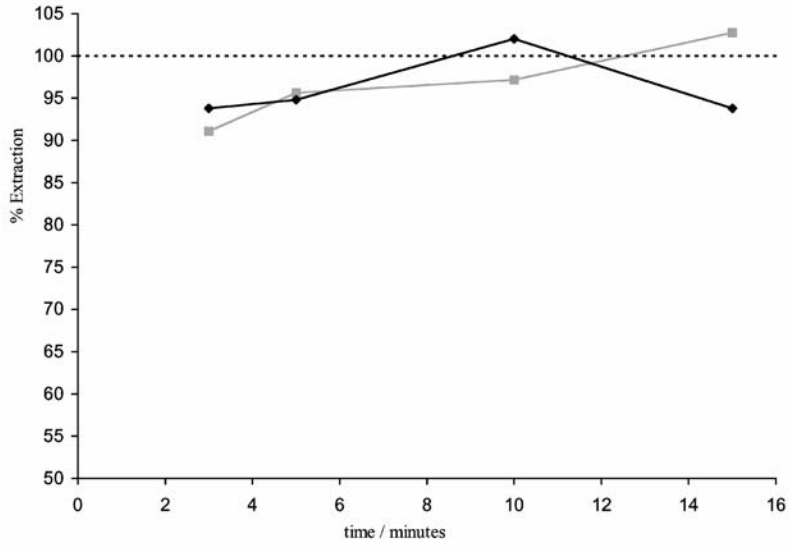

Fig. 3. Recovery of Buprofezin as a function of shaking time for the extraction with $CHCl_3$ of 30 mg of a sample containing 25% (w/w) pesticide, by employing ultrasonic (◆) and mechanical (▩) shaking.

needs more time than the ultrasonic mode to achieve a total extraction of Buprofezin and, additionally, less repetitive results were found. Because of that, sonication was selected as the extraction mode most convenient for Buprofezin determination, as it gave the best extraction for 10 min shaking. However, for a shaking time of 15 min a reduction on FT-IR band intensity, was found which probably indicates that free radicals generated in the system could affect the stability of the pesticide, as was observed in previous studies [11].

3.5. Off-line PLS determination of Buprofezin

From FT-IR absorbance spectra obtained between 4000 and 900 cm^{-1} for a calibration set of five Buprofezin standard solutions in $CHCl_3$, data were mean centred, the spectral region defined according to results reported in Table 3 and the number of factors selected by cross-validation using the minimum value of the predicted residual error sum of squares (PRESS) criterion. Calibration models for different spectral regions were considered and for a region between 1455 and 1342 cm^{-1}, corrected with a baseline established at 2052 cm^{-1}, a minimum PRESS of 0.0036 was obtained when three factors were selected, explaining more than 99.9% of the variance.

Repeatability, calibration error and accuracy of the different PLS models assayed are depicted in Table 3. To assure that the procedure was free from matrix effect, a recovery assay was carried out. Different amounts of Buprofezin standard from 5.18 to 11.93 mg were added to commercial formulations of this insecticide and recoveries from 100.5 ± 0.6 to 97.1 ± 0.6% were found. The mean recovery was statistically equal to 100% thus indicating that the developed method provides precise and accurate results in product analysis.

3.6. Effect of FIA variables on the determination of Buprofezin

In order to develop a fully mechanised procedure for FT-IR determination of Buprofezin, the FIA

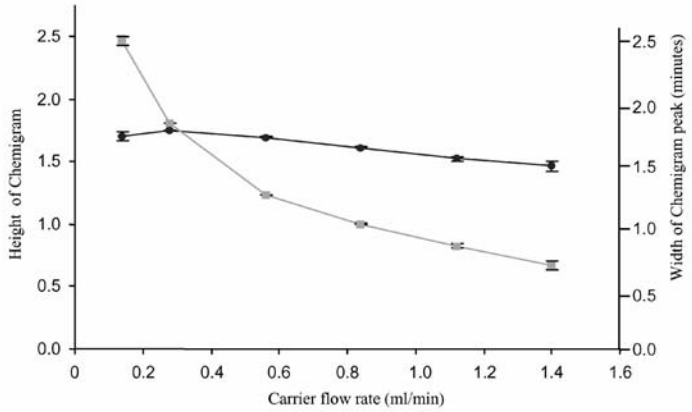

Fig. 4. Effect of $CHCl_3$ carrier flow rate on the FIA–FT-IR determination of Buprofezin. Experimental conditions: 3.16 mg ml^{-1} Buprofezin standard solution in $CHCl_3$. Height values in arbitrary units (●) are the averages of three independent measurements, accumulating two scans at a resolution of 4 cm^{-1}. The time (▣) in minutes correspond to the width of the chemigram base peak.

approach was assayed. The carrier flow rate and the volume of sample injected in the FIA manifold affect the sensitivity and reproducibility of the procedure, so the effect of both parameters was evaluated.

In a previous study different flow rates, from 0.14 to 1.12 ml min^{-1}, for a fixed sample volume of 500 μl, and sample volumes, from 100 to 1000 μl, for a fixed carrier of 0.56 ml min^{-1}, were tested and the peak areas between 1415 and 1349 cm^{-1}, using a baseline defined from 1417 to 1347 cm^{-1}, were measured to create the corresponding transient chemigrams.

As can be seen in Fig. 4, the height of the chemigrams decreases on increasing the carrier flow rate and the width of the peaks also decreases on increasing the flow rate. So a compromise value must be selected in order to obtain the highest possible sensitivity with an appropriate sampling frequency. A carrier flow

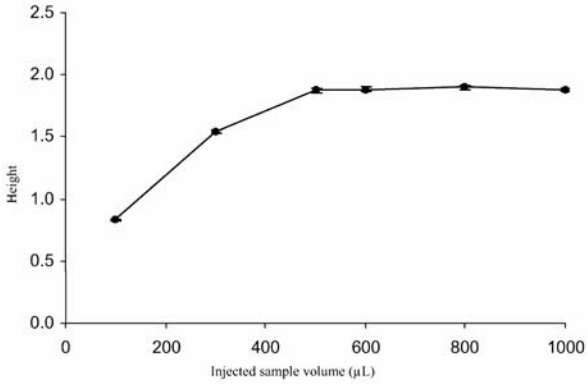

Fig. 5. Effect of the injected sample volume on the chemigram peak height measured for a 3.0 mg ml^{-1} Buprofezin standard by FIA–FT-IR.

rate of 0.56 ml min^{-1} was selected for the FIA–FT-IR determinations, giving a sampling frequency of 48 h^{-1}, a 46% higher than that achieved when the carrier flow rate was 0.28 ml min^{-1}, with a 3% decrease in the peak height signal.

On the other hand, Fig. 5 shows that the injection of a sample volume ≥500 μl provides the steady-state signal for a carrier flow of 0.56 ml min^{-1}. Thus, a 500 μl extract volume was selected.

3.7. On-line extraction of Buprofezin

A commercial pesticide, Buprofezin 25% (w/w) as a wetting powder was extracted on-line with 3 ml of $CHCl_3$, using the manifold depicted in Fig. 1, to evaluate the effect of the extraction flow rate, from 0.84 to 2.80 ml min^{-1}, on the time required to achieve a complete extraction of the pesticide and so to reach a steady-state signal (see Fig. 6).

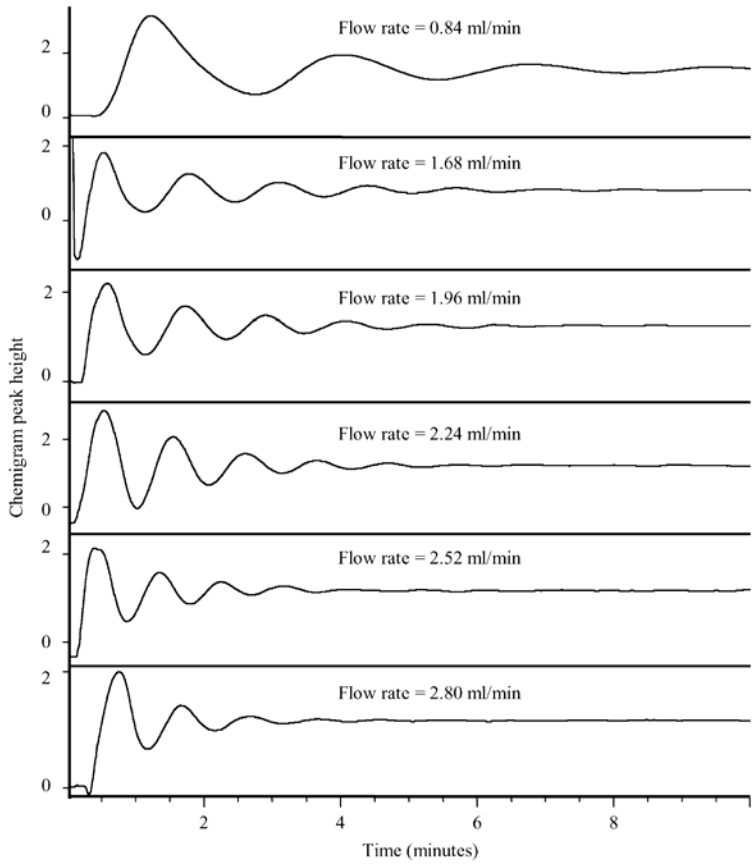

Fig. 6. Transient signals found during on-line extraction of Buprofezin with $CHCl_3$. Data were obtained for peak area measurements, as function of time established, from 1415 to1349 cm^{-1}, corrected using a baseline defined from 1417 to 1347 cm^{-1}, measured for a 40 mg sample containing Buprofezin 25% (w/w) and extracted with 3 ml of $CHCl_3$.

Fig. 6 shows that the time required for the quantitative extraction of Buporofezin decreases on increasing the extraction carrier flow rate. For an extraction, flow rate of 1.68 ml min^{-1}, 6 min was enough. To extract Buprofezin, the use of this flow rate avoids bubble formation inside the extraction manifold, thus increasing the reproducibility of the procedure and, because of that, it was selected for further experiments.

The use of an empty cartridge placed after the sample cartridge in the FIA manifold of Fig. 1 reduces the time needed to reach the steady state because has an effect similar to a mixing chamber, thus improving the homogenisation of the extracts and reducing bubble formation.

A minimum $CHCl_3$ extraction volume of 3 ml was chosen in order to ensure the correct transport through the closed extraction circuit and to be able to obtain three replicates of an injection volume of 500 μl for each extracted sample.

3.8. Analytical characteristics of FIA–FT-IR determination of Buprofezin

The sensitivity of the fully mechanised FIA–FT-IR analysis of Buprofezin corresponds to an absorbance of 0.584 mg^{-1} ml. Using the recommended procedure, the limit of detection was 20 μg ml^{-1}, which correspond to 0.12% (w/w) for a 30 mg sample, and provided a relative standard deviation of 0.8%. Buprofezin external calibration in the selected conditions gave ($n = 6$) the expression $A = [0.01 \pm 0.01] + [0.584 \pm 0.004]C$ (mg ml^{-1}) with $R^2 = 0.9994$, where A is the peak height absorbance, which is of the same order than that found for stopped-flow measurements.

3.9. Comparison between the different strategies tested

For a commercial sample containing 25% (w/w) Buprofezin, concentration values of 25.7 ± 0.5% and 25.5 ± 0.2% (w/w) were found for the FIA and stopped-flow PLS, respectively, thus, indicating that both strategies developed in this study provide accurate results for Buprofezin determination in commercial samples with relative errors <3%. However, the on-line extraction and FT-IR measurements compared with the stopped-flow PLS strategy involve a fully mechanised determination, which improves the productivity of laboratories (an analysis throughput of 6 h^{-1} instead of 4 h^{-1}) and reduces, as much as possible, the reagent consumption and waste generation (3 ml versus 25 ml for each sample extraction), also avoiding contact of operator with the pesticide.

Moreover, the processing time required for sample preparation by on-line extraction is less than that for off-line extraction, allowing faster Buprofezin determination way. So it can be concluded that the on-line extraction and FIA–FT-IR determination of Buprofezin is the best alternative for practical analysis.

Acknowledgements

Authors acknowledge the financial support of the Generalitat Valenciana Project GV01-249 and the grant provided by the Laboratorio de Higiene Laboral y Ambiental of the Universitat de Valencia to carry out this study.

References

[1] C. de Liñan, Vademecum de productos fitosanitarios y nutricionales, Editorial Agrotécnica S.L., Madrid, 2000.
[2] M. Nakamura, T. Suzuki, S. Yamada, Anal. Chim. Acta 428 (2001) 219.
[3] A. Kaihara, K. Yoshii, Y. Tsumura, Y. Nakamura, S. Ishimitsu, Y. Tonogai, J. Health Sci. 46 (2000) 336.
[4] M.C. Pablos-Espada, A. Garrido-Frenich, J.L. Martinez Vidal, P. Parrilla, Anal. Lett. 34 (2001) 597.
[5] P. Cabras, A. Angioni, V.L. Garau, F.M. Pirisi, F. Cabitza, M. Pala, Food Addit. Contam. 17 (2000) 855.
[6] H.J. Stan, J. Chromatogr. A 892 (2000) 347.
[7] D.K. Morgan, N.D. Danielson, J.E. Katon, Anal. Lett. 18 (1985) 979.
[8] D.J. Curran, W.G. Collier, Anal. Chim. Acta 177 (1985) 259.
[9] S. Garrigues, M. de la Guardia, Flow injection analysis. Fourier transform infrared spectroscopy (FIA–FT-IR), in: J.M. Chalmers, P.R. Griffiths (Eds.), Handbook of Vibrational Spectroscopy, Vol. 2, Wiley, Chichester, 2002, pp. 1661–1675.
[10] F. Cadet, M. de la Guardia, Infrared quantitative analysis, in: R.A. Meyers (Ed.), Encyclopedia of Analytical Chemistry, Wiley, Chichester, 2000. pp. 10879–10909.
[11] R. Cassella, R.J. Cassella, S. Garrigues, R.E. Santelli, R.C. de Campos, M. de la Guardia, Analyst 125 (2000) 1829.
[12] J.M. Garrigues, A. Pérez-Ponce, S. Garrigues, M. de la Guardia, Analyst 124 (1999) 783.
[13] Z. Bouhsain, J.M. Garrigues, S. Garrigues, M. de la Guardia, Vib. Spectrosc. 21 (1999) 143.
[14] D. Lin-Vien, N.B. Colthup, W.G. Fateley, J.G. Grasselli, Infrared and Raman Characteristic Frequencies of Organic Molecules, Academic Press, London, 1991.

FTIR approaches for Diuron determination in commercial pesticide formulations

Sergio Armenta, Guillermo Quintás, Asunción Morales, Salvador Garrigues and Miguel de la Guardia
Department of Analytical Chemistry, Universitat de València. Edifici Jeroni Muñoz, 50th Dr Moliner, 46100 Burjassot, Valencia, Spain.

Journal of Agricultural and Food Chemistry 53 (2005) 5842-5847.

Impact factor of this journal (2004): 2.327
Source: Journal citation reports ISI Web of Knowledge, 2004.

5842 J. Agric. Food Chem. 2005, 53, 5842–5847

JOURNAL OF AGRICULTURAL AND FOOD CHEMISTRY

FTIR Approaches for Diuron Determination in Commercial Pesticide Formulations

SERGIO ARMENTA, GUILLERMO QUINTÁS, ASUNCIÓN MORALES, SALVADOR GARRIGUES,* AND MIGUEL DE LA GUARDIA

Department of Analytical Chemistry, University of Valencia, Edifici Jeroni Muñoz, 50 Dr. Moliner, 46100 BURJASSOT, Valencia, Spain

Two strategies have been developed for Diuron determination by FTIR spectrometry, an off-line extraction and stopped-flow determination and a fully mechanized procedure, based on the on-line extraction of Diuron and FIA−FTIR measurement of the extracts. The aforementioned procedures have been compared with a reference chromatographic method. The off-line FTIR spectra were obtained at a nominal resolution of 4 cm^{-1} from 4000 to 900 cm^{-1} by accumulating 25 scans. Diuron was determined using peak height measurements at 1582 cm^{-1} corrected using a baseline defined between 1562 and 1614 cm^{-1}. The waste generation of the off-line procedure was 3.4 mL chloroform for each sample, and the method provided a LOD of 40 $\mu g\ g^{-1}$, corresponding to 0.8% (w/w) Diuron in the original sample. The fully mechanized FIA method provided a LOD of 35 $\mu g\ g^{-1}$, which corresponds to 0.7% (w/w) in the solid sample and a maximum sampling frequency of the whole procedure of 30 h^{-1}, with a waste generation of 9.3 mL per sample, taking into account the volume of $CHCl_3$ required for sample dissolution and that need as a carrier. All those methods consume less organic solvent than a HPLC method, which involves the use of 39 mL of acetonitrile per sample and a sampling frequency of 12 h^{-1}.

KEYWORDS: Diuron; FTIR determination; flow injection analysis; stopped-flow; pesticide formulations

1. INTRODUCTION

Diuron (3(3,4-dichlorophenyl)-1,1-dimethylurea) is a substituted urea herbicide used to control a wide variety of annual and perennial broadleaf and grassy weeds, as well as mosses. It is used on noncrop areas and many agricultural crops such as fruit, cotton, sugar cane, alfalfa, and wheat. Diuron works by inhibiting photosynthesis. Diuron is slightly toxic for mammalians, the oral LD_{50} in rats being 3400 mg/kg (*1*).

Diuron may be found in formulations as wettable powders (80% w/w) (*2*) and suspension concentrates (50% w/v) (*3*).

Diuron determination can be carried out in different types of samples by high performance liquid chromatography (HPLC) (*4*−*7*), capillary electrophoresis (*8*, *9*), gas chromatography with electron capture (*10*, *11*), or mass spectrometry detection (*12*, *13*).

FTIR spectrometry has been employed for the quantification of different active principles in commercially available pesticide formulations, such as carbaryl (*14*), buprofezin (*15*), fluometuron (*16*), folpet and metalaxyl (*17*), and chlorpyriphos-ethyl (*18*), showing the high suitability of FTIR to carry out this kind of analysis. However, to our knowledge, there is no precedent on the determination of Diuron by using FTIR spectrometry.

One of the main drawbacks of the FTIR spectrometry is the general use of chlorinated solvents because of their high toxicity and environmental damage. Despite this, there is a widespread use of this type of solvent because of their high transparency in the mid-IR range and the high solubility of a great number of pesticides in them. However, to develop low contaminant procedures, the chlorinated waste generation and the reagent consumption must be minimized.

The aim of this work was the development of fast and low waste generation procedures that may be able to carry out in a simple way the precise and accurate determination of Diuron (*19*) in commercial formulations without any previous clean up or chromatographic steps, suitable to be employed in both the manufacturing process and in the quality control of finished products. In this sense, we propose a direct extraction of Diuron from agrochemicals using a reduced volume of chloroform and, after off-line filtration, its transport and introduction in a microflow cell and FTIR measurement in the stopped-flow mode. Alternatively, to reduce the sample manipulation and the operator exposition with the pesticide and chlorinated solvent, a mechanized approach, based on sample extraction in a vial followed by on-line filtration and continuous flow measurement, is also proposed to improve green analytical chemistry.

2. EXPERIMENTAL PROCEDURES

2.1. Apparatus and Reagents. A Nicolet (Madison, WI) Magna 750 FTIR spectrometer, equipped with a temperature-stabilized deuterated tryglycine sulfate (DTGS) detector, was employed for spectral

* Corresponding author. E-mail: salvador.garrigues@uv.es.

10.1021/jf050268f CCC: $30.25
Published on Web 06/28/2005

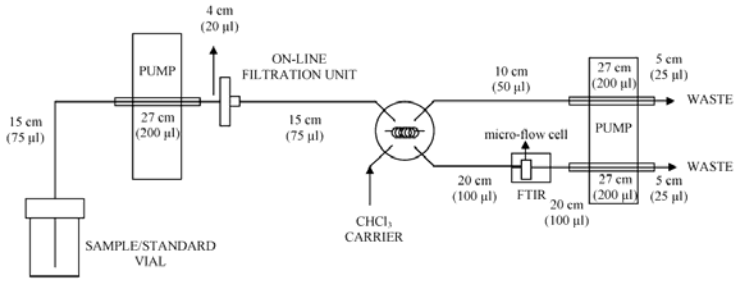

Figure 1. Manifold employed for the FIA–FTIR determination of Diuron in commercial pesticide formulations. Lengths of connections and an estimation of the internal volumes (values between parentheses) are indicated.

measurements, using a Specac (Orpington, UK) 10450 series microflow cell, with a ZnSe and CaF_2 window and a path length of 0.11 mm, that provides an internal volume of 5.5 μL. Spectra treatment and data manipulation have been carried out using Omnic 2.1 and QuantIR 1.2 software from Nicolet (Madison, WI).

To carry out the on-line extraction and FIA−FTIR determination of Diuron, the manifold depicted in **Figure 1** was made by employing a six-way Rheodyne 5041 injection valve (Cotati, CA) and two Gilson Minipuls peristaltic pumps (Villiers-le-Bel, France) furnished with Viton (iso-versinic) tubes (1 mm i.d. and 3 mm o.d.) placed before the filtration unit and after the measurement cell, to perform the Diuron extraction with $CHCl_3$ and sample transport and the carrier aspiration through the system while avoiding bubble formation. The connecting tubes employed in the setup were made of PTFE with a 0.8 mm i.d., and their lengths were adjusted to reduce the internal volume of the manifold. The filtration unit was made with a polypropylene 13 mm diameter syringe filter with a porous size of 0.45 μm. The six-way valve was used to select sample and standard injections and to insert a selected volume in the carrier stream.

A Hewlett-Packard HPLC Series 1050 high performance liquid chromatograph, equipped with a Kromasil C-18 column of 250 mm length and 4.6 mm i.d. with a 5 μm particle diameter was used. A variable wavelength UV−vis detector was employed for the analysis of Diuron formulations, this methodology being used as a reference procedure for the validation of FTIR measurements.

A Hewlett-Packard 8452 diode array spectrophotometer was employed for the measurements of UV spectra of Diuron standards.

The Diuron standard (99.4% w/w) was supplied by Fluka (Buchs, Switzerland). Analytical grade chloroform, stabilized with 150 mg L^{-1} amylene, was supplied by Scharlau (Barcelona, Spain) and employed for the preparation of samples and standards.

Wetting powder samples 1−3 were obtained directly from the Spanish market, containing approximately 80% w/w Diuron. Sample 4 was prepared from sample 1 by the addition of $CaCO_3$ with a final concentration of 40% Diuron. Sample 5, with a final content of 20% Diuron, was made from sample 2 by adding $CaCO_3$ and propylene glycol monooleate.

2.2. Reference HPLC Procedure. A total of 10 mg of sample was accurately weighed inside a 25 mL volumetric flask and diluted to the volume with CH_3CN. One milliliter of the slurry was diluted to 10 mL with CH_3CN and filtered through a 0.22 μm nylon filter. Twenty microliters of this solution was directly injected in a 85:15 acetonitrile/water mobile phase of 1 mL min^{-1}, and Diuron was determined in the isocratic mode by absorbance measurements at 254 nm. Area values of the chromatographic peaks obtained at 3.3 min for samples were interpolated in an external calibration established from five standard solutions of Diuron containing between 10.9 and 43.7 mg L^{-1}.

2.3. FTIR Off-Line Procedure. An accurate mass of sample (from 15 to 60 mg as a function of the Diuron content) was dispersed in 5 g of $CHCl_3$ by manual shaking. After homogenization, this slurry was off-line filtered, and afterward, the solution was introduced into the measurement cell by using a peristaltic pump. Then, the flow was stopped, and the FTIR spectra were recorded from 4000 to 900 cm^{-1}, using a nominal resolution of 4 cm^{-1}, accumulating 25 scans and employing a background spectrum of the cell filled with $CHCl_3$ measured in the same instrumental conditions.

A set of five Diuron chloroformic external standards, with concentrations from 1.3 to 4.5 mg g^{-1}, were prepared, and their FTIR spectra were obtained in the same conditions as those of the samples. Peak height absorbance values at 1582 cm^{-1} corrected using a linear baseline defined between 1562 and 1614 cm^{-1} were used for quantification purposes.

2.4. Flow Injection FTIR Procedure. A total of 15−60 mg of sample was weighed in a 10 mL vial, and 4 g of chloroform was added. The sample vial was installed in the manifold depicted in **Figure 1** on which the slurry was shaken and aspirated through an on-line connected 0.45 μm polypropylene filter. After that, 500 μL of the extract was sampled by using the sample loop of the injection valve and then injected in a chloroform carrier stream of 2.96 mL min^{-1}. The FTIR spectra, between 4000 and 900 cm^{-1}, were continuously recorded as a function of time, using a nominal resolution of 4 cm^{-1} and accumulating two scans per spectrum. Analytical measurements for Diuron were carried out from a representation of the peak height measurements at 1582 cm^{-1}, corrected with a linear baseline defined between 1562 and 1614 cm^{-1}, as a function of time (chemigram). The peak height values obtained for sample chemigrams were interpolated in an external calibration line established from the injection of five standard solutions containing between 0.7 and 4.7 mg g^{-1} Diuron, prepared in chloroform and measured in the same conditions as the samples.

3. RESULTS AND DISCUSSION

3.1. HPLC−UV Diuron Determination. Figure 2 shows the chromatograms of two Diuron standards containing 10.9 and 32.8 mg L^{-1} and that of a sample extract with a Diuron concentration of 20.5 mg L^{-1}. In this **Figure 2**, the UV spectrum of Diuron in CH_3CN in the wavelength region from 190 to 350 nm is also shown, in which case the presence of an intense band at 254 nm can be observed, which is extremely useful for Diuron monitoring. As can be seen in **Figure 2**, a sample diluted in CH_3CN and filtered provides the same chromatogram than the standards of pure Diuron.

The calibration line established in terms of area values of the chromatographic peaks obtained at a retention time of 3.3 min was $A = (8 \pm 6) + (70.4 \pm 0.2)C$ (mg L^{-1}), with a coefficient of determination $r^2 = 0.9999$. The limit of detection achieved, established from 3 times the standard deviation of the area values obtained for five independent injections of a standard containing 10.9 mg L^{-1} Diuron divided by the calibration slope, was 27 ng mL^{-1} that corresponds to 0.0013% w/w Diuron in the original sample. The sample injection frequency achieved using this procedure was 12 h^{-1}. For the validation of this method, we carried out recovery studies of

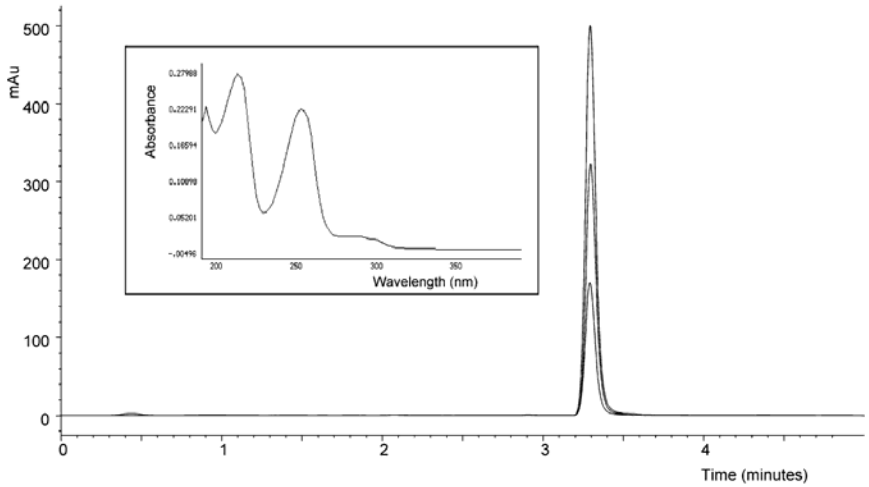

Figure 2. HPLC–UV chromatograms of two Diuron standards and a commercial sample extract with concentrations of 10.9, 32.8, and 20.5 mg L^{-1}, respectively. Inset: UV spectrum of a Diuron standard solution of 5.3 mg L^{-1} in CH_3CN obtained between 190 and 400 nm.

spiked pesticide samples and the analysis of synthetic samples (results not shown).

3.2. FTIR Absorbance Spectrum of Diuron. Figure 3 shows the spectra, in the wavenumber range of 1850−975 cm^{-1}, of a Diuron standard chloroformic solution of 2.7 mg g^{-1} and five insecticide sample extracts. As can be seen in **Figure 3**, the spectrum of every sample and that of the standard is very similar, and the same bands are present, thus indicating that practically only Diuron was extracted from the samples when $CHCl_3$ was used. The most intense bands were the carbonyl peak at 1672 cm^{-1} and the benzene ring stretching at 1514, 1477, and 1392 cm^{-1}. Other less important absorption bands are located at 1582 cm^{-1}, due to the C═C stretching in chloroalkenes, and 1297 and 1175 cm^{-1}, corresponding to amide and benzene ring breathing, respectively (*20*).

3.3. Selection of FTIR Bands for Diuron Determination. The object of this study was to find the measurement conditions that provide the best sensitivity and repeatability for Diuron determination. **Table 1** shows the figures of merit of different external calibration lines obtained from the main Diuron bands in the spectral region of 2000−1250 cm^{-1} and using different baseline and measurement criteria.

The limits of detection achieved, established from the standard deviation of six measurements of a blank solution divided by the calibration slope, varied from 10 to 86 $\mu g\ g^{-1}$, corresponding to 0.2 and 1.7% w/w Diuron in the original sample, respectively, for a sample mass of 15 mg, being adequate for the determination of this active principle in commercially available formulations.

Peak area values were in general 1 order of magnitude more sensitive than peak height ones. However, the band at 1582 cm^{-1} was selected because it does not overlap with any excipient band such as propylene glycol monooleate (see **Figure 4**) and because of the higher selectivity of this band in front of the carbonyl band at 1672 cm^{-1}. As can be seen in **Table 1**, the selected band peak height values provided have a lower LOD than the area ones. So, this measurement mode was selected and corrected with a baseline established from 1614 to 1562 cm^{-1} to avoid the effect of the presence of water in the formulations, which can interfere with the Diuron determination.

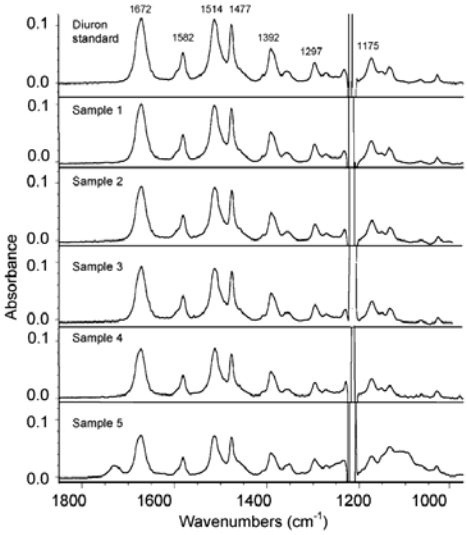

Figure 3. FTIR spectra of $CHCl_3$ solutions of a Diuron standard of 2.7 mg g^{-1} and three commercial pesticide formulations and two laboratory samples. Spectra are the average of 25 accumulated scans using a nominal resolution of 4 cm^{-1}. Commercial samples 1–3 containing 80% w/w Diuron and laboratory samples 4 and 5 with a Diuron content of 40 and 20% w/w, respectively. Note: mass of the different samples varies to provide a final concentration of Diuron of the same order than that of the standard.

Table 1. Analytical Characteristics for FTIR Determination of Diuron Using Different Measurement Modes, Bands, and Baseline Criteria

				calibration curve ($y = a + bC$ (mg g^{-1}))[a]					
band	measurement mode	wavelength	baseline correction	$a \pm s_a$[a]	$b \pm s_b$[a]	r^2[b]	LOD[c]	% LOD[d]	% RSD
1672	height	1672	1737–1633	0.0016 ± 0.0003	0.0349 ± 0.0001	0.9997	43	0.9	0.13
			1800	0.0012 ± 0.0003	0.0368 ± 0.0001	0.9998	25	0.5	0.15
	area	[1677–1 667]	1737–1633	0.013 ± 0.004	0.383 ± 0.002	0.9996	25	0.5	0.22
			1800	0.008 ± 0.004	0.405 ± 0.002	0.9997	10	0.2	0.11
1582	height	1582	1614–1562	0.0007 ± 0.0001	0.01500 ± 0.00006	0.9998	40	0.8	0.17
			1800	0.0003 ± 0.0001	0.01752 ± 0.00006	0.9998	32	0.6	0.39
	area	[1587–1577]	1614–1562	0.003 ± 0.001	0.1234 ± 0.0005	0.9997	48	1.0	0.35
			1800	0.003 ± 0.001	0.1216 ± 0.0005	0.9997	46	0.9	0.30
1514	height	1514	1556–1489	0.0004 ± 0.0002	0.0274 ± 0.0001	0.9997	72	1.5	0.31
			1556	0.0013 ± 0.0003	0.0329 ± 0.0001	0.9997	64	1.3	0.40
	area	[1519–1509]	1556–1489	0.007 ± 0.003	0.293 ± 0.001	0.9996	20	0.4	0.51
			1556	0.013 ± 0.004	0.358 ± 0.002	0.9996	32	0.6	0.12
1477	height	1477	1434–1490	0.0012 ± 0.0002	0.02299 ± 0.00006	0.9999	76	1.5	0.94
			1490	0.0010 ± 0.0001	0.02034 ± 0.00006	0.9999	83	1.6	1.41
	area	[1482–1472]	1434–1490	0.002 ± 0.002	0.1743 ± 0.0006	0.9998	28	0.6	0.87
			1490	0.000 ± 0.001	0.1468 ± 0.0006	0.9997	44	0.9	1.56
1392	height	1392	1425–1369	0.0003 ± 0.0001	0.01652 ± 0.00005	0.9998	50	1.0	1.77
			1407–1369	0.0004 ± 0.0001	0.01512 ± 0.00005	0.9999	44	0.9	1.46
	area	[1397–1 387]	1425–1369	0.001 ± 0.001	0.1439 ± 0.0006	0.9997	31	0.6	1.31
			1407–1369	0.001 ± 0.001	0.1309 ± 0.0005	0.9998	17	0.3	1.33
1297	height	1297	1282–1316	0.00017 ± 0.0008	0.00859 ± 0.00003	0.9999	86	1.7	0.44
	area	[1302–1292]	1282–1316	0.0002 ± 0.0006	0.0724 ± 0.0002	0.9998	57	1.1	2.10

[a] a and b are the intercept and the slope of the calibration lines. [b] Regression coefficient. [c] Limit of detection for the chloroform solution (in μg g^{-1}) obtained from the standard deviation of six measurements of a blank solution, established for a probability level of 99.6% ($K = 3$). [d] LOD in the original sample (% w/w).

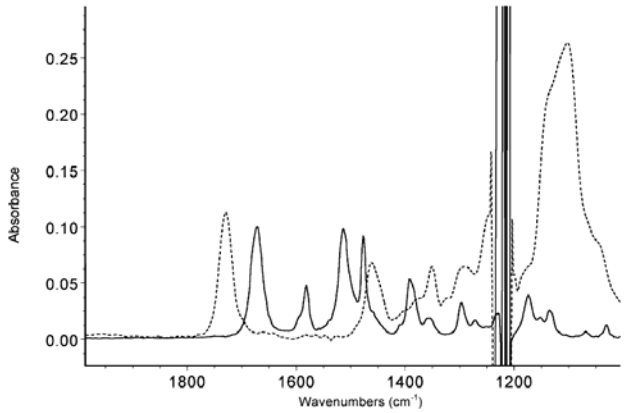

Figure 4. FTIR spectra of a Diuron standard chloroformic solution of 2.7 mg g^{-1} (solid line) and propylen glycol monooleate of 2.1 mg g^{-1} (dashed line).

4. OFF-LINE PROCEDURE

4.1. Off-Line Extraction of Diuron. A study of the time needed to carry out a quantitative extraction of Diuron by ultrasonic shaking was carried out, and it was confirmed that the extraction of Diuron from pesticide formulations was completed even without sonication. So it can be concluded that the high solubility of this compound in $CHCl_3$ permits a direct extraction from the samples by hand shaking.

4.2. Evaluation of the Matrix Effect on the Off-Line FTIR Diuron Determination. To ensure that the FTIR procedure was free from matrix effects, the slope of an external calibration line and that of a standard addition regression line were compared, obtaining $H = (0.0007 \pm 0.0001) + (0.01500 \pm 0.00006)C$ (mg g^{-1}) with $r^2 = 0.9998$ and $H = (0.054 \pm 0.001) + (0.0150 \pm 0.0002)C$ (mg added g^{-1}) with $r^2 = 0.999$, respectively, being that both slope values were statistically comparable for a confidence level of 95% (the t calculated value being 0.14, clearly lower than 1.71, the theoretical one).

5. ON-LINE PROCEDURE

5.1. Effect of Measurement Variables on the Determination of Diuron. The use of different sample injection volumes, from 100 to 500 μL, was tested to obtain as high a sensitivity as possible in the on-line measurement of Diuron. A volume of 500 μL was selected for further measurements because it provided peak height values statistically comparable with those found in the stopped-flow mode (see **Figure 5**), thus indicating the reduced dispersion of the solution from the injection loop to the measurement cell.

The effect of the carrier flow on the peak height values of the chemigrams of Diuron was studied in the range of 1−5 mL min^{-1} for an injection volume of 500 μL, and comparable data

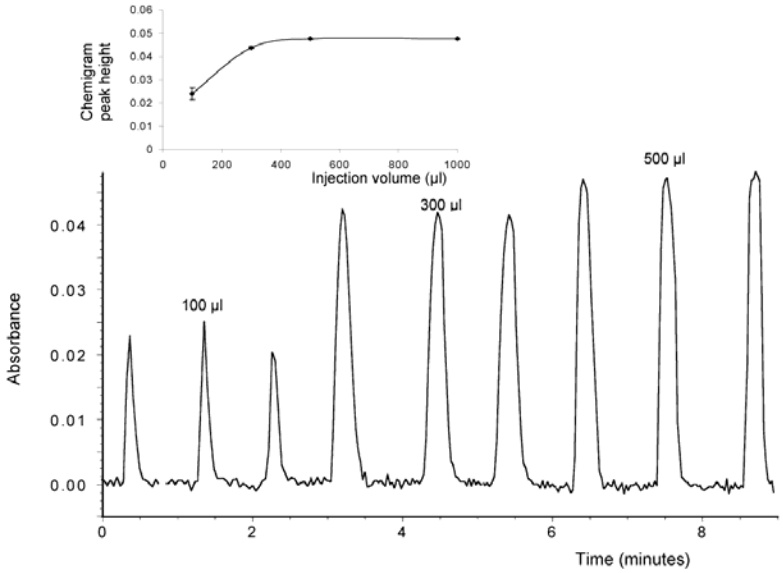

Figure 5. Effect of sample volume injected on the peak height of the Diuron chemigram established from measurements at 1582 cm^{-1} corrected using a baseline from 1614 to 1562 cm^{-1} on a Diuron standard solution of 3.13 mg g^{-1}. Experimental conditions: carrier flow 2.96 mL min^{-1}, nominal resolution 4 cm^{-1}, and two scans per spectrum. Values indicated correspond to the average of three independent injections ± the standard deviation. The peak height at 1000 μL corresponds to the Diuron standard solution measured in the stopped-flow mode, accumulating 25 scans. FIA recordings in this figure correspond to each one of the three injections made for the different volumes assayed.

Table 2. Determination of Diuron in Pesticide Formulations by Off-Line FTIR, FIA–FTIR, and HPLC–UV Procedures[a]

	FTIR			FIA–FTIR			HPLC–UV		
	$S = (0.0007 \pm 0.0001) + (0.01500 \pm 0.00006)C$; $r^2 = 0.9998$			$S = (-0.0001 \pm 0.0001) + (0.01296 \pm 0.00005)C$; $r^2 = 0.9999$			$S = (8 \pm 6) + (70.4 \pm 0.2)C$; $r^2 = 0.9999$		
sample	FTIR	CV (%)[b]	% relative accuracy error[c]	FIA–FTIR	CV (%)	% relative accuracy error	HPLC–UV	CV (%)	% active substance labeled
1	83.1 ± 0.3	0.4	0.5	80.8 ± 0.8	1.0	2.3	82.7 ± 0.3	0.4	80
2	82.6 ± 0.5	0.6	0.0	84 ± 2	2.4	1.7	82.6 ± 0.4	0.5	80
3	83.0 ± 0.7	0.8	0.0	84 ± 2	2.4	1.2	83.0 ± 0.4	0.5	80
4	40.1 ± 0.6	1.5	−0.5	42 ± 2	4.8	4.2	40.3 ± 0.5	1.2	40
5	20.8 ± 0.5	2.4	1.5	20.9 ± 0.4	1.9	2.0	20.5 ± 0.6	2.9	20

[a] Concentration values (% w/w) are the average of three independent analyses ± standard deviation. [b] Coefficient of variation for three replicates. [c] % error calculated as 100([FTIR] − [HPLC])/[HPLC], where [FTIR] and [HPLC] are the concentrations found using the FTIR or FIA–FTIR procedure and the HPLC–UV procedure, respectively.

were obtained with that found in the stopped-flow mode. However, using a carrier flow rate of 2.96 mL min^{-1}, the best precision of analytical data was found; thus, this value was selected, as a sample throughput of 30 h^{-1} was obtained.

5.2. Analytical Characteristics of FIA−FTIR Determination of Diuron. The sensitivity of the fully mechanized FIA−FTIR analysis of Diuron corresponds to 0.1296 absorbance units mg^{-1} mL. Using the recommended procedure, the limit of detection was 35 μg mL^{-1}, which correspond to 0.7% (w/w), for 20 mg of sample and provided a repeatability of 0.5% (expressed as relative standard deviation). For Diuron external calibration in the selected conditions, the expression $A = [-0.0001 \pm 0.0001] + [0.01296 \pm 0.00005]C$ (mg mL^{-1}) with $r^2 = 0.9999$ was found.

For actual sample analysis, a relative standard deviation between 1.0 and 2.8% for five replicate determinations and a maximum sampling frequency of the whole procedure of 30 h^{-1} was found.

6. COMPARISON BETWEEN THE DIFFERENT STRATEGIES ASSAYED

Commercially available Diuron formulations were analyzed by the HPLC−UV reference procedure and by the proposed FTIR method, using both off-line and FIA−FTIR measurements. As can be seen in **Table 2**, data found by the three methods are of the same order with average relative standard deviation values of 0.4−2.4% for stopped-flow measurements and 1.0−4.8% for FIA−FTIR measurements being the average accurate relative errors from −0.5 to 1.5% and from 1.2 to 4.2%, respectively, which is evidence that all the methods are comparable within their precision levels.

Additional statistical treatment of data in **Table 2** provides regression lines of $C_{FTIR} = (0.1 \pm 0.3) + (0.998 \pm 0.004)C_{HPLC}$ with $r^2 = 0.9993$ and $C_{FIA-FTIR} = (0.6 \pm 0.7) + (0.99 \pm 0.01)C_{HPLC}$ with $r^2 = 0.997$ for the comparison between data found by FTIR in the stopped flow and FIA mode and those obtained by HPLC. The slope and intercept values of these equations are statistically comparable (t_{exp}= 0.50 and 0.33 for the stopped flow and t_{exp}= 1.00 and 0.86 for the FIA mode) with values of 0 and 1 for the intercept and slope of the regression line (t_{theor}=1.70) for a probability level of 95% and 30 degrees of freedom, thus indicating that methodologies developed do not require blank correction nor present systematic relative errors as compared with the reference procedure.

It must be indicated that the sensitivity provided by HPLC measurements is higher than that found by FTIR. However, for this kind of concentrate sample, the advantage offered by a strong reduction of the volume of organic solvent required (39.1 mL for HPLC, 3.4 mL for stopped flow FTIR, or 9.3 mL for FIA−FTIR measurements) and the increase of the sampling frequency from 12 h^{-1} in the case of HPLC to 30 h^{-1} for FIA−FTIR and 60 h^{-1} for the stopped flow FTIR clearly recommend the use of FTIR measurements for the control of Diuron concentration in pesticide formulations.

LITERATURE CITED

(1) EXTOXNET. *Extensión Toxicology Network Pesticide Information Profiles*; Oregon State University: Corvallis, OR, 1996.

(2) de Liñan, C. In *Vademecum de productos fitosanitarios y nutricionales*; Agrotécnica S. L., Ed.; Madrid, Spain, 2000.

(3) Bayer Crop Science. Hawthorn, Victoria, 2002; http://www.bayercropscience.com.

(4) Efficient analysis of pesticide and herbicide residues in food. *Chrompack Application Note* M2807, **2001**, 1.

(5) Pesticides. *Chrompack Application Note* 544-HPLC, **2001**, 1.

(6) Draper, W. M. Electrospray liquid chromatography quadrupole ion trap mass spectrometry determination of phenyl urea herbicides in water. *J. Agric. Food Chem.* **2001**, *49*, 2746−2755.

(7) Vessella, J.; Acobas, F.; Benanou, D.; Guinamant, J. L. Liquid chromatography coupled with time-of-flight mass spectrometery. The new way for environmental analysis. *Spectra Anal.* **2001**, *220*, 32−36.

(8) Rodriguez, R.; Pico, Y.; Font, G.; Manes, J. Determination of urea-derived pesticides in fruits and vegetables by solid-phase preconcentration and capillary electrophoresis. *Electrophoresis* **2001**, *22*, 2010−2016.

(9) Zhang, M. Q.; El-Rassi, Z. Capillary electrochromatography with polyacrylamide monolithic stationary phases having bonded dodecyl ligands and sulfonic acid groups: evaluation of column performance with alkyl phenyl ketones and neutral moderately polar pesticides. *Electrophoresis* **2001**, *22*, 2593−2599.

(10) Berrada, H.; Molto, J. C.; Font, G. Gas chromatographic behavior of urea herbicides. *Chromatographia* **2001**, *54*, 360−364.

(11) Sanusi, A.; Millet, M.; Mirabel, P.; Wortham, H. Gas-particle partitioning of pesticides in atmospheric samples. *Atmos. Environ.* **1999**, *33*, 4941−4951.

(12) Gerecke, A. C.; Tixier, C.; Bartels, T.; Schwarzenbach, R. P.; Mueller, S. R. Determination of phenylurea herbicides in natural waters at concentrations below one nanogram per liter using solid-phase extraction, derivatization, and solid-phase microextraction−gas chromatography−mass spectrometry. *J. Chromatogr. A* **2001**, *930*, 9−19.

(13) Wittke, K.; Hajimiragha, H.; Dunemann, L.; Begerow, J. Determination of dichloroanilines in human urine by GC−MS, GC−MS−MS, and GC−ECD as markers of low-level pesticide exposure. *J. Chromatogr., B* **2001**, *755*, 215−228.

(14) Galignani, M.; Garrigues, S.; Martinez-Vidal, A.; de la Guardia, M. Determination of carbaryl in pesticide formulations by Fourier transform infrared spectrometry with flow analysis. *Analyst* **1993**, *118*, 1043−1048.

(15) Armenta, S.; Quintás, G.; Moros, J.; Garrigues, S.; de la Guardia, M. Fourier transform infrared spectrometric strategies for the determination of Buprofezin in pesticide formulations. *Anal. Chim. Acta* **2002**, *468*, 81−90.

(16) Quintás, G.; Morales-Noé, A.; Parrilla, C.; Garrigues, S.; de la Guardia, M. Fourier transform infrared determination of Fluometuron in pesticide formulations. *Vib. Spectrosc.* **2003**, *31*, 63−69.

(17) Quintás, G.; Armenta, S.; Morales-Noé, A.; Garrigues, S.; de la Guardia, M. Simultaneous determination of folpet and metalaxyl in pesticide formulations by flow injection Fourier transform infrared spectrometry. *Anal. Chim. Acta* **2003**, *480*, 11−21.

(18) Almond, M. J.; Knowles, S. J. Quantitative analysis of agrochemical formulations by multivariate spectroscopic techniques. *Appl. Spectrosc.* **1999**, *53*, 1128−1131.

(19) Collaborative International Pesticide Analytical Council. *Guidelines on method validation to be performed in support of analytical methods for agrochemical formulations (CIPAC 3507)*; Black Bear Press: Cambridge, 1999.

(20) Lin-Vien, D.; Colthup, N. B.; Fateley, W. G.; Grasselli, J. G. *Infrared and Raman characteristic frequencies of organic molecules*; Academic Press: London, 1991.

Received for review February 4, 2005. Revised manuscript received May 3, 2005. Accepted May 23, 2005. The authors acknowledge the financial support of the Generalitat Valenciana (Project GV04B-247 and Grupos 03-118) and the FPU Grant of the Ministerio de Educación, Cultura y Deporte (Ref. AP2002-1874) to S.A.

JF050268F

A validated and fast procedure for FTIR determination of Cypermethrin and Chlorpyrifos

Sergio Armenta, Guillermo Quintás, Salvador Garrigues and Miguel de la Guardia
Department of Analytical Chemistry, Universitat de València. Edifici Jeroni Muñoz, 50th Dr Moliner, 46100 Burjassot, Valencia, Spain.

Talanta 67 (2005) 634-639.

Impact factor of this journal (2004): 2.532
Source: Journal citation reports ISI Web of Knowledge, 2004.

Available online at www.sciencedirect.com
SCIENCE DIRECT®
Talanta 67 (2005) 634–639
Talanta
www.elsevier.com/locate/talanta

A validated and fast procedure for FTIR determination of Cypermethrin and Chlorpyrifos

Sergio Armenta, Guillermo Quintás, Salvador Garrigues *, Miguel de la Guardia

Department of Analytical Chemistry, University of Valencia, Edifici Jeroni Muñoz, 50th Dr. Moliner, 46100 BURJASSOT, Valencia, Spain

Received 15 November 2004; received in revised form 21 January 2005; accepted 15 March 2005
Available online 12 April 2005

Abstract

A FTIR methodology has been developed for the simultaneous determination of Cypermethrin and Chlorpyrifos in pesticide commercially available formulations. The method involves the extraction of both active principles with $CHCl_3$ and direct measurement of the peak area values between 1747 and 1737 cm^{-1} corrected with a baseline defined at 2000 cm^{-1} for Cypermethrin and peak height values established at 1549 cm^{-1} corrected using a baseline situated at 1650 cm^{-1} for Chlorpyrifos.

The limits of detection achieved were of the order of 0.7 and 0.4% (w/w), and the relative standard deviation 0.4 and 0.2% for Cypermethrin and Chlorpyrifos, respectively. The developed procedure provided statistically comparable results with those obtained by HPLC, for a series of commercial samples, which validated the FTIR method. The procedure developed reduces organic solvent consumption, per sample preparation, from 51 ml CH_3CN required for HPLC to 2.5 ml $CHCl_3$, and reduces waste generation also increasing the sample measurement frequency, from 3 to 30 samples/h, as compared with the HPLC–UV reference method.

Keywords: Cypermethrin; Chlorpyrifos; Pesticide formulations; FTIR

1. Introduction

Cypermethrin, (*R*,*S*)-alpha-cyano-3-phenoxybenzyl(1*RS*)-*cis*,*trans*-3-(2,2-dichlorovinyl)-2,2-dimethylcyclopropane-carboxylate, is a synthetic pyrethroid insecticide used to control many pests, including moth pests of cotton, fruit and vegetable crops. It is also used for crack, crevice and spot treatment to control insect pests in stores, industrial buildings, laboratories and on ships, buses and aircraft. It may be also used in non-food areas in schools, nursing homes, hospitals, restaurants, in food processing plants and as a barrier treatment insect repellent for horses. This pesticide is light stable and it is available as an emulsifiable concentrate or wettable powder (WP) [1].

Cypermethrin is an alpha-cyano (type II pyrethroids) that causes neurotoxicity in mammals and insects. It is a moderately toxic material by dermal absorption or ingestion [2,3]. EPA reports an oral LD_{50} of 150–500 mg/kg in rats [3].

Chlorpyrifos, *O*,*O*-diethyl-*O*-3,5,6-trichloro-2-pyridyl phosphorothioate, is a broad-spectrum organophosphate insecticide. Chlorpyrifos is effective in controlling cutworms, cockroaches, flea beetles, flies, termites and lice. It is used as an insecticide on grain, cotton, field, fruit, nut and vegetable crops and well as on lawns and ornamental plants. It is also registered for direct use on sheep and turkeys, for horse site treatment, domestic dwellings, farm buildings, storage bins and commercial establishments. This product is available as granules, wettable powder, dustable powder and emulsifiable concentrate [1].

Chlorpyrifos is moderately toxic. The oral LD_{50} for chlorpyrifos in rats is 95–270 mg/kg, 60 mg/kg in mice and 1000 mg/kg in rabbits [4].

Chlorpyrifos has a half-life between 16 and 72 days, depending on the pH of the solution. Direct photo transformation was observed in buffer solutions and river waters, under both natural and artificial lighting conditions [5].

* Corresponding author. Tel.: +34 963543158; fax: +34 963544838.
E-mail address: salvador.garrigues@uv.es (S. Garrigues).

0039-9140/$ – see front matter © 2005 Elsevier B.V. All rights reserved.
doi:10.1016/j.talanta.2005.03.008

The use of agrochemical formulations with more than one active principle is a common practice in order to improve their crop protective action. The determination of several active principles in a same formulation requires, in many cases, the use of different analytical techniques, thus involving long and tedious procedures. The Collaborative International Pesticide Analytical Council (CIPAC) recommends the use of high performance liquid chromatography with UV detection (HPLC-UV) or gas chromatography with flame ionization detection (GC-FID) for the determination of Cypermethrin [6] and the use of high performance liquid chromatography with UV detection for the determination of Chlorpyrifos [7].

In recent years, it has been published a series of procedures based on gas chromatography with mass spectrometry detection (GC-MS) for the simultaneous determination of Cypermethrin and Chlorpyrifos in different matrices, such as fruits and vegetables [8], food [9], soil [10], plants [11] or water [12]. All these methods are very convenient for determination of residues at trace levels, but not well justified for the analysis of formulations.

Gas chromatography with electron capture detection (GC-ECD) or nitrogen–phosphorous detection (GC-NPD) [13], high performance liquid chromatography with mass spectrometry (HPLC-MS) [14] or fluorescence detection (HPLC-FLD) [15], thin layer chromatography (TLC) [16] and micellar electrokinetic chromatography (MEKC) [17] have been also proposed for the determination of Cypermethrin and Chlorpyrifos.

The concentration range in which Cypermethrin and Chlorpyrifos are individually present in commercial formulations varies between 0.33–20% (w/w) and 1.5–75% (w/w), respectively [18]. On the other hand, when both pesticides are co-formulated, the concentration of Cypermethrin and Chlorpyrifos is between 2.0 and 4.5% (w/w) and from 36 to 45.5% (w/w), respectively [18].

FTIR spectrometry has been employed for the determination of different active principles in commercially available pesticide formulations such as Buprofezin [19], Fluometuron [20] and Folpet and Metalaxyl [21] showing the high suitability of FTIR to carry out this kind of analysis.

The single FTIR precedents concerning the determination of the aforementioned pesticides in formulations correspond to the work of Almond et al. [22], who determined Chlorpyrifos by ATR-FTIR on using multivariate spectroscopy on samples dissolved in Solvesso and that of Sharma et al. [23], who determined Cypermethrin in emulsifiable concentrated formulations after thin layer chromatography separation and dissolution of the compound in $CHCl_3$ measuring the absorbance at 1749 cm^{-1} with a baseline established between 1770 and 1720 cm^{-1}.

The evaluation of the experimental conditions for FTIR determination of Chlorpyrifos and Cypermethrin in pesticide formulations has been the main objective of the present work.

2. Experimental

2.1. Apparatus and reagents

A Magna 750 FTIR spectrometer (Nicolet, Madison, WI, USA.), equipped with a temperature-stabilized DGTS detector, a long-lasting Ever-Glo source and a KBr beamsplitter, was employed for spectral measurements, using a microflow cell (Specac, Orpington, UK) with ZnSe and BaF_2 windows and 0.10 mm pathlength. The equipment employs the 2.1 version of the OMNIC software developed by Nicolet Corporation, for the acquisition and processing of the FTIR absorbance data.

It has been employed a Gilson Minipuls 2 peristaltic pump (Villiers-le-Bel, France) equipped with solvent resistant viton tubes of 3 mm o.d. and 1 mm i.d. for the introduction of samples and standards in the flow cell.

A Hewlett-Packard HPLC Series 1050 High Performance Liquid Chromatograph (Palo Alto, CA, USA), equipped with a Kromasil column (C-18, 250 mm × 4.6 mm i.d. and 5 μm particle diameter), and a variable wavelength UV–vis detector was employed for the analysis of pesticide formulations.

Chlorpyrifos PESTANAL® reagent grade standard was obtained from Fluka (Buchs, Switzerland). Cypermethrin technical standard was supplied by Afrasa, S.A. (Valencia, Spain). Extra pure chloroform stabilized with 150 ppm of amylene and HPLC grade acetonitrile were supplied by Scharlau (Barcelona, Spain) and were employed for the preparation of samples and standards, using also Mili-Q grade water for the mobile phase.

Emulsifiable concentrates (EC) and wettable powder formulations containing Cypermethrin or/and Chlorpyrifos were obtained directly from the Spanish market. Sample 1 (EC) contains a nominal concentration of 10.0% (w/w) Cypermethrin. Samples 2 (EC) and 3 (EC) contain 46.0 and 50.0% (w/w) Chlorpyrifos, respectively. Sample 4 (WP) contains 2.1% (w/w) Cypermethrin and 37.0% (w/w) Chlorpyrifos and sample 5 (WP) contains 4.3% (w/w) Cypermethrin and 45.0% (w/w) Chlorpyrifos.

2.2. Reference procedure

Ten milligrams of sample were accurately weighted, inside a 25 ml volumetric flask and diluted to the volume with CH_3CN. One milliliters of the solution was diluted to 10 ml and filtered through a 0.22 μm nylon filter. Twenty microliters of this latter solution were directly injected in a 80:20 acetonitrile:water mobile phase using 1 ml min^{-1} carrier flow. Both pesticides were determined in the isocratic mode by absorbance measurements at 278 nm. For quantification, it was used area values of the chromatographic peaks obtained for Chlorpyrifos at a retention time of 11.9 min. In the case of Cypermethrin, the sum of the areas of the peaks found at 16.8, 17.2 and 17.6 min for the pesticide isomers were employed. Data found for samples were interpolated in external calibration lines established from the measurement of six standard

solutions of 4.32–43.2 $\mu g\,g^{-1}$ Chlorpyrifos and from 4.64 to 46.4 $\mu g\,g^{-1}$ Cypermethrin.

2.3. FTIR procedure

Twenty-five milligrams of sample were accurately weighted and diluted with 4 g of $CHCl_3$. The sample slurry were passed through a 0.22 μm nylon filter and then introduced in the FTIR measurement cell by using a peristaltic pump. The spectra were obtained in the stopped flow mode, at 4 cm^{-1} nominal resolution and accumulating 25 scans per spectrum, in the range from 4000 to 850 cm^{-1} and using a background of the cell filled with the solvent.

The concentrations of Cypermethrin and Chlorpyrifos in commercial formulations were calculated by interpolating absorbance values measured in the sample spectra in external calibration lines.

Two individual sets of Cypermethrin (five standards from 0.64 to 1.87 $mg\,g^{-1}$) and Chlorpyrifos (five standards from 1.61 to 4.70 $mg\,g^{-1}$) external standard solutions in $CHCl_3$ were prepared and their FTIR spectra were obtained in the same conditions as samples. A calibration line was established for Cypermethrin by measuring peak area values between 1747 and 1737 cm^{-1}, corrected using a baseline defined at 2000 cm^{-1}. For Chlorpyrifos determination, measurements of the peak height at 1549 cm^{-1}, corrected using a baseline established at 1650 cm^{-1}, were employed.

3. Results and discussion

3.1. FTIR spectra of Cypermethrin and Chlorpyrifos

Fig. 1 shows the absorbance FTIR spectra in the wavenumber region from 2000 to 900 cm^{-1} of pure standard solutions in $CHCl_3$ of Cypermethrin and Chlorpyrifos and different sample extracts in chloroform. As can be seen in this figure, the Cypermethrin spectrum has absorption bands at 1742, 1587,1488, 1449 and 1076 cm^{-1}, due to carbonyl stretching, C=C stretching in chloroalkenes, ring vibration of benzene, CH_2 deformation in R–CH_2–CN structure and (C=O)–O– stretching, respectively.

The absorption bands of Chlorpyrifos are located at 1549, 1412, 1339, 1165, 1088, 1025 and 968 cm^{-1}, due to C=N stretching, pyridine stretching, ring vibration, ring breathing, Cl–C stretching, trigonal ring breathing and P=S stretching [24], respectively.

Sample spectra provide the characteristic bands of the active principles additionally than some small bands coming from inert and solvent components of the pesticide formulations.

3.2. Measurement conditions

The effects of the number of accumulated scans and the nominal resolution employed for data acquisition were evaluated in order to improve the measurement conditions. The number of accumulated scans was modified from 5 to 50, and the nominal resolution varied from 2 to 16 cm^{-1}.

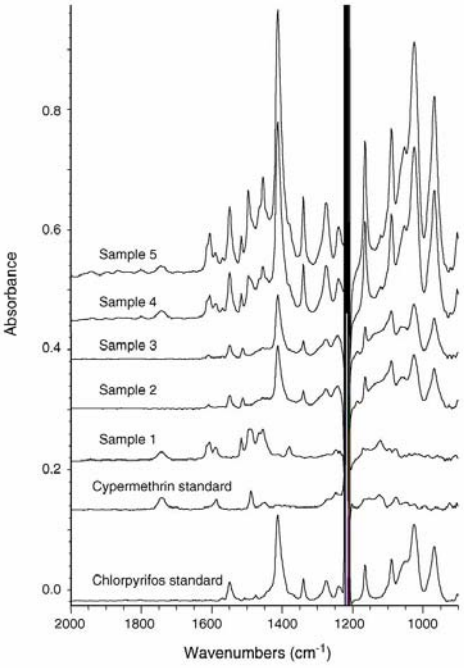

Fig. 1. FTIR spectra of $CHCl_3$ solutions of Cypermethrin, Chlorpyrifos and five commercial pesticide formulations containing these compounds. Spectra are the average of 25 accumulated scans using a nominal resolution of 4 cm^{-1}. Concentrations of standards correspond to 6.73 $mg\,g^{-1}$ Cypermethrin and 5.36 $mg\,g^{-1}$ Chlorpyrifos. Thirty-three milligrams of sample 1, 29 mg of sample 2, 24 mg of sample 3, 170 mg of sample 4 and 120 mg of sample 5 were diluted with 4 g $CHCl_3$ to obtain these spectra.

As can be seen in Fig. 2, the highest signal to noise ratio, established as the ratio between the spectral area calculated between 1747 and 1737 cm^{-1} corrected with a single point baseline established in 2000 cm^{-1}, for a 1.21 $mg\,g^{-1}$ Chlorpyrifos standard and the noise measured in the same region for a blank spectrum and expressed as root mean square (RMS) was found for a 2 cm^{-1} nominal resolution and accumulating 50 scans per spectra. However, in order to ensure a compromise between measurement frequency and sensitivity, 25 accumulated scans and a nominal resolution of 4 cm^{-1} were selected with a relative loss of sensitivity of 7% as compared with the best signal, but reducing the measurement time from 109 to 30 s.

3.3. Band selection

In order to choose the best analytical performance of the FTIR determination of Cypermethrin and Chlorpyrifos in for-

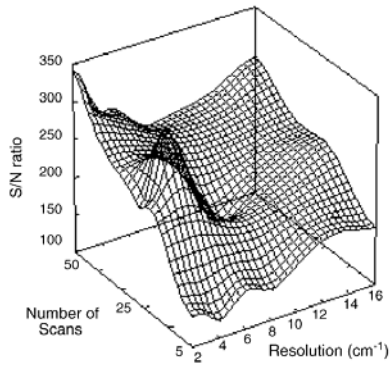

Fig. 2. Effect of the nominal resolution and number of accumulated scans on signal to noise ratio of a Chlorpyrifos standard of 1.21 mg g^{-1}.

mulated samples, different bands and baseline criteria were evaluated, as can be seen in Table 1. In every case, it was also considered the use of both, peak height and peak area, absorbance measurements.

In terms of sensitivity, it is clear that peak area measurements provide one order of magnitude better sensitivity than peak height values, but in general, all the studied conditions provide appropriate characteristics for pesticide formulations analysis. Peak area measurements between 1747 and 1737 cm^{-1} were selected for the determination of Cypermethrin because for these conditions, no overlapping effects were found in all samples analysed. On the other hand, the peak height at 1549 cm^{-1} was selected for Chlorpyrifos determination because in these conditions there is no overlapping with any Cypermethrin band.

Data in Table 1 also reports the limit of detection (LOD) values found on using different bands. LOD's were established, as recommended by the IUPAC as the pesticide concentration, which provides an absorbance value equal to three times the standard deviation of 10 blank solutions (99.6% confidence level). The aforementioned values divided by the slope of the calibration line and multiplied by the sample dilution factor used in the recommended procedure provided the limit of detection in the actual samples in terms of %, w/w.

3.4. Study of interferences

From sample spectra reported in Fig. 1, it can be seen that the main bands correspond to those of Cypermethrin and Chlorpyrifos being absent the characteristic bands of the typical excipients employed in these formulations like calcium carbonate, surfactants, cyclohexanone and other solvents. So, the mutual overlapping of bands of the considered pesticides could be the main source of interferences. It was carried out a series of mutual interference studies to verify the possibilities of the simultaneous determination of Cypermethrin and Chlorpyrifos in a same sample.

It was studied the effect on the absorbance measurements at 1548 cm^{-1} of increasing Cypermethrin concentrations, from 0 to 19.88 mg g^{-1}, for a fixed concentration of 2.39 mg g^{-1} Chlorpyrifos. On the other hand, it was evaluated the interference of increasing Chlorpyrifos concentrations, from 0 to 20.00 mg g^{-1}, for a fixed concentration of 1.47 mg g^{-1} Cypermethrin. In both cases, it can be concluded that in the selected conditions, the simultaneous determination of Cypermethrin and Chlorpyrifos could be done without interferences. The methodology developed is extremely valuable for the simultaneous determination of the two considered

Table 1
Analytical features of the FTIR determination of Cypermethrin and Chlorpyrifos using different bands and baseline criteria

Measurement mode	Wavelength (cm^{-1})	Baseline correction	$a \pm s_a$	$b \pm s_b$	r^2	R.S.D. (%)	L.O.D. (% w/w)	L.O.Q. (% w/w)
Cypermethrin calibration curve ($y = a + b\,C$ (mg g^{-1}))								
Height	1742	2000	0.0002 ± 0.0001	0.00953 ± 0.00004	0.9993	0.3	0.6	2
Area	1747–1737	2000	0.0017 ± 0.0008	0.1007 ± 0.0008	0.9998	0.4	0.7	2.3
Height	1587	1650	0.00031 ± 0.00009	0.00926 ± 0.00003	0.9999	0.9	0.3	1
Area	1592–1982	1650	0.002 ± 0.001	0.082 ± 0.001	0.9997	0.8	0.5	1.7
Height	1488	1530	0.0003 ± 0.0002	0.01514 ± 0.00005	0.9998	1.0	0.3	1
Area	1493–1483	1530	0.000 ± 0.002	0.147 ± 0.002	0.9995	1.1	0.6	2
Height	1076	1097–1061	0.0003 ± 0.0002	0.00558 ± 0.00008	0.997	1.2	1.4	4.7
Area	1081–1071	1097–1061	0.000 ± 0.002	0.070 ± 0.002	0.998	0.9	1.0	3.3
Chlorpyrifos calibration curve ($y = a + b\,C$ (mg g^{-1}))								
Area	1554–1544	1650	0.002 ± 0.001	0.0527 ± 0.0004	0.9993	0.10	0.2	0.67
Height	1549	1650	0.0009 ± 0.0002	0.00639 ± 0.00007	0.9993	0.2	0.4	1.3
Height	1549	1650–1527	0.0004 ± 0.0002	0.00600 ± 0.00004	0.9992	0.2	0.5	1.7
Height	1412	2000	0.0006 ± 0.0004	0.0290 ± 0.0001	0.9996	0.3	0.2	0.67
Area	1417–1407	2000	0.009 ± 0.005	0.270 ± 0.002	0.9995	0.4	0.9	3
Height	968	2000	0.0008 ± 0.0003	0.01839 ± 0.00009	0.9996	0.4	0.9	3
Area	973–963	2000	0.007 ± 0.004	0.207 ± 0.002	0.9994	0.6	0.8	2.7

Note: The linear range was in all the cases from 0.64 to 1.87 mg g^{-1} Cypermethrin and from 1.61 to 4.70 mg g^{-1} Chlorpyrifos, being employed five standard solutions measured three times each one to make the calibration.

Table 2
Determination of Cypermethrin and Chlorpyrifos in pesticide formulations by HPLC-UV and FTIR procedures

Sample	Active substance	HPLC-UV[a]	FTIR[a]	Relative accuracy error (%)[b]	t_{exp}
1	Cypermethrin	12.1 ± 0.1	12.2 ± 0.1	0.82	1.58
2	Chlorpyrifos	46.2 ± 0.2	46.4 ± 0.8	0.4	0.54
3	Chlorpyrifos	50.2 ± 0.1	50.3 ± 0.5	0.20	0.44
4	Chlorpyrifos	37.2 ± 0.5	37.6 ± 0.8[a]	1.08	0.95
	Cypermethrin	2.10 ± 0.05	2.08 ± 0.07	−0.9	0.52
5	Chlorpyrifos	45.3 ± 0.3	45.1 ± 0.2[a]	−0.44	1.24
	Cypermethrin	4.35 ± 0.04	4.32 ± 0.05	−0.69	1.05

t_{tab} = 1.812 with a probability level of 95% and 10 freedom degree.
[a] Concentration values (%, w/w) are the average of three independent duplicate analyses ± standard deviation.
[b] %Error calculated as 100 × ([FTIR] − [HPLC])/[HPLC], where [FTIR] and [HPLC] are the concentrations found using the FTIR procedure and the HPLC-UV one, respectively.

pesticides in a same sample containing a big range of relative concentrations.

4. Determination of Cypermethrin and Chlorpyrifos in pesticide formulations

To validate the proposed FTIR procedure, one sample containing Cypermethrin, two samples with Chlorpyrifos and two samples with the two aforementioned active principles were analysed by both, the FTIR developed procedure and the HPLC reference method, and results found are indicated in Table 2.

The accuracy errors obtained from the difference between results found by FTIR and HPLC range from −0.9 to 0.82% in the case of Cypermethrin and from −0.44 to 1.08% for Chlorpyrifos.

On the other hand, the regression between all the data found for samples assayed provided regression equation of $C_{FTIR} = (-0.014 \pm 0.016) + (1.002 \pm 0.002) C_{HPLC}$ with $r^2 = 0.9997$ for Cypermethrin and $C_{FTIR} = (0.0 \pm 0.9) + (1.00 \pm 0.02) C_{HPLC}$ with $r^2 = 0.996$ for Chlorpyrifos. Statistically, the aforementioned regression lines present slope and intercept values comparable with 1 and 0, respectively, which evidence that, as compared with the reference method, the developed FTIR procedure does not need any blank correction and does not present constant relative errors.

On the other hand, the statistical comparison of paired results (summarized in Table 2) provides t_{exp} values that are, in all the cases, lower than 1.82, the theoretical t value for a confidence level of 95%.

5. Conclusions

The FTIR procedure developed in this work provides statistically comparable results, for a probability level of 95%, with those obtained by the HPLC reference method.

In spite of the fact that HPLC provides a LOD of 0.24 and 0.16 mg l^{-1} for Cypermethrin and Chlorpyrifos, respectively, which are three orders of magnitude lower than those found by FTIR, it can be concluded that both techniques are appropriate for the concentration of pesticides in commercial formulations.

The reagent consume and waste generation were minimized, and then the FTIR procedure used only 2.5 ml of chloroform instead of 51 ml acetonitrile per sample required in the HPLC–UV method.

The sample analysis frequency was increased from 3 to 30 samples/h, by reducing the sample pre-treatment, being unnecessary any clean-up previous step to the FTIR measurement of the sample extracts.

So, it can be concluded that the FTIR procedure developed is a simple, fast and accurate alternative for the quality control analysis of pesticide formulations containing Cypermethrin and Chlorpyrifos, and provides an enhanced methodology as compared with previous studies focussed on FTIR measurement of Cypermethrin after a long and tedious treatment or that based on a multivariate approach for Chlorpyrifos determination.

Acknowledgements

Authors acknowledge the financial support of the Oficina de Ciència i Tecnològia de la Conselleria d' Innovació i Competitivitat de la Generalitat Valenciana (Project GV04B/247 and Grupos 03/118), and S. Armenta, the FPU Grant of the Ministerio de Educacion Cultura y Deporte AP2002-1874 to carry out this study.

References

[1] Extension Toxicological Network (EXTOXNET), University of California-Davis, Oregon State University, Michigan State University and the University of Idaho, 1996. http://ace.orst.edu/info/extoxnet/pips/ghindex.html.
[2] D.E. Ray, Pesticides derived from plants and other organisms, in: W.J. Hayes, E.R. Laws (Eds.), Handbook of Pesticide Toxicology, Academic Press, New York, 1991, p. 2.
[3] U.S. Environmental Protection Agency. Pesticide Fact Sheet Number 199: Cypermethrin. Office of Pesticides and Toxic Substances, Washington, DC, 1989, p. 2.

[4] M.A. Gallo, N.J. Lawryk, Organic phosphorus pesticides, in: W.J. Hayes, E.R. Laws (Eds.), Handbook of Pesticide Toxicology, Academic Press, New York, 1991, p. 5.
[5] WHO specifications and evaluations for public health pesticides. Geneva, 2004.
[6] Collaborative International Pesticides Analytical Council (CIPAC) Handbook, Volume 1C, CIPAC Ltd., 1994, p. 2047.
[7] Collaborative International Pesticides Analytical Council (CIPAC) Handbook, Volume 1C, CIPAC Ltd., 1994, p. 2028.
[8] R.J. Fussell, K.J. Addie, S.L. Reynolds, M.F. Wilson, J. Agric. Food Chem. 50 (2002) 441.
[9] A. Vongbuddhapitak, K. Atisook, G. Thoophom, B. Sungwaranond, Y. Lertreungdej, J. Suntudrob, L. Kaewklapanyachareon, J. AOAC Int. 85 (2002) 134.
[10] L.R. Zimmerman, E.M. Thurman, K.C. Bastian, Sci. Total Environ. 248 (2000) 169.
[11] H.J. Stan, J. Chromatogr. A. 892 (2000) 347.
[12] K.S. Liapis, G.E. Miliadis, N.G. Tsiropoulos, Bull. Environ. Contam. Toxicol. 65 (2000) 811.
[13] S. Jaggi, C. Sood, V. Kumar, S.D. Ravindranath, A. Shanker, J. Agric. Food Chem. 49 (2001) 5479.
[14] I.G. Zenkevich, O.K. Ostroukhova, V.I. Dolzhenko, J. Anal. Chem. (Transl. Zh. Anal. Khim.) 57 (2002) 35.
[15] J. Fillion, F. Sauve, J. Selwyn, J. AOAC Int. 83 (2000) 698.
[16] A. Mohammad, I.A. Khan, N. Jabeen, J. Planar Chromatogr. Mod. TLC. 14 (2001) 283.
[17] W.L. Klotz, M.R. Schure, J.P. Foley, J. Chromatogr. A. 930 (2001) 145.
[18] C. de Liñan, Vademecum de productos fitosanitarios y nutricionales, Ediciones Agrotécnicas S.L., Madrid, 2000.
[19] S. Armenta, G. Quintás, J. Moros, S. Garrigues, M. de la Guardia, Anal. Chim. Acta 468 (2002) 81.
[20] G. Quintás, A. Morales-Noé, C. Parrilla, S. Garrigues, M. de la Guardia, Vib. Spectrosc. 31 (2003) 63.
[21] G. Quintás, S. Armenta, A. Morales-Noé, S. Garrigues, M. de la Guardia, Anal. Chim. Acta 418 (2003) 11.
[22] M.J. Almond, S.J. Knowles, Appl. Spectrosc. 53 (1999) 1128.
[23] K.K. Sharma, S. Gupta, S.K. Handa, Talanta 44 (1997) 2075.
[24] D. Lin-Vien, N.B. Colthup, W.G. Fateley, J.G. Grasselli, Infrared and Raman Characteristic Frequencies of Organic Molecules, Academic Press, London, 1991.

FTIR determination of Aspartame and Acesulfame-K in tabletop sweeteners

Sergio Armenta, Salvador Garrigues and Miguel de la Guardia
Department of Analytical Chemistry, Universitat de València. Edifici Jeroni Muñoz, 50th Dr Moliner, 46100 Burjassot, Valencia, Spain.

Journal of Agricultural and Food Chemistry 52 (2004) 7798-7803.

Impact factor of this journal (2004): 2.327
Source: Journal citation reports ISI Web of Knowledge, 2004.

7798 J. Agric. Food Chem. 2004, 52, 7798–7803

JOURNAL OF AGRICULTURAL AND FOOD CHEMISTRY

FTIR Determination of Aspartame and Acesulfame-K in Tabletop Sweeteners

SERGIO ARMENTA, SALVADOR GARRIGUES,* AND MIGUEL DE LA GUARDIA

Department of Analytical Chemistry, Universitat de València, Edifici Jeroni Muñoz, 50th Dr. Moliner, 46100 Burjassot, Valencia, Spain

Two different strategies for sweeteners determination in tabletop samples by Fourier transform middle-infrared (FTIR) spectrometry, an off-line and a fully mechanized extraction of Aspartame and Acesulfame-K with different mixtures of chloroform and methanol, have been developed. The off-line method involves the extraction of both active principles by sonication of samples with 25:75 v/v $CHCl_3$/CH_3OH and direct measurement of the peak height values at 1751 cm^{-1}, corrected using a baseline defined at 1850 cm^{-1} for Aspartame, and measurement of the peak height at 1170 cm^{-1} in the first-order derivative spectra, corrected by using a horizontal baseline established at 1850 cm^{-1}, for Acesulfame-K. Limit of detection values of 0.10 and 0.9% w/w and relative standard deviations of 0.17 and 0.5% were found for Aspartame and Acesulfame-K, respectively. The time needed for the sweeteners determination is reduced from 35 min for the HPLC method to 7 min by FTIR. On the other hand, the fully mechanized on-line extraction avoids the contact of the operator with toxic solvents and differentiates between samples that contain Aspartame and Acesulfame-K and those that include only Aspartame, reducing the time needed for the analysis of the last kind of samples to 5 min.

KEYWORDS: Sweeteners; Aspartame; Acesulfame-K; FTIR; on-line FTIR

INTRODUCTION

Aspartame, *N*-L-*a*-aspartyl-L-phenylalanine methyl ester, is an artificial sweetener used throughout the world in foods and beverages. It contains two amino acids, aspartic acid and phenylalanine. Studies in a number of animal species indicate that aspartame is quickly and extensively metabolized to its constituent amino acids and methanol. Aspartame is reported to have low toxicity in experimental model systems. The oral LD_{50} of aspartame in rats and mice is >10 g/kg per day (*1*).

Aspartame is coformulated in combination with Acesulfame-K in tabletop commercial sweeteners due to their synergistic sweetening effect (*2*).

Acesulfame-K, a potassium salt of 3,4-dihydro-6-methyl-1,2,3-oxathiazine-4-one-2,2-dioxide, is a high-intensity and noncaloric sweetener. It is not metabolized by the body and is excreted unchanged. Acesulfame-K is currently used in food, beverage, oral hygiene, and pharmaceutical products in about 90 countries. The oral LD_{50} reported is >7 g/kg in rats (*2*).

High-performance liquid chromatography (HPLC) is the most commonly used method nowadays for Aspartame and Acesulfame-K determination, based on isocratic reversed-phase (RP) chromatographic separation and ultraviolet absorbance detection (*3*). Moreover, ion chromatography (IC) with UV (*4*) and electrochemical (*5*) detection offers an attractive alternative to traditional HPLC methods. In recent years, micellar electrokinetic chromatography (MEKC) has been applied to the determination of several sweeteners in foods (*6*). Other methods less commonly used for sweetener determination are amperometry based on the use of bilayer lipid membranes (*7*), spectrophotometry based on the complexation of Aspartame with Cu (*8*), and a biosensor for Aspartame determination (*9*).

Although there are no precedents in the literature on the use of FTIR spectrometry for sweetener determination, it is clear that direct spectrometric measurements on chloroformic solutions could be an alternative to HPLC procedures in quality control processes of active principles in commercial formulations due to their relatively simple matrix and high analyte content (*10*, *11*).

The main objective of this work is the development of an FTIR method for the simultaneous determination of Aspartame and Acesulfame-K in tabletop formulations, and thus a comparison has been made between different strategies in order to be able to carry out these analyses in the best conditions from both aspects, the analytical figures of merit and the environmental side effects.

EXPERIMENTAL PROCEDURES

Apparatus and Reagents. A Bruker Tensor 27 (Bremen, Germany) spectrometer equipped with a temperature-stabilized deuterated lanthanum triglycine sulfate (DLATGS) detector was employed for spectral measurements, using a 0.11 mm path length microflow cell (Graseby-Specac, Orpington, U.K.) with ZnSe and CaF_2 windows. Spectra treatment and data manipulation have been carried out using Omnic

* Author to whom correspondence should be addressed (e-mail salvador.garrigues@uv.es; fax 34 96 35 44 838).

10.1021/jf049218l CCC: $27.50
Published on Web 12/01/2004

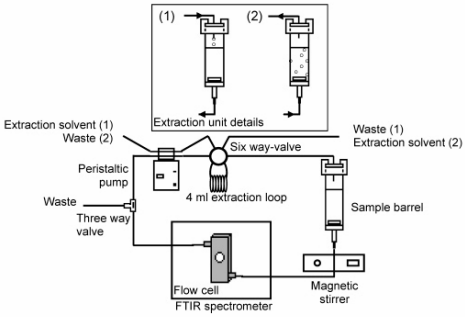

Figure 1. Manifold employed for on-line FTIR extraction of Aspartame and Acesulfame-K in tabletop sweetener samples: (1) configuration used in strategies A and B; (2) design employed in strategy C (air is circulated).

2.1 and OmnicMacros 2.1 software from Nicolet (Madison, WI). To carry out the on-line extraction of sweeteners, the manifold depicted in **Figure 1** was built by employing one six-way Rheodyne 5041 injection valve (Cotati, CA) and a Gilson Minipuls 2 peristaltic pump (Villiers-le-Bel, France) furnished with Viton (isoversinic) tubes (1 mm i.d. and 3 mm o.d.). The connecting tubes employed were made of PTFE of 0.8 mm i.d.

A Hewlett-Packard series 1050 (Palo Alto, CA) high-performance liquid chromatograph, equipped with a variable wavelength UV−vis detector and a Kromasil C-18 column (250 × 4.6 mm i.d. and 5 μm particle diameter), was also used for the analysis of tabletop sweetener samples, this methodology being employed as a reference for the validation of the FTIR determination procedures.

A J.P. Selecta ultrasonic water bath (Barcelona, Spain) was employed to improve a fast sweetener extraction in off-line experiments.

An SBS A-01 magnetic stirrer (Barcelona, Spain), working at medium rotation speed, was employed to improve the sweetener extraction in the manifold depicted in **Figure 1**.

Guinama (Barcelona, Spain) supplied Aspartame standard (99% w/w) and Fluka (Buchs, Switzerland) provided Acesulfame-K standard (98.9% w/w). Analytical grade chloroform stabilized with 150 mg L^{-1} amylene and HPLC grade methanol (Scharlau, Barcelona, Spain) were employed for the preparation of FTIR samples and standards. KH_2PO_4 and HPLC grade acetonitrile supplied by Scharlau (Barcelona, Spain), were used for the preparation of HPLC samples and standards. Commercial sweeteners employed in this study, containing Aspartame and/or Acesulfame-K, also contain lactose, sodium carboxymethylcellulose, L-leucine, and glycine as excipients. Samples analyzed were obtained directly from the Spanish market.

HPLC-UV Reference Procedure. A whole sweetener tablet (60 mg) was accurately weighed (±0.1 mg) inside a 25 mL volumetric flask, diluted to the volume with 0.02 M KH_2PO_4/acetonitrile (90:10 v/v), and sonicated during 5 min in an ultrasonic water bath to extract Aspartame and Acesulfame-K from the matrix. Half a milliliter of the extract was diluted to 10 mL with the same solvent mixture and filtered through a 0.22 μm nylon membrane; 20 μL of this latter solution was directly injected in a 0.02 M KH_2PO_4/acetonitrile (90:10 v/v) mobile phase using a constant 0.75 mL min^{-1} carrier flow, and Aspartame and Acesulfame-K were determined in the isocratic mode by absorbance measurements at 205 nm peak area values of the chromatogram obtained at 28.5 and 5.9 min, for Aspartame and Acesulfame-K, respectively, and were interpolated in the corresponding calibration lines obtained from six standards of the two studied compounds (from 10.49 to 41.97 mg g^{-1} for Aspartame and between 6.83 and 54.65 mg g^{-1} for Acesulfame-K). Each sample or standard solution was injected three times.

Calibration lines obtained in the aforementioned conditions were $A_1 = (0.6 \pm 0.8) + (42.58 \pm 0.04)C_{AS}$ with $R^2 = 0.99992$ and $A_2 = (-0.3 \pm 0.5) + (35.58 \pm 0.02)C_{AK}$ with $R^2 = 0.99998$ for Aspartame (C_{AS}) and Acesulfame-K (C_{AK}), respectively, A_1 and A_2 being the area values found at the aforementioned elution times and C being the concentration in mg L^{-1}.

The repeatabilities, established as the relative standard deviation, were 0.1 and 0.03% of five independent analyses of a 10.5 mg L^{-1} Aspartame standard and 6.8 mg L^{-1} Acesulfame-K, respectively, and limit of detection values (established as $3s_{blank}$/calibration slope) of 0.016 and 0.03% w/w, for Aspartame and Acesulfame-K, respectively, were achieved by this procedure.

Off-Line Extraction FTIR Procedure. A whole tablet of sample (60 mg) was accurately weighed (±0.1 mg) and diluted with 4 g of a mixture of $CHCl_3$ and methanol in a ratio of 25:75 (v/v). The mixture was sonicated for 5 min in an ultrasonic water bath. Sample extract was passed through a 0.22 μm nylon filter and introduced into the FTIR measurement cell by using a peristaltic pump. The spectra were obtained per triplicate in the stopped-flow mode at 4 cm^{-1} nominal resolution and accumulating 25 scans per spectrum from 4000 to 850 cm^{-1} using a background of the cell filled with the solvent mixture.

Two individual external calibration sets of Aspartame (six standards from 1.26 to 4.28 mg g^{-1}) and Acesulfame-K (six standards from 1.32 to 3.45 mg g^{-1}) were prepared and their FTIR spectra obtained under the same conditions employed for samples. A calibration line was established for Aspartame by measuring peak height values at 1751 cm^{-1}, corrected using a baseline defined at 1850 cm^{-1}. For Acesulfame-K determination, measurements of the peak height at 1170 cm^{-1} in the first-order derivative spectra, corrected by using a horizontal baseline established at 1850 cm^{-1}, were employed. The concentrations of Aspartame and Acesulfame-K in samples were calculated by interpolation of the absorbance data in the above calibration plots.

On-Line Extraction FTIR Procedure. For on-line extraction of Aspartame and Acesulfame-K three different strategies, which all provide quantitative and comparable results, were used.

Strategy A. A whole tablet of sample (60 mg) was accurately weighed (±0.1 mg) and introduced inside a homemade glass syringe barrel of 6 mL internal volume that includes a porous glass filter. The syringe was placed in the manifold of **Figure 1**. A 25:75 mixture of $CHCl_3$ and methanol was introduced through a 4 mL loop. The solvent was circulated in the closed system for 7 min with the magnetic stirrer on at medium speed level. After that, the spectrum was recorded per triplicate, accumulating 25 scans and employing a nominal resolution of 4 cm^{-1}.

The concentrations of Aspartame and Acesulfame-K in samples were calculated by interpolation of the absorbance data obtained for samples in the spectral conditions indicated before in the calibration plots obtained from standard solutions in $CHCl_3$ and methanol as indicated for off-line extraction.

The manifold includes a three-way valve, as can be seen in **Figure 1**, to clean the closed system before the introduction of other sample.

Strategy B. A whole sample tablet (60 mg) was weighed (±0.1 mg) and introduced inside a glass syringe barrel; after that, the syringe was placed in the manifold of **Figure 1**. A 50:50 mixture of $CHCl_3$ and methanol was introduced through the 4 mL loop. The solvent was circulated in the closed system during 5.5 min (magnetic stirrer on), and after that, the FTIR spectrum was recorded per triplicate using a nominal resolution of 4 cm^{-1} and accumulating 25 scans. Under these conditions, the concentration of Aspartame in samples was calculated by interpolation of the peak height of the absorbance spectra at 1751 cm^{-1} corrected with a horizontal baseline located at 1850 cm^{-1} in a calibration line established from standard solutions in 50:50 $CHCl_3$/methanol as indicated before.

For sample spectra that present two intense bands located at 1600 and 1150 cm^{-1} indicating the presence of Acesulfame-K, the loop was filled again with pure methanol, which was introduced in the glass syringe. The resulting solvent mixture was circulated for 7 min, and the spectrum was acquired in the aforementioned conditions but employing a background registered for a solvent mixture of 25:75 chloroform/methanol. Acesulfame-K was determined by using the first-order derivative spectra and the conditions indicted before.

Strategy C. A third strategy was employed, based on the same principle as that described for strategy B but including a step based on the circulation of an air current through the syringe barrel containing both the sample and the solvent mixture. In this case air bubbles provide

Table 1. Analytical Features of the FTIR Determination of Aspartame and Acesulafame-K Using Different Bands, Baseline Criteria, and Measurement Modes

measurement mode	wavenumber (cm^{-1})	baseline correction	$a \pm s_a$	$b \pm s_b$	R^2	% RSD	LOD[a] ($\mu g\ g^{-1}$)	LOD[b] (% w/w)	Er[c] % w/w
			Aspartame Calibration Curve [$y = a + bC$ (mg g^{-1})]						
height	1751	1850	−0.0005 ± 0.0002	0.01039 ± 0.00002	0.9996	0.17	14	0.10	0.5
area	1756−1746		−0.008 ± 0.001	0.0970 ± 0.0006	0.9996	0.10	5	0.03	6.0
height	1690		−0.0003 ± 0.0005	0.0115 ± 0.0002	0.996	0.16	12	0.08	32
area	1695−1685		−0.005 ± 0.004	0.110 ± 0.002	0.996	0.09	60	0.4	40
height	1606		−0.0010 ± 0.0004	0.0143 ± 0.0002	0.998	0.3	50	0.3	43
area	1611−1601		−0.011 ± 0.004	0.136 ± 0.002	0.998	0.2	30	0.19	48
			Acesulfame-K Calibration Curve [$y = a + bC$ (mg g^{-1})]						
height	1652	1850	0.0004 ± 0.0005	0.0284 ± 0.0004	0.999	0.14	7	0.05	58
area	1657−1647		0.002 ± 0.005	0.246 ± 0.004	0.998	0.17	14	0.10	66
height	1575		0.0000 ± 0.0001	0.01367 ± 0.00008	0.9997	0.7	20	0.13	94
area	1580−1570		−0.002 ± 0.001	0.130 ± 0.001	0.9996	0.6	40	0.3	94
height	1176		0.0009 ± 0.0003	0.0449 ± 0.0002	0.9998	0.4	13	0.09	8.5
area	1181−1171		0.002 ± 0.003	0.401 ± 0.002	0.9997	0.4	18	0.12	11
height	945		0.0009 ± 0.0003	0.0118 ± 0.0002	0.997	3.0	100	0.7	−16
area	950−940		0.005 ± 0.003	0.094 ± 0.002	0.996	1.4	200	1.3	12

[a] Limit of detection values were established for a probability level of 99.6% from the expression $3S_{blank}/b$, S_{blank} being the standard deviation of six measurements of a blank of chloroform/methanol 25:75 solution and b the slope of the calibration line. [b] Limit of detection in tabletop formulations for a sample mass of 60 mg. [c] Accuracy error in percent calculated from three independent determinations of sample 1 that contains 11.88 ± 0.02% (w/w) Aspartame and 11.71 ± 0.02% (w/w) Acesulfame-K.

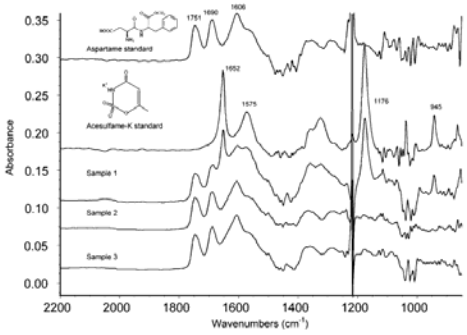

Figure 2. FTIR spectra of Aspartame and Acesulfame-K standard and three tabletop commercial samples extracted with a 25:75 v/v $CHCl_3$/CH_3OH solvent mixture. Spectra are the average of 25 scans using a nominal resolution of 4 cm^{-1}. Concentrations of standards correspond to 3.45 mg g^{-1} Aspartame and 3.13 mg g^{-1} Acesulfame-K. Sample 1 contains 11.88% w/w Aspartame and 11.71% w/w Acesulfame-K, and samples 2 and 3 contain 38.5 and 38.7% w/w of Aspartame, respectively.

a fast and complete extraction of Aspartame and Acesulfame-K from the samples, and FTIR measurements were made as indicated before.

RESULTS AND DISCUSSION

FTIR Transmission Spectrum of Artificial Sweeteners. **Figure 2** shows the FTIR spectra of an Aspartame standard solution with a concentration of 3.45 mg g^{-1}, an Acesulfame-K standard solution with a concentration of 3.13 mg g^{-1}, and three commercial tabletop sweeteners, one containing Aspartame and Acesulfame-K and two only Aspartame.

The most intense bands present in the Aspartame spectra are the C═O band in the ester group at 1751 cm^{-1}, that of 1700 cm^{-1} due to the C═O stretch in carboxylic acids, and the band at 1650 cm^{-1} due to the C═O stretch in amides.

The most intense bands of Acesulfame-K are those located at 1680 and 1150 cm^{-1} due to C═O stretch and NH_2 rock in amides. Other less intense absorption bands are located at 1600 and 1356 cm^{-1} due to SO_2 stretch and C═C stretch in cyclohexenes, respectively (*12*).

Selection of FTIR Absorbance Bands for Aspartame and Acesulfame-K Determination. To choose the best analytical conditions for Aspartame and Acesulfame-K determination in tabletop sweeteners by FTIR, different bands and baseline criteria were evaluated. In every case, the use of peak height and peak area absorbance measurement was considered.

Table 1 summarizes the main analytical features of the FTIR determination of Aspartame and Acesulfame-K using a typical stopped-flow approach for sample extraction in $CHCl_3$/methanol. As can be seen, the sensitivity found by peak area measurements was in all the cases 1 order of magnitude better than that obtained by using peak height. However, the limit of detection (LOD) values obtained (see footnote of **Table 1** for details) varied from 0.03 to 0.3% w/w and from 0.05 to 1.6% w/w for Aspartame and Acesulfame-K, respectively, and this latter parameter strongly depends on the stability of absorbance measurements as well as the sensitivity.

As can be seen in **Figure 2**, the Aspartame bands at 1690 and 1606 cm^{-1} highly overlap with the Acesulfame-K bands at 1652 and 1575 cm^{-1}. Therefore, despite the good regression coefficients and LOD values obtained, these bands could not be used for the determination of the two studied compounds in samples containing a mixture of both.

Therefore, the band selected to carry out Aspartame determination was that presented at 1751 cm^{-1}. From a comparison of peak height and peak area measurements it can be concluded that the use of peak area provides in general 1 order of magnitude greater sensitivity than the use of peak height. However, the mean relative errors achieved when peak area measurements were used were higher than those obtained for peak height values, so the latest measurement mode was selected for the Aspartame determination in tabletop sweeteners.

On the other hand, the Acesulfame-K band at 945 cm^{-1} does not overlap with any Aspartame band, but the low signal-to-noise (S/N) ratio in this region when compared with that achieved in the 2000−1100 cm^{-1} range increases the LOD

Table 2. Analytical Features of the FTIR Determination of Acesulafame-K by Using First-Order Derivative Spectra and Evaluating Different Bands and Measurement Modes

			Acesulfame-K calibration curve [$y = a + bC$ (mg g^{-1})]						
measurement mode	wavenumber (cm^{-1})	baseline correction	$a \pm s_a$	$b \pm s_b$	R^2	% RSD	LOD[a] (μg g^{-1})	LOD[b] (% w/w)	Er[c] % w/w
height	1647		0.00006 ± 0.00005	0.00282 ± 0.00002	0.9996	0.17	40	0.3	−20
area	1652–1642		−0.0001 ± 0.0004	0.0185 ± 0.0001	0.9995	0.08	50	0.4	−21
height	1170	1850	0.00008 ± 0.00006	0.00225 ± 0.00002	0.9992	0.5	140	0.9	1.0
area	1175–1165		0.0004 ± 0.0002	0.01839 ± 0.00008	0.9998	0.6	70	0.5	−4.3
height	938		0.00002 ± 0.00008	0.00122 ± 0.00003	0.994	1.4	200	1.3	−12
area	943–933		0.0004 ± 0.0004	0.0071 ± 0.0001	0.996	3.3	300	2.2	−18

[a] Limit of detection established for a probability level of 99.6% from the expression $3S_{blank}/b$, S_{blank} being the standard deviation of six measurements of a blank of chloroform/methanol 25:75 solution and b the slope of the calibration line. [b] Limit of detection in tabletop formulations for a sample mass of 60 mg. [c] Accuracy error in percent calculated from three independent determinations of sample 1 containing 11.71 ± 0.02% (w/w) Acesulfame-K.

values obtained from peak height measurement. Therefore, for Acesulfame-K determination the band located at 1176 cm^{-1} corrected with a single-point baseline located at 1850 cm^{-1} was selected. In these conditions, an accuracy relative error of the order of 8% w/w was obtained for the analysis of a commercially available sample containing Aspartame and Acesulfame-K.

To improve the Acesulfame-K determination in tabletop samples, the first-order derivative spectra were obtained and, as can be seen in **Table 2**, different bands and measurement modes were tested.

As can be seen, the limits of determination achieved are worse than those obtained using zero-order spectra, being between 0.3 and 2.2% w/w. Peak height values at 1170 cm^{-1} corrected with a single-point baseline located at 1850 cm^{-1} were selected because a mean accuracy relative error of 1.0% w/w was achieved on the analysis of actual samples.

Study of Interferences. From the manufacturer's information the main excipient present in the samples studied is lactose. This compound is very slightly soluble in alcohol and insoluble in $CHCl_3$, and it remains undissolved after the complete extraction of Aspartame and Acesulfame-K. Other excipients present, at a low level, are sodium carboxymethylcellulose (insoluble in alcohol), glycine (soluble, 0.06 g/100 mL of alcohol), and L-leucine (soluble, 0.07 g in 100 mL of alcohol). Because of that, spectral interferences expected were simply the mutual ones between both studied sweeteners.

To ensure the accuracy of the Aspartame and Acesulfame-K determination in commercial formulations containing both products, a series of studies was carried out on the influence of the concentration of each of these compounds on the other. For a fixed concentration of 0.88 mg g^{-1} Aspartame the effect of increasing amounts of Acesulfame-K, from 0.97 to 3.05 mg g^{-1}, was studied, and for a fixed concentration of 0.86 mg g^{-1} Acesulfame-K the effect of Aspartame, from 1.01 to 2.31 mg g^{-1}, was also evaluated.

The presence of Acesulfame-K does not interfere with the Aspartame determination when peak height values at 1751 cm^{-1}, corrected with a baseline defined at 1850 cm^{-1}, were used.

However, Aspartame clearly interferes with Acesulfame-K determination when peak height values at 1176 cm^{-1} (corrected with a baseline defined at 1850 cm^{-1}) in the zero-order spectra were used. Therefore, to avoid this interference, first-order derivative spectra were employed for Acesulfame-K determination. When peak height values at 1170 cm^{-1} with a baseline defined at 1850 cm^{-1} were used, the interference of Aspartame on Acesulfame-K determination was avoided.

Off-Line Extraction of Sweeteners. To reduce the time needed to carry out the extraction of Aspartame and Acesulfame-K from solid samples, different sonication times from 2 to 12 min were applied to extract both compounds with a $CHCl_3$/methanol (25:75 v/v) mixture; it was found that 5 min of sonication is enough for the quantitative recovery of the two compounds under study.

Effect of Experimental Variables on the On-Line Extraction of Aspartame and Acesulfame-K. To develop a fully mechanized procedure for FTIR determination of Aspartame and Acesulfame-K in tabletop sweeteners, the on-line approach described in the experiment set was assayed. Different parameters, such as carrier flow rate, direction of flow, or geometry of the extraction cell, were evaluated to improve the extraction by reducing the time required.

Carrier flow rate was modified between 0.5 and 2.75 mL min^{-1}. As can be seen in **Figure 3**, this parameter is not decisive because the time needed for the dissolution of the sweeteners in the sample cartridge is higher than the recirculation solvent time.

Another parameter evaluated was the solvent recirculation direction. Two different configurations based on the solvent recirculation in a closed system and the air bubbling through the mixture of the sample and solvent, remaining all the time inside the syringe barrel, were assayed. However, as can be seen in **Figure 4** both air and solvent circulation provided a complete Aspartame extraction, but the use of air bubbles seems to be more effective, requiring 6 min instead 7 min for a complete extraction.

Different sample extraction cell geometries were tested to minimize the extraction time: a 35 mL volume, 7.78 cm length, and 2.67 cm i.d. plastic syringe barrel; two glass cells of 6 mL volume, 5.48 cm length, and 1.14 cm i.d.; and a 9 mL volume with 3.70 cm length and 1.69 cm i.d. As can be seen in **Figure 5**, a syringe barrel of 6 mL internal volume was selected because it facilitates the homogenization and avoids the deposition of solid particles on the sample cell internal surface.

ANALYTICAL FIGURES OF MERIT

To verify the absence of matrix effect on the FTIR determination of Aspartame and Acesulfame-K, external calibration and standard addition lines were compared, employing in both cases the previously selected measurement conditions.

The typical calibration line obtained by the standard addition for Aspartame was $A = (0.01820 \pm 0.00008) + (0.01040 \pm 0.00006)C$ (mg g^{-1} Aspartame added), with $R^2 = 0.9997$, which is comparable to the external calibration line $A = (-0.0005 \pm$

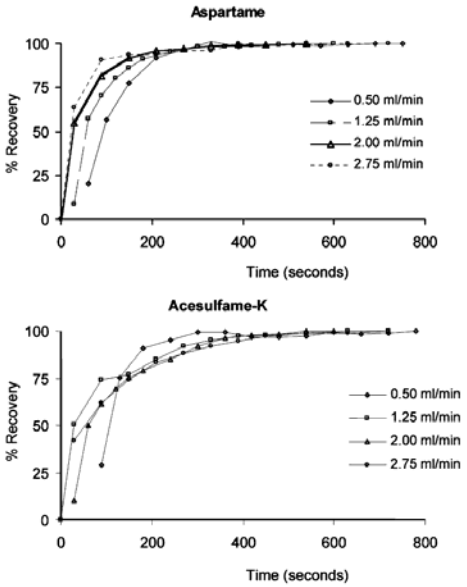

Figure 3. Effect of carrier flow rate and extraction time on Aspartame and Acesulfame-K recovery. For Aspartame peak height values at 1751 cm^{-1} corrected using a baseline defined at 1850 cm^{-1} were used, and for the Acesulfame-K peak height values at 1170 cm^{-1} with a baseline defined at 1850 cm^{-1} in the first-order derivative spectra were employed. The percentage recovery was calculated using the concentration of both sweeteners in sample 1 found by the HPLC reference procedure.

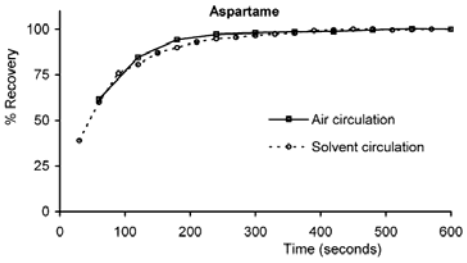

Figure 4. Effect of solvent circulation on Aspartame extraction by using air (□) and solvent (○) circulation with a flow of 2.00 mL min^{-1}. Measurement conditions were as indicated in **Figure 3**.

0.0002) + (0.0104 ± 0.0001)C (mg g^{-1} Aspartame), with R^2 = 0.9990.

On the other hand, in the case of Acesulfame-K, the calibration line obtained from first-derivative spectra by standard addition was A = (0.00188 ± 0.00006) + (0.00224 ± 0.00005)C (mg g^{-1} Acesulfame-K added), with a regression coefficient of R^2 = 0.998, which is comparable to the external calibration line A = (0.00008 ± 0.00004) + (0.00225 ± 0.00002)C (mg g^{-1} Acesulfame-K), with R^2 = 0.9995.

Therefore, on the basis of these results it can be concluded that the selected conditions for Aspartame and Acesulfame-K determination are free from matrix interferences, and thus external calibration can be employed.

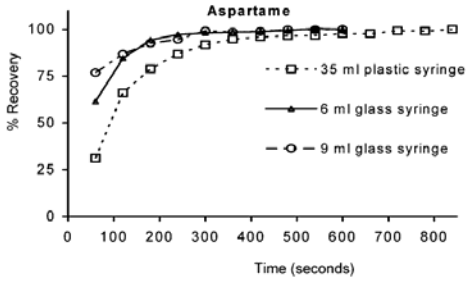

Figure 5. Effect of sample syringe geometries on Aspartame extraction time. The conditions employed are the same as those indicated in **Figure 3**. The percentage recovery was calculated using the concentration of Aspartame in sample 1 found by the HPLC reference procedure.

Table 3. Determination of Aspartame and Acesulfame-K Content (Percent w/w) in Commercially Available Tabletop Formulations

sample	active substance	HPLC[a]	FTIR off-line[a]	t_{exp}[b]	FTIR on-line[a]	t_{exp}
1	Aspartame	11.88 ± 0.02	11.83 ± 0.08	1.36	11.9 ± 0.2	0.22
	Acesulfame-K	11.71 ± 0.02	11.74 ± 0.14	0.47	11.8 ± 0.3	0.52
2	Aspartame	38.5 ± 0.2	38.4 ± 0.2	0.79	38.6 ± 0.3	0.62
3	Aspartame	38.7 ± 0.2	38.70 ± 0.10	0.00	38.9 ± 0.4	1.00

[a] Average of three independent analyses ± standard deviation. [b] t_{tab} = 2.132, for a probability level of 95% and 4 freedom degrees.

Table 4. Comparison of the Analysis Time and Organic Solvent Consumption for the Measurement Step among the Developed Procedures

	Aspartame	Acesulfame-K	total	
	analysis time (min)	analysis time (min)	time (min)	volume (mL)
HPLC	30	7	35	6.5
FTIR off-line	7	7	7	4
FTIR on-line				
strategy A	6.5	7	7	4
strategy B	5.5	7	12.5	4
strategy C	5	6	11	4

COMPARISON AMONG THE DIFFERENT METHODOLOGIES DEVELOPED

Off-line and on-line FTIR procedures developed in this work provide statistically comparable results (for a probability level of 95%) with those obtained by the HPLC reference method, as can be seen in **Table 3**.

The precision obtained by off-line FTIR (in terms of the relative standard deviation of results) is of the same order of magnitude as that found by the reference method, the results obtained by on-line FTIR being less precise than those determined by HPLC.

The limits of detection achieved by FTIR procedures were higher than those found by HPLC, being for Aspartame and Acesulfame-K 0.09 and 0.9% w/w and 0.016 and 0.03% w/w, respectively. However, due to the high concentration of these two compounds present in commercial formulations, FTIR procedures are sufficiently sensitive for their analysis.

FTIR strategies involve a strong reduction of the time of analysis as compared with the chromatographic procedures, as can be seen in **Table 4**. The time needed for the determination

of Aspartame and Acesulfame-K in tabletop samples was reduced from 35 to 7 min by using FTIR.

On the other hand, in this paper, a fully mechanized extraction procedure has been developed, in which the contact of the operator with the solvents is avoided. This strategy provides a clear differentiation between samples that contain only Aspartame and those that include Acesulfame-K. In the first case, Aspartame can be extracted and filtered on-line in only 5 min, and it could be determined by FTIR measurements. In tabletop samples containing Aspartame and Acesulfame-K, a second extraction step is necessary, increasing the time of analysis to 11 min.

FTIR procedures developed in this work are an alternative to the chromatographic procedures in the quality control of sweeteners in tabletop formulations.

LITERATURE CITED

(1) U.S. Department of Health and Human Services, Public Health Service. National Institutes of Health. *Ntp Technical Report on the Toxicity Studies of Aspartame (Case No. 22839-47-0)*; U.S. GPO: Washington, DC, 2003.

(2) International Sweeteners Association, Brussels, Belgium, 2004; http://www.isabru.org/frameset.html.

(3) Kobayashi, C.; Nakazato, M.; Ushiyama, H.; Kawai, Y.; Tateishi, Y.; Yasuda, K. Simultaneous determination of five sweeteners in foods by HPLC. *Shokuhin Eiseigaku Zasshi* **1999**, *40*, 166−171.

(4) Chen, Q. C.; Wang, J. Simultaneous determination of artificial sweeteners, preservatives, caffeine, theobromine and theophylline in food and pharmaceutical preparations by ion chromatography. *J. Chromatogr. A* **2001**, *937*, 57−64.

(5) Qu, F.; Qi, Z. H.; Liu, K. N.; Mou, S. F. Determination of aspartame by ion chromatography with electrochemical integrated amperometric detection. *J. Chromatogr. A* **1999**, *850*, 277−281.

(6) Boyce, M. C. Simultaneous determination of antioxidants, preservatives and sweeteners permitted as additives in foods by mixed micellar electrokinetic chromatography. *J. Chromatrogr. A* **1999**, *847*, 369−375.

(7) Nikolelis, D. P.; Pantoulias S. A minisensor for the rapid screening of acesulfame-K, cyclamate and saccharin based on surface-stabilized bilayer lipid membranes. *Electroanalysis* **2000**, *12*, 786−790.

(8) Fatibello-Filho, O.; Marcolino-Junior, LH.; Pereira, AV. Solid-phase reactor with copper(II) phosphate for flow-injection spectrophotometric determination of aspartame in tabletop sweeteners. *Anal. Chim. Acta* **1999**, *384*, 167−174.

(9) Odaci, D; Timur, S.; Telefoncu, A. Carboxyl esterase-alcohol oxidase based biosensor for the aspartame determination. *Food Chem.* **2004**, *84*, 493−496.

(10) Quintas, G.; Armenta, S.; Morales-Noe, A.; Garrigues, S.; de la Guardia, M. Simultaneous determination of folpet and metalaxyl in pesticide formulations by flow injection Fourier transform infrared spectrometry. *Anal. Chim. Acta* **2003**, *480*, 11−21.

(11) Armenta, S.; Quintas, G.; Moros, J.; Garrigues, S.; de la Guardia, M. Fourier transform infrared spectrometric strategies for the determination of Buprofezin in pesticide formulations. *Anal. Chim. Acta* **2002**, *468*, 81−90.

(12) Lin-Vien, D.; Colthup, N. B.; Fateley, W. G.; Grasselli, J. G. *Infrared and Raman Characteristic Frequencies of Organic Molecules*; Academic Press: London, U.K., 1991.

Received for review May 17, 2004. Revised manuscript received October 15, 2004. Accepted October 18, 2004. We acknowledge the financial support of the Generalitat Valenciana Project GV04B-247 and Grupos 03/118 to carry out this study. S.A. acknowledges an FPU Grant of the Ministerio de Educación, Cultura y Deporte (Ref. AP2002-1874).

JF049218L

Optimization of transmission near infrared spectrometry procedures for quality control in pesticide formulations

Sergio Armenta, Salvador Garrigues and Miguel de la Guardia
Department of Analytical Chemistry, Universitat de València. Edifici Jeroni Muñoz, 50th Dr Moliner, 46100 Burjassot, Valencia, Spain.

Analytical Chimica Acta Accepted for publication 2005.

Impact factor of this journal (2004): 2.588
Source: Journal citation reports ISI Web of Knowledge, 2004.

Optimization of transmission near infrared spectrometry procedures for quality control

Sergio Armenta, Salvador Garrigues*, Miguel de la Guardia

Department of Analytical Chemistry. Universitat de València. Edifici Jeroni Muñoz, 50th Dr. Moliner 46100 BURJASSOT. Valencia. SPAIN

Abstract:
The use of different response functions to be optimized in the frame of the use of near infrared spectrometry for quality control of active principles in agrochemical formulations has been evaluated. Both, simple functions, based on parameters like sensitivity, repeatability, accuracy, signal to noise ratio, limit of detection or sample throughput, and a complex function, considering all the aforementioned aspects, were employed in the developmenrt of a new method for the determination of iprodione in agrochemicals. Optimization strategies were based on the previous screening of the most important instrumental factors like number of cumulated scans, nominal resolution, mirror velocity and zero filling factor, based on a two-level full factorial design and on the search for the optimum conditions using central composite designs.
Data found evidenced the influence of the response function on the optimum values of experimental conditions and could be employed as a general guide to evaluate the experimental factors in routine use of near spectrometry.
Keywords: Optimization functions, Near infrared, PLS calibration, pesticide formulations

Introduction

The term optimization refers to an experimental design applied to determine in an efficient way the set of conditions that are required to obtain a product or process with desirable, often optimal, characteristics.

Actual optimization strategies try to obtain the largest number of good quality information carrying out a limited number of experiments [1].

The traditional one-at-a-time optimization strategy is simple and easy, and the individual effects of medium components can be seen on a graph without the need to revert to statistical analysis. Unfortunately, it frequently fails to locate the region of optimum response because the joint effects of factors on the response are not taken into account in such procedures [2]. On the other hand, the univariate optimization implies the continuous iteration until the best conditions

* Corresponding author. Tel.: +34 96 354 3158; fax: +34 96 354 4838.

E-mail address: salvador.garrigues@uv.es (S. Garrigues).

are obtained, thus involving a big number of experiments.

Multivariate optimization strategies involve the simultaneous consideration of as many as possible experimental variables and their concomitant effects which are considered in a series of sequential or simultaneous experiments.

One kind of sequential optimization strategy is based on the Simplex algorithm, which is useful for any type and number of parameters. The Simplex method has serious drawbacks mainly derived from its limited searching capability. The procedure is a hill climbing method in which the direction and increment of advance is dependent only on the experimental responses. The Simplex method will find an optimum but it might be a local optimum and no reversal order is detected. A possible route to avoid that a local optimum may be considered as a global optimum is to repeat the procedure with a different starting position. Consequently, super modified Simplex, weighted centroid methods have been advocated. Another drawback of the Simplex method is the large number of experiments and the total time needed to reach the optimum [3].

On the other hand, the so-called simultaneous or factorial, designs are used to determine the collective influence of a large number of factors on the variance in the results of a process. The simplest experimental design is a full factorial design (FFD) in which each factor can assume two levels. A two level full factorial design is a design where all combinations of parameter levels are made. This type of design would allow the determination of all main effects as well as all interaction effects. Since it is time consuming to perform as many experiments, a fraction of the full factorial design is commonly utilized.

Fractional factorial design (fFD) is a fraction of a full factorial design and, whilst a reduction in the number of experiments leads to some loss of information, this procedure maintains the statistical ability to identify the influence of each parameter and to check possible interactions between parameters. The linear model taking account interaction effects between factors obtained from a two level design may lead to erroneous conclusions about factor effects in the case where curvatures (second order effects) are neglected. In that case, a three level factorial design can be used.

A central composite design (CCD) consists of a 2^d factorial runs (or fractional factorial of resolution V), $2d$ axial or star runs and n center runs. Six replicates at the center point of the design and a pair of experiments along each coordinate axis permit to calculate the experimental error of the process and to determine response surfaces and the corresponding contour plots. For design with few variables the experiments to choose are obvious but for larger series computer aided selections are mandatory. Data from a CCD can be evaluated and plotted as a response surface by combining a statistical procedure that fits a quadratic response surface model to the data. Response surfaces can provide a graphical representation of the data over the range of the key parameters under study.

It is increasingly common to find examples in the bibliography of the application of

experimental design methodology in the optimisation of methods of extraction and analysis [4,5].

A very important step in experimental design is the selection of the response to be investigated. Usually, one models each response separately and tries to find the factor values yielding the highest or lowest response, but in practice, it is common that these results be conflicting. So, the response selection is a critical stage in the optimisation. It is common to optimise parameters such as the peak height or area [6], the variability [7], the correlation coefficient or other more complex functions [8] which indirectly evaluate the sensitivity, precision, sample throughput or cost. However, in our knowledge there is no precedent on the systematic optimization of quality control methodologies of agrochemical products based on the use of vibrational spectrometry.

Nowadays, there is an ongoing interest to develop safe, fast, reliable and cost effective analytical methods for the quality control of commercial products. In short, the aim of the present paper is to study the different possible responses to be optimized (sensitivity, precision, accuracy, limit of detection, signal to noise ratio and sample throughput), to compare and to establish the global-optimum conditions in the quality control analysis of commercially available formulations through the use of NIR spectrometry. In this sense, Iprodione, 3-(3,5-dichlorophenyl)-N-(1-methylethyl)2,4-dioxo-1-imidazoline-carboxamide, a dicarboximide contact fungicide used for a wide variety of crop diseases on vegetables, ornamentals, pome and stone fruit, root crops, cotton, and sunflowers as a post harvest fungicide has been selected as test molecule [9].

Iprodione is slightly toxic by ingestion, with reported oral LD_{50} values of 3500 mg/kg in rats. Iprodione is manufactured in several commercially available pesticide formulations as dusting powder, soluble concentrated or wetting powder [10].

The use of near infrared (NIR) has been proposed as a fast and environmentally friendly alternative to the use of chromatographic procedures for the determination of active principles in pesticide formulations and there are available methods for the determination of Diuron (11) and Buprofezin (12), which provide comparable values to those obtained by the CIPAC recommended methods (13). However, in our best knowledge there is no precedent on the use of NIR for the determination of Iprodione.

Experimental

Apparatus and reagents

A Bruker MPA (Bremen, Germany) Fourier transform near infrared (FT-NIR) spectrometer equipped with a quartz beamspliter, an air cooled NIR source, an InGaAs detector was used in this study. For measurement control, data acquisition and spectra treatment, the OPUS program, from Bruker was used.

For the optimization of the NIR instrumental parameters, the Minitab® Release 14 statistical

software from Minitab Inc. (State College, PA, USA) was used.

A Hewlett-Packard HPLC Series 1050 High Performance Liquid Chromatograph, eqquiped with a variable wavelength UV-Vis detector and a reversed phase C-18 (Kromasil) column of 250 mm length and 4.6 mm i.d. with 5 µm particle diameter, was employed for the analysis of the pesticide formulations, being used this methodology as a reference procedure for the validation of NIR measurements.

Iprodione PESTANAL® grade standard (99.8 % w/w) was supplied by Fluka (Buchs, Switzerland). Analytical grade acetonitrile supplied by Scharlau (Barcelona, Spain), was employed for the preparation of samples and standards. Iprodione wettable powder commercial formulations, containing a declared value of 50 % w/w, were obtained directly from the Spanish market.

Reference procedure

30 mg sample were accurately weighed, inside a 25 ml volumetric flask and diluted to the volume with acetonitrile, being sonicated during 5 minutes in an ultrasound water bath to extract Iprodione from the matrix. 1 ml of the extract was diluted to 25 ml and filtered through a 0.22 µm nylon filter. 10 µl of this latter solution were directly injected in a 85:15 acetonitrile:water mobile phase, at 1 ml min^{-1} carrier flow and Iprodione determined in the isocratic mode by absorbance measurements at 229 nm. Area values of the chromatogram peak obtained at 4.2 min for samples were interpolated in an external calibration line established from the measurement of six standard solutions of Iprodione containing from 5.85 to 23.40 mg l^{-1}.

Calibration line obtained in the aforementioned conditions was $A=(-0.2 \pm 0.2) + (21.853 \pm 0.014)C_{IP}$ with a $R^2=0.99996$ for Iprodione, concentrations expressed in mg l^{-1}. The repeatability, established as the relative standard deviation, was 0.1 % for five independent analysis of a 5.85 mg l^{-1} Iprodione standard and a limit of detection of 0.016 % w/w was achieved by this procedure.

FT-NIR procedure

15-20 mg of sample were dissolved with 750 mg acetonitrile by ultrasonic shaking for two minutes. This solution was filtered and transferred to a glass vial of 6.5 mm i.d. used as measurement cell. The FT-NIR spectrum was recorded from 12500 to 4000 cm^{-1} employing a background spectrum of the cell filled with acetonitrile measured in the same instrumental conditions used for samples.

A calibration line was established from Iprodione standard solutions in acetonitrile, in the concentration range between 5.25 and 27.58 mg g^{-1}, by measuring peak area values between 4915 and 4867 cm^{-1} corrected using a two points baseline defined between 4982 and 4810 cm^{-1}. Sample spectral data obtained in the same conditions as standards, were interpolated in the Iprodione calibration line.

Optimization procedure and experimental design

As indicated before, the optimization procedure involved two steps: i) the screening of significant instrumental variables affecting the function under study through a FFD and ii) the optimization of the functions through a CCD.

Screening by a fractional factorial design (FFD)

A 2^4 full factorial design, with a complete repetition and one center point performed in one run resulting in a total of 33 experiments, was employed to determine the instrument variables of the NIR spectrometry determination that affects significantly the different functions under study.

The number of cumulated scans, nominal resolution, mirror velocity and zero filling factor were selected as potentially affecting variables on the NIR transmission measurements. The setting of the four factors is given in Table 1. Each factor had the chance to be examined at a high level (+) and a low setting (-), and the corresponding center point (0), respectively. All the experiments were performed in a random order to avoid trends in data found.

Different functions were selected as response to be optimized, such as: i) sensitivity (s), as the slope of the calibration line in mg g^{-1} Iprodione per peak area values; ii) repeatability (% RSD), established as relative standard deviation; iii) accuracy relative error of the results (% Er) obtained by the NIR method for three commercial formulations of Iprodione with 50 % w/w concentration, compared with the chromatography reference procedure; iv) the limit of detection (LOD), established as three times the standard deviation of a blank signal divided by the slope of the calibration curve; v) signal to noise ratio (S/N), being established as the area, between 4915 and 4867 cm^{-1} corrected using a two points baseline defined between 4982 and 4810 cm^{-1}, of a 5.25 mg g^{-1} Iprodione standard solution divided by the noise obtained in the aforementioned region for an acetonitrile blank solution and vi) sample throughput, established as the number of measurements per hour.

Once the experiments were performed, the resulting normal probability plot is calculated and the effects were classified in significant and no significant using a confidence level of 95 % (α=0.05).

Optimization by a central composite design (CCD)

The instrumental variables that affect NIR determination significantly were optimized with a CCD design for each one of the response functions defined. Due to limitations in instrumentals variables it is not possible to apply a central composite circumscribed design (CCC) and the central composite face centred (CCF) design was used. In all the cases it was selected a value of α=1, for the design of axial points. The factors used on the CCD design

where those that affect significantly the different response functions studied. The responses were those used in the screening by FFD.

The analysis of the response surfaces can be done in several ways. The most immediate way of concluding the optimum conditions is the graphical inspection of the surfaces, since the 3D pictures give the complete overview of the systems. But when the number of factors is higher than 2, the response surfaces are projections of the response over two of the factors, and the graphical approach is not a correct way to get the optimum. In those cases, the Minitab's Response Optimizer application can be used to identify the combination of input variable settings that jointly optimize a single response or a combination of responses. The desirability (d) is a measure of how well the model has satisfied the combined goals for all the responses. Desirability has a range from 0 to 1, and takes into account the responses considered in the optimization. Optimal conditions are achieved when the membership value is close to 1.

Results and discussion

Screening of significant instrumental variables in the NIR determination

As a preliminary step for optimization, the most important instrumental factors were screened by applying the two-level full factorial design as indicated in the Experimental section.

The experimental design and the results of the FFD observations for each one of the optimization functions considered are summarized in Table 1. The main effects of the factors on the different responses studied are presented in Figure 1.

As can be seen, the sensitivity of the proposed methodology is affected by only a variable which is the nominal resolution and as the nominal resolution of NIR spectra increases, the sensitivity decreases. The repeatability of the procedure is significantly influenced by the number of cumulated scans and the mirror velocity. The accuracy relative error of the procedure is not affected by the studied factors if samples and standards were measured in the same instrumental conditions, as can be seen in Figure 1C. So this response was not taken into account in the optimization of the instrumental conditions.

The limit of detection is affected mainly by number of cumulated scans and the combined effect of this factor with nominal resolution and mirror velocity. On the other hand, the signal to noise ratio is affected by the nominal resolution and by the joint effect of nominal resolution and number of cumulated scans. The sample throughput is affected by the number of cumulated scans, the nominal resolution, the mirror velocity and the corresponding shared effects.

Optimization of the key factors

As can be seen in Figure 1, sensitivity is only dependent on the nominal resolution. So, a monoparametric study was undertaken to optimize this response. Figure 2 shows that the highest sensitivity was obtained when a minimum nominal resolution of 1 cm^{-1} was used.

In order to optimize the factors that affect significantly the repeatability, a central composite design was studied. According to Minitab, a full factorial CCD design of two factors (number of cumulated scans and mirror velocity) consisted of 14 runs made per duplicate (28 total combinations) in a single block (8 cubic points with 6 center points in cube and 8 axial points with 6 axial center points), and the details are indicated in Table 2. As can be seen in Figure 3A, the optimum values to improve the signal repeatability of

Table 1

Experimental design of the 2^4 full factorial model for the screening of factors which affect NIR measurements

	Experimental conditions				Results of the optimization functions						
Trial	Scans	Resolution cm^{-1}	Mirror velocity kHz	Zero filling factor	S	% RSD	% Er	LOD	S/N	throughput	Complex function
1	-	+	-	-	0.1384	0.6	0.4	0.007	95847	621	28.7
2	+	+	-	+	0.1394	0.9	0.6	0.02	35551	63	3.7
3	-	+	-	+	0.1394	0.08	0.5	0.02	416825	621	25.6
4	-	+	-	-	0.1374	0.56	0.07	0.007	48439	623	25.3
5	-	-	+	-	0.1482	0.13	0.8	0.02	49723	468	11.6
6	-	-	-	+	0.1484	0.13	0.9	0.013	53977	118	2.9
7	+	+	-	+	0.1384	0.89	0.06	0.03	25900	62	1.0
8	-	+	+	-	0.1387	0.07	1.2	0.010	201116	2400	1214.1
9	+	-	+	+	0.1479	0.21	0.8	0.012	31089	47	3.6
10	-	+	+	-	0.1377	0.09	0.4	0.010	135077	2410	418.5
11	-	+	+	+	0.1398	0.05	0.9	0.03	232373	2400	907.4
12	-	+	-	+	0.1384	0.09	0.10	0.02	75042	620	68.4
13	+	-	+	-	0.1479	0.26	0.7	0.013	37475	47	13.6
14	+	+	-	-	0.1388	0.29	0.9	0.03	46166	63	0.6
15	+	-	+	+	0.1469	0.19	0.3	0.012	21789	50	2.7
16	-	-	+	+	0.1481	0.07	1.0	0.04	30587	468	10.5
17	+	-	-	-	0.1481	0.16	0.7	0.018	60205	12	1.6
18	-	-	+	-	0.1476	0.14	0.5	0.02	33148	467	16.8
19	+	-	+	-	0.1469	0.28	0.2	0.013	26392	51	5.2
20	0	0	0	0	0.1465	0.39	1.5	0.04	37656	146	4.6
21	+	-	-	+	0.1489	0.13	1.0	0.008	63078	12	1.7
22	-	-	-	-	0.1488	0.31	2.3	0.04	27270	118	6.5
23	+	+	+	-	0.1392	0.63	1.7	0.07	52506	240	23.2
24	-	+	+	+	0.1388	0.04	0.3	0.03	61977	2350	516.7
25	+	+	-	-	0.1378	0.31	0.11	0.03	29026	59	2.8
26	+	+	+	-	0.1382	0.60	0.19	0.07	20489	241	1.7
27	+	+	+	+	0.1397	0.22	2.1	0.07	44458	240	7.5
28	+	-	-	+	0.1479	0.12	0.4	0.008	49009	13	3.3
29	-	-	-	+	0.1474	0.10	0.4	0.014	43624	120	1.4
30	+	-	-	-	0.1471	0.14	0.13	0.018	43376	14	1.4
31	-	-	-	-	0.1478	0.30	0.5	0.04	16741	115	2.2
32	-	-	+	+	0.1471	0.08	0.3	0.04	24330	451	9.1
33	+	+	+	+	0.1386	0.20	0.012	0.07	19469	242	91.7

Details on the optimization functions employed are indicated in the Experimental section.

Where number of cumulated scans (scans) varied from 10 to 100 (- and + in codified values, respectively, being 0, 50 cumulated scans per spectrum); nominal resolution varied from 2 to 16 cm^{-1} (- and +), being 0, 8 cm^{-1} nominal resolution), mirror velocity factor varied from 5 to 20 kHz (- and +), being 0, 10 kHz mirror velocity) and zero filling factor varied from 2 to 16 (- and +), being 0, 8 zero filling).

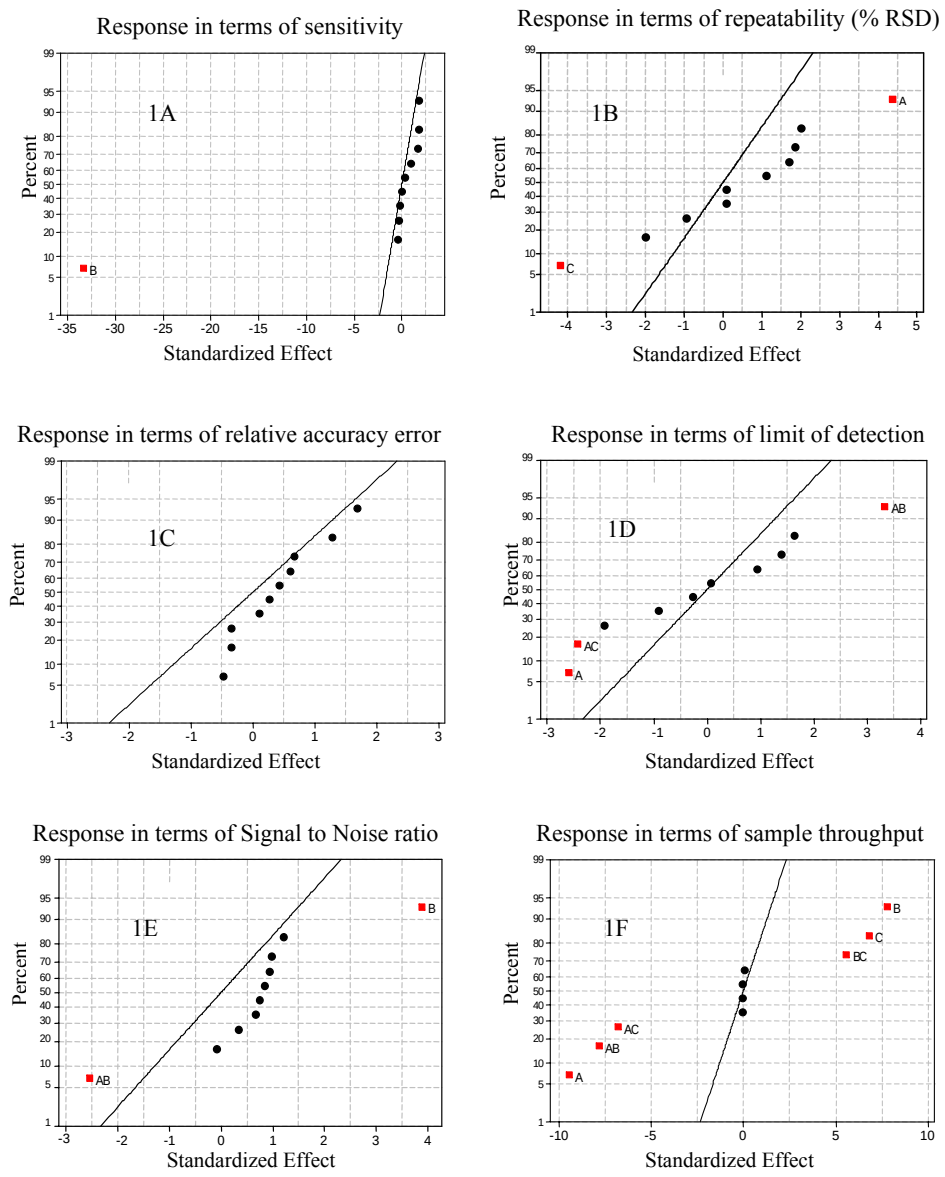

Fig. 1. Normal probability plot in the full factorial 2^4 design for the different response functions under study: □, significant effect; •, not significant effect. Factor: A= number of cumulated scans, B= nominal resolution, C= mirror velocity, D= zero filling.

Iprodione were 10 scans per spectrum and 20 kHz mirror velocity.

Number of cumulated scans, nominal resolution and zero filling were the factors to be optimized when the limit of detection was chosen as response. So, a central composite design of these factors consisted of 20 runs made per duplicate (40 total combinations) in two different blocks (16 cubic points with 8 center points in cube and 12 axial points with 4 center points in axial), and the details are illustrated in Table 3. Optimum conditions for response of each factor were calculated using the desirability function (target value: 0.08 mg g^{-1}, maximum acceptable: 0.2 mg g^{-1}). As can be see in Figure 4A, the optimum conditions to improve the LOD of Iprodione were 10 cumulated scans, 16 cm^{-1} nominal resolution and 22.6 zero filling factor. However, due to the instrumental limitations a 16 zero filling factor was selected.

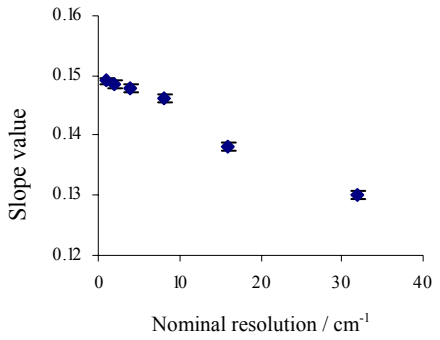

Fig. 2. Monoparametric study of the effect of the resolution on the sensitivity obtained for Iprodione determination.

To optimize the factors according to the signal to noise ratio a CCD design of two factors (number of cumulated scans and nominal resolution) consisted of 13 runs made per duplicate (26 total combinations) in a single block (8 cubic points with 10 center points in cube and 8 axial points with 0 axial center points), and the details are summarized in Table 4. In this study 50 scans per spectrum and 16 cm^{-1} resolution were obtained as the optimum values (see Figure 3B).

Using sample throughput as response, a central composite design of three factors consisted of 20 combinations made per duplicate (40 total combinations) in a single block (16 cubic points with 12 center points in cube and 12 axial points with 0 axial center points), and the details are indicated in Table 5. Optimum conditions for the response of each factor were calculated using the desirability function (target value: 2100 h^{-1}, minimum acceptable: 100 h^{-1}). The optimum conditions obtained were 10 scans per spectrum, 16 cm^{-1} nominal resolution and 20 kHz mirror velocity, as can be seen in Figure 4B.

Evaluation of the optimum conditions studied

Table 6 summarizes the different optimum values obtained depending on the response function employed. As can be seen, the sensitivity reaches the optimum value when a nominal resolution of 1 cm^{-1} is used. However,

other analytical parameters, such as S/N ratio, LOD or sample throughput uses 16 cm^{-1} nominal resolution to obtain the optimum value. In the same way, to obtain the best S/N ratio it is required to accumulate 50 scans per spectrum but this value is not appropriate for repeatability, LOD or sample throughput used as response functions.

Table 2

Experimental design of the 2^2 central composite model for the evaluation of the optimum conditions to obtain the best repeatability

Trial	Scans	Mirror velocity / kHz	% RSD
1	0	0	0.06
2	+	+	0.05
3	+	-	0.07
4	0	0	0.05
5	0	0	0.05
6	0	0	0.04
7	0	0	0.04
8	+	+	0.04
9	-	+	0.05
10	0	0	0.03
11	-	+	0.04
12	-	-	0.06
13	+	-	0.05
14	-	-	0.03
15	-	0	0.02
16	-	0	0.04
17	+	0	0.03
18	0	0	0.04
19	0	0	0.03
20	0	0	0.03
21	+	0	0.03
22	0	0	0.03
23	0	0	0.03
24	0	-	0.05
25	0	+	0.01
26	0	-	0.04
27	0	+	0.03
28	0	0	0.03

Where number of cumulated scans (scans) varied from 10 to 50 (- and + in codified values, respectively, being 0, 30 cumulated scans per spectrum) and mirror velocity varied from 5 to 20 kHz (- and +), being 0, 10 kHz mirror velocity.

Table 3

Experimental design of the 2^3 central composite model for the evaluation of the optimum conditions to obtain the best limit of detection

Trial	Scans	Resolution cm^{-1}	Zero filling	LOD
1	0	0	0	0.012
2	+	-	-	0.005
3	-	+	-	0.011
4	-	+	+	0.0005
5	0	0	0	0.013
6	+	-	+	0.013
7	0	0	0	0.016
8	-	-	+	0.011
9	0	0	0	0.018
10	+	+	+	0.021
11	+	+	-	0.020
12	+	-	-	0.016
13	0	0	0	0.020
14	0	0	0	0.011
15	-	-	-	0.019
16	+	+	-	0.013
17	-	-	+	0.013
18	0	0	0	0.010
19	+	+	+	0.021
20	-	-	-	0.019
21	+	-	+	0.019
22	0	0	0	0.015
23	-	+	-	0.007
24	-	+	+	0.011
25	+	0	0	0.021
26	0	0	-	0.024
27	0	+	0	0.025
28	0	-	0	0.006
29	-	0	0	0.025
30	0	0	0	0.024
31	0	0	0	0.023
32	0	0	+	0.018
33	0	0	0	0.019
34	0	0	0	0.024
35	0	+	0	0.023
36	-	0	0	0.016
37	0	-	0	0.009
38	0	0	+	0.025
39	0	0	-	0.028
40	+	0	0	0.012

Where number of cumulated scans (scans) varied from 10 to 50 (- and + in codified values, respectively, being 0, 30 cumulated scans per spectrum); nominal resolution varied from 2 to 16 cm^{-1} (- and +, being 0, 8 cm^{-1} nominal resolution) and zero filling factor varied between 2 to 32 (- and +, being 0, 16 zero filling).

It is clear that the obtained results are conflicting, thereby supporting the importnace of the optimization function on the experimental conditions obtained as the best ones. However it is clear that in the real world there is no interest on a single analytical figure of merit and, because of that, it was assigned a complex function, in which a combination of the considered analytical parameters with their respective weights, was defined.

It was taken into consideration that the NIR analytical procedure for the determination of Iprodione was developed for the quality control of commercially available formulations, and thus, a hierarchical estimation of the importance of the considered parameters was established. For example, the maximum importance of the analytical productivity was fixed at a level of 4, the repeatability and sensitivity in a reduced level of 3 and 2 respectively and considered signal to noise ratio and LOD only as residual parameters with a level of importance of 1. So, it can be defined the following optimization function:

$$Response = \frac{0.1818S \times 0.0909S/N \times 0.3636t}{0.2727R \times 0.0909LOD}$$

where *S*, *S/N*, *t*, *R* and LOD are the sensitivity, signal to noise ratio, sample throughput, repeatability and limit of detection, respectively.

Table 4

Experimental design of the 2^2 central composite model for the evaluation of the optimum conditions to obtain the best signal to noise ratio

Trial	Scans	Resolution cm^{-1}	S/N
1	0	0	233579
2	0	0	234119
3	+	-	116853
4	-	+	432795
5	0	-	141110
6	0	0	172845
7	+	0	179014
8	0	0	210418
9	-	0	216892
10	0	0	287363
11	0	+	699564
12	+	+	214549
13	+	-	141855
14	0	0	169843
15	0	0	213834
16	-	-	116147
17	+	+	1172281
18	-	0	220551
19	0	0	357871
20	0	+	560926
21	-	-	119245
22	+	0	207923
23	0	0	410022
24	-	+	718589
25	0	-	121836
26	0	0	190858

Where number of cumulated scans (scans) varied from 10 to 50 (- and + in codified values, respectively, being 0, 30 cumulated scans per spectrum) and nominal resolution varied from 2 to 16 cm^{-1} (- and +, respectively, being 0, 8 cm^{-1} nominal resolution).

In this function the accuracy is not present because it was probed that this parameter does not depend on the experimental conditions studied when standards and samples are measured in the same conditions, as it has been aforementioned.

This function has been used as response in the full factorial design described in the results and discussion section, taking into account that only the number of cumulated scans, nominal resolution, mirror velocity and the corresponding shared effects affect significantly the response (see Figure 5A).

For the complex response function a central composite design of three factors, similar to those applied for the analysis of sample throughput, was constructed (results are shown in Table 5). The optimum conditions for response of each factor were calculated using the desirability function (target value: 2300, minimum acceptable: 10). So, 10 scans per spectrum, 16 cm^{-1} nominal resolution and 20 kHz mirror velocity were the optimum conditions obtained for this response as can be seen in Figure 5B.

Analytical figures of merit of the developed procedure

In the experimental conditions optimized for the complex function it was obtained the main analytical figures of merit of the NIR method developed and, it can be seen from Table 7 that, although the limit of detection is three orders of magnitude better in the chromatographic procedure, the residue generation is reduced from 50 ml to 1 ml of acetonitrile and the sample throughput is increased from 12 to 2400 h^{-1}, obtaining a repeatability, as relative standard deviation of the same order than that obtained by the reference method.

Analysis of commercial formulations of agrochemicals

Three different lots of a wettable powder commercial formulation, containing a declared value of 50 % w/w Iprodione were analyzed by both, the NIR procedure and the reference chromatographic method and concentration values of 49.90 ± 0.15, 48.80 ± 0.15 and 50.00 ± 0.12 were obtained being comparables to 48.94 ± 0.03, 49.04 ± 0.02 and 50.22 ± 0.02, with a relative man accuracy error of 0.96%.

So, it can be concluded that the method developed is suitable as an accurate alternative to the chromatographic determination offering the additional advantage of the absence of residues, because the use of glass vials for direct determination of Iprodione in samples treated with acetonitrile permits to use the sample cells as recipients to store the samples for further comparative studies.

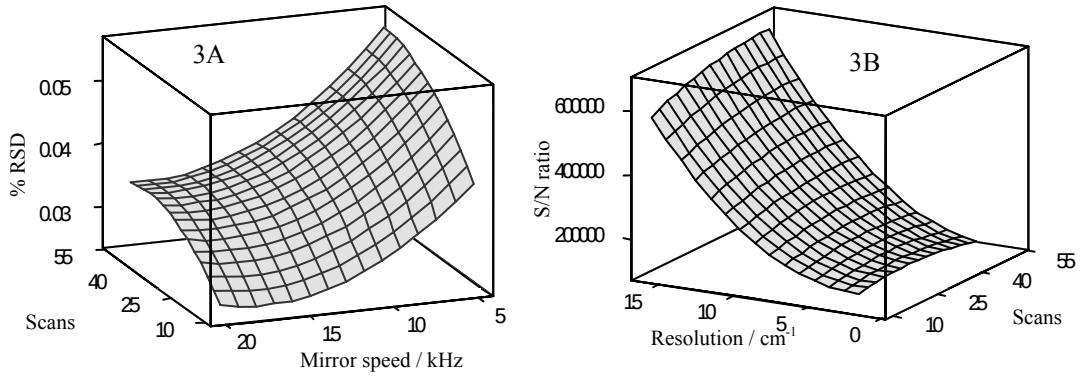

Fig. 3. Surface plot of the theoretical responses: 3A) %RSD as a function of the number of scans and mirror velocity and 3B) S/N ratio as a function of number of scans per spectrum and nominal resolution.

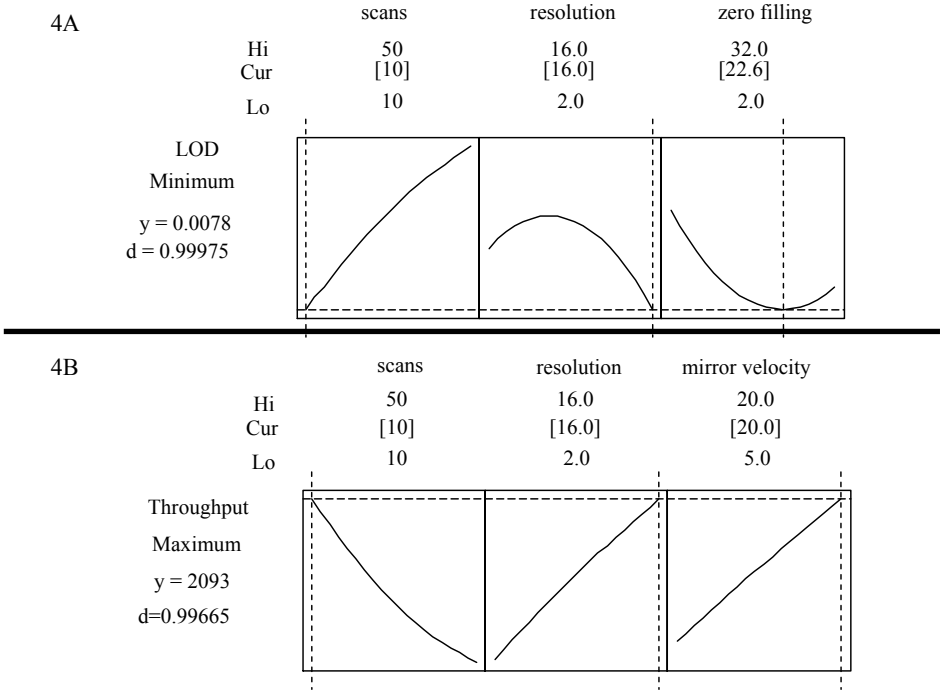

Fig. 4. Representation of four-dimensional response surface for LOD (4A) and sample throughput (4B) as a function of the experimental parameters which significantly affect these functions. Note: "y" indicates the value obtained as the optimum, and "d" the desirability in the optimum conditions. Hi, Lo and Cur correspond to the high, low and optimum values of the experimental variables.

Table 5

Experimental design of the 2^3 central composite model for the evaluation of the optimum conditions to obtain the best sample throughput and the maximum value of a complex function which includes all the analytical characteristics together.

Trial	Scans	Resolution / cm^{-1}	Mirror velocity	Sample throughput	Complex function
1	0	0	+	503	7.0
2	0	0	-	130	3.0
3	+	+	-	127	1.1
4	-	-	+	467	23.9
5	+	0	0	154	10.8
6	0	0	+	503	41.4
7	+	+	+	481	132.1
8	0	0	0	257	44.7
9	+	+	+	481	110.0
10	0	0	0	257	35.2
11	0	0	-	130	9.1
12	-	+	+	2416	2309.5
13	-	+	-	636	170.9
14	0	0	0	257	32.5
15	0	0	0	249	25.0
16	+	-	-	24	3.8
17	+	-	+	93	4.7
18	-	+	+	2056	794.5
19	0	0	0	257	29.4
20	0	-	0	78	5.5
21	+	-	-	24	6.4
22	-	0	0	772	48.4
23	0	0	0	242	18.3
24	-	-	+	467	7.5
25	-	0	0	772	152.7
26	-	-	-	118	4.9
27	0	-	0	74	4.7
28	+	0	0	154	2.1
29	-	+	-	636	47.8
30	-	-	-	118	4.2
31	0	0	0	257	7.0
32	0	0	0	257	5.9
33	0	0	0	252	10.8
34	0	0	0	257	15.0
35	0	0	0	257	4.6
36	+	-	+	93	5.1
37	0	0	0	257	5.0
38	+	+	-	127	3.3
39	0	+	0	415	11.9
40	0	+	0	415	15.8

Where number of cumulated scans (scans) varied from 10 to 50 (- and + in codified values, respectively, being 0, 30 cumulated scans per spectrum); nominal resolution varied from 2 to 16 cm^{-1} (- and +), being 0, 8 cm^{-1} nominal resolution and mirror velocity factor varied from 5 to 20 kHz (- and +), being 0, 10 kHz mirror velocity.

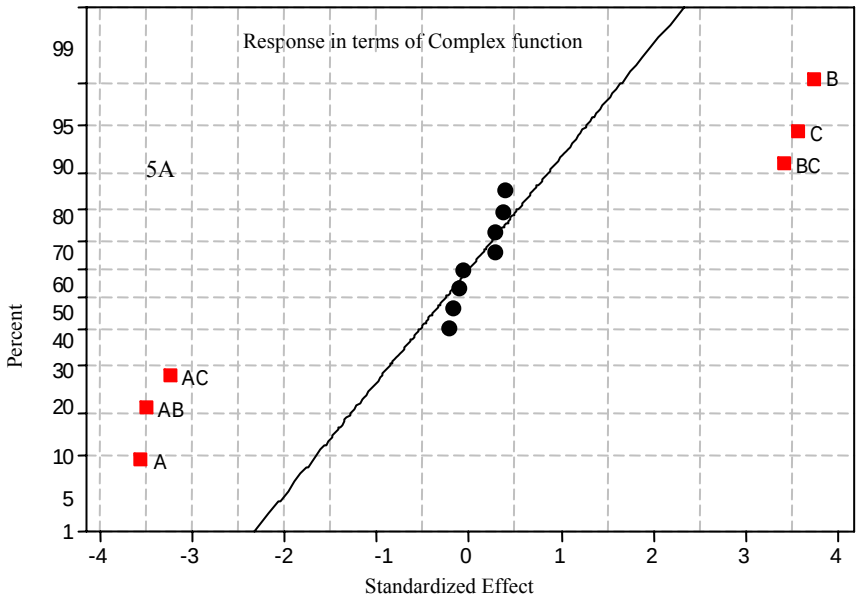

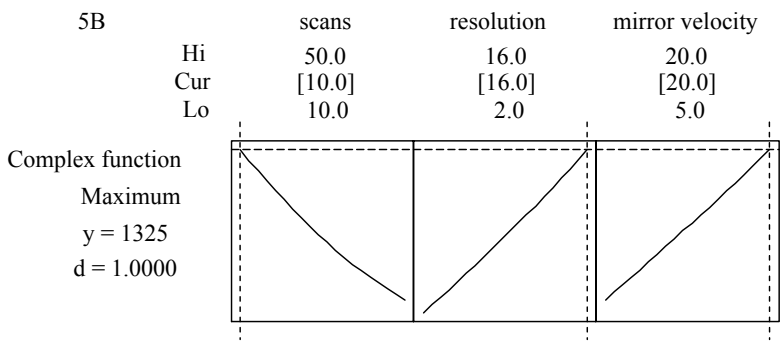

Fig. 5. Optimization of the experimental variables on using a complex function which includes all the analytical figures of merit. 5A) Normal probability plot in the full factorial 2^4 design for the complex function. Note: □, significant effect; •, not significant effect. Factor A= number of cumulated scans, B= nominal resolution, C= mirror velocity, D= zero filling. 5B) Representation of four-dimensional response surface for the complex function y. See legend of Figure 4 for details.

Table 6

Different optimum conditions obtained in function of the response evaluated.

Response	Scans	Resolution / cm^{-1}	Mirror velocity / kHz	Zero filling[a]
Sensitivity	-	1	-	-
Repeatability	10	-	(20) 17.5*	-
Accuracy	-	-	-	-
S/N	50	16	-	-
LOD	10	16	-	(16) 22.6*
Sample throughput	10	16	20	-
Complex function	10	16	20	-

[a] A zero filling factor of 2 was employed in all the cases as a default value.

* Due to instrumental limitations the number between brackets was selected as optimum.

Table 7. Figures of merit of NIR determination of Iprodione.

Regression line	$A=(0.02 \pm 0.02) + (0.1387 \pm 0.0007)\ C_{Iprodione}$ (mg g^{-1})
Sensitivity	0.1387
LOD (mg g^{-1})	0.010
Repeteability (% RSD)	0.07
Sample througput (h^{-1})	2400
Reagent consume (ml)	1

Conclusion

Results obtained in the optimization of different analytical responses separately for the NIR determination of Iprodione in agrochemicals are contradictories. So, the usefulness of the use of complex functions including several parameters has been proved for solving the conflict between the optimisation of the different analytical parameters under study. The use of complex function permits us to arrive at a compromise solution and to reach a global optimum which fulfils the specifications imposed by the researcher and because of that we strongly recommend to establish carefully the function to be optimized to be in agreement with the objectives of each work.

On the other hand, the NIR procedure developed could be considered as a fast and environmentally friendly alternative to the Iprodione determination in agrochemicals by liquid chromatography, being evidenced that the NIR method is suitable for this kind of analysis.

Acknowledgement

The authors acknowledge the financial support of the Direcció General d'Universitats i Investigació de la Generalitat Valenciana (**Project GV04B/247** and **Grupos 03-118**), Universitat de València (**Project UV-AE-20050203**) and Ministerio de Educación y Ciencia (**Project CTQ2005-05604/BQU**). S. Armenta also acknowlwdges the FPU Grant of the MECD (**Ref. AP2002-1874**).

References

[1] R.V. Lenth, *J. Am. Stat. Assoc.*, 2002, **97**, 924-924.

[2] C.F. Jeff Wu and M. Hamada, in Experiments: Planning, Analysis, and Parameter Design Optimization, ed. John Wiley and sons Inc, Chichester, England, 2000.

[3] N.R. Draper and D.K.J. Lin, in Response surface designs. Handbook of Statistics, 1996, **13**, 343-375.

[4] A.M. Siouffi and R. Phan Tan Luu, *J. Chromatogr. A*, 2000, **892**, 75-106.

[5] J.L. Gomez-Ariza,, T. Garcia-Barrera, F. Lorenzo and A. Gustavo Gonzalez, *Anal. Chim. Acta*, 2005, **540**, 17–24.

[6] M.I. Acedo-Valenzuela, T. Galeano-Díaz, N. Mora-Díez and A. Silva-Rodríguez, *Talanta*, 2005, **66**, 952-960.

[7] M. E. Rueda, L. A. Sarabia, A. Herrero and M. C. Ortiz, *Anal. Chim. Acta*, 2003, **479**, 173-184.

[8] F. Safa and M.R. Hadjmohammadi, *Anal. Chim. Acta*, 2005, **540**, 121-126.

[9] Extension Toxicological Network (EXTOXNET), University of California-Davis, Oregon State University, Michigan State University and the University of Idaho, 1996. http://ace.orst.edu/info/extoxnet/pips/ghindex.html.

[10] Infoagro.com, 2001. http://www.infoagro.com/agrovademecum/

[11] J. Moros, S. Armenta, S. Garrigues, M. de la Guardia, *Anal. Chim. Acta,* 2005, **543**, 124–129

[12] S. Armenta, J. Moros, S. Garrigues, M. de la Guardia, *J. Near Infrared Spec.,* 2005, **13**, 161-168.

[13] Collaborative International Pesticides Analytical Council, CIPAC Methods, Abingdon, England. http://www.cipac.org

Automated Fourier transform near infrared determination of buprofezin in pesticide formulations

Sergio Armenta, Javier Moros, Salvador Garrigues and Miguel de la Guardia
Department of Analytical Chemistry, Universitat de València. Edifici Jeroni Muñoz, 50th Dr Moliner, 46100 Burjassot, Valencia, Spain.

Journal of Near Infrared Spectroscopy 13 (2005)161-168.

Impact factor of this journal (2004): 1.027
Source: Journal citation reports ISI Web of Knowledge, 2004.

S. Armenta *et al.*, *J. Near Infrared Spectrosc.* **13,** 161–168 (2005)

Automated Fourier transform near infrared determination of buprofezin in pesticide formulations

Sergio Armenta, Javier Moros, Salvador Garrigues and Miguel de la Guardia

Department of Analytical Chemistry, Universitat de València. Edifici Jeroni Muñoz, 50th Dr Moliner, 46100 Burjassot, Valencia, Spain.
E-mail: salvador.garrigues@uv.es

An automated procedure has been developed for Fourier transform near infrared (FT-NIR) determination of buprofezin in pesticide formulations. This methodology is based on on-line pesticide extraction with acetonitrile from solid samples and its determination by using peak area absorbance measurements between 2147 and 2132 nm, corrected with a horizontal baseline established at 2091 nm. The repeatability, as a relative standard deviation of five independent analyses of 18.9 mg g^{-1} of buprofezin, was 0.06% and the limit of detection 5 mg L^{-1}. The reagent consumption was clearly reduced compared with a chromatographic reference procedure from 40.4 mL acetonitrile per sample, required by high performance liquid chromatography (HPLC), to 2 mL acetonitrile consumed for FT-NIR. The sample measurement throughput obtained by the FT-NIR methodology was 30 h^{-1}, five times higher than that obtained by HPLC (6 h^{-1}). It can be concluded that the proposed vibrational spectroscopic method is appropriate for the quality control of commercial pesticide formulations. The on-line sample treatment avoids contact by the operator with toxic products and this method is an environmentally friendly alternative to the measurement in the mid infrared which requires the use of $CHCl_3$.

Keywords: near infrared, flow analysis, pesticide, formulations, agrochemicals, quality control

Introduction

The last two decades have seen a substantial increase in the use of near infrared (NIR) spectroscopy in analytical chemistry. The simplicity, precision and accuracy of this technique, in combination with the advances in chemometrics, have extended its use to all industrial areas.[1]

NIR is particularly useful in the quality control process due to its flexibility for both qualitative[2] and quantitative analysis, being employed for the determination of active principles in pharmaceuticals,[3,4] foods[5] and coal.[6] In addition, NIR has been used for the on-line monitoring of fermentation processes.[7] However, there are no precedents for the use of NIR in the quality control of agrochemical formulations.[8]

NIR spectra depend not only on the chemical composition of samples, but also on the physical properties of their matrix, including particle size, shape and distribution and degree of sample compaction, which could significantly affect the signals. All these effects create difficulties in applying NIR to the quantitative determination of active principles in solid samples and because of this have involved the use of multivariate calibration methods based on partial least squares (PLS),[9] principal component regression (PCR)[10] or multiple linear regression (MLR)[11] to obtain accurate results.

The aim of the present paper has been to develop a simple Fourier transform (FT)-NIR methodology, based on the use of classical least squares calibration, for the automated determination of buprofezin in pesticide formulations. In this sense, an appropriate solvent was selected to carry out the on-line extraction of buprofezin from solid samples, avoiding the typical problems related with the direct measurement of solid samples by diffuse reflectance.

Buprofezin (2-*tert*-butylimino-3-isopropyl-5-phenyl-1,3,5-thiadiazinan-4-one) is an insecticide and acaricide with persistent parvicidal action against *Homopterasome coleoptera* and acarina. Buprofezin is effective against leafhoppers in rice and potatoes, whitefly in citrus plants, cotton and vegetables and also for *coccidae*, *diaspididae* (scale insects) and *pseudococcidae* (mealybugs) in citrus plants. It is an insecticide with contact and stomach side effects.

Buprofezin is manufactured in several commercially available pesticide formulations as wetting powder in a 25% (w/w) concentration.[12]

Chromatographic techniques have been the most widely used procedures for the determination of buprofezin residues at trace levels. This pesticide has been determined in fruits by high performance liquid chromatography/mass spectrometry,[13] in wines by head-space gas chromatography

with electron capture detection[14] and in air by gas chromatography/mass spectrometry.[15]

There is only a single precedent for the determination of buprofezin in pesticide formulations,[16] which is based on pesticide extraction with chloroform and subsequent measurement in the mid-infrared region (FT-IR).

In short, the main objective of this paper is to develop an automated, fast, simple and environmentally friendly FT-NIR method for the determination of buprofezin for quality control of commercially available formulations which could avoid the use of ozone depleting solvents such as chloroform, which are requirements for working in the mid infrared (MIR) range, which could offer a fast alternative to the more sensitive but time-consuming chromatographic procedures.

Experimental

Apparatus and reagents

A Bruker MPA (Ettlingen, Germany) FT-NIR spectrometer equipped with a quartz beamsplitter, an air cooled NIR source, an InGaAs detector and a 5 mm micro quartz flow cell was used for NIR transmission measurements. Diffuse-reflection FT-NIR spectra were obtained using an integrating sphere accessory. For measurement control and data acquisition, the Opus program (version 4.1) from Bruker (Ettlingen, Germany) was employed. Spectral treatment and data manipulation were carried out using Omnic 2.1 software from Nicolet (Madison, WI, USA).

To carry out the on-line extraction and NIR determination of buprofezin, the manifold depicted in Figure 1 was built by employing a six-way Rheodyne 5041 injection valve (Cotati, CA, USA) and two Gilson Minipuls 2 peristaltic pumps (Villiers-le-Bel, France) furnished with Viton (iso-versinic) tubes (1 mm i.d. and 3 mm o.d.). A plastic syringe of 2.67 cm i.d. and 35 mL internal volume was used for solid sample treatment and an SBS A-01 magnetic stirrer (Barcelona, Spain), working at medium rotation speed, was employed to improve the buprofezin extraction. For the introduction and measurement of standards, a three-way directional valve was employed.

For the optimisation of the FT-NIR instrumental parameters, the Minitab Release 14 statistical software from Minitab Inc. (State College, PA, USA) was used.

A Hewlett-Packard HPLC Series 1050 high-performance liquid chromatograph, equipped with a variable wavelength UV-vis detector and a reversed-phase C-18 (Kromasil) column of 250 mm length and 4.6 mm i.d. with 5 µm particle diameter, was employed for the analysis of buprofezin formulations, being used as a reference procedure for the validation of FT-NIR measurements.

Buprofezin standard (99.4% w/w) was supplied by Fluka (Buchs, Switzerland). HPLC grade (99.85% w/w) acetonitrile supplied by Scharlau (Barcelona, Spain) was employed for the preparation of samples and standards. Buprofezin 25% (w/w) wetting powder commercial formulations were obtained from the Spanish market.

Reference procedure

20 (±0.01) mg of sample were accurately weighed, into a 25 mL volumetric flask and diluted to the volume with CH_3CN. After manual stirring, buprofezin was dissolved and 0.1 g of the clear solution was diluted to 5 g and filtered through a 0.22 µm nylon filter. 20 µL of this solution was injected directly into a 90:10 acetonitrile:water mobile phase of 1 mL min^{-1} carrier flow and buprofezin determined, in the isocratic mode, by absorbance measurements at 240 nm. Area values of the chromatograms peaks obtained at 7.40 min for samples were interpolated in an external calibration line established from five standard solutions of buprofezin containing up to 50.7 mg L^{-1}.

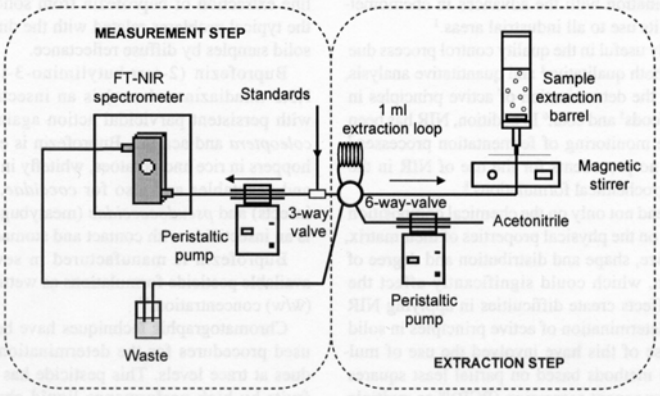

Figure 1. Manifold employed for on-line extraction and FT-NIR determination of buprofezin in commercial pesticide formulations.

A typical calibration line obtained in the aforementioned conditions was $A=(0.4\pm0.5)+(0.717\pm0.005)C_{Bup}$ with an $R^2=0.9994$, A being the area values of the chromatographic peaks and C_{Bup} the concentration of buprofezin in mg L^{-1}. The repeatability, established as the relative standard deviation, of five independent analyses of 10.8 mg L^{-1} buprofezin was 0.19% and a limit of detection of 0.06 mg L^{-1} was achieved by this procedure.

FT-NIR procedure

40 (±0.01) mg of sample were accurately weighed into a plastic syringe barrel of 35 mL internal volume that included a porous glass filter in the bottom. The barrel was placed in the manifold of Figure 1 and 1 mL acetonitrile was injected and transported by air carrier flow to the cartridge. The air current circulation and the magnetic stirring make a complete buprofezin extraction possible in only 60 seconds. After that, the flow was reversed and the FT-NIR transmission spectra of sample extract was recorded in the stopped flow mode, from 2500 to 833 nm, by accumulating 36 scans at a nominal resolution of 16 cm^{-1} and using a zero filling factor of 2 and a scan velocity of 40 Hz. A background spectrum of the cell filled with acetonitrile was obtained under the same instrumental conditions.

The system was cleaned with 1 mL acetonitrile after each sample measurement in order to avoid possible memory effects.

Peak area values between 2147 and 2132 nm, corrected with a horizontal baseline established at 2091 nm, were employed to quantify buprofezin in samples using an external calibration line obtained with five standard solutions of the pesticide dissolved in acetonitrile in the concentration range between 9.7 and 37.9 mg g^{-1} (introduced in the flow cell by using a three-way directional valve), measured under the same instrumental conditions as the samples and adjusted by classical least squares regression.

Results and discussion

FT-NIR spectra of buprofezin

Figure 2 shows the diffuse reflection FT-NIR spectra of a buprofezin standard mixed with NaCl and a commercial sample containing buprofezin (25% w/w), both placed in glass vials with an effective base diameter of 10 mm.

From this spectrum, it can be seen that the main bands appear between 2100 and 2500 nm. The bands located between 2139 and 2179 nm are probably due to C=O stretching and Amide III and the rest of the bands in this region are due to combination vibrations of aliphatic and aromatic C–H. Another, less important, absorption band is the CH aromatic stretching first overtone, located at 1688 nm and the CH_2 and CH_3 stretching first overtone at 1749 nm.[17]

As has been mentioned in the introduction, problems related to physical properties of the sample, which could be corrected by using multiplicative scatter correction to equalise the scatter effects in each sample[18] and those related to the standardisation with solid standards, gave us the idea to evaluate alternatives based on the extraction of the pesticide in an appropriate solvent and the use of an external calibration adjusted by classical least squares. In this case, the use of acetonitrile as the solvent to do the quantitative extraction of buprofezin was evaluated.

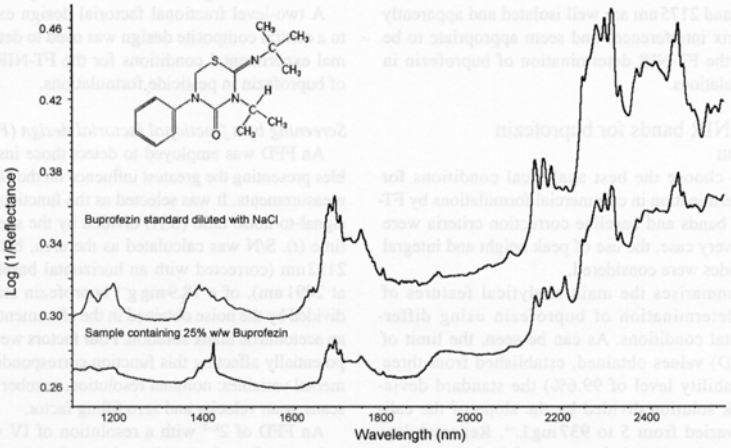

Figure 2. FT-NIR reflection spectra of a 25% w/w standard of buprofezin diluted with NaCl and a solid sample containing 25% w/w buprofezin. Note: spectra were shifted on the y axis to show their bands clearly. Instrumental conditions: 36 scans, 16 cm^{-1} nominal resolution.

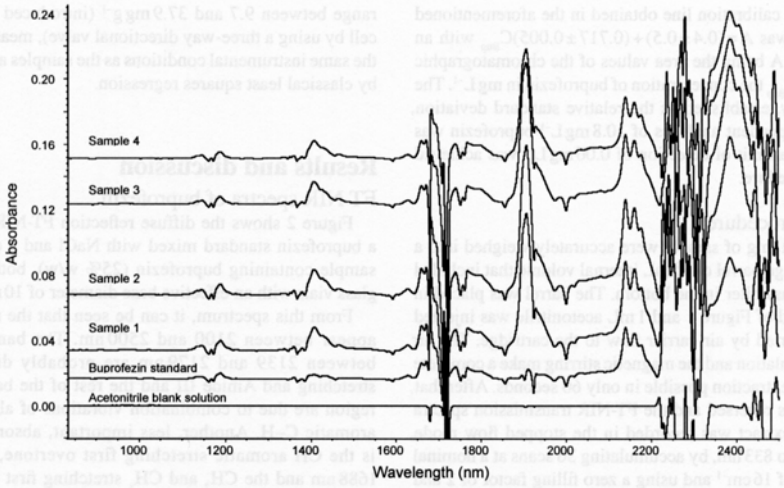

Figure 3. FT-NIR transmission spectra of a 18.9 mg g^{-1} buprofezin standard dissolved in acetonitrile, those of four pesticide sample extracts and a blank of acetonitrile. Spectra are the average of 36 accumulated scans using a nominal resolution of 16 cm^{-1}.

Figure 3 shows the transmission FT-NIR spectra, in the wavelength range from 2500 to 850 nm, of an 18.9 mg g^{-1} buprofezin standard dissolved in acetonitrile, those of four pesticide sample extracts and that of an acetonitrile blank. The presence of negative bands is due to the use of the cell filled with acetonitrile for the background measurement.

As can be seen in this figure, the spectrum of buprofezin standard and those of the samples present the same absorption bands and it can be concluded that the bands located between 2125 and 2175 nm are well isolated and apparently free from matrix interferences and seem appropriate to be employed for the FT-NIR determination of buprofezin in pesticide formulations.

Selection of NIR bands for buprofezin determination

In order to choose the best analytical conditions for buprofezin determination in commercial formulations by FT-NIR, different bands and baseline correction criteria were evaluated. In every case, the use of peak height and integral absorbance modes were considered.

Table 1 summarises the main analytical features of the FT-NIR determination of buprofezin using different experimental conditions. As can be seen, the limit of detection (LOD) values obtained, established from three times (a probability level of 99.6%) the standard deviation of a blank solution divided by the slope of the calibration line, varied from 5 to 937 mg L^{-1}. Repeatability values, established as the relative standard deviation of five measurements of a 18.9 mg g^{-1} buprofezin standard, ranged from 0.06 to 1.1%.

In short, the use of a band area measurement between 2147 and 2132 nm, with a single point baseline correction fixed at 2091 nm, provides a variation coefficient of 0.06%, a limit of detection of 5 mg L^{-1} and a limit of quantification of 15 mg L^{-1}. These spectral measurement conditions were selected for the FT-NIR determination of buprofezin in pesticide formulations.

Statistical design of instrumental parameters

A two-level fractional factorial design expanded further to a central composite design was used to determine the optimal experimental conditions for the FT-NIR determination of buprofezin in pesticide formulations.

Screening by a fractional factorial design (FFD)

An FFD was employed to detect those instrumental variables presenting the greatest influence on the NIR transmission measurements. It was selected as the function to optimise the signal-to-noise ratio (S/N) divided by the spectra acquisition time (t). S/N was calculated as the area, between 2147 and 2132 nm (corrected with an horizontal baseline established at 2091 nm), of a 18.9 mg g^{-1} buprofezin standard solution divided by the noise obtained in the aforementioned region for an acetonitrile blank solution. Four factors were considered as potentially affecting this function corresponding to the instrumental variables: nominal resolution, number of accumulated scans, scan velocity and zero filling factor.

An FFD of 2^{k-1} with a resolution of IV was selected in order to reduce the number of experiments to be carried out.

As suggested by the software employed, experiments concerning the extreme values were made in triplicate and

Table 1. Analytical characteristics of NIR determination of buprofezin using different measurement modes, bands and baseline corrections.

Peak height (nm)	Baseline correction (nm)	Regression line $y=(a\pm s_a)+(b\pm s_b)\,C$ ($g\,g^{-1}$)	R^2	*RSD %*	*LOD* ($mg\,L^{-1}$)	*LOQ* ($mg\,L^{-1}$)
2139	2091	$y=(0.00038\pm0.00011)+(2.263\pm0.005)$ [buprofezin]	0.9999	0.07	16	53
2139	2044	$y=(0.00015\pm0.00011)+(2.332\pm0.004)$ [buprofezin]	0.9999	0.18	62	206
2161	2151	$y=(0.00013\pm0.00002)+(0.6192\pm0.0010)$ [buprofezin]	0.99996	0.13	324	1080
2161	2044	$y=(0.00001\pm0.00008)+(2.015\pm0.003)$ [buprofezin]	0.99996	0.3	24	81
2177	2044	$y=(-0.00054\pm0.00014)+(1.428\pm0.006)$ [buprofezin]	0.9997	0.7	937	3124

Peak area (nm)	Baseline correction (nm)	Regression line $y=(a\pm s_a)+(b\pm s_b)\,C$ ($g\,g^{-1}$)	R^2	*RSD %*	*LOD* ($mg\,L^{-1}$)	*LOQ* ($mg\,L^{-1}$)
2132–2147	**2091**	**$y=(0.010\pm0.003)+(59.13\pm0.12)$ [buprofezin]**	**0.9999**	**0.06**	**5**	**15**
2132–2147	2150	$y=(0.0064\pm0.0014)+(18.19\pm0.06)$ [buprofezin]	0.9998	0.18	64	214
2132–2147	2044	$y=(0.003\pm0.003)+(61.25\pm0.12)$ [buprofezin]	0.9999	0.19	80	266
2155–2166	2150–2172	$y=(0.0024\pm0.0007)+(11.89\pm0.03)$ [buprofezin]	0.9999	0.13	31	103
2155–2166	2151	$y=(0.0007\pm0.0007)+(11.12\pm0.03)$ [buprofezin]	0.9999	0.19	156	519
2155–2166	2172	$y=(0.0041\pm0.0007)+(12.65\pm0.03)$ [buprofezin]	0.9999	0.3	194	647
2172–2181	2172–2186	$y=(0.0010\pm0.0003)+(3.888\pm0.012)$ [buprofezin]	0.9999	1.1	25	84

[a] Relative standard deviation values of five independent measurements of a buprofezin solution of 18.9 $mg\,g^{-1}$

[b] Limit of detection values were established from three times (a probability level of 99.6%) the standard deviation of a blank solution divided by the slope of the calibration line

[c] Limit of quantification values established as 10 times the standard deviation of a blank solution divided by the slope of the calibration line

were also measured at a central point. So a total of 25 runs were made in a single block. The experiment run order was randomised to protect against the effect of hidden variables.

As can be seen from results summarised in Table 2, the number of accumulated scans, resolution and their interaction effect had a statistically significant effect on the (S/N)/*t* data, showing that the influence of each variable depended upon the levels at which the other one was tested.

A reduced model was designed using only the factors identified with statistically significant effect on (S/N)/*t*, screening out the unimportant instrumental variables. The reduced model is much simpler and fits the data almost as well as the previous one, as can be seen in Table 2. When the *p*-value for one variable in the four-factors model was less than 0.05 (95% probability level) it was employed in the central composite design. It was confirmed in all cases (see Table 2) that scan number and spectral resolution are the significant variables which control the optimisation functions. For the following experiments, a zero filling factor of 2 and a scan velocity of 40 Hz were selected in order to reduce the acquisition time.

Optimisation by a central composite design (CCD)

The FFD was expanded further to a CCD and a total of 39 runs in a single block. In order to provide orthogonal blocking and rotatability of the design, a value of $\alpha=1.414$ was selected, α being the experimental design of axial points. The values corresponding to the high, low, central and axial points for the number of cumulated scans were 64, 8, 36, 75 and 2 and for the nominal resolution, 16, 2, 8, 32 and 1, respectively.

The response surface obtained is depicted in Figure 4 and, as can be seen, the signal-to-noise ratio increases when the nominal resolution and the number of accumulated scans rise, achieving an optimum value for 16 cm^{-1} nominal resolution

Table 2. Estimated effects found in the fractional factorial design (FFD) for the buprofezin determination by NIR.

Variables	4-factors model		2-factors model	
	Response	*p*-value*	Response	*p*-value*
A Scans	–24847	0.014	–40343	<0.001
B Resolution	36930	0.001	42411	<0.001
C Scan velocity	12381	0.190		
D Zero filling	–6680	0.470		
AB Scans–Resolution	–20750	0.036	–26231	<0.001
AC Scans–Scan velocity	–7908	0.394		
AD Scans–zero filling	10129	0.279		

* significance *p*-value: probability level of 0.05
Alias structure: it must be noticed that the experimental design based on 25 experiments could confound the following effects: A with BCD, B with ACD, C with ABD, D with ABC, AB with CD, AC with BD and AD with BC

and 36 cumulated scans and also considering the acquisition time of the signals.

Effect of experimental variables on the on-line extraction of buprofezin

To develop an automated procedure for the FT-NIR determination of buprofezin in commercial formulations, the on-line approach described in the experimental section was assayed.

A fixed volume of 1 mL acetonitrile was used for the following experiments because it was the minimum amount required to fill the appropriate height of the sample cartridge and to facilitate the handling of the solutions, avoiding an excessive dilution of the analyte in the organic extract. Different parameters, such as shaking time and geometry of the extraction cell, were evaluated to improve the extraction of buprofezin in acetonitrile by reducing the time required.

Three different sample extraction cell geometries were tested to minimise the extraction time: (i) a 35 mL volume, 7.78 cm length and 2.67 cm i.d. syringe barrel; (ii) a 2 mL volume, 6.5 cm length and 8.9 mm i.d. and (iii) a 1 mL volume with 5.7 cm length and 5.6 mm i.d. obtaining buprofezin recoveries of 100 ± 2, 82 ± 7 and 95 ± 15%, respectively. Thus, the syringe barrel with 35 mL internal volume was selected because it facilitates the homogenisation of the solution and the dispersion of solid particles.

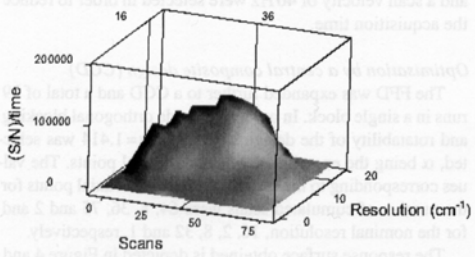

Figure 4. Surface plot of signal-to-noise ratio divided by the acquisition time versus resolution and number of accumulated scans.

Sixty seconds were enough to assure the complete on-line extraction of buprofezin from solid agrochemical formulations using 1 mL acetonitrile.

Analytical figures of merit

A recovery study, carried out on actual samples containing 18.0 mg g^{-1} buprofezin, spiked with known amounts of buprofezin, from 6.9 to 22.8 mg g^{-1}, provided mean recoveries of 99.8 ± 0.8%. The absence of a matrix effect was confirmed by comparing the slopes of the external calibration and the standard addition regression lines. The equations obtained for $n=5$ standards were $y=(1.003\pm0.002)+(58.0\pm0.17)C\,g\,g^{-1}$ with $R^2=0.9998$ and $y=(0.004\pm0.008)+(57.9\pm0.3)C\,mg\,g^{-1}$ with $R^2=0.9991$ for the standard addition and the external calibration, respectively, showing that the slope values of those regression equations are statistically comparable.

Analysis of formulation samples

The FT-NIR methodology proposed in this paper provided statistically comparable results with those obtained by the HPLC reference method for the analysis of buprofezin in commercial formulations, as can be seen in Table 3. It was found that, in all cases, experimental *t* values were lower than 1.812 for a paired *t* test for a probability level of 95% and 10 freedom degrees (six data found by each method minus two parameters).

Table 3. Determination of buprofezin in pesticide formulations by HPLC-UV and NIR procedures.

Sample	HPLC-UV (% w/w)[a]	NIR (% w/w)[a]	t_{exp} [b]
1	26.72±0.16	26.80±0.07	1.024
2	26.86±0.06	26.79±0.05	1.431
3	26.70±0.16	26.78±0.04	1.085
4	25.50±0.10	25.41±0.07	1.649

[a]Concentration values are the average of two independent analyses measured in triplicate ± the standard deviation of the six values found

[b]t_{tab} = 1.812 for a probability level of 95% for 10 freedom degrees.

Comparison of the developed procedure with other alternatives

Table 4 resumes the analytical characteristics of the different methods employed for the buprofezin determination in pesticide formulations. As can be seen, the limit of detection achieved by the HPLC procedure (0.06 mg L^{-1}) is two orders of magnitude lower than that obtained by FT-IR (20 mg L^{-1}) and FT-NIR (5 mg L^{-1}) procedures. However, due to the high concentration of buprofezin present in commercial formulations, vibrational spectroscopic procedures are sufficiently sensitive for their analysis and the use of high sensitive procedures which involve high dilution levels seem unjustified.

FT-NIR strategy provides a strong enhancement of sampling measurement frequency (30 h^{-1} instead 6 h^{-1} provided by the reference HPLC method and 10 h^{-1} for FT-IR determination) and reduces the amount of reagents used as compared with the FT-IR and HPLC procedures.

As compared with the previous developed methodology for FT-IR determination of buprofezin, the possibility of using acetonitrile in the NIR, in spite of chlorinated solvents, such as chloroform, is an environmentally friendly characteristic which helps avoid the depletion of the ozone layer.

Comparison

It has been shown that FT-NIR spectroscopy can be applied to the determination of buprofezin in commercially available formulations after previous extraction with acetonitrile. This provides a selective approach, which can be applied using external calibrations based on solutions of buprofezin in acetonitrile and so avoid the problems associated with the search of appropriate standards for multiparametric calibration in the presence of sample matrices.

Acknowledgements

The authors acknowledge the financial support of the Direcció General d'Universitats i Investigació de la Generalitat Valenciana (*Project GV04B/247 and Grupos 03-118*) and Universitat de València (*Project UV-AE-20050203).* S. Armenta also acknowledges the FPU Grant of the MECD (*Ref. AP2002-1874*).

References

1. M. Blanco, M.A. Romero and M. Alcalà, *Talanta* **64,** 597 (2004).
2. W. Plugge and C. Van der Vlies, *J. Pharm. Biomed. Anal.* **11,** 435 (1993).
3. Y.L. Ren, Y.H. Gou, Z. Tang, P.Y. Liu and Y. Guo, *Anal. Lett.* **33,** 69 (2000).
4. M. Blanco, D. Valdes, M.S. Bayod, F. Fernandez-Mari and I. Llorente, *Anal. Chim. Acta* **502,** 221 (2004).

Table 4. Comparison of the analytical features of the different procedures employed for the determination of Buprofezin in pesticide formulations.

	LOD (mg L^{-1})[a]	*% RSD*[b]	Sampling frequency[c]	Solvents consumed (mL)[d]	Solvent
HPLC	0.06	0.19	6	40.4	Acetonitrile
MIR	20	0.8	10	3	Chloroform
NIR	5	0.06	30	2	Acetonitrile

[a]Limit of detection values were established from three times (a probability level of 99.6%) the standard deviation of a blank solution divided by the slope of the calibration line. Note: in the case of HPLC, the limit of detection was established as three times the standard deviation of a 10.8 mg L^{-1} buprofezin standard solution divided by the slope of the calibration curve.
[b]Relative standard deviation values of five independent measurements
[c]Number of sample measurements per hour
[d]Solvent consumed corresponds with the analysis of a single sample

5. O.V. Brenna and N. Berardo, *J. Agric. Food Chem.* **52,** 5577 (2004).
6. T.F. Yeh, H.M. Chang and J.F. Kadla, *J. Agric. Food Chem.* **52,** 1435 (2004).
7. G. Vaccari, S. Tosi, A. Trilli and E. Tamburini, *Appl. Spectrosc.* **57,** 132 (2003).
8. S. Armenta, G. Quintás, S. Garrigues and M. de la Guardia, *Trends Anal. Chem.* **24,** 772 (2005).
9. A. Eustaquio, P. Graham, R.D. Jee, A.C. Moffat and A.D. Trafford, *Analyst* **123,** 2303 (1998).
10. M. Blanco, J. Coello, H. Iturriaga, S. Maspoch and C. de la Pezuela, *J. Near Infrared Spectrosc.* **5,** 67 (1997).
11. H.W. Czarnik-Matusewicz and A. Korniewicz, *J. Near Infrared Spectrosc.* **6,** A181 (1998).
12. C. de Liñan, *Vademecum de productos fitosanitarios y nutricionales*. Agrotécnica SL, Madrid, Spain, (2000).
13. D. Ortelli, P. Edder and C. Corvi, *Anal. Chim. Acta* **520,** 33 (2004).
14. M. Correia, C. Delerue-Matos and A. Alves, *J. Chromatogr. A* **889,** 59 (2000).
15. F.J. Egea-Gonzalez, A. Mena-Granero, C.R. Glass, A. Garrido-Frenich and J.L. Martinez-Vidal, *Rapid Commun. Mass Spectrom.* **18,** 537 (2004).
16. S. Armenta, G. Quintas, J. Moros, S. Garrigues and M. de la Guardia, *Anal. Chim. Acta* **468,** 81 (2002).
17. D.A. Burns and E.W. Ciurczak (Eds), *Handbook of near infrared spectroscopy*. Marcel Deker, Inc., New York, USA (1992).
18. T. Isaksson and T. Naes, *Appl. Spectrosc.* **42,** 1273 (1988).

Received: 10 May 2005
Accepted: 8 August 2005
Web Publication: 30 September 2005

ATTENUATED TOTAL REFLECTANCE SPECTROSCOPY

Attenuated total reflection-Fourier transform infrared analysis of the fermentation process of pineapple

Sergio Armenta[a], Salvador Garrigues[a], Miguel de la Guardia[a] and Philippe Rondeau[b]

[a]*Department of Analytical Chemistry, Universitat de València. Edifici Jeroni Muñoz, 50th Dr Moliner, 46100 Burjassot, Valencia, Spain.*

[b]*Laboratoire de Biochimie et Génétique Moléculaire, Faculté des Sciences et Technologies, Université de la Réunion, BP 7157, 97715 Saint-Denis, France.*

Analytical Chimica Acta 545 (2005) 99-106.

Impact factor of this journal (2004): 2.588
Source: Journal citation reports ISI Web of Knowledge, 2004.

Available online at www.sciencedirect.com
SCIENCE DIRECT
Analytica Chimica Acta 545 (2005) 99–106
ANALYTICA CHIMICA ACTA
www.elsevier.com/locate/aca

Attenuated Total Reflection-Fourier transform infrared analysis of the fermentation process of pineapple

Sergio Armenta [a], Salvador Garrigues [a], Miguel de la Guardia [a], Philippe Rondeau [b,*]

[a] Department of Analytical Chemistry, Faculty of Chemistry, University of Valencia, Edifici Jeroni Muñoz, 50th Dr. Moliner, 46100 Burjassot, Valencia, Spain
[b] Laboratoire de Biochimie et Génétique Moléculaire, Faculté des Sciences et Technologies, Université de La Réunion, BP 7151, 97715 Saint-Denis, France

Received 3 January 2005; received in revised form 20 April 2005; accepted 20 April 2005
Available online 31 May 2005

Abstract

A direct and reagent free procedure has been developed to monitor the fermentation process of pine apple nectar using Attenuated Total Reflectance Fourier-transform mid-infrared spectrometry (FT-IR) and multivariate analysis. A classical 4^2 design for standards was employed for calibration using the information in the spectral range from 907 to 1531 cm^{-1} of the first order derivative spectra after mean centering of infrared data. The root mean square error of calibration (RMSEC) of 0.040, 0.021, 0.063 and 0.074% w/w were obtained for glucose, fructose, saccharose and ethanol, respectively, and a mean relative validation error of 2.9, 2.1, 2.6 and 3.6% was achieved for glucose, fructose, saccharose and ethanol. Results obtained by the proposed procedure for the alcohol content at different fermentation levels were statistically comparable with those obtained by a reference spectrometric method. So, FT-IR spectrometry provides a fast alternative to long and tedious classical procedures to ethanol determination and sugar enzymatic analysis.

Keywords: FT-IR; ATR; PLS; PCA; Monitorization; Fermentation; Bioprocess

1. Introduction

Process analytical technologies (PAT) are systems for analysis and control of manufacturing processes based on timely measurements of critical quality parameters and performance attributes of raw materials and in-process products, to assure acceptable end-product quality at the completion of the process [1].

Bioprocesses involving enzymes or active cells are used to produce a wide variety of chemicals from alcohols, organic and amino acids, to insulin, enzymes, and antibiotics. Different kinds of fermentations are widely used in industrial scale in production of food, beverages, enzymes, pharmaceuticals, biogas, etc. Continuous monitoring of biotechnological processes is urgently needed for improving efficient management and optimization as well as for quality control with the aim of high quality final products. In fermentation processes of sugar rich products, the continuous control of alcohol provides a way to understand these processes and to predict the quality of the final product. Currently, alcohol measurements use on site semi-quantitative measurements (i.e. ebullioscopy) or involve enzymatic extraction and preparation of samples for laboratory analysis (i.e. distillation prior to gravimetric analysis). In recent years, gas chromatography has been accepted as standard procedure for ethanol assay [2]. However, the relatively high-cost and 'off-line' nature of these analyses has restricted its use in fermentation monitoring. As a result, extensive research has been undertaken to develop techniques that will allow for the continuous monitoring of ethanol levels during fermentation processes. For example, headspace analysis of ethanol fermentations using gas sensors has been attempted [3,4].

Infrared spectroscopy offers an alternative to conventional chemical analysis. This analytical technique has been applied successfully in a lot of bioprocess such as

* Corresponding author. Tel.: +33 262938643; fax: +33 262938237.
E-mail address: rophil@univ-reunion.fr (P. Rondeau).

0003-2670/$ – see front matter © 2005 Elsevier B.V. All rights reserved.
doi:10.1016/j.aca.2005.04.057

acetone–butanol–ethanol fermentation [5], glucoamylase fermentation [6], determination of sorbitol and sorbose in fermentation broth [7], and for monitoring glucose, glutamate, glutamine, lactate and ammonium [8]. Additionally, we developed a fast methodology for the quantitative analysis of ethanol in beer based on ATR measurements [9], which could open the way for the on-line control of this compound in bioprocesses.

A literature survey revealed a precedent about on-line baker's yeast fermentation monitoring by mid-IR based on the use of a diamond attenuated total reflection cell [10] and that ethanol production from pineapple has been already done in a reactor using immobilized yeast cells (*Saccharomyces cerevisiae*) through the use of gas chromatography [11].

In our work, the bioprocess media studied is a pine apple nectar not inoculated with yeast cells and submitted to a natural maturation process. Vibrational spectroscopy coupled with chemometric analysis has been used to determine the concentration of chemical components like glucose, fructose, saccharose and ethanol during the fermentation of pine apple juice.

2. Experimental

2.1. Apparatus and reagents

A Nicolet (Madison, WI, USA) 460 Protege FT-IR spectrometer, equipped with a temperature-stabilized deuterated tryglycine sulphate (DTGS) detector and a KBr beam-splitter, was employed for infrared measurements, using a Specac (Orpington UK) horizontal ATR (attenuated total reflectance) system, with a Ge crystal for the reflectance measurements.

Spectra treatment and data manipulation were carried out using Omnic 4.1 (Thermo Nicolet Corp., Madison, WI, USA). PLS calibration models were applied by using TurboQuant Analyst 6.0 software (Thermo Nicolet Corp., Madison, WI, USA).

A Hewlett Packard HP 8453 UV–vis (Palo Alto, CA, USA) diode array spectrophotometer coupled to User Data version software was used for the acquisition and storage of the UV–vis spectra on using the reference procedures for both alcohol and glucose determination. The 1 cm plastic cuvettes were used for spectral analysis.

Glucose levels were determined by an enzymatic colorimetric glucose oxidase assay.

Standards of D(+)-Glucose (Biochemistry quality), D(−)-Fructose (for analysis) and D(+)-Saccharose (for analysis) were supplied by Prolabo (Fontenay, France), Sigma (Lyon, France) and Labosi (Elancourt, France) respectively. Ethanol (99.8% v/v) was supplied by Merck (Paris, France). Sulfuric acid and potassium dichromate employed in the determination of ethanol were obtained from Sigma (Lyon, France).

2.2. Sampling method

Fresh Victoria Pine apple (*Ananas comosus* (L.) Merill) were growth at La Reunion Island and were peeled and blended in a household juicer to obtain a turbid juice. Juice was extracted by filtering and solid matter was removed by centrifugation at 10,000 × *g* for 10 min. 58 g of juice contained 13.2% w/w of total sugars was supplemented with 41 g of commercial concentrated sugar canne (82.5% w/w) and 184 g of water for having a final nectar with 14% w/w of total sugars. The final solution was divided into two sets of equal volume. One of them was sterilized by using an autoclave (20 min at 120 °C until 12 psi of vacuum) prior to incubation and the second one was employed directly to study the fermentation process.

Solutions of pine apple nectar were incubated at 37 °C during 30 days. Four milliliter of sample were collected every 24 h. A total of 23 samples were collected, frozen and stored at −20 °C until they were analyzed.

2.3. ATR FT-IR procedure

The mid-FT-IR spectra of the nectar samples have been recorded at room temperature in the ATR cell between 4000 and 650 cm^{-1} at 8 cm^{-1} nominal resolution, accumulating 50 scans per spectrum and with a mirror velocity of 0.158 cm s^{-1} employing a background of the empty cell. The equipment was continuously purged with a flow of dry nitrogen gas to eliminate any contributions from air humidity to the spectra.

The cell was cleaned after each sample measurement with water and detergent and a blank spectra was registered to asses that the memory effects are avoided.

The proposed PLS model was made using sixteen standards for calibration and four standards for validation. These standards correspond to different mixtures of glucose, fructose, saccharose and ethanol at two different concentration levels (4^2). Glucose was fixed at 0.10 and 5.05% w/w, fructose was evaluated at 0.10 and 2.09% w/w, saccharose at 1.86 and 12.83% w/w and ethanol at 0 and 6.57% w/w. Concentration of these components in samples was calculated employing the PLS calibration using the information of the spectral range from 907 to 1531 cm^{-1} in the first derivative spectra.

2.4. Statistical analysis

Principal component analysis (PCA) performed on the full set of spectra of non-sterilized nectar, was carried out with the commercial analysis software "The Unscrumbler", developed and published by Camo ASA. The principles of principal component analysis (PCA) have been described in detail in several papers [12,13].

2.5. Ethanol reference procedure

The reaction used for the determination of ethanol by UV–vis method involves mixing ethanol with acidified potassium dichromate and measuring the chromium(III) that is formed. This method is well explained [14]: an accurate amount of 1–2 g of nectar sample was diluted with 60 ml

of water inside a round bottom flask and distilled at 100 °C. Forty milliliter of the distillate were collected in a volumetric flask and washed with water until a final volume of 50 ml. After homogenization, an aliquot of 1 ml was added to 1 ml of 0.2 M $K_2Cr_2O_7$ in 4 M H_2SO_4. After 30 min, absorbance measurements at 600 nm were made using water as a blank.

A calibration line was established by measuring the absorbance at 600 nm for pure ethanol standards from 0.0024 to 0.14% w/w treated with $K_2Cr_2O_7$.

2.6. Enzymatic assay for glucose determination

Glucose levels were determined by an enzymatic colorimetric glucose oxidase assay commercially available from Sigma as described by Huggett and Nixon [15]. The basic principle is well described: glucose + O_2 + $H_2O \xrightarrow{glucose\ \ oxidase}$ gluconate + H_2O_2. Subsequently, there is a reaction between H_2O_2 and orthodianisidine catalyzed by peroxidase to produce a yellow complex, which become pink in acid media.

Two hundred and fifty microliter of nectar sample, previously diluted with water (exactly dilution), were mixed with 500 μL of reagent, containing glucose oxidase, peroxydase and o-dianisidine dichlorate in a tris–phosphate buffer pH = 7, and incubated for 30 min at 37 °C. 1 mL of HCl 5 M was added before reading the absorbance at 525 nm. A calibration line was established from the absorbance at 525 nm of a series of glucose standards in the concentration range between 0 and 0.006% w/w treated in the same way than samples.

3. Results and discussion

3.1. ATR FT-IR spectra

Fig. 1 shows the ATR-FT-IR spectra of pure glucose, fructose, saccharose and ethanol standards in water and those of the pineapple nectar, before and after fermentation.

The most intense bands present at sugar spectra are those located between 1200 and 900 cm^{-1} due to C–O–C stretching vibrations [13,16]. From these bands it can be seen that there are no band isolated to be employed in the external calibration.

For ethanol, the most intense bands are located at 1087 and 1045 cm^{-1} due to C–O stretching. Other less intense bands located between 3020 and 2800 cm^{-1} are due to CH stretching [17].

As can be seen in the figure, pineapple nectar presents the main characteristic bands of sugar and fermented nectar also shows the ethanol band at 1044 cm^{-1}.

3.2. Morphological analysis

PCA was performed on spectra of 23 samples of non-sterilized nectar at different stage of maturation process, in the region 900–1200 cm^{-1} corresponding to the major bands of sugars and ethanol. These spectra are featured in Fig. 2a. The decrease of several bands (1137, 1106, 1056 and 996 cm^{-1}) symbolised with downing arrows can be noted with the progress of maturation process. These bands correspond to the major component of the nectar (i.e. sucrose). The increase of bands at 1087 and 1045 cm^{-1} corresponding to ethanol is also observed.

Twenty two axes were calculated and cross validation was the method used to estimate the prediction error. The first axis explains about 97.8% of the information. The spectral pattern illustrated in Fig. 2b corresponds to the first axis and summarize well the antagonist effect between the decrease of bands of sucrose (positive peaks) and increase of bands of ethanol (negative peaks) during the maturation process.

3.3. Effect of FT-IR measurement conditions

The effect of the nominal resolution, the number of accumulated scans and the mirror velocity were tested in order to improve the measurement conditions. The nominal resolution varied between 2 and 16 cm^{-1}, the number of accumulated scans was modified from 5 to 75 and the mirror velocity between 0.1581 and 0.9494 cm s^{-1}.

Fig. 3a shows that the signal to noise ratio increased when the nominal resolution was increased being also increased the standard deviation of several measurements of the same solution. The signal was established from the spectral area calculated between 1090 and 1010 cm^{-1} corrected with a single point baseline established in 2515 cm^{-1}, for a standard with 8.6% w/w glucose, 9.0% w/w fructose, 11.2% w/w saccharose and 16.3% w/w ethanol, and the noise was measured in the same region for a blank spectrum and expressed as root mean square (RMS). As can be seen, the best signal-to-noise ratio was found for a 16 cm^{-1} nominal resolution, but it also causes a loss of repeatability and spectral information. Because of that, 8 cm^{-1} resolution was chosen for further measurements.

Fig. 3b, shows that the signal to noise ratio increases when the number of accumulated scans were increased till to reach practically a plateau for more than 50 scans. It must be also considered that the increase of the cumulated scans also increase the acquisition time, thus reducing the sampling frequency. So, in order to ensure a compromise between these two factors, 50 scans were selected for further experiments.

Fig. 3c evidences that the increase of the mirror velocity causes an important decrease in the signal to noise ratio. So, a 0.1581 value was selected for this study.

3.4. PLS determination of sugars and ethanol during nectar fermentation

A multivariate calibration technique based on the partial least squares (PLS) treatment of the ATR FT-IR data of both, zero and first order derivative spectra was employed. A classical design of 4^2 standards for the four analytes considered

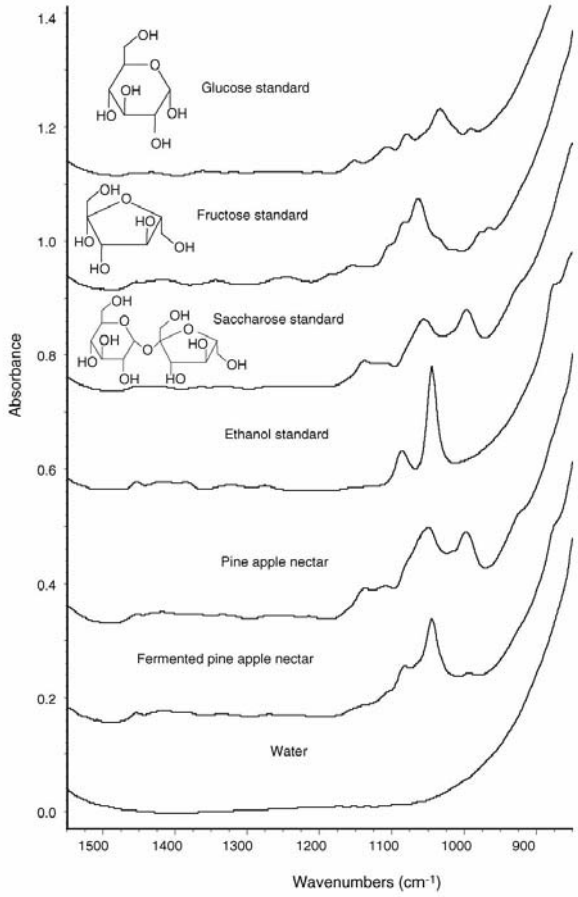

Fig. 1. Attenuated total reflectance—FT-IR spectra of glucose, fructose, saccharose and ethanol standard aqueous solutions at concentration levels of 6.0, 8.0, 7.0, and 8.1% w/w and those of pine apple nectar before and after fermentation. Spectra were obtained by accumulating 50 scans and using a spectral resolution of 8 cm^{-1}.

(glucose, fructose, saccharose and ethanol), at two concentration levels, was used as starting point.

Table 1 shows the analytical features of the PLS model applied to the different compounds under study as a function of the use of different spectral regions in the zero order spectra. It has been indicated the number of factors required for prediction of each analyte concentration with the minimum predicted residual error sum of squares (PRESS), the R^2 of the calibration model, the root mean square error of calibration (RMSEC) and the mean absolute validation errors established for four mixtures of the four considered compounds.

As can be seen, in the best conditions, using the information of the spectral range from 907 to 1531 cm^{-1} and 2800 to 3031 cm^{-1} for glucose and fructose and only between 907 and 1531 cm^{-1} for saccharose and ethanol, RMSEC of 0.08, 0.048, 0.102, and 0.095% w/w and mean relative validation errors of 5.8, 15.7, 4.4 and 3.1% were obtained for glucose, fructose, saccharose and ethanol, respectively, thus indicating a lack of accuracy, specially for the analytical control of fructose.

In order to improve the aforementioned results the first order derivative spectra were employed and, as can be see in Table 2, different regions were tested.

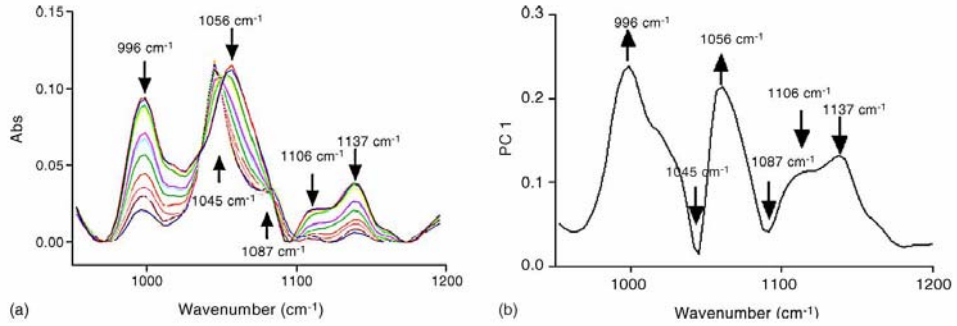

Fig. 2. Following of the maturation process of non sterilized nectar: FT-IR spectra (900–1200 cm^{-1}) of samples at different time of maturation (a), first principal axis spectral representation of PCA applied on all nectar samples (b).

On using the PLS calibration model with the information of the spectral region from 907 to 1531 cm^{-1} of the first order derivative spectra, in all the cases, it can be seen that the RMSEC obtained was 0.040, 0.021, 0.063 and 0.074% w/w, and the mean relative validation error were reduced to 2.9, 2.1, 2.6 and 3.6% for glucose, fructose, saccharose and ethanol, respectively, thus providing a clear enhancement of the prediction value.

3.5. *Study of interferences*

In order to assure the accuracy of the ATR-FT-IR developed procedure, it was evaluated the interference of increasing amounts of ethanol on the determination of sugars. For a fixed concentration of glucose (2.3% w/w), fructose (1.3% w/w) and saccharose (4.5% w/w) the interference of increasing concentrations of ethanol from 0 to 4.5% w/w was

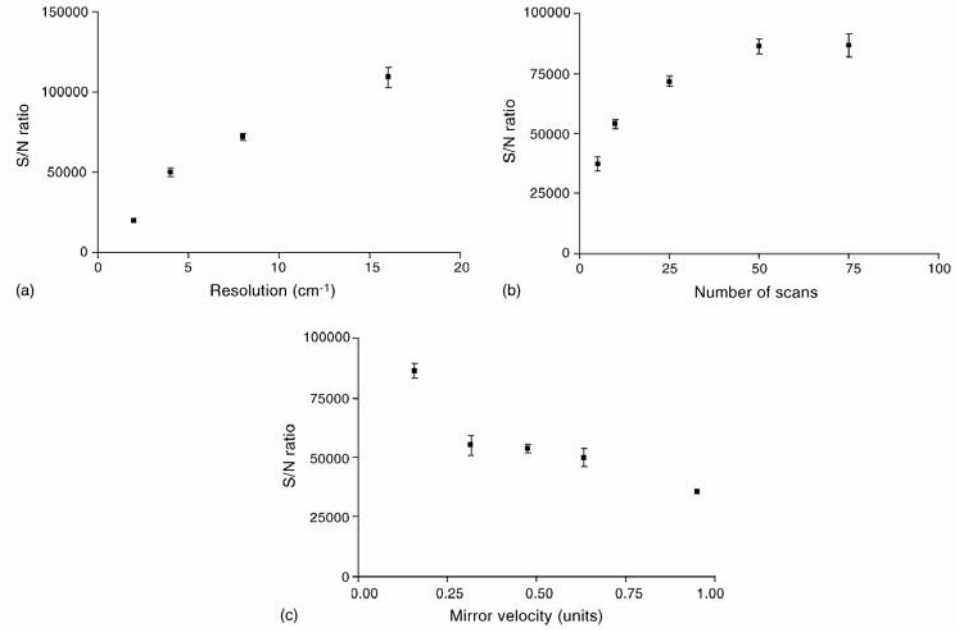

Fig. 3. Effect of measurement conditions on the signal to noise ratio of a standard solution containing 8.6, 9.0, 11.2 and 16.3% w/w glucose, fructose, saccharose and ethanol, respectively. (a) Effect of resolution, (b) effect of the number of cumulated scans and (c) effect of the mirror velocity.

Table 1
Analytical features of different wavenumber ranges employed for PLS zero order ATR FT-IR spectra monitoring of pine apple nectar fermentation process

Data employed (cm^{-1})		Component	Analytical characteristics found			
Region	Baseline		Factors[a]	R^{2}[b]	RMSEC[c]	Mean validation error[d] (%)
4000–907	None	Glucose	7	0.9991	0.075	9.9
		Fructose	8	0.996	0.060	17.5
		Saccharose	5	0.9998	0.089	5.0
		Ethanol	6	0.9993	0.107	4.2
3021–907	None	Glucose	7	0.9992	0.073	11.6
		Fructose	8	0.995	0.070	23.7
		Saccharose	5	0.9997	0.105	5.1
		Ethanol	6	0.9993	0.111	3.7
1531–907	None	Glucose	7	0.9995	0.060	7.5
		Fructose	8	0.998	0.039	31.3
		Saccharose	5	0.9997	0.102	4.4
		Ethanol	6	0.9995	0.0095	3.1
1531–907	None	Glucose	7	0.9990	0.080	5.8
3031–2800	None	Fructose	8	0.998	0.048	15.7
		Saccharose	5	0.9997	0.113	11.8
		Ethanol	6	0.9992	0.119	3.9
1531–907	None	Glucose	7	0.9990	0.080	5.8
3031–2800	None	Fructose	8	0.998	0.048	15.7
1531–907	None	Saccharose	5	0.9997	0.102	4.4
		Ethanol	6	0.9995	0.095	3.1

[a] The number of latent variables was chosen in order to obtain the minimum PRESS.
[b] Regression coefficient.
[c] Root mean square calibration error for a cross-validation.
[d] Relative error (%) found for validation without considering the sign.

Table 2
Analytical features of different wavenumber ranges employed for PLS first order derivative ATR FT-IR spectra monitoring of pine apple nectar fermentation process

Data employed (cm^{-1})		Component	Analytical characteristics found			
Region	Baseline		Factors[a]	R^{2}[b]	RMSEC[c]	Mean validation error[d] (%)
4000–907	None	Glucose	7	0.9999	0.029	3.9
		Fructose	8	0.9999	0.009	41.2
		Saccharose	5	0.9999	0.048	3.5
		Ethanol	6	0.9999	0.038	3.0
3021–907	None	Glucose	7	0.9998	0.033	3.7
		Fructose	8	0.9998	0.013	10.1
		Saccharose	5	0.9999	0.058	2.3
	7	Ethanol	6	0.9999	0.055	2.6
1531–907	None	Glucose	7	0.9998	0.040	2.9
		Fructose	8	0.9996	0.021	2.1
		Saccharose	5	0.9999	0.063	2.6
		Ethanol	6	0.9997	0.074	3.6
1531–907	None	Glucose	7	0.9998	0.037	3.8
3031–2800	None	Fructose	8	0.9998	0.016	3.9
		Saccharose	5	0.9999	0.060	2.3
		Ethanol	6	0.9997	0.071	2.9
1531–907	None	Glucose	7	0.9998	0.040	3.5
3031–2800	None	Fructose	8	0.999	0.037	3.6
		Saccharose	5	0.9999	0.060	2.3
		Ethanol	6	0.9997	0.074	2.8

[a] The number of latent variables was chosen in order to obtain the minimum PRESS.
[b] Regression coefficient.
[c] Root mean square calibration error for a cross-validation.
[d] Relative error (%) found for validation without considering the sign.

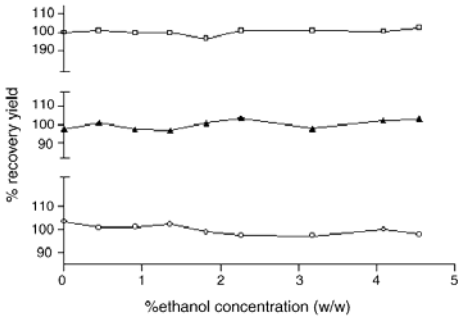

Fig. 4. Effect of increasing concentrations of ethanol on the recovery yield of (▲) glucose, (◯) fructose and (□) saccharose.

evaluated. Fig. 4 gives the recovery values for glucose, sucrose and fructose respectively mixed with varying amount of ethanol. The recovery value corresponds to the ratio of concentration obtained by calibration model between pure sugar and sugar mixed with ethanol. We can notice that whatever the sugar involved and the concentration of ethanol, the recovery values stay around 100%. The presence of ethanol does not interfere on glucose, fructose and sucrose determination.

4. Analysis of fermented nectar

Results obtained for glucose, fructose, saccharose and ethanol concentration at different state of pine apple incubation at 37 °C are shown in Fig. 5 for the non-sterilized nectar (A) as well as for the sterilized nectar (B). For untreated nectar, ethanol concentration increased from 0 to 4.3% w/w while saccharose concentration decreased from 12.6 to 3.6% w/w. No variations of concentration of the four analytes were observed for the sterilized sample incubation.

Ethanol concentrations obtained by the proposed methodology were comparable with those obtained by the reference method for ethanol determination. The regression between the concentrations found by FT-IR and those obtained by reference procedure during the pine apple fermentation provided a regression line ($C_{FT\text{-}IR} = (0.04 \pm 0.05) + (1.01 \pm 0.02)C_{UV}$, with a $R^2 \pm 0.995$) which has intercept and slope values statistically comparable to 0 and 1, respectively, for a probability level of 95%. So it can be concluded the absence of systematic absolute or relative errors and the useless of carrying out a blank correction.

On the other hand (results not shown) an enzymatic assay for the glucose assessment was made obtaining comparable results with those provided by the ATR-FT-IR procedure.

5. Conclusions

In this study, we verified that FT-IR spectroscopy coupled with PLS regression analysis offers an useful analytical tool for monitoring industrial fermentation process based on ATR measurements on the first order derivative spectra. The developed method provided simultaneously good estimations for the four analytes considered (glucose, fructose, saccharose and ethanol) during the fermentation of pine apple nectar.

The aforementioned analyte concentrations can be predicted with the accuracy and precision demanded for process monitoring. The novel method has shown itself to be rapid, as it does not require any sample pre-treatment and can be easily mechanized. Additionally, there is no reagent consumption nor waste generation, thus offering an environmentally friendly tool in front of reference procedures.

The ability of the ATR sampling technique to handle difficult and varied samples, and the total analysis capability of FT-IR spectroscopy with chemometric data processing, makes this technique suitable for the monitoring of other fermentation and industrial processes where the measurement of one or more analytes is required.

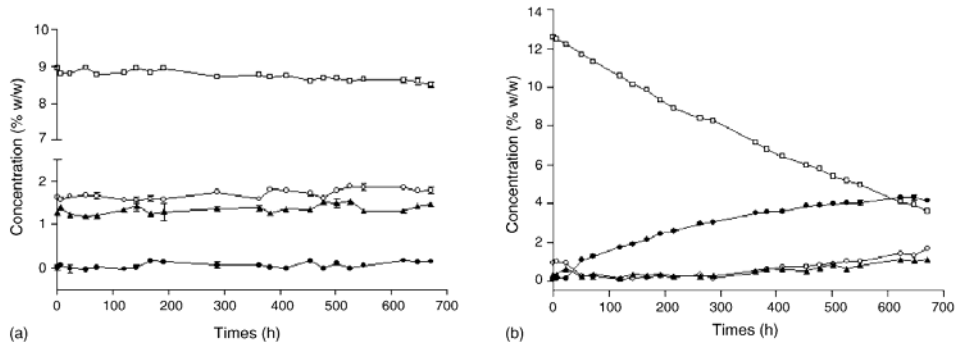

Fig. 5. Monitorization of the fermentation process of sterilized (a) and unsterilized (b) pine apple nectar by ATR FTIR spectrometry. (▲) glucose, (◯) fructose, (□) saccharose and (●) ethanol.

Acknowledgement

S. Armenta acknowledges the FPU Grant of the Ministerio de Educación, Cultura y Deporte (Ref. AP2002-1874).

References

[1] FDA, bPAT-A Framework for Innovative Pharmaceutical Manufacturing and Quality Assurance (Draft Guideline)Q, 2003. http://www.fda.gov/cder/OPS/PAT.htm.
[2] A.T. James, A.J.P. Martin, Biochem. J. 50 (1952) 679.
[3] C.F. Mandenius, O. Holst, B. Mattiasson, Acta Chem. Scand. 8 (1983) 746.
[4] W.J. Criddle, K.W. Parry, T.P. Jones, Analyst 112 (1987) 615.
[5] M. Grube, J.R. Gapes, K.C. Schuster, Anal. Chim. Acta 471 (2002) 127.
[6] J. Qiu, H.C. Pan, C.J. Han, Q. Ye, S.L. Zhang, Guangpuxue-Yu-Guangpu-Fenxi 19 (6) (1999) 831–833.
[7] J. Qiu, M.Z. Huang, H.F. Hang, C.J. Han, Q. Ye, S.L. Zhang, Appl. Spectrosc. 55 (2001) 794.
[8] M. Riley, H. Crider, Talanta 52 (2000) 473.
[9] F.J. Rambla, S. Garrigues, N. Ferrer, M. de la Guardia, Proceeding of the Second Mediterranean Basin Conference on Analytical Chemistry, 1997.
[10] G. Mazarevica, J. Diewok, J.R. Baena, E. Rosenberg, B. Lendl, Appl. Spectrosc. 58 (2004) 804.
[11] J.M. Nigam, J. Biotech. 80 (2000) 189.
[12] F. Cadet, M. de la Guardia, Encyclopedia of Analytical Chemisty, Wiley, 2000.
[13] P. Rondeau, S. Sers, D. Jhurry, F. Cadet, Appl. Spectrosc. 57 (2003) 466.
[14] P.J. Fletcher, J.F. van-Staden, Anal. Chim. Acta 499 (2003) 123.
[15] St.G. Huggett, D.A. Nixon, The Lancet 270 (1957) 368.
[16] M. Kansiz, J.R. Gapes, D. McNaughton, B. Lendl, K.C. Schuster, Anal. Chim. Acta 438 (2001) 175.
[17] D. Lin-Vien, N.B. Colthup, W.G. Fateley, J.G. Grasselli, Infrared and Raman Characteristic Frequencies of Organic Molecules, Academic Press, London, 1991.

DIFFUSE REFLECTANCE SPECTROSCOPY

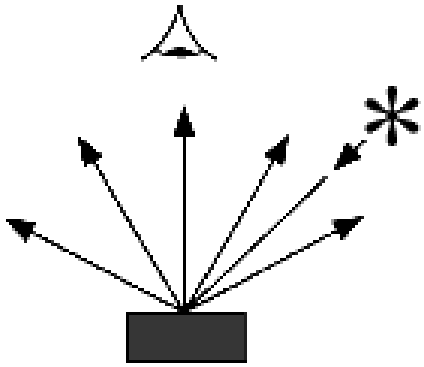

Quality control of agrochemical formulations by diffuse reflectance near infrared spectrometry

Sergio Armenta, Salvador Garrigues and Miguel de la Guardia
Department of Analytical Chemistry, Universitat de València. Edifici Jeroni Muñoz, 50th Dr Moliner, 46100 Burjassot, Valencia, Spain.

Analytical Chimica Acta Sent for publication 2006.

Impact factor of this journal (2004): 2.588
Source: Journal citation reports ISI Web of Knowledge, 2004.

Quality control of agrochemical formulations by diffuse reflectance near infrared spectrometry

Sergio Armenta, Salvador Garrigues*, Miguel de la Guardia

Department of Analytical Chemistry. Universitat de València. Edifici Jeroni Muñoz, 50th Dr. Moliner 46100 BURJASSOT. Valencia. SPAIN

Abstract:

A near infrared-based methodology (NIR) was developed for the determination of 11 pesticides in commercially available formulations. This solvent free, fast and environmentally friendly method was based on the direct measurement of the diffuse reflectance spectra of solid samples and a multivariate calibration model to determine the active principle concentration in agrochemicals.

The proposed PLS model was made from a common calibration set composed by 11 well characterized commercial samples and 22 additional doped samples (11 under and 11 over dosed), and 22 different formulations have been employed as the validation set. For Buprofezin, Chlorsulfuron, Cyromazine, Daminozide, Diuron and Iprodione determination, the information in the spectral range between 1618 and 2630 nm of the reflectance spectra was employed. On the other hand, for Bensulfuron, Fenoxycarb, Metalaxyl, Procymidone and Tricyclazole determination the information of the first order derivative spectra in the range between 1618 and 2630 nm was used. In both cases, a linear remove correction was applied as data pre-treatment.

The developed PLS/NIR method does not consume any solvent as no sample preparation is necessary. So, the developed methodology improves the laboratory efficiency without sacrifice the accuracy and avoids the contact of the operator with toxic solvents.

Keywords: ***Diffuse reflectance, Near infrared, Partial least squares calibration, pesticide formulations***

Introduction

Agriculture is the world's major industry, over 50 percent of the world's population being dependent upon agriculture for its livelihood.

In 1974, The World Food Conference recognized that a greatly increased use of fertilizers and pesticides is among the measures essential for achieving the massive expansion needed in food production (1).

It has been evidenced by data reported in 2000 and 2001 that the world pesticide expenditures totalize more than 32.5 billion dollars per year

* Corresponding author. Tel.: +34 96 354 3158; fax: +34 96 354 4838.

E-mail address: salvador.garrigues@uv.es (S. Garrigues).

and that the amount used of these products exceeded 5.0 billion pounds per year (2).

Pesticides are intended to effectively control organisms that destroy or endanger man's food, health or environment, under some circumstances and at concentrations above a certain threshold. The registration and sale of a pesticide formulation implies a number of different controls among which its evaluation, safety and composition are the most important. In order to characterize a pesticide formulation, it is necessary to be able to determine its composition and chemical and physical properties.

Many standardized methods are available to analyze technical products and commercial formulations, such as those of the Collaborative International Pesticides Analytical Council (CIPAC) (3) and the Association of Official Analytical Chemists (AOAC) (4). Chromatographic techniques have been the most widely used procedures. However the concentration range of the active principles in the samples allows that vibrational spectrometry-based procedures could be employed as a serious alternative in the quality control of pesticide commercial formulations.

In the last year a series of methodologies for the quality control of agrochemical formulations by mid-infrared spectrometry have been developed, being available methods for Artemisinin (5), Buprofezin (6), Chlorsulfuron (7), Cyromazine (8), Fenoxycarb (9), Fenvalerate (10) and Metalaxyl (11) determination after their extraction in an appropriate solvent, generally a chlorinated one.

Near infrared (NIR) based methodologies have been successfully applied in the quality control of end products in other industrial areas, such as food (12), petrochemical (13), pharmaceutical (14), clinical and biomedical (15), and environmental (16) sectors. However in the agrochemical sector there are only few precedents in the quality control of pesticides, Diuron (17), Buprofezin (18) and Hexythiazox (19) were determined by us in commercial formulations, after extraction with acetonitrile and subsequent transmittance measurement.

The main advantages of the NIR spectrometry are its non-destructive nature, the possibility to analyze products in real time, the low cost of equipment maintenance, the fast response times and the possibility to measure directly solid samples, with no sample pre-treatment. However, in most cases the use of chemometrics is required to extract relevant information because the overlapped bands of the NIR spectra are influenced by a number of chemical, physical and structural variables. Additionally, the use of previously analyzed or synthetic samples as calibration sets is necessary to incorporate the physical and chemical variability of samples in the calibration and to provide an enhancement of the predictive capability of the model (14).

On the other hand, the reduced number of available formulations that contain a specific pesticide complicates the development of classical multivariate calibration models.

The aim of the present study was to develop a direct, fast, accurate, environmentally friendly and affordable NIR procedure to the quality

control of pesticides in commercial formulations and in order to do it, a series of 11 pesticides commonly used in the treatment of crops were selected and the available formulations in the market employed to build a model for the analytical control of the production of a factory.

Experimental

Apparatus and reagents

A Bruker MPA (Bremen, Germany) FT-NIR spectrometer equipped with a quartz beamspliter, an air cooled NIR source, an InGaAs detector and an integrating sphere accessory was employed for diffuse reflectance measurements. For measurement control and data acquisition it was used the OPUS program (version 4.1) from Bruker. Spectra treatment and data manipulation was carried out using Omnic 2.1 software from Nicolet (Madison, WI, USA). PLS calibration models were established by using TurboQuant Analyst 6.0 software from Thermo Nicolet Corp. (Madison, WI, USA).

A Hewlett-Packard HPLC Series 1050 (Palo Alto, CA, USA) High Performance Liquid Chromatograph, equipped with a variable wavelength UV-Vis detector and a reversed phase C-18 (Kromasil) column of 250 mm length and 4.6 mm i.d. with 5 µm particle diameter, was employed for the analysis of the pesticide formulations, being used this methodology as a reference procedure for the validation of NIR measurements.

Bensulfuron (99.5% w/w), Buprofezin (99.1% w/w), Chlorsulfuron (99.8% w/w), Cyromazine (99.9%, w/w), Daminozide (99.9% w/w), Diuron (99.4% w/w), Fenoxycarb (99.7% w/w), Iprodione (99.8% w/w), Metalaxyl (99.7% w/w), Procymidone (99.1%, w/w) and Tryciclazol (99.7% w/w) PESTANAL® reagent grade standards were supplied by Fluka (Buchs, Switzerland). Acetonitrile and methanol HPLC gradient grade were purchased from Scharlab (Barcelona, Spain). Calcium carbonate was obtained from Probus (Barcelona, Spain) and kaolin, technical product, and commercial pesticide formulations were obtained directly from the local market.

Reference procedure

High performance liquid chromatography (HPLC)-based procedures were employed as reference methods to analyze the samples. The aforementioned procedures and the analytical characteristic are summarized in Table 1.

The indicated amounts of pesticide samples were accurately weighted inside 25 ml volumetric flasks and diluted to the volume in each case with the mobile phase. After appropriate dilution, solutions were filtered and discrete volumes were directly injected in the corresponding mobile phase, at a flow rate of 1 ml min^{-1}, except in the case of Daminozide for which 0.5 ml min^{-1} was employed. The active principles were determined in the isocratic mode by absorbance measurements at different wavelengths. Area values of the chromatographic peaks obtained at the reported retention times were interpolated in external

calibration lines established from standard solutions prepared in the mobile phases employed in each case.

Table 1

High performance liquid chromatography reference procedures and their analytical characteristics for the determination of different pesticides in commercial formulations

Pesticide	Sample amount (mg)	Volume Injected (µl)	Mobile phase	Wavelength (nm)	% RSD[a]	LOD (µg l^{-1})
Bensulfuron	40	20	20:80 ACN:phosphate buffer (pH=3)	250	0.1	77
Buprofezin	20	20	90:10 ACN:water	240	0.19	62
Chlorsulfuron	40	20	85:15 MetOH:water (pH=4)	226	0.02	13
Ciromazine	20	5	25:75 ACN:phosphate buffer (pH=3)	230	0.05	20
Daminozide	40	20	50:50 MetOH:ammonium acetate 10mM	218	0.15	70
Diuron	10	20	85:15 ACN:water	254	0.08	27
Fenoxycarb	40	10	85:15 ACN:water	282	0.2	40
Iprodione	30	10	85:15 ACN:water	229	0.1	20
Metalaxyl	80	20	80:20 ACN:water	250	0.11	64
Procymidone	40	20	90:10 ACN:water	238	0.2	12
Tricyclazole	15	20	85:15 ACN:water	275	0.06	10

[a] RSD values were established for four independent analysis of a standard containing a pesticide concentration of the order of mg l^{-1}.

PLS/NIR procedure

Wetting powder samples were introduced in standard chromatographic glass vials and the reflectance NIR spectra were recorded using 8 cm^{-1} nominal resolution and 36 cumulated scans per spectra. Water-Dispersible Granules were previously homogenized in an agate mortar.

The proposed PLS model was built using three independent measurements of a common calibration set composed by 11 well characterized commercial samples and 22 additional doped samples (11 under and 11 over dosed). 22 different known formulations were used for validation. The 11 over-dosed samples were obtained directly by addition to 100 mg of commercial pesticide formulations of known amounts of the active principle, till to reach a spiked amount of the same order than that present in the original sample. On the other hand, different amounts of an inert ingredient present in the commercial formulation (kaolin or calcium carbonate), were added to 100 mg of pesticide samples till to reach final concentrations of a half of the original one in order to obtain the 11 under-dosed samples.

For Buprofezin, Chlorsulfuron, Cyromazine, Daminozide, Diuron and Iprodione determination, the information in the reflectance spectra from 1618 to 2630 nm was employed. For Bensulfuron, Fenoxycarb, Metalaxyl, Procymidone and Tricyclazole determination the first order derivative spectra in the range between 1618 and 2630 nm were used. In both cases, a linear remove correction was applied.

The PLS factors used for the determination of Bensulfuron, Buprofezin, Chlorsulfuron, Cyromazine, Daminozide, Diuron, Fenoxycarb, Iprodione, Metalaxyl, Procymidone and Tricyclazole were 18, 22, 13, 23, 16, 22, 16, 16, 17, 19 and 19, respectively.

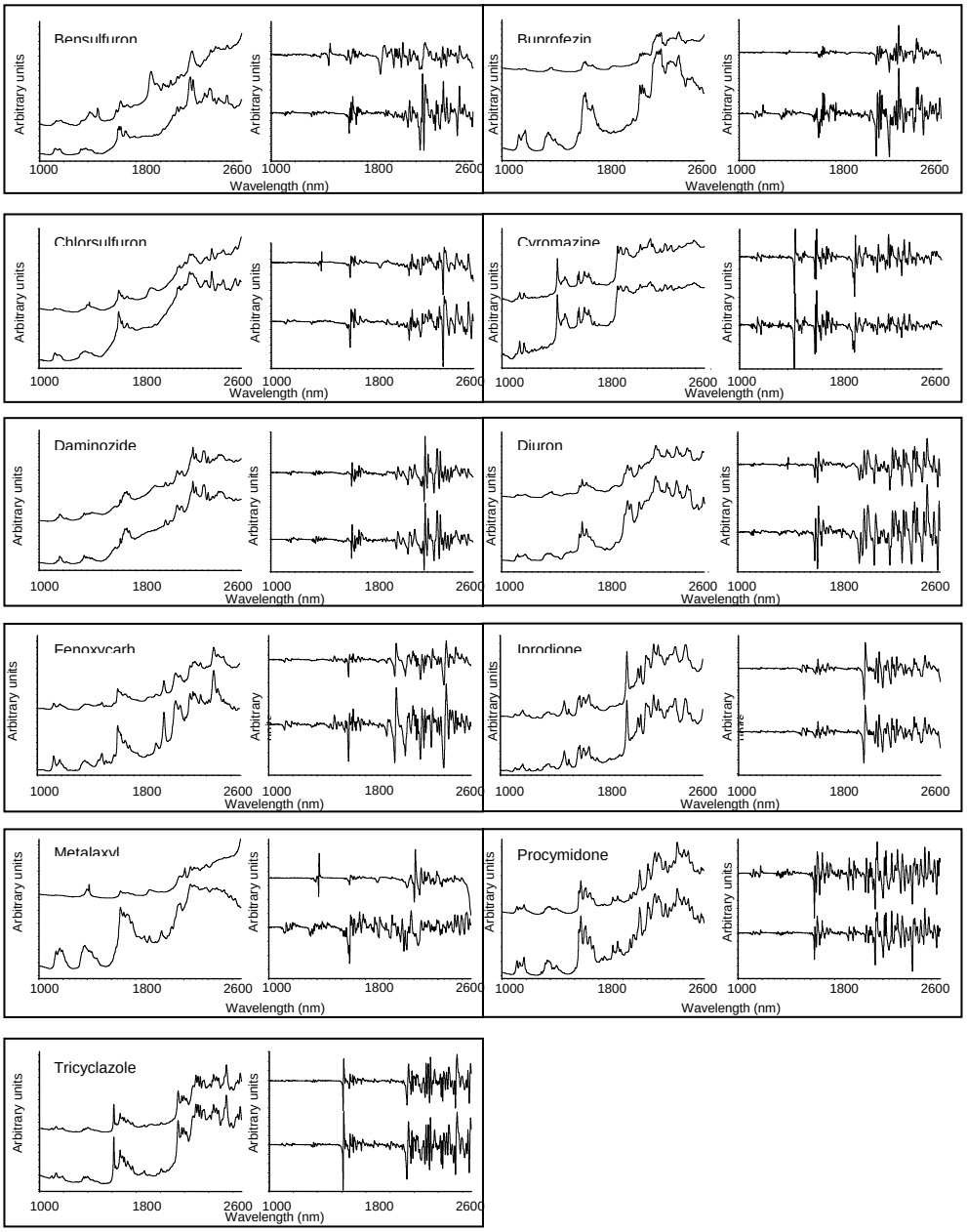

Fig. 1. NIR reflectance zero and first order derivative spectra of the different pesticides under study. Bensulfuron, Buprofezin, Chlorsulfuron, Cyromazine, Daminozide, Diuron, Fenoxycarb, Iprodione, Metalaxyl, Procymidone and Tryciclazole. Notes: Spectra of standard and commercial formulations containing 60% w/w Bensulfuron, 25% w/w Buprofezin, 75% w/w Chlorsulfuron, 75% w/w Cyromazine, 85% w/w Daminozide, 80% w/w Diuron, 25% w/w Fenoxycarb, 50% w/w Iprodione, 25% w/w Metalaxyl, 50% w/w Procymidone and 75% w/w Tryciclazole were obtained for the solid products placed in glass vials with a base diameter of 10 mm. Spectra were shift on the y axis to clearly show their bands. Instrumental conditions: 36 scans, 8 cm^{-1} nominal resolution.

Results and discussion

NIR spectra of pesticide formulations

Figure 1 shows the NIR zero and first order derivative reflectance spectra of different pesticide standards together with those of commercial formulations containing these products. All spectra were obtained by diffuse reflectance measurements on the solid products placed inside chromatographic glass vials with a base diameter of 10 mm.

Figure 1 shows the tremendous possibilities offered by the NIR technique to do the direct determination of active principles in solid agrochemicals due to the number and intensity of the bands present in the pesticide spectra which can be recognised in the samples.

Through examination of the spectra depicted in Figure 1 the PLS/NIR model for pesticide determination can be based on data in the spectral range from 1400 to 2630 nm which contains the main characteristic near infrared bands of the studied products.

PLS determination of pesticides in commercial formulations

The possibility to use a multivariate calibration technique, such as the partial least squares (PLS) for the treatment of the NIR data was evaluated based on the use of commercial samples to build the calibration set.

Table 2 shows the analytical features of the use of a PLS/NIR model, based on the use of 11 well characterized commercial samples as calibration set, for the determination of the selected active principles in pesticide formulations as a function of the use of different spectral regions and baseline criteria. First order derivative spectra were also tested with the aim of isolate absorption bands and flatten spectral baseline at the same time.

It must be noticed that all considered pesticides were formulated in single products and, because of that the model only uses a commercial formulation and 10 blanks for the determination of each one of the pesticides.

Mean centering spectra data pre-treatment was employed to eliminate common spectral information. The leave one out cross-validation procedure was used to obtain the best number of latent variables for each pesticide using the predicted residual error sum of squares (PRESS). It has been also indicated the R^2 of the calibration model, the root mean square error of calibration (RMSEC) and the mean accuracy errors found as compared data predicted by PLS/NIR with HPLC data and the % recovery yield obtained for doped samples.

It is noteworthy that the application of a linear removed correction to correct shifts and drifts in baseline improves the regression coefficients, the RMSEC and the mean accuracy errors found.

Table 2
Analytical features of PLS/NIR determination of pesticides in commercial formulations using different calibration models.

Data employed (nm)				Analytical characteristics found					
Region	Baseline	Spectra pre-treatment	Pesticide	Factors[a]	$R^{2,b}$	RMSEC[c]	Mean accuracy Error[d] (%)	% Recovery	
								UD*	OD*
1618-2630	Linear removed	None	Bensulfuron	6	0.9998	0.336	0.6	129.4 ± 0.1	44 ± 1
			Buprofezin	11	1.0000	0.0084	1.4	90.1 ± 0.2	78.1 ± 0.1
			Chlorsulfuron	11	1.0000	0.0297	1.1	104.6 ± 0.2	92.5 ± 0.2
			Cyromazine	4	0.999	1.07	0.8	110.6 ± 0.3	69.5 ± 0.3
			Daminozide	3	0.98	5.14	5.0	113.6 ± 0.1	77.4 ± 0.7
			Diuron	5	0.997	1.80	1.9	109.6 ± 0.5	113.6 ± 0.3
			Fenoxycarb	3	0.96	1.95	6.2	131.3 ± 0.2	83.3 ± 0.2
			Iprodione	3	0.94	5.01	7.2	96.8 ± 0.6	76.3 ± 0.6
			Metalaxyl	6	0.996	0.614	2.7	138.4 ± 0.5	49.4 ± 0.1
			Procymidone	5	0.9996	0.414	2.4	68.7 ± 0.2	57.9 ± 0.2
			Tricyclazole	8	0.99999	0.0819	1.2	118.4 ± 0.3	108.7 ± 0.1
Data employed (nm)				Analytical characteristics found					
Region	Baseline	Spectra pre-treatment	Pesticide	Factors[a]	$R^{2,b}$	RMSEC[c]	Mean accuracy Error[d] (%)	% Recovery	
								UD*	OD*
1618-2630	Linear removed	First derivative	Bensulfuron	5	0.998	1.11	0.7	127.1 ± 0.9	65.8 ± 0.6
			Buprofezin	6	0.99992	0.099	0.9	97.5 ± 0.2	80.6 ± 0.4
			Chlorsulfuron	11	0.99999	0.0879	1.1	101.6 ± 0.7	93.7 ± 0.3
			Cyromazine	4	0.9997	0.551	0.9	115.9 ± 0.8	72.1 ± 0.6
			Daminozide	3	0.996	2.21	1.2	123.2 ± 0.6	92.7 ± 0.2
			Diuron	6	0.9998	0.465	1.4	116.1 ± 0.5	108.6 ± 0.5
			Fenoxycarb	5	0.9990	0.357	0.9	143.2 ± 0.2	98.4 ± 0.2
			Iprodione	6	0.9998	0.253	2.4	110.7 ± 0.3	85.4 ± 0.4
			Metalaxyl	10	0.99997	0.0522	1.0	129.7 ± 0.7	57.1 ± 0.7
			Procymidone	3	0.9995	0.478	2.1	86.2 ± 0.6	66.1 ± 0.2
			Tricyclazole	2	0.99	3.02	1.5	114.0 ± 0.2	101.6 ± 0.3

[a]. The number of factors were chosen in order to obtain the minimum PRESS.
[b]. R^2 is the correlation coefficient of the regression line between predicted and actual values of analyte concentration in the calibration set.
[c]. Root mean square calibration error for a cross-validation.
[d]. Mean accuracy error (%) found from the comparison with results obtained by HPLC.
*UD: under-dosed samples. OD: over-dosed samples.

However, as it can be seen in the table, the recovery yield values found by the models that use only commercial formulations that contain a single active principle as calibration set, were unacceptable for the determination of these principles in unknown samples. It demonstrates the tremendous importance of the physical properties associated with the inert ingredients of the formulation, such as degree of compaction, manufacturing process, etc additionally than the recognition of each pesticide spectrum in the NIR determination and makes necessary the introduction of a serie of samples containing different concentrations of each pesticide in the calibration set.

The initial model was improved by addition of eleven under and eleven over-dosed samples to the calibration set, prepared as it has been aforementioned in the experimental section, in order to obtain a more robust PLS model than the previous one.

Table 3
Analytical features of the selected PLS/NIR determination of pesticides in commercial formulations.

Data employed (nm)			Analytical characteristics found						
Region	Baseline	Spectra pre-treatment	Pesticide	Factors[a]	$R^{2,b}$	RMSEC[c]	Mean accuracy Error[d] (%)	% Recovery	
								UD*	OD*
1618-2630	Linear removed	First derivative	Bensulfuron	18	0.9998	0.388	1.2	100.9 ± 0.3	99.1 ± 1.0
		None	Buprofezin	22	0.9993	0.310	0.8	99.3 ± 0.6	100.8 ± 0.2
			Chlorsulfuron	13	0.998	1.30	0.7	98.7 ± 0.7	99.0 ± 0.3
			Cyromazine	23	0.9993	0.800	2.0	101.4 ± 0.3	99.7 ± 0.3
			Daminozide	16	0.998	1.30	1.1	102.6 ± 0.1	98.5 ± 0.8
			Diuron	22	0.9998	0.441	3.1	100.6 ± 0.9	102.8 ± 0.6
		First derivative	Fenoxycarb	16	0.998	0.648	1.4	102.6 ± 0.8	100.1 ± 0.3
		None	Iprodione	16	0.995	1.60	2.7	103.9 ± 0.4	98.2 ± 0.2
		First derivative	Metalaxyl	17	0.9996	0.259	0.3	102.8 ± 0.4	101.6 ± 0.2
			Procymidone	19	0.9998	0.345	3.1	100.1 ± 0.9	101.5 ± 0.3
			Tricyclazole	19	0.9998	0.338	0.5	100.8 ± 0.5	99.3 ± 0.4

[a]. The number of factors were chosen in order to obtain the minimum PRESS.
[b]. R^2 is the correlation coefficient of the regression line between predicted and actual values of analyte concentration in the calibration set.
[c]. Root mean square calibration error for a cross-validation.
[d]. Mean accuracy error (%) found from the comparison with results obtained by HPLC.
*UD: under-dosed samples. OD: over-dosed samples.

Table 3 shows the analytical features of the use of the selected PLS/NIR model, based on the use of 11 commercial formulations and 22 doped samples as calibration set for the determination of the 11 pesticides under study.

Figure 2 shows the PRESS and the mean accuracy errors obtained for the pesticide analysis by introduction each additional factor of the selected model. As can be seen from this figure, the mean accuracy errors exposed show clearly the importance of a carefully selection of the wavelength range and the number of factors to be used. The high number of factors needed in the PLS/NIR determination of active principles in pesticide formulations is probably due to the high number of blanks introduced for the determination of each pesticide with a different spectral contribution (one for each formulation) and the differences in physical properties of the sample matrices.

The principal component spectra (PCS) were obtained in order to explain the contribution of factors on the analysis of each pesticide. As an example, the principal component spectra, obtained for the determination of Cyromazine, additionally than the spectra of a commercial formulation containing this pesticide were represented in Figure 3 in order to evaluate the correlation between the concentration of Cyromazine in wetting powder samples and the spectral data.

The principal components 4, 5, 6, 8, 14, 16 and 23 provide practically the characteristic spectra of Cyromazine commercial samples being necessary the other factors to modelize the corresponding matrix and to differentiate this active principle from the rest of the studied pesticides.

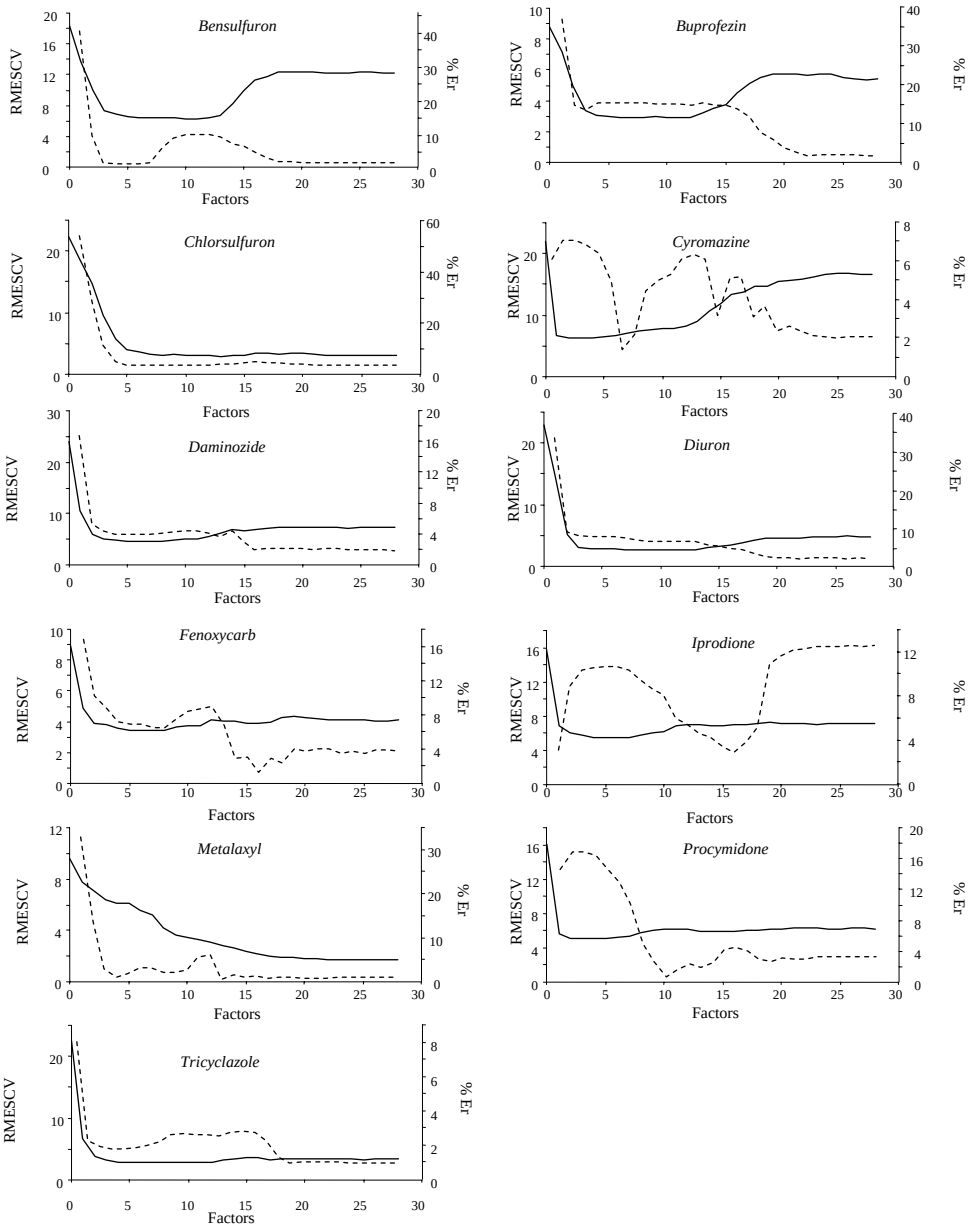

Fig. 2. RMSECV (solid line) and the mean accuracy errors (dashed line) obtained as a function of the number of factors employed to build the PLS model for determination of 11 active principles in commercial formulations.

In the light of the results, there are no important differences between the use of zero or first order derivative spectral data. So the best criterion must be selected in each case in terms of precision and accuracy.

In short, for Buprofezin, Chlorsulfuron, Cyromazine, Daminozide, Diuron and Iprodione determination, the information in the zero order reflectance spectral range between 1618 and 2630 nm was employed, and for the other studied pesticides the information of the first order derivative spectra in the same region was used, applying, in both cases, a linear remove correction for data pre-treatment. On using the aforementioned conditions it was found mean accuracy errors between 0.5 and 3.1% for the validation of samples.

Analysis of doped samples

A validation set of 22 doped samples (different than those employed for calibration) was used to determine the accuracy of the developed PLS/NIR method for pesticide quality control in agrochemical formulations.

Once again, eleven over-dosed samples obtained by addition of different known amounts of the active principle to the commercial formulations and eleven under-dosed samples prepared by addition of different amounts of the inert ingredient present in the commercial formulations (kaolin and calcium carbonate) were used.

The doped samples were analyzed in the same instrumental conditions that original samples and the concentration of active principle was determined employing the aforementioned PLS model.

The mean average recovery was 101.2 ± 1.6% and 100.1 ± 1.5% for over and under dosed samples, respectively, as can be seen in Table 3, thus indicating the lack of systematic errors.

Analysis of commercial samples

Table 4 summarizes the data found for the HPLC and PLS/NIR determination of the selected pesticides in the commercial formulations assayed, which were employed as validation data set in PLS, and it can be seen that results found by the recommended method compared well with those obtained by the reference chromatographic procedure.

On the other hand, the regression between all the data found for commercial samples assayed by the PLS/NIR and chromatographic methods provided an equation of $C_{NIR}=(0.6 \pm 0.8) + (0.98 \pm 0.04)C_{HPLC}$ with $R^2=0.997$. Statistically the aforementioned regression line present slope and intercept values comparable with 1 and 0 respectively which evidence that, as compared with the reference method, the developed procedure does not present constant nor relative errors.

Conclusion

This paper demonstrates the high potential of diffuse reflectance NIR and multivariate calibration for the quality control of pesticide formulations in the agrochemical industry, in spite of the limited number of different samples

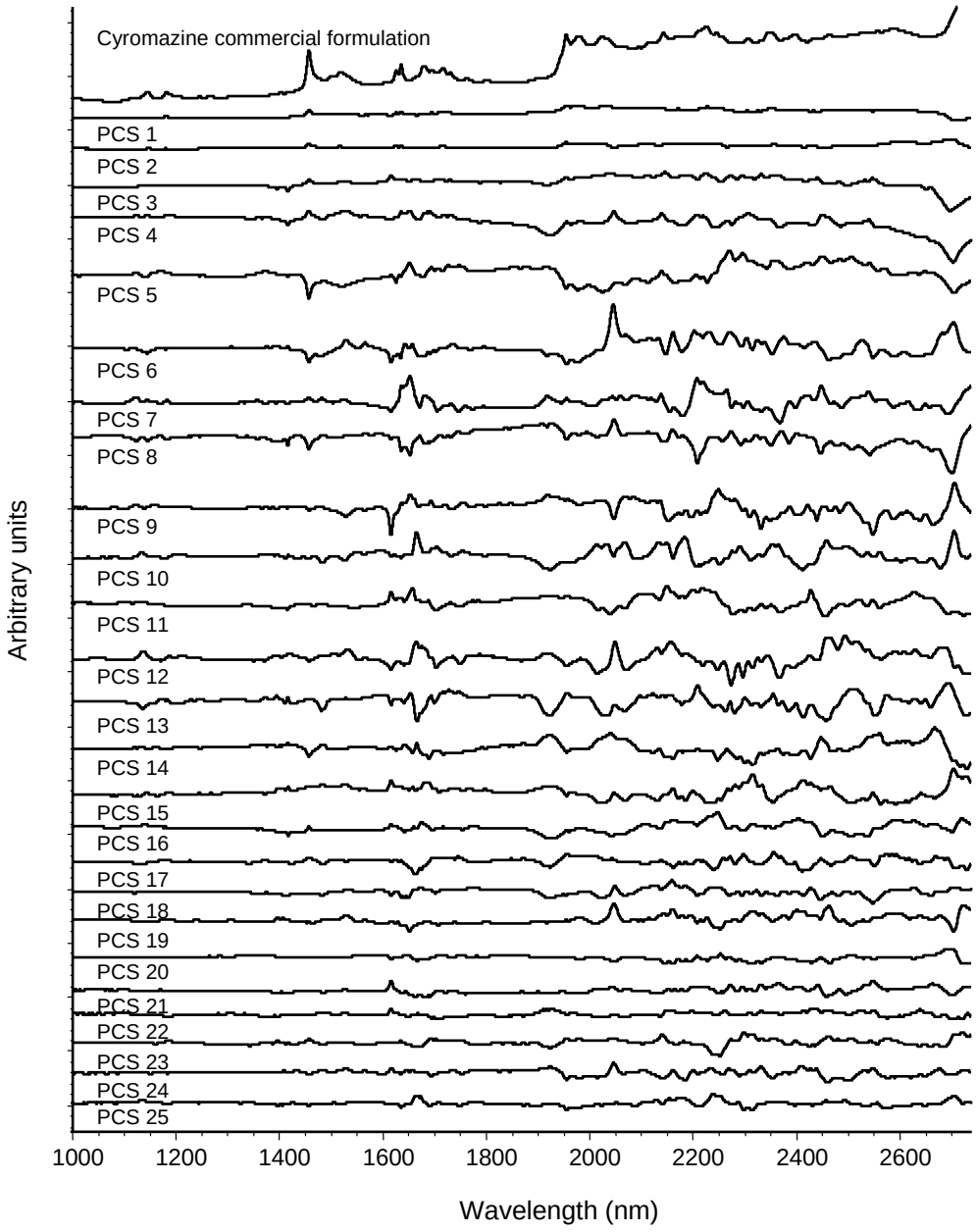

Fig. 3. Principal component spectra diagnostic applied to verify the effect of the increasing number of factors on the signals of Cyromazine pesticide formulations. Note: spectra of Cyromazine samples was included for comparison purposes.

Table 4
Determination of active principles in pesticide commercial formulations by HPLC-UV and NIR procedures.

Pesticide	Sample	HPLC (% w/w)	NIR (% w/w)	% Relative accuracy error
Bensulfuron	1	61.7 ± 0.6	60.6 ± 0.4	1.8
	2	60.9 ± 0.3	60.8 ± 0.5	0.5
Buprofezin	3	26.86 ± 0.06	27.2 ± 0.2	1.3
	4	26.70 ± 0.16	26.8 ± 0.2	0.4
Chlorsulfuron	5	76.4 ± 0.2	76.48 ± 0.07	0.10
	6	76.4 ± 0.2	77.41 ± 0.2	1.3
Cyromazine	7	76.8 ± 0.3	77.4 ± 0.8	0.8
	8	75.4 ± 0.2	73.0 ± 1.1	3.2
Daminozide	9	85.47 ± 0.03	85.60 ± 0.11	0.11
	10	85.3 ± 0.3	83.5 ± 0.2	2.1
Diuron	11	82.6 ± 0.4	80.3 ± 0.9	2.8
	12	83.0 ± 0.4	80.2 ± 0.8	3.3
Fenoxycarb	13	23.50 ± 0.10	23.9 ± 0.4	1.6
	14	24.00 ± 0.06	24.3 ± 0.2	1.2
Iprodione	15	48.94 ± 0.03	50.3 ± 0.2	2.8
	16	49.04 ± 0.03	50.2 ± 0.3	2.6
Metalaxyl	17	25.44 ± 0.11	25.33 ± 0.12	0.3
	18	25.16 ± 0.05	25.1 ± 0.2	0.3
Procymidone	19	51.6 ± 0.2	48.6 ± 1.1	3.7
	20	50.5 ± 0.3	50.3 ± 0.5	2.4
Tricyclazole	21	75.5 ± 0.2	74.9 ± 0.8	0.8
	22	75.5 ± 0.1	75.4 ± 1.5	0.14

[a] Concentration values are the average of three independent analysis measured in triplicate ± the corresponding standard deviation of the 6 values found.

produced for each pesticide and the diversity of formulated compounds.

NIR is a very rapid quantitative analytical method once it has been validated, but the requisite calibrations are time consuming. It requires the production of a range of samples that differ from their commercial available counterparts solely in concentration. Model-building also requires an optimisation step, i.e. the choice of a regression method and spectral pre-treatments strongly informed by the data set. Once one has dealt with all these aspects, NIR can be used as a far faster technique than HPLC for quality control of agrochemicals. Moreover the developed procedure does not consume any solvent as no sample preparation is necessary.

So, the main advantages of the application of the developed PLS/NIR methodology are that it improves the laboratory efficiency without sacrifice the accuracy and avoids the contact of the operator with the pesticide.

Acknowledgements

The authors acknowledge the financial support of the Direcció General d'Universitats i Investigació de la Generalitat Valenciana (Project GV04B/247 and Grupos 03-118) and S. Armenta the FPU Grant of the MECD (Ref. AP2002-1874).

References

[1] Food and Agriculture Organization (FAO) of the United Nations, International Code of Conduct on the Distribution and Use of Pesticides, Rome, 2002.

[2] EPA: Pesticides - 2000/2001 Pesticide Sales and Usage Report Biological and analysis division Office of pesticide programs, Washington, 2002. http://www.epa.gov/oppbead1/pestsales/01pestsales/sales2001.html

[3] Collaborative International Pesticide Analytical Council (CIPAC) Methods, Abingdon, England.

[4] Official Methods of Analysis of AOAC International. 17th Edition, Gaithersburg, MD, 2002.

[5] B.Y. Liu, H.J. Tian, J. Cui, Z.J. Song. Yaowu Fenxi Zazhi 14, 47-48, 1994.

[6] S. Armenta, G. Quintas, J. Moros, S. Garrigues and M. de la Guardia, Anal. Chim. Acta. 468 (2002) 81-90.

[7] G. Quintas, S. Armenta, A. Morales-Noe, S. Garrigues and M. de la Guardia Spectroscopy lett. 36 (2003) 511–525.

[8] S. Armenta, G. Quintás, S. Garrigues and M. de la Guardia, Anal. Chim. Acta, 524 (2004) 257-264.

[9] G. Quintás, S. Armenta, S. Garrigues and M. de la Guardia Ciencia, 11 (2003) 319-327.

[10] S. Gupta, K.K. Sharma, S.K. Handa. J. AOAC Int. 79 (1996) 1260-1262.

[11] G. Quintás, S. Armenta, A. Morales-Noé, S. Garrigues and M. de la Guardia Anal. Chim. Acta, 480 (2003) 11-21.

[12] K. C. Volkers, M. Wachendorf, R. Loges, N. J. Jovanovic and F. Taube Anim. Feed Sci. Tech. 109 (2003) 183-194.

[13] J.J. Kelly, C.H. Barlow, M. Jinguji, J.B. Callis, Anal. Chem. 61 (1989) 1419-1424.

[14] M. Blanco, M. A. Romero and M. Alcalà Talanta, 64 (2004) 597-602.

[15] X. Kexin, O. Qingjun, J. Jingying and Y. Xiuyan Opt. Lasers Eng. 43 (2005) 1096-1106.

[16] P. Bowyer and F.M. Danson Remote Sens. Environ. 92 (2004) 297-308.

[17] J. Moros, S. Armenta, S. Garrigues, M. de la Guardia Anal. Chim. Acta 543 (2005) 124-129.

PHOTOACOUSTIC SPECTROSCOPY

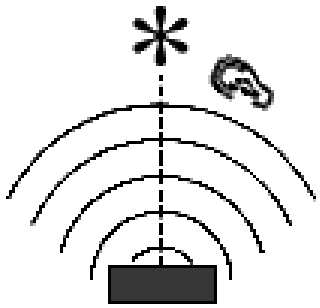

Direct determination of Mancozeb by Photoacoustic spectrometry

Sergio Armenta, Javier Moros, Salvador Garrigues and Miguel de la Guardia
[a]*Department of Analytical Chemistry, Universitat de València. Edifici Jeroni Muñoz, 50th Dr Moliner, 46100 Burjassot, Valencia, Spain.*

Analytical Chimica Acta Accepted for publication 2006.

Impact factor of this journal (2004): 2.588
Source: Journal citation reports ISI Web of Knowledge, 2004.

+ Model
ARTICLE IN PRESS
Available online at www.sciencedirect.com
SCIENCE DIRECT
ELSEVIER
Analytica Chimica Acta xxx (2006) xxx–xxx
ANALYTICA CHIMICA ACTA
www.elsevier.com/locate/aca

Direct determination of Mancozeb by photoacoustic spectrometry

Sergio Armenta, Javier Moros, Salvador Garrigues *, Miguel de la Guardia

Department of Analytical Chemistry, Universitat de València, Edifici Jeroni Muñoz, 50th Dr. Moliner, 46100 Burjassot, Valencia, Spain

Received 9 January 2006; received in revised form 6 March 2006; accepted 8 March 2006

Abstract

A solvent free, fast and environmentally friendly photoacoustic-infrared-based methodology (PAS-FTIR) was developed for the determination of Mancozeb in agrochemicals. This methodology was based on the direct measurement of the transmittance spectra of solid samples and a multivariate calibration model to determine the active ingredient concentration. The proposed partial least squares (PLS) model was made using nine standards prepared by mixing different amounts of kaolin and Mancozeb, with concentrations between 5.43 and 88.10% (w/w).

A hierarchical cluster analysis was made in order to classify the samples in terms of similarity in the PAS-FTIR spectra. From their spectra different commercially available fungicide samples were classified in four groups, attending to the presence of other active ingredients co-formulated with Mancozeb. Different PLS models were applied for the analysis of each group of samples.

So, for samples containing copper oxychloride (group 1), the information in the spectral range from 1543 to 1474 and 1390 to 1269 cm^{-1} was employed. For samples co-formulated with Fosetyl-Al (group 2) the range between 3334 and 3211 cm^{-1}, corrected with a single point baseline located at 3055 cm^{-1}, was used. For samples containing Metalaxyl (group 3) it was used the information in the spectral range from 1543 to 1474 cm^{-1} was used to determine Mancozeb. Finally, the range between 1456 and 1306 cm^{-1} was used for Mancozeb determination in samples containing Cymoxanil (group 4).

The PLS factors used for Mancozeb determination depends on the PLS model employed. 3, 2, 2 and 3 factors were used for Mancozeb determination in commercially available pesticides for groups 1, 2, 3 and 4, respectively. The mean accuracy errors found were 3.1, 2.1, 2.5 and 3.0% for groups 1, 2, 3 and 4, respectively. The developed PAS-FTIR methodology does not consume any solvent, as no sample preparation is necessary it improves the laboratory efficiency without sacrifice the accuracy and avoids the contact of the operator with toxic substances.

Keywords: Mancozeb; Photoacoustic infrared spectrometry; Partial least squares calibration; Pesticide formulations

1. Introduction

Mancozeb, a [[1,2-etilenbisdithiocarbamate](2-)] of manganese and zinc mixture, is used to protect many fruit, vegetable, nut and field crops against a wide spectrum of fungal diseases, including potato blight, leaf spot, scab (on apples and pears), and rust (on roses). It is also used for seed treatment of cotton, potatoes, corn, safflower, sorghum, peanuts, tomatoes, flax, and cereal grains [1]. Mancozeb is practically non-toxic via the oral route with reported oral LD_{50} of greater than 5000 mg kg^{-1} to greater than 11,200 mg kg^{-1} in rats [2] and due to this property is one of the most used pesticides around the world [3]. It is commonly found in combination with other pesticides like Cymoxanil, Metalaxyl, Fosetyl-Al or copper oxychloride [4].

Mancozeb is practically insoluble in common organic and inorganic solvents and indirect methods for its determination include spectrophotometry [5], gas chromatography (GC) [6], headspace solid phase microextraction GC [7] or reversed phase ion-pair chromatography [8] determination of the reaction products liberated after reduction, in an acidic medium, to carbon disulfide. It is important to note that these methods are typically unable to distinguish among various dithiocarbamates since most of them can be degraded to CS_2. Other methods for determination of ethylenebisdithiocarbamates rely on the measurement of the metallic portion of the compounds, and therefore, many of these methods are similar to those for detection of inorganic manganese or zinc [9]. However, these methodologies assure the content of metal but cannot evaluate the possible degradation of pesticide molecules.

Liquid chromatography has been employed after transformation of dithiocarbamates onto water-soluble sodium

* Corresponding author. Tel.: +34 96 354 3158; fax: +34 96 354 4838.
E-mail address: salvador.garrigues@uv.es (S. Garrigues).

0003-2670/$ – see front matter © 2006 Elsevier B.V. All rights reserved.
doi:10.1016/j.aca.2006.03.031

salts, methylation and ultraviolet detection at 272 nm [10] to determine and distinguish thiocarbamates and dithiocarbamates.

Mancozeb has been determined by FTIR spectrometry based on the ratio between the absorbance of a characteristic band of Mancozeb and that of an internal standard measured in the FTIR spectra obtained from KBr pellets [11]. However, this procedure is tedious and time consuming.

Photoacoustic spectroscopy (PAS) has been widely used to investigate the chemical and physical properties of many samples. The theoretical basis for the photoacoustic effect in solids was laid by Rosencwaig and Gersho in the mid-1970s in the so-called R–G theory. The photoacoustic signal is proportional to the temperature rise in a sample irradiated with a light source and thus to the absorbed energy [12].

PAS offers the advantage that it can be used for highly absorbing, layered or highly scattering samples, which were previously difficult or impossible to be measured by ordinary transmission and reflection methods. On using PAS, the FTIR spectra of solid substances can be obtained without any previous treatment of the sample.

PAS coupled with FTIR detection has been previously used with quantitative purposes in solid substances for the analysis of depth profiling in coated papers [13], chemical composition of woods [14], microbiological studies [15], characterisation of potato chips [16] and process analysis of bio-films [17]. However, there are no PAS precedents on the use of this technique for the determination of pesticides in agrochemical formulations [18].

So, the aim of this paper is to present an environmentally friendly methodology with no sample pre-treatment that can be used for routine determination of Mancozeb in commercially formulated fungicides as a serious alternative to tedious, time and reagent consuming reference procedures, taking also advantage on the difficulties offered to dissolve Mancozeb.

2. Experimental

2.1. Apparatus and reagents

A Bruker IFS66/v (Bremen, Germany) FT-IR spectrometer, equipped with a KBr beamsplitter, was employed for infrared measurements, using a helium-purged PAC300 MTEC (Ames, Iowa, USA) photoacoustic detector cell.

For measurement control and data acquisition, the OPUS program (version 4.1) from Bruker (Bremen, Germany) was employed. Spectra treatment and data manipulation were carried out using Omnic 2.1 software from Nicolet (Madison, WI, USA). PLS calibration models were obtained by using TurboQuant Analyst 6.0 software developed by Thermo Nicolet Corp. (Madison, WI, USA).

A Dionex P680 High Performance Liquid Chromatograph (Sunny Vale, CA, USA), equipped with a C-18 reversed phase (Kromasil) column (250 mm × 4.6 mm i.d. and 5 μm particle diameter), and an UVD 170U variable wavelength UV–vis detector was employed for the determination of Mancozeb as reference methodology.

Mancozeb standard (88.1%, w/w) was supplied by Riedel-de-Haën (Seelze, Germany) and acetonitrile, chloroform, hexane, methanol (HPLC gradient grade), and sodium hydroxide were purchased from Scharlau (Barcelona, Spain). EDTA disodium salt 2-hydrate was supplied by Panreac (Barcelona, Spain) and tetrabutylammonium hydrogen sulfate, methyl iodide and 1,2-propanediol were obtained from Fluka (Buchs, Switzerland). Kaolin was purchased from Afrasa S.A. (Valencia, Spain) and commercially available Mancozeb samples were obtained directly from the Spanish market.

Samples were classified in different groups according to their PA spectra and were shown to be in good agreement with their composition. So, group 1 is composed of samples that contain Mancozeb and copper oxychloride. Group 2 is formed by samples that present in their composition Mancozeb and Fosetyl-Al and finally groups 3 and 4 are composed of samples of Mancozeb co-formulated with Metalaxyl or Cymoxanil, respectively.

2.2. Reference procedure

The reference procedure employed for Mancozeb determination was a high performance liquid chromatography one based on the method of Gustaffson and Thompson [19] for determination of dithiocarbamates after a methylation process. Lo et al. [10] also used this methodology to determine and distinguish between different dithiocarbamates such as Propineb, Thiram and Mancozeb, Maneb and Zineb.

Ten to twenty milligrams sample were weighted inside a 100 ml beaker and 50 ml of 0.25 M EDTA in 0.45 M sodium hydroxide (pH 9.5–9.6) were added (the pH of the EDTA-sodium hydroxide solution should not be lower than 9.5 in order to obtain an efficient transformation of the dithiocarbamate to the water-soluble complex in 10 min) and stirred during 10 min. The EDTA extracts were filtered through a Whatman 42 (Brentford, Middlesex, UK), 2.5 μm pore size cellulose filter paper. The extraction beaker and the filter were rinsed with 20 ml water. The pH of the solution was adjusted to 6.5–8.5 by addition of 8 ml of HCl (2 M) and 5 ml of aqueous tetrabutylammonium hydrogen sulfate solution (0.4 M). The mixture was shaken in a separatory funnel for 5 min with 30 ml of methyl iodide (0.05 M) in chloroform:hexane 3:1. The organic phase was collected and the aqueous phase was rinsed with 10 ml of methyl iodide solution. Both organic phases were combined and concentrated by rotary evaporation at 30 °C after the addition of 5 ml of 1,2-propanediol in chloroform (20%, v/v). The residue was transferred to a 10 ml volumetric flask and diluted to the volume with methanol. After manual stirring 0.5 g of the solution were diluted to 10 g with methanol and 20 μl of this solution were directly injected in a 1:1 acetonitrile:water mobile phase of 1 ml min^{-1} carrier flow and Mancozeb determined, in the isocratic mode, by absorbance measurements at 272 nm. Area values of the chromatogram peaks obtained at 9.3 min for samples were interpolated in an external calibration line established from five standard solutions of Mancozeb containing up to 92.5 mg l^{-1}.

Additionally, samples of group 2 that contains Fosetyl-Al, were previously mixed with 50 ml slightly hot water (60 °C)

to solve this active ingredient and to avoid its interference in the determination. After that, the slurry was centrifuged during 3 min at 3000 rpm and the procedure continued by the aforementioned way.

Samples of group 1 cannot be analyzed by using the selected methodology due to copper oxychloride interferences. So, values provided by the manufacturer were taken as reference for data evaluation.

2.3. PA-FTIR procedure

Untreated samples were placed in the standard stainless steel holder of 1 cm i.d. and 3.7 mm height. The cell was purged for 5 min by helium to provide a CO_2 and moisture free environment. The spectra were collected with a nominal resolution of 4 cm^{-1}, accumulating 25 scans per spectra and with a mirror velocity of 2.2 kHz. A carbon black reference was used to collect the corresponding reference spectrum for spectra-intensity normalization.

The PLS models were built using nine external standards prepared by mixing different amounts of Kaolin and Mancozeb with concentrations ranging between 5.43 and 88.10% (w/w), as calibration set.

A hierarchical cluster analysis was made in order to evaluate the similarity of samples in terms of their PAS-FTIR spectra and to assess the number of characteristic subsets in which the available samples could be divided. Four different sample groups were obtained corresponding to the samples classified attending the co-formulated active ingredients.

For samples of group 1 containing Copper oxychloride, the information in the spectral ranges from 1543 to 1474 and 1390 to 1269 cm^{-1} was employed. For group 2, which contains Fosetyl-Al the range between 3334 and 3211 cm^{-1} corrected with a single point baseline located at 3055 cm^{-1} was used. For samples of group 3 co-formulated with Metalaxyl the information in the spectral range from 1543 to 1474 cm^{-1} was used to determine Mancozeb. Finally, the range between 1456 and 1306 cm^{-1} was used for Mancozeb determination in samples of group 4, which contain Cymoxanil.

The PLS factors used for Mancozeb determination depend on the PLS model employed. So 3, 2, 2 and 3 factors were used for Mancozeb determination in commercially available pesticides of groups 1, 2, 3 and 4, respectively.

3. Results and discussion

3.1. PAS spectra of Mancozeb

Fig. 1 shows the PAS-FTIR spectra, in the wavenumber region from 3600 to 800 cm^{-1}, of a 20% (w/w) Mancozeb standard and different commercial samples of agrochemicals. The spectra of standard and sample present the main absorption bands corresponding to the Mancozeb molecule, and in addition, sample spectra also present characteristic absorption bands of the other active ingredients present in the formulations; copper oxychloride in group 1, Fosetyl-Al in group 2, Metalaxyl in group 3 and Cymoxanil in group 4.

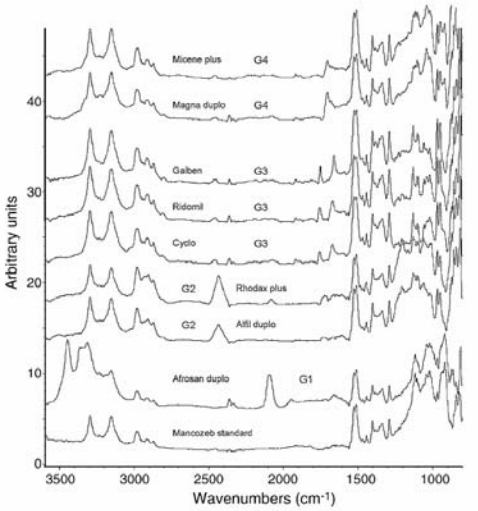

Fig. 1. PAS-FTIR spectra of a 20% (w/w) Mancozeb standard diluted with kaolin and nine commercial samples. Afrosan duplo belongs to group 1 (containing Mancozeb and Copper oxychloride), Alfil duplo and Rhodax plus are from group 2 (formulated with Mancozeb and Fosetyl-Al), Cyclo, Ridomil and Galben belongs to group 3 (containing Mancozeb and Metalaxyl) and Magna duplo and Micene plus are from group 4 (formulated with Mancozeb and Cymoxanil). *Note*: Spectra were shift on the *y*-axis to clearly show their bands. Instrumental conditions: 25 scans, 4 cm^{-1} nominal resolution and 2.2 kHz mirror speed.

The bands located at 1528 and 1512 cm^{-1}, are due to the amide II band in CSNH structures and seems to be free from matrix interferences and thus could be useful for Mancozeb determination in pesticide formulations. Other less intense absorption bands are located at 1402, 1335, 1287 1039 and 968 cm^{-1} due to CNH stretching-bending, CNH stretch-open, C=S and CNC stretching and NCS deformation, respectively [20].

3.2. Effect of measurement conditions

A monoparametric study was made to evaluate the effect of the instrumental variables, such as nominal resolution, scan velocity and number of cumulated scans on the signal to noise ratio and acquisition time of spectra. The signal to noise ratio was established as the area, between 1535 and 1501 cm^{-1} (corrected with a baseline defined between 1589 and 1481 cm^{-1}) of a 20% (w/w) Mancozeb standard divided by the noise obtained, in the aforementioned region, for a blank spectrum, obtained for the black carbon reference in the same conditions used for Mancozeb measurements.

Nominal resolution was varied between 2 and 8 cm^{-1} and, as can be seen in Fig. 2, values higher than 4 cm^{-1} of nominal resolution cause the deformation of the absorption bands and the loss of spectral information. So, a nominal resolution of 4 cm^{-1}

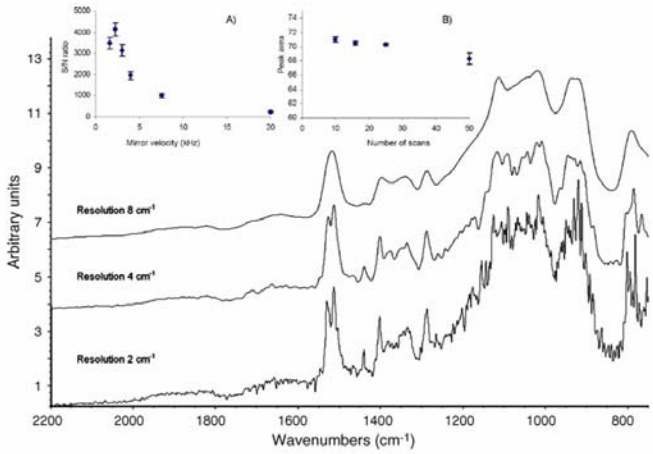

Fig. 2. Effect of the experimental variables on the PAS-FTIR signal of a 20% (w/w) Mancozeb standard, accumulating 25 scans per spectrum. *Note*: Spectra were shift on the *y*-axis to clearly show their bands using 2, 4 and 8 cm^{-1} nominal resolution, respectively. Inset A: Effect of the mirror speed on the signal to noise ratio for the Mancozeb standard. Inset B: Effect of the number of cumulated scans on the repeatability of three measurements of the peak area of the Mancozeb standard.

was selected and provided a signal to noise ratio higher than that obtained with 2 cm^{-1} and a low acquisition time.

The scan velocity (mirror velocity) of the interferometer was modified between 1.6 and 20 kHz to select the most appropriate conditions of measurement. As can be seen in the inset A of Fig. 2, a scan velocity of 2.2 kHz provides the highest signal to noise ratio and an acceptable acquisition time of 96 s.

The number of cumulated scans per spectra was also tested, being varied between 10 and 50. As can be seen in the inset B of Fig. 2, the highest precision of the peak area measured between 1535 and 1501 cm^{-1}, with a two points baseline established from 1589 to 1481 cm^{-1}, was obtained when 25 scans were accumulated. So, 25 cumulated scans per spectrum were selected, as this value is a good compromise between sensitivity and measurement throughput.

3.3. Hierarchical cluster analysis

In hierarchical cluster analysis, the similarity between samples is established using the distance concept, calculated from mathematical relationships of numerical properties of the samples [21]. In a successive procedure, each sample was linked to the closest sample or group of samples and a characteristic distance was used to describe this union. The distance between groups of samples can be evaluated in different ways and is the main difference among common linkage methods. These groups are called classes or clusters [22]. The group formation can be represented graphically in a dendrogram (see Fig. 3), which shows the different groups at a normalised or rescaled distance of each kind of samples from the others, when it is read from right to left. For the cluster analysis the region between 3550 and 706 cm^{-1} with no pre-processing was used. The algorithm used was the Standard method, which calculates the Euclidean distance between the test spectrum and the reference spectrum. As can be seen in Fig. 3, four groups can be established as a function of the differences in the PAS-FTIR spectra, those groups being based on the composition of samples regarding the presence of additional active ingredients.

3.4. PLS modelization of Mancozeb

An external monoparametric calibration was tested for the determination of Mancozeb in commercial formulations by PA-FTIR spectrometry. The use of the peak area values between 1542 and 1474 cm^{-1} employing two points baseline correction located between 2224 and 1474 cm^{-1} was assayed but provide

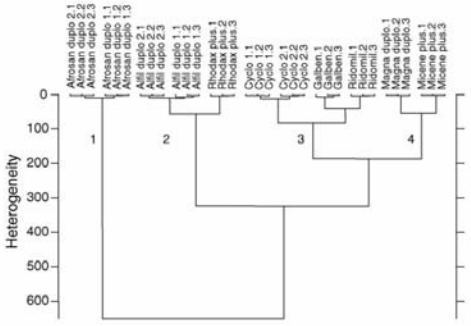

Fig. 3. Dendrographic classification of agrochemical samples using the Euclidean distance of the PAS-FTIR spectra and applying the Ward linkage method. *Note*: For the cluster analysis the region between 3550 and 706 cm^{-1} with no pre-processing was used. The algorithm used was the Standard method.

Table 1
Analytical features of PAS-FTIR determination of Mancozeb in commercial formulations using different PLS calibration models.

Region (cm^{-1})	Baseline correction (cm^{-1})	R^2[a]	Number of factors[b]	RMSEC[c]	E_r (%, w/w)[d]
Group 1					
3334–3080	3055	0.999	2	1.45	179
1543–1269	None				
1543–1269	None	0.998	2	1.65	22
1390–1269	None	0.9995	3	0.9	4.6
1390–1269	None	0.9992	3	1.1	3.1
1543–1474	None				
Group 2					
3334–3080	3055	0.999	2	1.45	10
1543–1269	None				
1543–1269	None	0.998	2	1.65	32
1543–1474	None	0.9990	2	1.3	2.6
3334–3211	3055	0.997	2	2.1	2.1
3334–3211	3055	0.9996	2	0.81	4.1
1543–1474	None				
Group 3					
3334–3080	3055	0.999	2	1.45	4.4
1543–1269	None				
1543–1269	None	0.998	2	1.65	4.7
1543–1474	None	0.9991	2	1.3	2.5
Group 4					
3334–3080	3055	0.999	2	1.45	10
1543–1269	None				
1543–1269	None	0.998	2	1.65	11
1456–1306	None	0.9996	3	0.812	4.4

[a] R^2 is the correlation coefficient of the regression line between predicted and actual values of analyte concentration in the calibration set.
[b] The number of factors was chosen in order to obtain the minimum PRESS.
[c] Root mean square calibration error for a cross-validation.
[d] Mean accuracy error (%) found from the comparison with results obtained by HPLC.

a very poor linearity and relative errors of the order of 5, 18, 36 and 27% for samples of groups 1, 2, 3 and 4, respectively. So, the possibility to use a multivariate calibration technique, such as the partial least squares (PLS) for the treatment of the PAS-FTIR data was evaluated.

Table 1 shows the analytical features of a PLS-PAS-FTIR model, based on the use Mancozeb standards prepared by mixing the pure compound with kaolin, as calibration set, for its determination in pesticide formulations as a function of the use of different spectral regions and baseline criteria. Mean centering spectra data pre-treatment was employed to eliminate common spectral information.

The leave one out cross-validation procedure was used to obtain the best number of latent variables for each formulation using the predicted residual error sum of squares (PRESS). It has been also indicated the R^2 value of the calibration model, the root mean square error of calibration (RMSEC) and the mean accuracy errors have also included and compared with data predicted by PLS-PAS-FTIR with HPLC data.

As can be seen, when a single model was used for Mancozeb determination, using the spectral information in the range from 3334 to 3080 cm^{-1} and from 1543 to 1269 cm^{-1}, mean accuracy errors of the order of 179, 9.9, 4.4 and 9.7% (w/w) were obtained for the different groups. The aforementioned data clearly show that the presence of different active ingredients co-formulated with Mancozeb strongly affect the prediction capability of the

Table 2
Determination of Mancozeb in pesticide formulations by HPLC-UV and PAS-FTIR procedures

Sample	HPLC-UV (%, w/w)[a]	PAS-FTIR (%, w/w)[a]	% E_r[b]
Group 1			
Afrosan duplo 1	17.5[c]	17.1 ± 0.5	−2.3
Afrosan duplo 2	17.5[c]	16.8 ± 0.4	−3.9
Group 2			
Alfil duplo 1	36.3 ± 0.8	35.9 ± 1.3	−1.0
Alfil duplo 2	34.2 ± 1.0	33.1 ± 1.4	−3.3
Rhodax plus	35 ± 0.7	34.3 ± 1.0	−2.0
Group 3			
Cyclo 1	78.1 ± 0.7	75.7 ± 0.4	−3.1
Cyclo 2	67.0 ± 0.9	71.4 ± 0.4	6.5
Galben	76.2 ± 1.6	74.7 ± 1.3	−2.8
Ridomil	74.0 ± 1.4	74.0 ± 0.3	−0.003
Group 4			
Magma duplo	39.7 ± 0.5	37.0 ± 0.7	−6.7
Micene plus	50.9 ± 1.7	50.1 ± 0.3	−1.5

[a] Concentration values are the average of two independent analysis measured in triplicate ± the corresponds standard deviation of the six values found.
[b] Mean accuracy error (%) found from the comparison with results obtained by HPLC.
[c] Data reported by the producer.

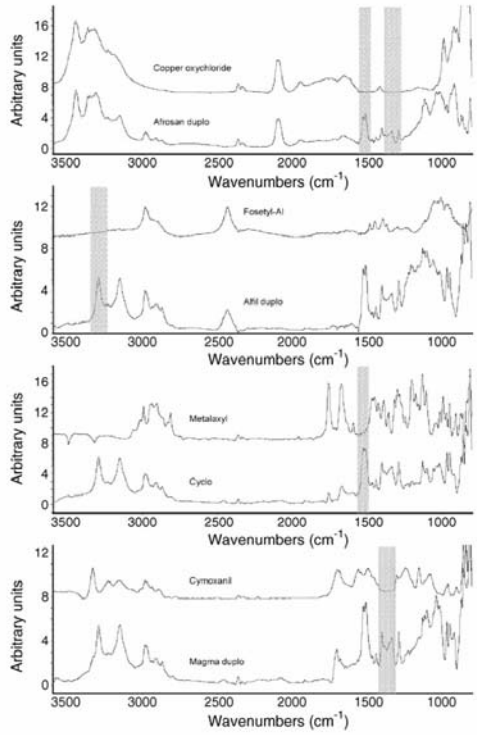

Fig. 4. PAS-FTIR spectra of each group of samples and active ingredient co-formulated with Mancozeb. *Note*: Regions selected for the PLS calibration models are indicated for each type of samples.

PLS model, due to the spectral overlapping of the bands provided by these latter compounds (see Fig. 4).

So, one model was constructed for each group of samples selected from the hieralchical cluster analysis. As can be seen in the table, the best results, in terms of accuracy, were obtained for different regions of the spectra (see Fig. 4). The mean accuracy errors found were 3.1, 2.1, 2.5 and 3.0% for groups 1, 2, 3 and 4, respectively.

3.5. Analysis of commercially available formulations

PAS-FTIR methodology, proposed in this paper, provided statistically comparable results with those obtained by HPLC reference method or manufacturer values (group 1) for Mancozeb analysis in commercial formulations. As can be seen in Table 2, in all cases experimental t values were lower than 1.812 for a paired two tails t-test, for a probability level of 95% and 10 degrees of freedom (six data found by each method minus two parameters).

On the other hand, the regression between all the average values of the data found for commercial samples assayed by the PLS-PAS-FTIR and chromatography provided an equation of $C_{\text{PAS-FTIR}} = (-0.6 \pm 1.4) + (1.00 \pm 0.03) C_{\text{HPLC}}$ with $r = 0.997$. Statistically the aforementioned regression line presents slope and intercept values comparable with 1 and 0, respectively, which provides evidence that the developed procedure does not present constant nor relative errors, as compared with the reference method.

4. Conclusion

The main advantages offered by the developed vibrational procedure are: (i) a strong reduction of the volume of reagents consumed and waste generated as compared with HPLC, and (ii) the increase of the measurement frequency from $2\,h^{-1}$ in the case of HPLC to $45\,h^{-1}$ for PAS-FTIR.

It can be concluded that the proposed spectrometric methodology is a fast, without sample pre-treatment and environmentally friendly alternative to the classic reference and chromatographic procedures for the quality control of Mancozeb in commercial formulations in the agrochemical sector. Additionally, the developed PAS-FTIR methodology could analyze the different types of samples without matrix interferences and using mixtures of Mancozeb and Kaolin as a calibration set.

Acknowledgements

The authors acknowledge the financial support of the Ministerio de Educación y Ciencia of Spain (Project CTQ2005-05604) and S. Armenta the FPU Grant (Ref. AP2002-1874).

References

[1] Extension Toxicology Network (EXTOXNET) Pesticide Information Profiles. Cornell University, Oregon State University, University of Idaho, University of California-Davis and Institute for Environmental Toxicology, Michigan State University, 1996. http://ace.orst.edu/info/extoxnet/pips/ghindex.html.
[2] I.R. Edwards, D.G. Ferry, W.A. Temple, Fungicides and related compounds, in: W.J. Hayes, E.R. Laws (Eds.), Handbook of Pesticide Toxicology, Academic Press, New York, 1991.
[3] EPA: Pesticides-2000/2001 Pesticide Sales and Usage Report Biological and analysis division Office of pesticide programs, Washington, 2002. http://www.epa.gov/oppbead1/pestsales/01pestsales/sales2001.html.
[4] C. de Liñan, Vademecum de productos fitosanitarios y nutricionales, Ediciones Agrotécnicas S.L., Madrid, Spain, 2000.
[5] E.D. Caldas, M.H. Conceiçao, M.C.C. Miranda, L.C.K.R. de Souza, J.F. Lima, J. Agric. Food Chem. 49 (2001) 4521.
[6] A. Zena, P. Conte, A. Piccolo, Fresenius Environ. Bull. 8 (1999) 116.
[7] M. Bekbolet, Chim. Acta Turc. 18 (1990) 53.
[8] H. van-Lishaut, W. Schwack, J. AOAC. Int. 83 (2000) 720.
[9] R.J. Cassella, V.A. Salim, S. Garrigues, R.E. Santelli, M. de la Guardia, Anal. Sci. 18 (2002) 1253.
[10] C.C. Lo, M.H. Ho, M.D. Hung, J. Agric. Food Chem. 44 (1996) 2720.
[11] S. Armenta, S. Garrigues, M. de la Guardia, Talanta 65 (2005) 971.
[12] J.F. McClelland, R.W. Jones, S.J. Bajic, FTIR photoacoustic spectrometry, in: J.M. Chalmers, P.R. Griffiths (Eds.), Handbook of Vibrational Spectroscopy, John Wiley & sons Ltd, Chichester, 2002.
[13] M.W.C. Wahls, E. Kentta, J.C. Leyte, Appl. Spectrosc. 54 (2000) 214.
[14] S. Bjarnestad, O. Dahlman, Anal. Chem. 74 (2002) 5851.

[15] J. Irudayaraj, H. Yang, S. Sakhamuri, J. Mol. Struct. 606 (2002) 181.
[16] S. Sivakesava, J. Irudayaraj, J. Sci. Food Agric. 80 (2000) 1805.
[17] T. Schmid, C. Helmbrecht, U. Panne, C. Haisch, R. Niessner, Anal. Bioanal. Chem. 375 (2003) 1124.
[18] S. Armenta, G. Quintas, S. Garrigues, M. de la Guardia, Trac-Trends Anal. Chem. 24 (2005) 772.
[19] K.H. Gustaffson, R.A. Thompson, J. Agric. Food Chem. 29 (1981) 729.
[20] D. Lin-Vien, N.B. Colthup, W.G. Fateley, J.G. Grasselli, Infrared and Raman Characteristic Frequencies of Organic Molecules, Academic Press, London, 1991.
[21] K.R. Beebe, R.J. Pell, M.B. Seasholiz, Chemometrics: A Practical Guide, John Wiley & Sons, New York, 1998.
[22] J. Moros, F.A. Iñón, S. Garrigues, M. de la Guardia, Anal. Chim. Acta 538 (2005) 181.

RAMAN SPECTROSCOPY

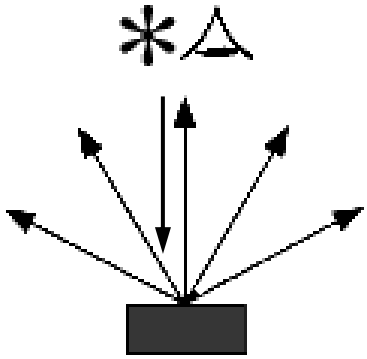

Determination of Cyromazine in pesticide commercial formulations by vibrational spectrometric procedures

Sergio Armenta, Guillermo Quintás, Salvador Garrigues and Miguel de la Guardia
[a]*Department of Analytical Chemistry, Universitat de València. Edifici Jeroni Muñoz, 50th Dr Moliner, 46100 Burjassot, Valencia, Spain.*

Analytical Chimica Acta 524 (2004) 257-264.

Impact factor of this journal (2004): 2.588
Source: Journal citation reports ISI Web of Knowledge, 2004.

Available online at www.sciencedirect.com
SCIENCE DIRECT®
Analytica Chimica Acta 524 (2004) 257–264
ANALYTICA CHIMICA ACTA
www.elsevier.com/locate/aca

Determination of cyromazine in pesticide commercial formulations by vibrational spectrometric procedures

Sergio Armenta, Guillermo Quintás, Salvador Garrigues*, Miguel de la Guardia

Department of Analytical Chemistry, Faculty of Chemistry, University of Valencia, Edifici Jeroni Muñoz, 50th Dr. Moliner, 46100 Burjassot, Valencia, Spain

Received 5 November 2003; received in revised form 19 January 2004; accepted 24 February 2004
Available online 24 April 2004

Abstract

Two vibrational spectrometry-based methodologies were developed for Cyromazine determination in solid pesticide formulations: a Fourier transform infrared (FTIR) procedure, based on the extraction of Cyromazine by CH_3OH and direct determination in the extracts by peak height measurement at 1622 cm^{-1} corrected using a baseline defined at 1900 cm^{-1}, and a FT-Raman determination, made directly on the powdered solid products using standard chromatographic glass vials as sample cells and measuring the Raman intensity between 633 and 623 cm^{-1} for a baseline established between 663 and 601 cm^{-1}. The sensitivity obtained was 0.01631 absorbance g^{-1} mg for FTIR determination and 2.23 area values g^{-1} g for FT-Raman. A repeatability of 0.2 and 0.4% as relative standard deviation (R.S.D.) and a limit of detection of 0.2 and 0.8% (w/w) were obtained for FTIR and FT-Raman determination, respectively.

FTIR determination provides a sampling frequency of 60 h^{-1}, higher than the FT-Raman and LC ones, which were 25 and 6 h^{-1}, respectively. On the contrary FT-Raman reduces to the minimum the reagents consumption and waste generation, also avoiding sample handling and contact of the operator with the pesticide. Results obtained by both developed procedures were statistically comparable with those found by a reference liquid chromatography procedure. It can be concluded that the proposed methods are appropriate for quality control in pesticide commercial formulations.

Keywords: Cyromazine; Pesticide formulations; FTIR; FT-Raman; Solid samples

1. Introduction

Cyromazine, *N*-cyclopropyl-1,3,5-triazine-2,4,6-triamine, is an insect growth regulator used as a chitin synthesis inhibitor for fly control in cattle manure, field crops, vegetables and fruits [1]. It is characterized by a rapid stiffening of the cuticle, and it seems to have more specificity than the benzoylphenylureas, affecting mostly larvae of Diptera [2]. Cyromazine is slightly toxic by ingestion, with reported oral LD_{50} values of 3387 mg^{-1} kg in rats [3].

Cyromazine formulations are commercially available as wettable powder with concentrations between 25 and 75% (w/w). On the other hand, Cyromazine is not co-formulated with other pesticides.

Cyromazine has been determined at trace levels in water samples by luminescence bioassays [4,5] and by liquid chromatography with UV detection (LC–UV) [6,7], in soils by HPLC–UV [8,9] and in crops by gas chromatography with mass spectrometry detection (GC–MS) [10,11] and by thermolysis–atmospheric pressure ionization tandem mass spectrometry [12].

One of the main drawbacks of the use of vibrational spectrometry for pesticide analysis is its rather low sensitivity as compared with that achieved by chromatography. However, it has been evidenced the applicability of Fourier transform infrared (FTIR) spectrometry for the determination of Carbaryl [13], Buprofezin [14], Fluometuron [15], Folpet and Metalaxyl [16] and Chlorpyriphos [17] in pesticide formulations providing fast and reliable alternative methods of analysis for this kind of samples. One of the useful features of Raman spectroscopy concerns the possibility to carry out direct measurements on solids. In spite of this, Raman spectroscopy has been scarcely used for the qualitative and

* Corresponding author. Tel.: +34-96-354-3158; fax: +34-96-354-4838.
E-mail address: salvador.garrigues@uv.es (S. Garrigues).

0003-2670/$ – see front matter © 2004 Elsevier B.V. All rights reserved.
doi:10.1016/j.aca.2004.02.063

quantitative analysis of active principles in commercial pesticide formulations there being the few precedents related to the determination of Diazinon [18] and Fenthion [19] in liquid solutions.

On the other hand, the development of surface-enhanced Raman scattering (SERS) increases dramatically the sensitivity of Raman measurements and provided new possibilities on the analysis of pesticides like chlorinated [20] and organophosphorus [21] pesticides.

Raman and surface-enhanced Raman spectra of Cyromazine have been reported [22], but no application of Raman or FTIR spectrometry have been described previously for the determination of Cyromazine.

The main objective of this work has been the development of fast and environmentally friendly methodologies for the determination of Cyromazine in agrochemical formulations employing vibrational spectroscopy like FTIR or FT-Raman, and avoiding the use of a chlorinated solvent.

2. Experimental

2.1. Apparatus and reagents

A Nicolet (Madison, WI, USA) Magna 750 FTIR spectrometer, equipped with a temperature-stabilized deuterated tryglycine sulphate (DGTS) detector, was employed for infrared measurements, using a micro-flow cell with ZnSe and CaF_2 windows and a pathlength of 0.10 mm. The equipment employs the 2.1 version of the OMNIC software developed by Nicolet Corporation, for the acquisition and processing of the FTIR absorbance data.

A Brücker (Bremen, Germany) RFS 100/S FT-Raman spectrometer equipped with a liquid cooled Ge detector and a 2 W maximum power Nd:YAG laser, that emits at 1064 nm, was employed to obtain FT-Raman spectra of solid samples, using 2 ml standard glass chromatographic vials (12 mm × 32 mm) as sample cells.

A Hewlett-Packard (Palo Alto, CA) HPLC Series 1050 high performance liquid chromatograph, equipped with a Kromasil C-18, 250 mm × 4.6 mm i.d. and 5 μm particle diameter column, and a variable wavelength UV-Vis detector was also employed for the analysis of herbicide formulations, being employed this methodology as a reference for the validation of FTIR and Raman determinations. Control of chromatograph and data acquisition was carried out using the Hewlett-Packard HPLC 2D Chemstation software package.

A J.P. Selecta (Barcelona, Spain) ultrasonic water bath was used to carry out the pesticide extraction with CH_3OH for FTIR determinations and HPLC validation.

Cyromazine PESTANAL® reagent grade standard (99.9%, w/w) was supplied by Fluka (Buchs, Switzerland). Sodium chloride, reagent grade (99.8%, w/w), HPLC grade (99.99%, w/w) methanol and (99.85%, w/w) acetonitrile supplied by Scharlau (Barcelona, Spain) and phosphoric acid, reagent grade, supplied by Sigma–Aldrich (Madrid, Spain) were employed for the preparation of samples and standards.

Cyromazine wettable powder commercial pesticide formulations were obtained directly from the Spanish market. From different commercial presentation units representative laboratory samples were taken and stored in glass vials after their homogenisation by grinding.

2.2. HPLC reference procedure

Twenty milligrams of sample was accurately weighted inside a 25 ml volumetric flask and diluted to volume with CH_3OH, being sonicated for 5 min in an ultrasonic water bath to extract Cyromazine from the matrix 0.5 ml of the extract was diluted to 25 ml, and 5 μl of this solution, previously passed through a 0.22 μm nylon filter was directly injected in a 1:3 acetonitrile:(10 mM) phosphate buffer at pH 3 mobile phase of 1 ml min^{-1} carrier flow and Cyromazine was determined in the isocratic mode by measurement the area of the peak with a retention time of 6.50 min from the chromatogram obtained at 230 nm for samples which were interpolated in an external calibration line established from 12 methanolic solutions of Cyromazine (with a concentration range from 7.52 to 22.56 mg l^{-1}) processed and measured under the same chromatographic conditions.

2.3. FTIR procedure

Twenty-five milligrams of sample were accurately weighed and diluted with 4 g of CH_3OH. The mixture was sonicated for 5 min in an ultrasonic water bath. After that, the sample extract was passed through a 0.22 μm nylon filter and then introduced in the FTIR measurement cell by using a peristaltic pump. The spectra were obtained from 4000 to 800 cm^{-1} in the stopped-flow mode at 4 cm^{-1} nominal resolution and accumulating 25 scans per spectrum versus a background of the cell filled with the solvent.

A calibration line was established for Cyromazine by measuring peak height values at 1622 cm^{-1} corrected using a baseline defined at 1900 cm^{-1}. Sample absorbance spectra measured in the same conditions as standards were interpolated in the Cyromazine calibration line.

2.4. FT-Raman procedure

Two hundred milligrams of commercial sample was mixed with 100 mg of sodium chloride. The mixture was ground and homogenized for 5 min in an agate mortar, before to be introduced in a chromatographic glass vial. FT-Raman spectra were obtained directly for the sample confined in the glass vial, at 4 cm^{-1} nominal resolution and accumulating 25 scans per spectrum. The Nd:YAG laser power employed was fixed at 750 mW. A Blackman-Harris 4 apodization function, a scan velocity of 1.0 (2.2 KHz), a zero filling factor of 2 and an aperture of 10 mm were also employed for the acquisition of spectra.

Calibration was achieved with a solid Cyromazine standard diluted with sodium chloride at levels, from 32.2 to 92% (w/w). For quantitative purposes peak area values between 623 and 613 cm^{-1} Raman shift, corrected using a baseline defined between 663 and 601 cm^{-1}, were used.

3. Results and discussion

3.1. FTIR transmittance spectrum of Cyromazine

Fig. 1 shows the absorbance spectra, in the range 2000–1000 cm^{-1}, of a Cyromazine standard methanolic solution of 3.70 $mg\,g^{-1}$ and that of a insecticide sample extract, both obtained using a background established with the cell filled with CH_3OH. As can be seen in this figure, the spectra of both sample and standard present at the same wavenumber the main bands, which evidences the little or no solubility in methanol of other matrix components.

The Cyromazine molecule presents three characteristic absorption bands in the mid IR, located at 1622, 1586 and 1566 cm^{-1}, due to NH in-plane bending, triazine stretching and C–N stretching, respectively, [23] and so, these bands were assayed for the quantification of Cyromazine.

3.2. Effect of FTIR measurement conditions on Cyromazine determination

The effect of the number of accumulated scans and the nominal resolution employed for spectra acquisition were evaluated in order to improve the measurement conditions. The number of accumulated scans was modified from 5 to 50, and the nominal resolution varied from 2 to 16 cm^{-1}.

As can be seen in Fig. 2, for the peak at 1622 cm^{-1} and 25 cumulated scans per spectrum, the highest absorbance was obtained for a 2 cm^{-1} nominal resolution, but in these instrumental conditions noisy spectra were found. On the other hand, the 1.6% signal enhancement achieved with a 2 cm^{-1} resolution reduces to a 50% the sample throughput as compared with that obtained using a 4 cm^{-1} resolution. So, despite of the lost of sensitivity obtained as compared with 2 cm^{-1} it was selected a 4 cm^{-1} nominal resolution for further measurements in order to ensure a compromise between the sensitivity and the sample throughput.

The same criterion was employed for the selection of the number of accumulated scans. An increase in the number of accumulated scans also increases the signal-to-noise ratio. However, in order to obtain as faster as possible measurements 25 scans were selected for the determination of Cyromazine.

3.3. FTIR determination of Cyromazine

Table 1 summarizes the regression lines obtained for peak height or peak area measurements using different bands. In every case a, good linear fit was obtained with R^2 values >0.999. The precision, as relative standard deviation (R.S.D.), ranged between 0.2 and 1.3% independent of the use of peak height or peak area values, and the limit of detection obtained was between 0.2 and 0.7% for peak height and from 1.4 to 1.8% for area values, which are appropriate for Cyromazine determination in commercial pesticide formulations.

The best results were obtained when the band at 1622 cm^{-1} was used. It was selected the use of peak height measurements at 1622 cm^{-1} corrected with an horizontal baseline fixed at 1900 cm^{-1}, because the LOD and R.S.D. (%) obtained under these conditions were the lowest of the different possibilities tested.

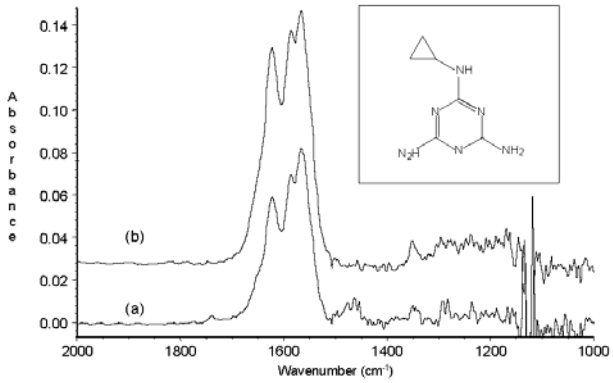

Fig. 1. FTIR spectra of Cyromazine: (a) 3.7 $mg\,g^{-1}$ Cyromazine standard in CH_3OH and (b) CH_3OH extract of a sample containing 4.1 $mg\,g^{-1}$ Cyromazine. *Inset*: Chemical structure of Cyromazine.

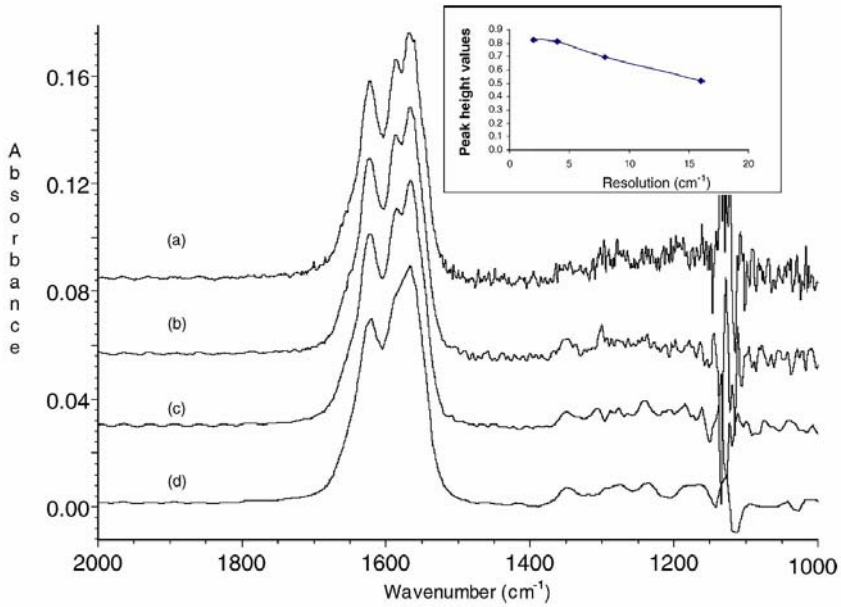

Fig. 2. Effect of the nominal resolution on peak height values of Cyromazine measured at 1622 cm^{-1} with a single point baseline established at 1900 cm^{-1}. Spectra of a Cyromazine standard of 3.7 $mg\,g^{-1}$ obtained accumulating 25 scans per spectrum registered at 2 cm^{-1} (a), 4 cm^{-1} (b), 8 cm^{-1} (c) and 16 cm^{-1} (d) nominal resolution.

3.4. FT-Raman spectra of Cyromazine

Fig. 3 shows the FT-Raman spectra of a solid Cyromazine standard diluted with sodium chloride (55.4%, w/w), a commercial fungicide with a Cyromazine concentration of 66.7% (w/w) and those of pure calcium carbonate and sodium chloride. The most intense bands in the Cyromazine FT-Raman spectra are those present at 1193, 628 and 350 cm^{-1} due to cyclopropyl ring breathing, triazine in-plane and asymmetric bending and *N*-cyclopropyl bending, respectively. Other less intense bands are those located at 1359, 1240, 984, 839 and 721 cm^{-1} due to NH in-plane bending, CH bending, cyclopropyl in-plane bending (984 and 839 cm^{-1}) and triazine in plane bending, respectively [22].

It must be also noticed that the band at 1087 cm^{-1} is due to the calcium carbonate and that sodium chloride provides an excellent non scattered FT-Raman spectrum.

All the eight main bands found for Cyromazine were assayed to determine this product in pesticide formulations by FT-Raman.

3.5. Measurement conditions

The effects of the number of accumulated scans and that of the nominal resolution employed for FT-Raman data

Table 1
Analytical features of the FTIR determination of Cyromazine using different bands and measurement modes

Measurement mode	Wavenumber (cm^{-1})	Baseline correction	Cyromazine calibration curve ($y = a + bC$ ($mg\,g^{-1}$))			R.S.D. (%)	LOD (%, w/w)
			$a \pm S_a$	$b \pm S_b$	R^2 ($n = 15$)		
Height	1622	1900	0.00017 ± 0.00009	0.01631 ± 0.00003	0.99994	0.2	0.2
Area	1627–1617		−0.004 ± 0.002	0.1860 ± 0.0006	0.9998	0.5	1.4
Height	1586		0.0003 ± 0.0005	0.0186 ± 0.0002	0.999	1.2	0.7
Area	1591–1581		0.000 ± 0.005	0.176 ± 0.002	0.999	1.0	1.8
Height	1566		0.0003 ± 0.0005	0.0227 ± 0.0002	0.999	1.3	0.2
Area	1571–1561		−0.003 ± 0.005	0.257 ± 0.002	0.999	0.5	1.4

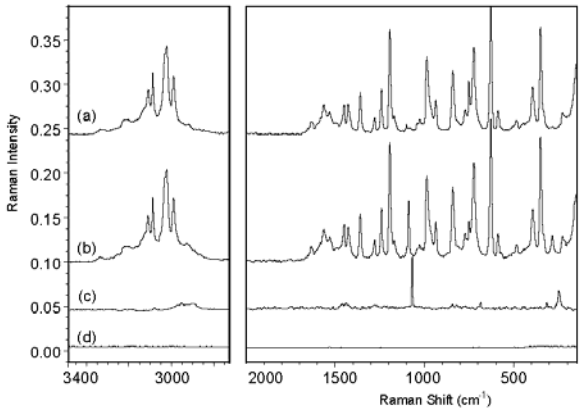

Fig. 3. FT-Raman spectra of a Cyromazine standard of 55.4% (w/w) diluted in sodium chloride (a), a commercial sample containing a concentration of 66.7% (w/w) of Cyromazine (b), calcium carbonate (c) and sodium chloride (d).

acquisition were evaluated. The number of accumulated scans was modified from 5 to 50, and the nominal resolution varied from 2 to 8 cm^{-1}.

As can be seen in Fig. 4, the best signal-to-noise ratio corresponds to the accumulation of 50 scans, but in order to ensure a compromise between measurement frequency and precision values, 25 accumulated scans were selected. On the other hand, it can be seen that the most intense signals were found for a 4 cm^{-1} nominal resolution.

The effect of the laser power on the peak area value between 633 and 623 cm^{-1} using a baseline correction between 663 and 601 cm^{-1} is shown in Fig. 5 in which it can be seen that the analytical signal increases on increasing the excitation laser power. However, if excitation power is too high, the sample may be excessively heated and it may thermally decompose. So, 750 mW was selected for further experiments.

In order to evaluate the effect of sample positioning changes and possible vial variations on the precision of

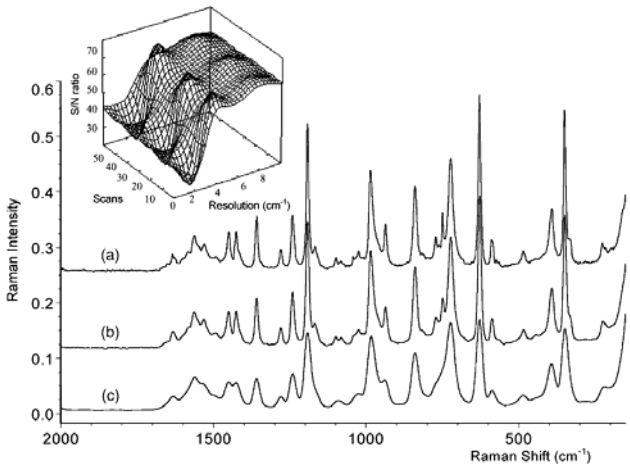

Fig. 4. Effect of the number of accumulated scans and nominal resolution on the signal-to-noise ratio of FT-Raman determination of Cyromazine. Data were obtained from the peak area values between 633 and 623 cm^{-1} of a standard containing 55.4% (w/w) Cyromazine. Experimental measurements were carried out with a laser power of 750 mW being spectra depicted those found for (a) 2 cm^{-1} (b) 4 cm^{-1} and (c) 8 cm^{-1} nominal resolution and 25 scans per spectra.

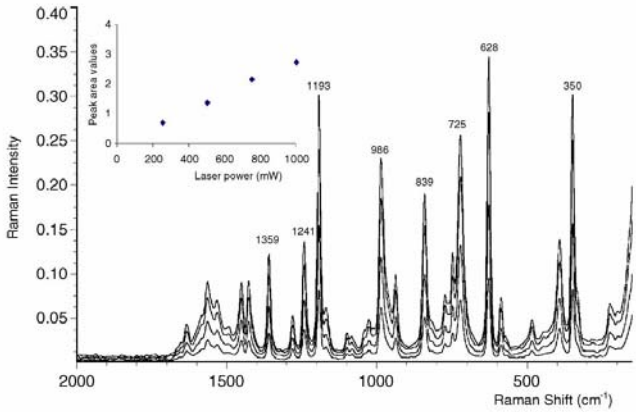

Fig. 5. Effect of the laser power on FT-Raman determination of Cyromazine. Inset: Peak area values were established between 633 and 623 cm^{-1} from the spectra of a Cyromazine standard of 55.4% (w/w) obtained accumulating 25 scans per spectrum at a nominal resolution of 4 cm^{-1}. The figure also includes the FT-Raman spectrum found in each case.

the measurements a Cyromazine standard was measured using two different vials and changing the vial position randomly four times. A relative standard deviation of 3.0% was found for measurements carried out on the same vial and 5.9% for the same sample into different vials thus showing that the direct FT-Raman measurements on solids confined in chromatography glass vials is appropriate to carry out the Cyromazine determination in commercial insecticides.

3.6. Selection of bands for Raman determination of Cyromazine

Searching for the best analytical performance of the FT-Raman determination of Cyromazine, different bands were considered, after also establishing the corresponding baseline with different criteria and both peak height and peak area measurements being considered. The obtained results are summarized in Table 2. It was found that the

Table 2
Analytical features of the FT-Raman determination of Cyromazine using different bands, baseline criteria and measurement modes

Measurement mode	Wavenumber (cm^{-1})	Baseline correction	Cyromazine calibration curve ($y = a + bC$ ($g\,g^{-1}$))			R.S.D. (%)	LOD (%, w/w)
			$a \pm S_a$	$b \pm S_b$	R^2 ($n = 12$)		
Height	1359	1388–1331	−0.0008 ± 0.0003	0.0894 ± 0.0006	0.9995	0.8	1.4
Area	1364–1354		−0.006 ± 0.002	0.724 ± 0.004	0.9997	0.5	1.9
Height	1241	1262–1216	−0.0010 ± 0.0005	0.0967 ± 0.0009	0.9991	1.6	1.1
Area	1246–1236		−0.006 ± 0.003	0.783 ± 0.006	0.9994	0.9	1.0
Height	1193	1215–1176	−0.0009 ± 0.0007	0.219 ± 0.001	0.9997	0.4	0.1
Area	1198–1188		−0.009 ± 0.004	1.675 ± 0.008	0.9998	0.8	0.9
Height	986	1006–900	−0.0005 ± 0.0007	0.159 ± 0.001	0.9994	0.8	0.2
Area	991–981		−0.003 ± 0.007	1.58 ± 0.01	0.9994	0.6	0.02
Height	839	873–796	−0.0018 ± 0.0009	0.138 ± 0.002	0.999	1.9	0.4
Area	844–834		−0.016 ± 0.008	1.18 ± 0.01	0.999	1.5	0.2
Height	725	789–659	−0.002 ± 0.001	0.186 ± 0.002	0.999	0.6	0.1
Area	730–720		−0.017 ± 0.009	1.62 ± 0.02	0.999	0.4	0.3
Height	628	663–601	−0.0002 ± 0.0009	0.281 ± 0.002	0.9996	0.7	1.2
Area	633–623		0.000 ± 0.007	2.23 ± 0.01	0.9997	0.4	0.8
Height	350	369–311	−0.005 ± 0.002	0.241 ± 0.004	0.997	1.0	0.1
Area	355–345		−0.03 ± 0.01	1.73 ± 0.03	0.998	0.9	0.7

Table 3
Recovery studies on Cyromazine added to formulate samples

FT-Raman				FTIR			
Cyromazine added (%, w/w)	Cyromazine found (%, w/w)	Recovery (%)	Mean recovery ± s	Cyromazine added (mg g^{-1})	Cyromazine found (mg g^{-1})	Recovery (%)	Mean recovery ± s
16.04	15.89 16.52 16.21	101 ± 3	101.5 ± 2.0	3.52	3.61 3.58 3.56	101.7 ± 0.8	100.6 ± 1.4
21.33	21.23 22.34 21.79	102 ± 4		4.36	4.42 4.39 4.41	100.9 ± 0.4	
58.46	60.61 59.98 60.30	103.1 ± 0.8		4.99	5.06 5.08 5.02	101.3 ± 0.7	
64.22	64.27 63.61 63.94	99.6 ± 0.7		6.91	6.79 6.84 6.80	98.6 ± 0.4	

band at 628 cm^{-1} provides the best sensitivity. However, the lowest limit of detection was found working with the area values at the band of 986 cm^{-1}. Finally peak area values from between 633 and 623 cm^{-1} corrected with a baseline established between 663 and 601 cm^{-1} were selected in order to improve both the analytical sensitivity and the precision of measurements (a R.S.D. value of 0.4% was found working with the aforementioned conditions which is better than that found working with the band at 986 cm^{-1}).

3.7. Analytical figures of merit of the developed procedures

In order to evaluate the accuracy of both vibrational procedures assayed a recovery study was carried out on spiked samples with known amounts of Cyromazine added to commercial pesticide samples, from 3.52 to 6.91 mg g^{-1} and 16.04 to 64.22% (w/w), for the FTIR and FT-Raman determination, respectively. Using an external calibration for FTIR and FT-Raman approaches, as can be seen in Table 3, the mean recovery values found were 101 ± 1% and 101 ± 2%, in each case, thus indicating the absence of systematic errors in the two developed procedures.

4. Stability of samples prepared for FT-Raman analysis

Three samples were analysed, using the same calibration set, after room temperature storage inside the glass vials for 3 months. The data found by FT-Raman were 76.3 ± 1.2%, 76.9 ± 0.7% and 76.2 ± 0.6% (w/w) which compare well with these obtained previously (75.6 ± 0.9, 76.4 ± 0.6 and 75.8 ± 0.9, respectively) for a probability level of 95%. So, it can be concluded that the FT-Raman procedures not only provides a fast and environmentally friendly alternative for Cyromazine determination but also offer an excellent way for storing in a safe way, the materials analysed in order to be able to verified the determinations after a period of time for at least 3 months.

5. Comparison between LC and vibrational methods

For the validation of the vibrational methodologies developed in this study, three different pesticide formulation samples were analysed by FTIR, FT-Raman and LC and results obtained are summarized in Table 4. Both vibrational methods provide statistically comparable results to those found

Table 4
Cyromazine concentrations found in three commercially available formulations by the two developed vibrational procedures and statistically compared with those obtained by a reference LC method

	$S^a_{HPLC} = (1 \pm 1) + (18.49 \pm 0.07)C_{HPLC}$		$S_{FTIR} = (0.00017 \pm 0.00009) + (0.01631 \pm 0.00003)C_{FTIR}$				$S_{FT\text{-}Raman} = (0.000 \pm 0.007) + (2.23 \pm 0.01)C_{FT\text{-}Raman}$			
	HPLC	R.S.D. (%)	FTIR	R.S.D. (%)	E_r (%)	t_{exp}	FT-Raman	R.S.D. (%)	E_r (%)	t_{exp}
S 1	76.3 ± 0.3	0.3	75.8 ± 0.8	0.7	−0.7	1.31	75.6 ± 0.9	1.1	−1.0	1.65
S 2	76.8 ± 0.3	0.4	76.3 ± 0.6	0.2	−0.6	1.67	76.4 ± 0.6	0.8	−0.5	1.33
S 3	75.4 ± 0.2	0.3	75.4 ± 0.8	0.7	0	0.00	75.8 ± 0.9	1.1	0.5	0.97

Student parameter $t = 1.821$ for a probability level of 95%.
[a] Calibration lines found for each one of the methodologies assayed, being S the analytical signal obtained for each method and C the Cyromazine concentration in mg l^{-1} for HPLC, mg g^{-1} for FTIR and g g^{-1} for FT-Raman.

by LC for a probability level of 95% calculated (t values were 1.821, the theoretical value) so showing the accuracy of these procedures.

Regarding the analytical repeatability, the R.S.D. values found were 0.2, 0.4 and 0.05% for FTIR, FT-Raman and LC. Limit of detection values found for FTIR, FT-Raman and LC were 0.2, 0.8 and 0.02% (w/w). So, it can be seen that HPLC provides the most precise and sensitive way for determination of Cyromazine. However, at the concentration level of commercial available samples, all three methods work well.

On considering the amount of reagents and solutions used, it is clear that LC involves the use of 50 ml CH_3OH and 11 ml of the CH_3CN mobile phase per sample in contrast to the 4 ml of CH_3OH consumed for FTIR measurements and the absence of sample preparation in FT-Raman.

Regarding sampling throughput Cyromazine determination by LC and FTIR require 5 min for sample sonication IR spectra being taken in 30 s before the 10 min required for each chromatogram. On the other hand, the total FT-Raman spectrum was obtained in 60 s directly from the solid sample confined in the glass vial used as a cell.

6. Conclusions

The proposed vibrational spectrometric procedures can be used for the determination of Cyromazine in pesticide commercial formulations providing fast, simple and environmentally friendly alternatives to the recommended LC procedure in spite of the lack of sensitivity and precision involved in vibrational measurements as compared with chromatographic ones. Both vibrational techniques, FTIR and FT-Raman, can be useful for the analysis of formulations containing more than one active ingredient, directly selecting adequate and not interfered characteristic bands or by means of the use of chemometrics for partially overlapping spectra.

Acknowledgements

The Authors acknowledge the financial support of the Generalitat Valenciana Project GV01-249, and the grant provided by the Laboratorio de Higiene Laboral y Ambiental of the Universitat de Valencia to carry out this study. S. Armenta acknowledges the FPU Grant of the Spanish Ministerio de Educación, Cultura y Deporte (ref. AP2002-1874).

References

[1] W.T. Thomson, Agricultural Chemicals, Book I, Insecticides, Thompson Publications, Fresno, CA, 1994.
[2] D. Davis, Insect Pest Management, CABI Bioscience, Ascot, UK, 2000.
[3] Federal Register Environmental Documments, US Environmental Protection Agency, PA, USA, 2000, http://www.epa.gov/fedrgstr/.
[4] A.R. Fernández-Alba, L. Hernando-Guil, G. Díaz-Lopez, Y. Chisti, Anal. Chim. Acta 451 (2002) 195–202.
[5] A.R. Fernández-Alba, L. Hernando-Guil, G. Díaz-Lopez, Y. Chisti, Anal. Chim. Acta 426 (2001) 289–301.
[6] P. Parrilla-Vazquez, M. Martinez-Galera, A. Garrido-Frenich, J.L. Martinez-Vidal, Anal. Sci. 16 (2000) 49–55.
[7] P. Cabras, M. Meloni, L. Spanedda, J. Chromatogr. 505 (1990) 413–416.
[8] R.A. Yokley, L.C. Mayer, R. Rezaaiyan, M.E. Manuli, M.W. Cheung, J. Agric. Food Chem. 48 (2000) 3352–3358.
[9] A. Kaune, R. Bruggemann, M. Sharma, A. Kettrup, J. Agric. Food Chem. 46 (1998) 335–343.
[10] J.P. Toth, P.C. Bardalaye, J. Chromatogr. 40 (1987) 335–340.
[11] P.C. Bardalaye, W.B. Wheeler, C.W. Meister, J. Assoc. Off. Anal. Chem. 70 (1987) 455–457.
[12] J.P. Toth, A.P. Snyder, Biol. Mass Spectrom. 20 (1991) 70–74.
[13] M. Gallignani, S. Garrigues, A. Martinez-Vidal, M. de la Guardia, Analyst 118 (1993) 1043–1048.
[14] S. Armenta, G. Quintás, J. Moros, S. Garrigues, M. de la Guardia, Anal. Chim. Acta 468 (2002) 81–90.
[15] G. Quintás, A. Morales-Noé, C. Parrilla, S. Garrigues, M. de la Guardia, Vib. Spectrosc. 31 (2003) 63–69.
[16] G. Quintás, S. Armenta, A. Morales-Noé, S. Garrigues, M. de la Guardia, Anal. Chim. Acta 480 (2003) 11–21.
[17] M.J. Almond, S.J. Knowles, Appl. Spectrosc. 53 (1999) 1128–1131.
[18] S.G. Skoulika, C.A. Georgiou, M.G. Polissiou, Talanta 51 (2000) 599–604.
[19] S.G. Skoulika, C.A. Georgiou, M.G. Polissiou, Appl. Spectrosc. 53 (1999) 1470–1474.
[20] A.M. Alak, T. Vo-Dinh, Anal. Chim. Acta 206 (1988) 333–337.
[21] A.M. Alak, T. Vo-Dinh, Anal. Chem. 59 (1987) 2149–2153.
[22] K. Mukherjee, S. Sanchez-Cortes, J.V. García-Ramos, Vib. Spectrosc. 25 (2001) 91–99.
[23] D. Lin-Vien, N.B. Colthup, W.G. Fateley, J.G. Grasselli, Infrared and Raman Characteristic Frequencies of Organic Molecules, Academic Press, London, 1991.

Vibrational spectrometric strategies for quality control of procymidone in pesticide formulations

Sergio Armenta, Salvador Garrigues and Miguel de la Guardia
[a]*Department of Analytical Chemistry, Universitat de València. Edifici Jeroni Muñoz, 50th Dr Moliner, 46100 Burjassot, Valencia, Spain.*

Spectroscopy letters 38 (2004) 703-720.

Impact factor of this journal (2004): 0.355
Source: Journal citation reports ISI Web of Knowledge, 2004.

Spectroscopy Letters, 38: 703–720, 2005

ISSN 0038-7010 print/1532-2289 online
DOI: 10.1080/00387010500315843

Taylor & Francis
Taylor & Francis Group

Vibrational Spectrometry Strategies for Quality Control of Procymidone in Pesticide Formulations

Sergio Armenta, Salvador Garrigues, and Miguel de la Guardia
Department of Analytical Chemistry, University of Valencia, Valencia, Spain

Abstract: Two vibrational spectrometry–based methodologies were developed for procymidone determination in wettable powdered pesticide formulations. The Fourier-transform infrared (FTIR) procedure was based on the selective extraction of procymidone by chloroform and determination by peak area measurement between 1451 and 1441 cm^{-1}, using a baseline correction established between 1490 and 1410 cm^{-1}, and a precision of 0.4% and a limit of detection of 0.01% w/w procymidone for a sample mass of 25 mg were obtained. For FT-Raman determination, the selected conditions were peak area measurement between 1005 and 995 cm^{-1} Raman shift, with a baseline correction fixed between 1030 and 947 cm^{-1}, and a relative standard deviation of 1% and a limit of detection of 0.8% procymidone in the original sample were obtained. The sample frequency for FTIR determination was 30 hr^{-1}, lower than that for Raman with 40 hr^{-1}. FT-Raman reduces to the minimum the reagent consumption and waste generation, also avoiding the sample handling and contact of the operator with the pesticide. It can be concluded that the proposed methods are appropriate for quality control in commercial pesticide formulations.

Keywords: FTIR, pesticide formulations, powder analysis, procymidone, Raman

Received 24 January 2005, Accepted 24 May 2005

This paper was by special invitation as a contribution to a special issue of the journal entitled "Quantitative Vibrational Spectrometry in the 21st Century." This special issue was organized by Professor Miguel de la Guardia, Professor of Analytical Chemistry at Valencia University, Spain.

Address correspondence to Salvador Garrigues, Department of Analytical Chemistry, University of Valencia, Edifici Jeroni Muñoz, 46100 Valencia, Spain. E-mail: salvador.garrigues@uv.es

INTRODUCTION

Procymidone, *N*-(3,5-dichlorophenyl)-1,2-dimethylcyclopropane-1,2-dicarboximide, is a dicarboximide fungicide with moderate generic activity. Although most uses involve foliar application, absorption through roots occurs with translocation to leaves and flowers. Procymidone inhibits spore germination, mycelial growth, and triglyceride synthesis in fungi. It is used in agriculture, horticulture, and viticulture against *Botrytis* sp., *Sclerotinia* sp., *Monilia* sp., *Aslternaria* sp., *Fusarium* sp., and *Rhizoctonia* sp.[1]

The main procymidone formulations commercially available are wettable powder (50% w/w), soluble concentrate (25% and 50% w/v), and water dispersable granules (50% and 75% w/w). In most cases, procymidone is not coformulated with other pesticides.[2]

Procymidone presents a low acute toxicity, its lethal dose (LD_{50}) being higher than 5000 mg/kg in rats and mice.[1]

The recommended method of the Collaborative International Pesticides Analytical Council (CIPAC) for the determination of procymidone in pesticide formulations is based on capillary gas chromatography with flame ionization detection (GC-FID) using dibutyl sebacate as internal standard.[3]

Procymidone has also been determined at trace levels in fruits and vegetables,[4,5] wine,[6] and human urine[7,8] by gas chromatography with tandem mass spectrometry; in vegetables,[9] wine,[10] and water[11] by gas chromatography with electron capture detection; in fruits and vegetables[12,13] by using micellar electrokinetic chromatography; and in synthetic mixtures by high-performance liquid chromatography (HPLC) with diode array detection.[14,15]

The use of vibrational spectrometry for pesticide analysis is a less common practice than the use of chromatography. The applicability of Fourier-transform infrared (FTIR) has been shown for the determination of carbaryl,[16] chlorpyriphos-ethyl,[17] buprofezin,[18] fluometuron,[19] chlorsulfuron,[20] folpet and metalaxyl[21] in pesticide formulations; Fourier-transform Raman spectrometry has been applied to the determination of pesticides in concentrated formulations based on the direct measurement of the Raman scattering of solid samples placed inside modified nuclear magnetic resonance tubes.[22–24] Recently, FT-Raman also has been employed for the direct determination of pesticides from solid[25] or liquid[26] samples or a previous dilution of the formulation with $CHCl_3$,[27] using in all cases standard chromatographic glass vials as a cell.

On the other hand, the development of surface-enhanced Raman scattering (SERS) increased dramatically the sensitivity of Raman measurements and provided new possibilities on the analysis of pesticides.[28,29] However, till now there exist no report on the use of FTIR nor on Raman for the determination of procymidone.

The main objective of this work was the development of fast and environmentally friendly methodologies for the analysis of pesticide formulations

containing procymidone that can be applied for quality control in the manufacturing industry.

EXPERIMENTAL

Apparatus and Reagents

A Nicolet (Madison, WI, USA) Magna 750 FTIR spectrometer, equipped with a temperature-stabilized deuterated tryglycine sulfate (DGTS) detector, was employed for infrared measurements, using a micro-flow cell (Graseby-Specac, Orpington, UK) with ZnSe and CaF_2 windows and a pathlength of 0.10 mm. The equipment employs the 2.1 version of the OMNIC software developed by Nicolet Corporation for the acquisition and processing of the FTIR absorbance data.

A Bruker RFS 100/S (Bremen, Germany) spectrometer equipped with a 2 W maximum power Nd:YAG laser that emits at 1064 nm and a Ge detector cooled with N_2 was employed to obtain Raman spectra of solid samples, using 2 mL and 12 × 32 mm internal diameter standard glass chromatographic vials as sample cells.

An ultrasonic water bath (J.P. Selecta, Barcelona, Spain) was used to improve a fast pesticide extraction.

An Agilent HPLC Series 1100 High Performance Liquid Chromatograph (Madrid, Spain), equipped with a reversed phase C-18 (Kromasil), 250 × 4.6 mm i.d. and 5-μm particle diameter column, and a diode array detector (DAD) was also employed for the analysis of fungicide formulations, this methodology being used as a reference for the validation of FTIR measurements.

Procymidone PESTANAL reagent grade standard (99.1% w/w) was supplied by Fluka (Buchs, Switzerland). Analytical grade chloroform stabilized with ethanol and sodium chloride, reagent grade (99.8% w/w) and supplied by Scharlau (Barcelona, Spain), was employed for the preparation of samples and standards. Procymidone wettable powder commercial formulations with a procymidone concentration of 50% w/w were obtained directly from the Spanish market.

HPLC-DAD Reference Procedure

Sample (40 mg) was accurately weighed inside a 25-mL volumetric flask and diluted to the volume with acetonitrile (CH_3CN), being sonicated during 5 min in an ultrasonic water bath to extract procymidone from the matrix. Extract (0.1 mL) was diluted to 10 mL and filtered through a 0.22-μm polyamide filter. Filtrate (20 μl) was directly injected in a 9 : 1 acetonitrile : water mobile phase of 1 mL min^{-1} flow rate. Procymidone was determined in the

isocratic mode by absorbance measurements at 238 nm and area values of the chromatograms peak obtained at 3.7 min. An external calibration was established with standard solutions of Procymidone in acetonitrile.

FTIR Procedure

Sample (25 mg) were accurately weighed into a glass vial and dissolved with 4 g of $CHCl_3$. The vial was closed with a cap and the mixture was sonicated for 5 min in an ultrasonic water bath. After that, the sample extract was passed through a 0.22-μm nylon syringe filter and then introduced into the FTIR measurement cell by using a peristaltic pump. The spectra were obtained in the stopped-flow mode at 4 cm^{-1} nominal resolution and accumulating 25 scans per spectrum from 4000 to 900 cm^{-1} using a background of the cell filled with the solvent.

Peak area values between 1451 and 1441 cm^{-1}, corrected with a baseline established between 1490 and 1410 cm^{-1}, were employed to quantify procymidone in samples using an external calibration line obtained with standard solutions of the pesticide in chloroform in the concentration range between 1.7 and 5.3 mg g^{-1}, measured in the same conditions than samples.

Raman Procedure

An amount approximately of 300 mg of commercial sample were grounded and homogenized for 5 min in an agate mortar. The sample was introduced in a chromatographic glass vial and the Raman spectra recorded between 3500 and 70 cm^{-1}, at 4 cm^{-1} resolution and accumulating 25 scans per spectrum. The Ng : YAG laser power was fixed at 750 mW. A Blackman-Harris 4 apodization function, a scan velocity of 1.0 (2.2 kHz), a zero filling factor of 2, and an aperture of 10 mm were also employed for the acquisition of the Raman spectra.

An external calibration curve was established with a solid procymidone standard diluted with sodium chloride at different levels, for 0.25 to 0.73 g g^{-1}. For quantitative purposes, peak area values between 1005 and 995 cm^{-1} corrected with a baseline defined between 1039 and 947 cm^{-1} were used.

RESULTS AND DISCUSSION

FTIR Spectrum of Procymidone

Figure 1 shows the absorbance spectra, in the wavenumber range from 2000 to 1000 cm^{-1}, of a procymidone standard chloroformic solution of 4.2 mg g^{-1}

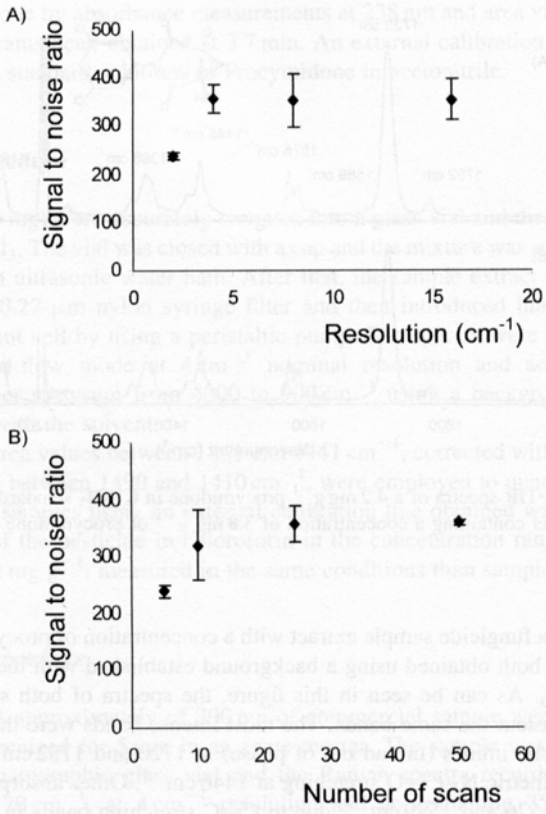

Figure 2. (A) Effect of the nominal resolution on signal to noise ratio of a procymidone standard of 3.31 mg g^{-1} obtained accumulating 25 scans for spectrum. (B) Effect of the number of accumulated scans on the signal to noise ratio. Data were obtained using a nominal resolution of 4 cm^{-1}. The signals were established for a procymidone standard of 3.31 mg g^{-1}.

50 scans, but in order to ensure a compromise between measurement frequency and precision values, 25 accumulated scans was selected.

Selection of FTIR Bands for Procymidone Determination

In order to select the best measurement conditions for FTIR procymidone determination, several bands, base-line criteria, and measurement mode (peak height and peak area values) were assayed and evaluated in terms of sensitivity, repeatability, and limit of detection. Table 1 shows the main

Table 1. Analytical features of the FTIR determination of procymidone using different bands, baseline criteria, and measurement modes

Measurement mode	Wavenumber (cm^{-1})	Baseline correction	Procymidone calibration curve [$y = a + b\ C$ (mg g^{-1})]				
			$a \pm s_a$	$b \pm s_b$	R^2	% RSD[a]	LOD[b] (% w/w)
Height	1782	1805–1757	0.0002 ± 0.0001	0.00564 ± 0.00004	0.9994	0.17	2.9
Area	1787–1777		-0.0002 ± 0.0008	0.0505 ± 0.0003	0.9996	0.3	1.0
Height	1720	1760–1666	0.0020 ± 0.0009	0.0656 ± 0.0003	0.9997	0.13	0.1
Area	1725–1715		0.014 ± 0.007	0.589 ± 0.002	0.9998	0.06	0.03
Height	1589	1631–1529	0.0000 ± 0.0002	0.01214 ± 0.0006	0.9996	0.4	1.2
Area	1594–1584		-0.001 ± 0.002	0.1070 ± 0.0006	0.9996	0.4	0.5
Height	1576	1631–1529	-0.0002 ± 0.0003	0.01787 ± 0.00008	0.9997	0.07	0.8
Area	1581–1571		-0.002 ± 0.002	0.1233 ± 0.0005	0.9997	0.3	0.2
Height	1446	1490–1410	-0.0003 ± 0.0003	0.02048 ± 0.00009	0.9997	0.4	0.4
Area	1451–1441		-0.003 ± 0.002	0.1611 ± 0.0007	0.9998	0.4	0.01
Height	1366	1410–1318	-0.0002 ± 0.0002	0.01522 ± 0.00006	0.9997	0.2	0.6
Area	1371–1361		-0.002 ± 0.002	0.1374 ± 0.0005	0.9998	0.13	0.2
Height	1159	1186–1138	-0.0002 ± 0.0003	0.0158 ± 0.0001	0.9994	0.3	1.2
Area	1164–1154		-0.006 ± 0.002	0.1474 ± 0.0008	0.9996	0.2	0.4

[a]RSD: Relative standard deviation for five measurements.
[b]LOD: Limit of detection in pesticide formulations for a sample mass of 25 mg and stablished for a probability level of 99.6%.

Table 1. Analytical features of the FTIR determination of procymidone using different bands, baseline criteria, and measurement modes

Measurement mode	Wavenumber (cm^{-1})	Baseline correction	Procymidone calibration curve [$y = a + b\ C$ (mg g^{-1})]				
			$a \pm s_a$	$b \pm s_b$	R^2	% RSD[a]	LOD[b] (% w/w)
Height	1782	1805–1757	0.0002 ± 0.0001	0.00564 ± 0.00004	0.9994	0.17	2.9
Area	1787–1777		−0.0002 ± 0.0008	0.0505 ± 0.0003	0.9996	0.3	1.0
Height	1720	1760–1666	0.0020 ± 0.0009	0.0656 ± 0.0003	0.9997	0.13	0.1
Area	1725–1715		0.014 ± 0.007	0.589 ± 0.002	0.9998	0.06	0.03
Height	1589	1631–1529	0.0000 ± 0.0002	0.01214 ± 0.0006	0.9996	0.4	1.2
Area	1594–1584		−0.001 ± 0.002	0.1070 ± 0.0006	0.9996	0.4	0.5
Height	1576	1631–1529	−0.0002 ± 0.0003	0.01787 ± 0.00008	0.9997	0.07	0.8
Area	1581–1571		−0.002 ± 0.002	0.1233 ± 0.0005	0.9997	0.3	0.2
Height	1446	1490–1410	−0.0003 ± 0.0003	0.02048 ± 0.00009	0.9997	0.4	0.4
Area	1451–1441		−0.003 ± 0.002	0.1611 ± 0.0007	0.9998	0.4	0.01
Height	1366	1410–1318	−0.0002 ± 0.0002	0.01522 ± 0.00006	0.9997	0.2	0.6
Area	1371–1361		−0.002 ± 0.002	0.1374 ± 0.0005	0.9998	0.13	0.2
Height	1159	1186–1138	−0.0002 ± 0.0003	0.0158 ± 0.0001	0.9994	0.3	1.2
Area	1164–1154		−0.006 ± 0.002	0.1474 ± 0.0008	0.9996	0.2	0.4

[a]RSD: Relative standard deviation for five measurements.
[b]LOD: Limit of detection in pesticide formulations for a sample mass of 25 mg and stablished for a probability level of 99.6%.

figures of merit of different external calibration lines obtained from the main procymidone bands in the spectral region from 2000 to 1000 cm^{-1}.

The limits of detection established from three times the standard deviation of blank values divided by the slope of the calibration line varied from 0.01% to 2.9% w/w procymidone for an original sample mass of 25 mg this being adequate for the determination of this active main component in commercially available formulations. A repeatability between 0.06% and 0.4% in terms of relative standard deviation of a solution containing 4.3 mg g^{-1} procymidone was obtained, thus indicating the good stability of FTIR measurements.

In terms of sensitivity, it is clear that peak area measurements provides one order of magnitude better sensitivity than peak height values, but the repeatability of area measurements in some cases works better than that of peak height.

The band at 1446 cm^{-1} was selected because is not overlapped with any excipient band and due to the higher selectivity of this band in front of the carbonyl band at 1720 cm^{-1}. As can be seen in Table 1, peak area values provided lower % RSD and % LOD than the use of peak height, so this measurement mode was selected.

FT-Raman Spectra of Procymidone

Figure 3 shows the FT-Raman spectra of a solid procymidone standard diluted in sodium chloride of 48.9% w/w of procymidone, a commercial fungicide

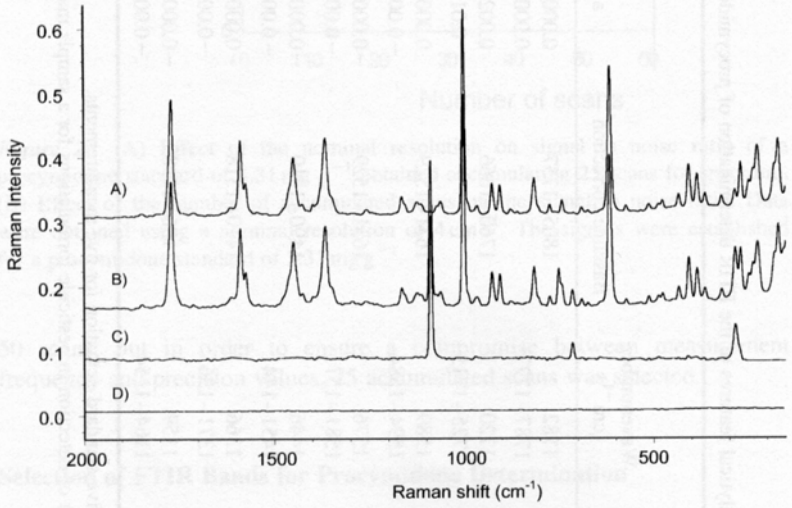

Figure 3. Raman spectra of a 48.9% w/w procymidone standard diluted in sodium chloride (A), a commercial sample containing a concentration of 50% w/w of procymidone (B), calcium carbonate (C), and sodium chloride (D) employed for the preparation of standards.

with a concentration of procymidone of 50% w/w, calcium carbonate, the main coadjuvant present in the sample, and that of a blank of sodium chloride. As can be seen, the spectrum of the sample and that of the standard present practically the same bands except those typical of $CaCO_3$, which can be clearly identified in the sample. The most intense bands in procymidone spectra are those present at 1770 and 1000 cm^{-1} Raman shift due to C=O stretching and trigonal ring breathing, respectively. Other less important bands are those located at 1588, 1449, 1365, and 615 cm^{-1} due to C=C stretching in chloroalkenes, pseudosymmetric N–C=O stretching, ring stretching in benzene and C–Cl stretching, respectively.[30]

Raman Measurement Conditions

In order to improve the Raman measurement conditions, the effect of the number of accumulated scans, the laser power, and the nominal resolution employed for data acquisition were evaluated for a standard of procymidone diluted in a sodium chloride matrix with a concentration of 48.9% w/w. The number of accumulated scans was modified from 5 to 50, the laser power changed between 250 and 1000 mW and the nominal resolution varied from 2 to 16 cm^{-1}.

The most precise and sensitive results were those obtained when accumulating 50 scans for a laser power of 1000 mW (Fig. 4A). However in order to ensure a compromise between measurement frequency and precision and to avoid the use of a high laser power, which can affect the thermal stability of samples, 25 accumulated scans and 750 mW were selected, also being confirmed that, for a nominal resolution of 4 cm^{-1} and 25 accumulated scans, the best signal to noise ratio was found on using 750 mW (Fig. 4B).

Concerning the nominal resolution, it was found that the use of a resolution between 2 and 16 cm^{-1} provided a signal to noise ratio, established as the ratio between the peak area measurement between 1005 and 995 cm^{-1} Raman shift, with a baseline correction between 1030 and 947 cm^{-1}, and the noise of a blank established in the same region, of the order 10,000 (Fig. 5), but a 4 cm^{-1} resolution was the best compromise between sensitivity and sampling speed, a sample measurement throughput of 40 hr^{-1} for this value being obtained.

The repeatability of procymidone Raman measurements in solid phase can be affected by the vial and sample holder position. In order to evaluate the effect of these variables, a procymidone standard was measured changing the vial position randomly and using different vials for the same sample. A relative standard deviation of 2.9% and 5.3%, respectively, was found for the Raman intensity of a 48.9% w/w procymidone standard determined with peak area values between 1005 and 995 cm^{-1}, which is acceptable to carry out determination of this pesticide in commercial formulations.

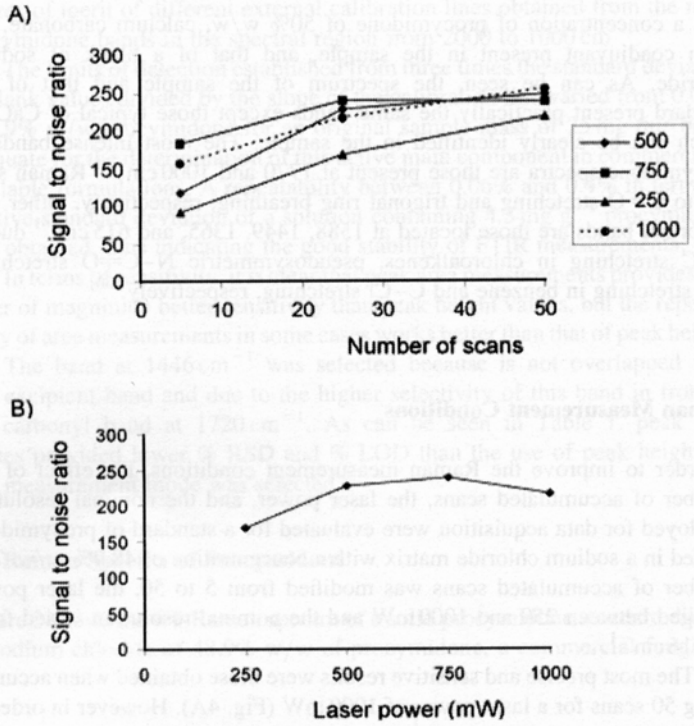

Figure 4. (A) Effect of the number of accumulated scans on the signal to noise ratio for different laser power. Data were obtained from the area between 1005 to 995 cm^{-1} shift of a standard containing 48.9% w/w procymidone. Experimental measurements were carried out with a nominal resolution of 4 cm^{-1} and laser powers between 250 and 1000 mW. (B) Signal to noise dependence from the laser power for 1000 cm^{-1} peak of a spectrum of a procymidone standard of 48.9% w/w obtained accumulating 25 scans per spectrum at a nominal resolution of 4 cm^{-1}.

Selection of Bands for Raman Determination of Procymidone

As indicated in Table 2, different bands were tested to do the Raman determination of procymidone in solid pesticide formulations. Peak height and peak area values were measured, also evaluating the use of different baseline criteria. The table shows the equations of the calibration lines obtained in each condition considered. It can be seen that the sensitivity of FT-Raman determination of procymidone varies from 0.215 to 5.6 intensity units (g^{-1} g), where peak height measurements are one order of magnitude less sensitive than when using peak area. In all the cases assayed, the limit of detection found was of the order 0.1% to 1.0% w/w independently of sample amount if it was enough to be excited and the emission could be done.

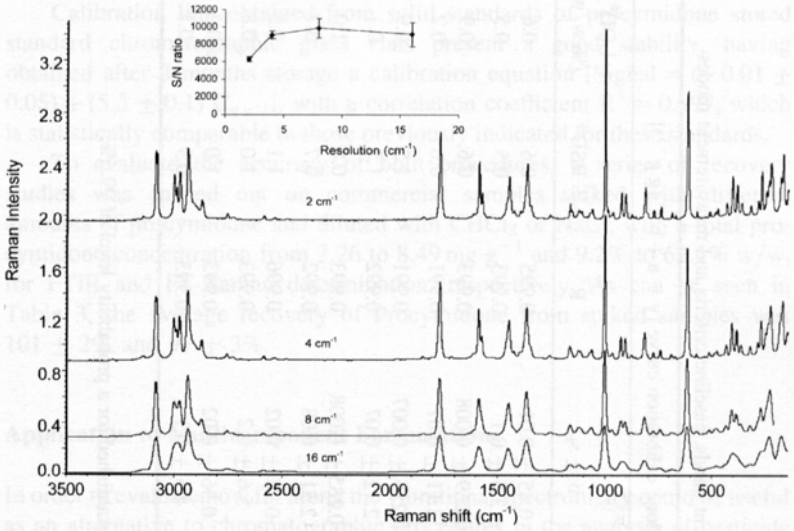

Figure 5. Effect of the nominal resolution on the Raman spectrum of a procymidone standard of 48.9% w/w obtained accumulating 25 scans for spectrum and a laser power of 750 mW. Inset: Signal to noise effect for peak area values between 1005 to 995 cm^{-1} Raman shift.

The use of the peak area measurement between 1005 and 995 cm^{-1} with a baseline fixed between 1030 and 947 cm^{-1} was selected because it presented the best sensitivity, a limit of detection of 0.8% w/w, and accuracy errors of the order 1.0%.

Analytical Figures of Merit of the Developed Procedures

The main characteristics of the FTIR method developed for the determination of procymidone in formulated products are indicated in Table 1. For peak area measurements between 1451 and 1441 cm^{-1}, corrected with a baseline established between 1490 and 1410 cm^{-1}, a calibration line [Absorbance = $(-0.003 \pm 0.002) + (0.1611 \pm 0.0007)\ C_{mg\,g^{-1}}$] with a correlation coefficient $R^2 = 0.9998$, a precision of 0.4%, and a limit of detection of 0.01% w/w procymidone for a sample mass of 25 mg were obtained.

For FT-Raman determination, the selected conditions were peak area measurement between 1005 and 995 cm^{-1} Raman shift, with a baseline correction fixed between 1030 and 947 cm^{-1}, obtaining a calibration line [Signal = $(0.00 \pm 0.06) + (5.6 \pm 0.2)\ C_{g\,g^{-1}}$, with a correlation coefficient $R^2 = 0.993$, a relative standard deviation of 1%, and a limit of detection of 0.8% Procymidone in the original sample.

Table 2. Analytical features of the Raman determination of procymidone using different bands, baseline criteria and measurement modes

Measurement mode	Wavenumber (cm^{-1})	Baseline correction	Procymidone calibration curve [$y = a + b\ C$ ($g\ g^{-1}$)]				
			$a \pm s_a$	$b \pm s_b$	R^2	% RSD[a]	LOD[b] (% w/w)
Height	1770	1800–1720	0.000 ± 0.004	0.45 ± 0.01	0.995	0.6	0.6
Area	1775–1765		0.01 ± 0.04	3.6 ± 0.1	0.993	0.5	0.5
Height	1588	1606–1551	0.000 ± 0.003	0.269 ± 0.008	0.993	0.6	0.9
Area	1593–1583		−0.01 ± 0.03	2.11 ± 0.07	0.991	0.6	0.2
Height	1419	1499–1414	0.000 ± 0.003	0.215 ± 0.007	0.991	1.5	0.9
Area	1454–1444		−0.01 ± 0.03	2.12 ± 0.07	0.992	1.5	0.1
Height	1365	1409–1320	0.000 ± 0.003	0.285 ± 0.008	0.993	0.8	1.0
Area	1454–1444		0.00 ± 0.03	2.51 ± 0.08	0.992	0.7	0.7
Height	1000	1030–947	0.002 ± 0.007	0.78 ± 0.02	0.996	1.1	0.5
Area	1005–995		0.00 ± 0.06	5.6 ± 0.2	0.993	1.0	0.8
Height	615	660–592	0.001 ± 0.006	0.56 ± 0.02	0.993	1.0	0.3
Area	620–610		0.00 ± 0.05	4.5 ± 0.1	0.993	0.9	0.1

[a]RSD: Relative standard deviation for five measurements.
[b]LOD: Limit of detection in pesticide formulations for a sample mass of 25 mg and stablished for a probability level of 99.6%.

Calibration line obtained from solid standards of procymidone stored standard chromatographic glass vials present a good stability, having obtained after 3 months storage a calibration equation [Signal = $(-0.01 \pm 0.05) + (5.5 \pm 0.1)\ C_{g\,g^{-1}}$], with a correlation coefficient $R^2 = 0.997$, which is statistically comparable to those previously indicated for these standards.

To evaluate the accuracy of both procedures, a series of recovery studies was carried out on commercial samples spiked with different amounts of procymidone and diluted with $CHCl_3$ or NaCl, with a total procymidone concentration from 3.26 to 8.49 mg g^{-1} and 9.2% to 62.5% w/w, for FTIR and FT-Raman determination, respectively. As can be seen in Table 3, the average recovery of Procymidone from spiked samples was $101 \pm 2\%$ and $97 \pm 3\%$.

Application to Multicomponent Formulations

In order to evaluate how far along the vibrational spectrometry could be useful as an alternative to chromatographic procedures in the analysis of pesticide formulations, the existence of agrochemicals containing additional pesticides than procymidone was checked and it was found that chlorothalonil is coformulated with the aforementioned compound.[31]

As it can be seen in Fig. 6, in both the FTIR (Fig. 6A) and Raman (Fig. 6B) spectra, the selected bands employed through this study can be clearly differentiated with those obtained for chlorothalonil, thus evidencing the tremendous possibilities to extract direct information from the vibrational spectra of mixtures of compounds, based on the presence of several isolated bands for each one of the compounds considered.

However, for complex mixtures containing several principles and additives, it must be employed a chemometric-based methodology for the calibration of signals based on a series of well-analyzed samples as we have suggested.[32]

Comparison Between Different Methodologies Developed

The different methodologies developed for the determination of procymidone in pesticide formulations provide statistically comparable results for a probability level of 95% (student statistical, calculated value, t_{exp}, being lower than 1.812, the theoretical one for 10 degrees of freedom, t_{tab}), as can be seen in Table 4.

The advantages offered by the vibrational procedures is a strong reduction of the volume of organic solvent required for the analysis (41.3 mL acetonitrile for HPLC-DAD, 2.7 mL chloroform for FTIR, and no solvent for FT-Raman) and the increase of the sampling frequency from 8.6 hr^{-1} on the case of HPLC-DAD to 30 hr^{-1} for FTIR and 40 hr^{-1} for FT-Raman.

Table 3. Recovery studies on procymidone added to formulate samples by using FTIR and FT-Raman spectrometry

FTIR				FT-Raman			
Total content of procymidone (mg g^{-1})	Procymidone found (mg g^{-1})	% Recovery	Mean recovery ± s	Total content of procymidone (% w/w)	Procymidone found (% w/w)	% Recovery	Mean recovery ± s
3.27	3.34	101.9 ± 0.3		9.26	9.04	99 ± 2	
	3.32				9.34		
	3.33				9.20		
5.19	5.32	102.5 ± 0.2		12.97	12.99	102 ± 2	
	5.33				13.02		
	5.33				13.57		
6.40	6.35	99.1 ± 0.2	101 ± 2	17.15	16.87	98 ± 2	97 ± 3
	6.33				16.90		
	6.34				16.51		
7.07	7.19	101.72 ± 0.09		40.1	37.76	93 ± 1	
	7.19				37.77		
	7.18				37.00		
8.49	8.43	99.0 ± 0.2		62.6	61.19	95 ± 3	
	8.39				58.68		
	8.41				57.90		

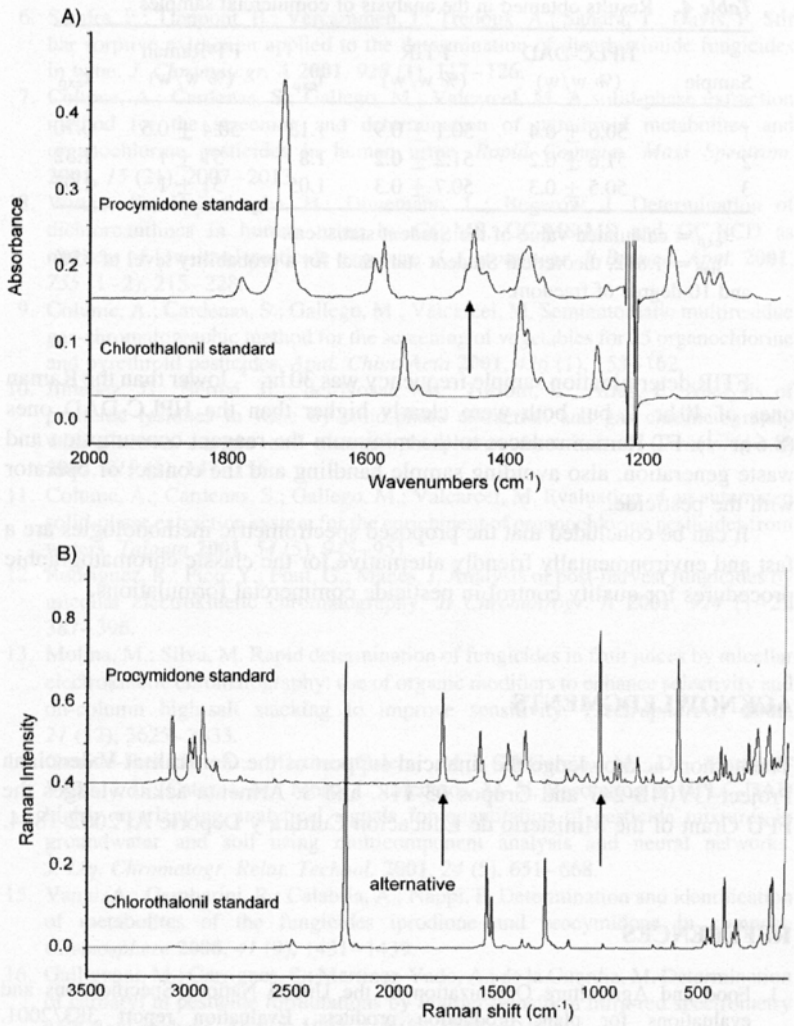

Figure 6. Vibrational spectra of procymidone and chlorothalonil: (A) FTIR spectra of standards dissolved in $CHCl_3$; (B) FT-Raman spectra obtained directly from the solid standards.

CONCLUSIONS

Results obtained in this paper show the possibilities of the absorption (FTIR) and emission (FT-Raman) vibrational techniques for the determination of principle active components in pesticide formulations.

Table 4. Results obtained in the analysis of commercial samples

Sample	HPLC-DAD (% w/w)	FTIR (% w/w)	t_{exp}	FT-Raman (% w/w)	t_{exp}
1	50.6 ± 0.4	50.1 ± 0.9	1.13	50.4 ± 0.5	0.70
2	51.6 ± 0.2	51.2 ± 0.2	1.8	51 ± 1	1.32
3	50.5 ± 0.3	50.7 ± 0.3	1.05	51 ± 1	1.07

t_{exp} = calculated value of the Student statistical.
t_{tab} = 1.812, theoretical Student statistical for a probability level of 95% and 10 degree of freedom.

FTIR determination sample frequency was 30 hr^{-1}, lower than the Raman ones of 40 hr^{-1}, but both were clearly higher than the HPLC-DAD ones (8.6 hr^{-1}). FT-Raman reduces to the minimum the reagent consumption and waste generation, also avoiding sample handling and the contact of operator with the pesticide.

It can be concluded that the proposed spectrometric methodologies are a fast and environmentally friendly alternative for the classic chromatographic procedures for quality control in pesticide commercial formulations.

ACKNOWLEDGMENTS

The authors acknowledge the financial support of the Generalitat Valenciana Project GV04B-247 and Grupos 03-118, and S. Armenta acknowledges the FPU Grant of the Ministerio de Educacion Cultura y Deporte AP2002-1874.

REFERENCES

1. Food and Agriculture Organization of the United Nations Specifications and evaluations for plant production products. Evaluation report 383/2001. Available at http:/www.fao.org/WAICENT/FAOINFO/AGRICULT/AGP/AGPP/Pesticid/.
2. de Liñan, C. *Vademecum de productos fitosanitarios y nutricionales*; Ediciones Agrotécnicas, S. L., Ed.; Madrid, Spain, 2000.
3. Methods Committee Reports. General referee reports. *J. AOAC Int.* **2001**, *84*, 187–189.
4. Gamon, M.; Lleo, C.; Ten, A.; Mocholi, F. Multiresidue determination of pesticides in fruit and vegetables by gas chromatography-tandem mass spectrometry. *J. AOAC Int.* **2001**, *84* (4), 1209–1216.
5. Colume, A.; Cardenas, S.; Gallego, M.; Valcarcel, M. Multiresidue screening of pesticides in fruits using an automatic solid-phase extraction system. *J. Agric. Food Chem.* **2001**, *49* (3), 1109–1116.

6. Sandra, P.; Tienpont, B.; Vercammen, J.; Tredoux, A.; Sandra, T.; Davis, F. Stir bar sorptive extraction applied to the determination of dicarboximide fungicides in wine. *J. Chromatogr. A* **2001**, *928* (1), 117–126.
7. Colume, A.; Cardenas, S.; Gallego, M.; Valcarcel, M. A solid-phase extraction method for the screening and determination of pyrethroid metabolites and organochlorine pesticides in human urine. *Rapid Commun. Mass Spectrom.* **2001**, *15* (21), 2007–2013.
8. Wittke, K.; Hajimiragha, H.; Dunemann, L.; Begerow, J. Determination of dichloroanilines in human urine by GC-MS, GC-MS-MS and GC-ECD as markers of low-level pesticide exposure. *J. Chromatogr. B Biomed. Appl.* **2001**, *755* (1–2), 215–228.
9. Colume, A.; Cardenas, S.; Gallego, M.; Valcarcel, M. Semiautomatic multiresidue gas-chromatographic method for the screening of vegetables for 25 organochlorine and pyrethroid pesticides. *Anal. Chim. Acta* **2001**, *436* (1), 153–162.
10. Jimenez, JJ.; Bernal, JL.; del-Nozal, MJ.; Toribio, L.; Arias, E. Analysis of pesticide residues in wine by solid-phase extraction and gas chromatography with electron capture and nitrogen-phosphorus detection. *J. Chromatogr. A* **2001**, *919* (1), 147–156.
11. Colume, A.; Cardenas, S.; Gallego, M.; Valcarcel, M. Evaluation of an automated solid-phase extraction system for the enrichment of organochlorine pesticides from waters. *Talanta* **2001**, *54* (5), 943–951.
12. Rodriguez, R.; Pico, Y.; Font, G.; Manes, J. Analysis of post-harvest fungicides by micellar electrokinetic chromatography. *J. Chromatrogr. A* **2001**, *924* (1–2), 387–396.
13. Molina, M.; Silva, M. Rapid determination of fungicides in fruit juices by micellar electrokinetic chromatography: use of organic modifiers to enhance selectivity and on-column high-salt stacking to improve sensitivity. *Electrophoresis* **2000**, *21* (17), 3625–3633.
14. Garrido-Frenich, A.; Martinez-Galera, M.; Gil-Garcia, M. D.; Martinez-Vidal, J. L.; Catasus, M.; Marti, L.; Mederos, M. V. Resolution of HPLC-DAD highly overlapping analytical signals for quantitation of pesticide mixtures in groundwater and soil using multicomponent analysis and neural networks. *J. Liq. Chromatogr. Relat. Technol.* **2001**, *24* (5), 651–668.
15. Vanni, A.; Gamberini, R.; Calabria, A.; Nappi, P. Determination and identification of metabolites of the fungicides iprodione and procymidone in compost. *Chemosphere* **2000**, *41* (9), 1431–1439.
16. Gallignani, M.; Garrigues, S.; Martinez-Vado, A.; de la Guardia, M. Determination of carbaryl in pesticide formulations by Fourier-transform infra-red spectrometry with flow analysis. *Analyst* **1993**, *118* (8), 1043–1048.
17. Almond, M. J.; Knowles, S. J. Quantitative analysis of agrochemical formulations by multivariate spectroscopic techniques. *Appl. Spectrosc.* **1999**, *53* (9), 1128–1131.
18. Armenta, S.; Quintás, G.; Moros, J.; Garrigues, S.; de la Guardia, M. Fourier transform infrared spectrometric strategies for the determination of Buprofezin in pesticide formulations. *Anal. Chim. Acta* **2002**, *468* (1), 81–90.
19. Quintás, G.; Morales-Noé, A.; Parrilla, C.; Garrigues, S.; de la Guardia, M. Fourier transform infrared determination of fluometuron in pesticide formulations. *Vib. Spectrosc.* **2003**, *31* (1), 63–69.
20. Quintas, G.; Armenta, S.; Morales-Noe, A.; Garrigues, S.; and de la Guardia, M. An infrared method, with reduced solvent consumption, for the determination of chlorsulfuron in pesticide formulations. *Spectrosc. Lett. 36* (5–6), 515–529.

21. Quintás, G.; Armenta, S.; Morales-Noé, A.; Garrigues, S.; de la Guardia, M. Simultaneous determination of folpet and metalaxyl in pesticide formulations by flow injection Fourier transform infrared spectrometry. *Anal. Chim. Acta* **2003**, *480* (1), 11–21.
22. Skoulika, S. G.; Georgiou, C. A.; Polissiou, M. G. FT-Raman spectroscopy: an analytical tool for routine analysis of diazinon pesticide formulations. *Talanta* **2000**, *51* (3), 599–604.
23. Skoulika, S. G.; Georgiou, C. A.; Polissiou, M. G. Quantitative determination of fenthion in pesticide formulations by FT-Raman spectroscopy. *Appl. Spectrosc.* **1999**, *53* (11), 1470–1474.
24. Skoulika, S. G.; Georgiou, C. A. Univariate and multivariate calibration for the quantitative determinations of methyl-parathion in pesticide formulations by FT-Raman spectroscopy. *Appl. Spectrosc.* **2000**, *54* (5), 747–752.
25. Armenta, S.; Quintás, G.; Garrigues, S.; de la Guardia, M. Determination of cyromazine in pesticide commercial formulations by vibrational spectrometric procedures. *Anal. Chim. Acta* **2004**, *524* (1–2), 257–264.
26. Quintás, G.; Garrigues, S.; Pastor, A.; de la Guardia, M. FT-Raman determination of Mepiquat chloride in agrochemical products. *Vib. Spectrosc.* **2004**, *36* (1), 41–46.
27. Quintás, G.; Garrigues, S.; de la Guardia, M. FT-Raman spectrometry determination of Malathion in pesticide formulations. *Talanta* **2004**, *63* (2), 345–350.
28. Alak, A. M.; Vo-Dinh, T. Surface-enhanced Raman spectrometry of organophosphorus chemical agents. *Anal. Chem.* **1987**, *59* (17), 2149–2153.
29. Alak, A. M.; Vo-Dinh, T. Surface-enhanced Raman spectrometry of chlorinated pesticides. *Anal. Chim. Acta* **1988**, *206* (1–2), 333–337.
30. Lin-Vien, D.; Colthup, N. B.; Fateley, W. G.; Grasselli, J. G. *Infrared and Raman Characteristic Frequencies of Organic Molecules*, Academic Press: London, 1991.
31. Vademecum de productos fitosanitarios **2004**. Available at http://www.infoagro.com/agrovademecum/default.htm.
32. Armenta, S.; Quintás, G.; Garrigues, S.; de la Guardia, M. Middle infrared and Raman spectrometry as tools for pesticide formulations quality control. *Trends Anal. Chem.* **2005**, *24* (8), 772–781.

Sweeteners determination in table top formulations using FT-Raman spectrometry and chemometric analysis

Sergio Armenta, Salvador Garrigues and Miguel de la Guardia
[a]*Department of Analytical Chemistry, Universitat de València. Edifici Jeroni Muñoz, 50th Dr Moliner, 46100 Burjassot, Valencia, Spain.*

Analytical Chimica Acta 521 (2004) 149-155.

Impact factor of this journal (2004): 2.588
Source: Journal citation reports ISI Web of Knowledge, 2004.

Available online at www.sciencedirect.com
SCIENCE DIRECT®
Analytica Chimica Acta 521 (2004) 149–155
ANALYTICA CHIMICA ACTA
www.elsevier.com/locate/aca

Sweeteners determination in table top formulations using FT-Raman spectrometry and chemometric analysis

Sergio Armenta, Salvador Garrigues*, Miguel de la Guardia

Department of Analytical Chemistry, Universitat de València Edifici Jeroni Muñoz, 50th Dr. Moliner, 46100 Burjassot, Valencia, Spain

Received 31 March 2004; received in revised form 27 May 2004; accepted 27 May 2004

Available online 22 July 2004

Abstract

A partial least squares (PLS) Fourier transform Raman spectrometry procedure based on the measurement of solid samples contained inside standard glass vials, has been developed for direct and reagent-free determination of sodium saccharin and sodium cyclamate in table top sweeteners. A classical 2^2 design for standards was used for calibration, but this system provides accuracy errors higher than 13% w/w for the analysis of samples containing glucose monohydrate. So, an extended model incorporating glucose monohydrate (2^3 standards) was assayed for the determination of sodium saccharin and sodium cyclamate in all the samples. Mean centering spectra data pre-treatment has been employed to eliminate common spectral information and root mean square error of calibration (RMSEC) of 0.0064 and 0.0596 was obtained for sodium saccharin and sodium cyclamate, respectively. A mean accuracy error of the order of 1.1 and 1.9% w/w was achieved for sodium saccharin and sodium cyclamate, in the validation of the method using actual table top samples, being lower than those obtained using an external monoparametric calibration. FT-Raman provides a fast alternative to the chromatographic method for the determination of the sweeteners with a three times higher sampling throughput than that obtained in HPLC. On the other hand, FT-Raman offers an environmentally friendly methodology which eliminates the use of solvents. Furthermore, the stability of samples and standards into chromatographic standard glass vials allows their storage for future analysis thus avoiding completely the waste generation.

Keywords: Sweeteners; Sodium saccharin; Sodium cyclamate; Raman; Powder analysis

1. Introduction

Sweeteners are the modern non-caloric alternatives to sugars as additives in foods and drinks. At present, six sweeteners are included in the European Union legislation to be used in foods: acesulfame K, aspartame, cyclamate, neohesperidine DC, saccharin and thaumatin [1] and additionally two new sweeteners were approved by the Scientific Committee for Food (SCF) in 2000, namely Sucralose and Twinsweet™, an aspartame and acesulfame salt.

Sweeteners can be used separately or in combination with others and it has been reported sinergistic effects in various sweetener combinations [1]. The most common artificial sweeteners include sodium saccharin, cyclamate and aspartame, which are all those permitted for use in about 90 countries.

Saccharin, 1,2-benzisothiazolin-3-one-1,1-dioxide, is the oldest and one of the strongest sweeteners on the market, possessing about 500 times the sweetening capacity of sugar. Sodium saccharin, which is often used because it dissolves better than saccharin, is still 450 times sweeter than sugar.

The acceptable daily intake (ADI) for saccharin was increased to 5.0 mg kg^{-1} by the Joint Expert Committee on Food Additives (JECFA) in 1993. The Scientific Committee on Food of the European Commission (SCFEC) increased the ADI for saccharin to 5.0 mg kg^{-1} in 1995 [1].

Cyclamate, cyclohexylsulfamic acid monosodium salt, is 35 times sweeter than sugar. Cyclamate is approved in more than 50 countries worldwide. ADI for cyclamate has been set at 11 mg kg^{-1} by the JECFA and at 7 mg kg^{-1} by the SCFEC (2000) [1].

Although a great variety of methods have been applied to the analysis of the aforementioned compounds in foods, only a few procedures are suitable for the simultaneous determination of sodium saccharin and sodium cyclamate in a same sample. High performance liquid chromatography

* Corresponding author. Tel.: +34 354 3158; fax: +34 354 4838.
E-mail address: salvador.garrigues@uv.es (S. Garrigues).

0003-2670/$ – see front matter © 2004 Elsevier B.V. All rights reserved.
doi:10.1016/j.aca.2004.05.077

(HPLC) is the most frequently technique used nowadays. Most HPLC procedures were based on isocratic [2] or gradient reversed-phase (RP) chromatographic separation and ultraviolet absorbance detection [3]. In addition, ion chromatography (IC) offers an attractive alternative to traditional HPLC methods [4]. In the past few years, micellar electrokinetic chromatography (MEKC) has been applied to the simultaneous determination of several kinds of sweeteners in foods [5]. Other methods less commonly used for saccharin and cyclamate determination are an amperometric method based on the use of bilayer lipid membranes [6], a flow injection spectrophotometry procedure for the determination of cyclamate after conversion to cycloheylamine and the subsequent reaction with 1,2-naphtoquinone-4-sulfonate and detection at 480 nm [7] and the use of an ion selective electrode for saccharin determination [8].

Even though FT-Raman spectroscopy offers the possibility to carry out direct measurements on solids [9,10] there are no precedents for the determination of sweeteners in table top commercial formulations by this technique.

The aim of the present study is the development of an accurate, fast and environmentally friendly methodology for the analysis of solid table top sweeteners that can be applied for quality control in the manufacturing industry.

2. Experimental

2.1. Apparatus and reagents

A Bruker RFS 100/S (Bremen, Germany) Fourier transform Raman spectrometer equipped with a 2 W maximum power Nd:YAG laser, that emits at 1064 nm, was employed to obtain Raman spectra of solid samples in the back scattering mode, using 2 ml volume and 12 mm internal diameter glass chromatographic vials as sample cells.

Spectra treatment and data manipulation were carried out using Omnic 2.1 and Omnic Macros 2.1 (Thermo Nicolet Corp., Madison, WI, USA). PLS calibration models were obtained by using TurboQuant Analyst 6.0 software (Thermo Nicolet Corp., Madison, WI, USA).

A Hewlett-Packard Series 1050 (Palo Alto, CA, USA) high performance liquid chromatograph, equipped with a variable wavelength UV-Vis detector and a Kromasil C-18, 250 mm × 4.6 mm i.d. and 5 μm particle diameter column was employed for the analysis of table top sweeteners, being used this methodology as a reference for the validation of FT-Raman determinations.

An ultrasonic water bath J.P. Selecta (Barcelona, Spain) was employed to improve a fast sweetener extraction or dissolution.

Sodium saccharin standard (99.3% w/w), sodium cyclamate (99.0% w/w) and glucose monohydrate (99.0% w/w) were supplied by Guinama (Barcelona, Spain). Additionally, sodium chloride, KH_2PO_4 and acetonitrile (99.8% v/v) supplied by Scharlau (Barcelona, Spain), were employed for the preparation of samples and standards or chromatographic analysis.

Commercial sweeteners were obtained directly from the Spanish market. The commercial table top sweeteners analysed can be separated in two different groups: group A integrated by sweeteners containing sodium saccharin, sodium cyclamate and glucose monohydrate (samples 1–3) and group B for sweeteners with sodium saccharin, sodium cyclamate, maltose, bicarbonate and citrate, without glucose monohydrate (samples 4–6).

2.2. HPLC-UV reference procedure

Twenty milligrams of sample were accurately weighted inside a 25 ml volumetric flask and diluted to the volume with 0.02 M KH_2PO_4:acetonitrile (90:10 v/v), being sonicated during 5 min in an ultrasonic water bath to extract sweeteners from the matrix. One milliliter of the extract was diluted to 10 ml and filtered through a 0.22 μm nylon membrane. Twenty microliters of this latter solution was directly injected in a 0.02 M KH_2PO_4:acetonitrile (90:10 v/v) mobile phase of 0.75 ml min^{-1} carrier flow and sodium saccharin and sodium cyclamate were determined in the isocratic mode by using absorbance measurements at 205 nm and from peak area values of the chromatogram obtained at 7.4 and 9.3 min, respectively.

Calibration lines obtained with the aforementioned conditions were $A_1 = (0.1 \pm 0.2) + (136.63 \pm 0.04)C_{SS}$ with an $R^2 = 0.99998$, and $A_2 = (0.3 \pm 0.2) + (0.241 \pm 0.001)C_{SC}$ with an $R^2 = 0.9997$ for sodium saccharin (C_{SS}) and sodium cyclamate (C_{SC}), respectively, being A_1 and A_2 area values found at the aforementioned elution times.

The repeatability, established as the relative standard deviation of 0.15 and 0.3% for five independent injections of a 0.7 mg l^{-1} sodium saccharin standard and a 16.5 mg l^{-1} sodium cyclamate, and a limit of detection of 0.0005 and 0.07% w/w for sodium saccharin and sodium cyclamate, respectively, were achieved by this procedure.

2.3. FT-Raman external monoparametric calibration procedure

Three hundred milligrams of commercial sweeteners of group A were grounded and homogenized for 5 min in an agate mortar, previously to be introduced in a chromatographic standard glass vial. The FT-Raman spectra was recorded between 3500 and 75 cm^{-1}, at 4 cm^{-1} nominal resolution and accumulating 64 scans per spectrum. The Nd:YAG laser power employed was fixed at 250 mW. A Blackman-Harris 4 apodization function, a scan velocity of 2.2 kHz, a zero filling factor of 2 and an aperture of 10 mm were also used for spectra acquisition.

For samples of group B, 100 mg were diluted with 300 mg of sodium chloride and were measured in the aforementioned conditions.

An external calibration curve was established with solid sodium saccharin and sodium cyclamate diluted with sodium chloride at different levels, from 0.98 to 10.26 and from 3.94 to 28.39% w/w, respectively. For sodium saccharin determination peak height values at 1592 cm^{-1} corrected using a baseline defined at 1975 cm^{-1} were used. Sodium cyclamate was quantified by using peak height values at 806 cm^{-1} corrected with a baseline defined at 1800 cm^{-1}.

2.4. PLS/FT-Raman procedure

FT-Raman spectra of the commercial samples were recorded under the aforementioned conditions.

The finally proposed PLS model was made using eight standards for calibration. These standards correspond to different mixtures of sodium saccharin, sodium cyclamate and glucose monohydrate at two different concentration levels (2^3). Sodium saccharin was fixed at 1.1 and 6.7% w/w, sodium cyclamate was evaluated at 5.7 and 67.6% w/w and glucose monohydrate at 14.7 and 88.7% w/w.

Concentration of sodium saccharin and sodium cyclamate in samples was calculated employing the PLS calibration using the information in the spectral range between 3003 and 2815, 1493–964, 2692–2642, 3113–3045, 955–259 and 3292–3255 cm^{-1}, corrected with baselines defined between 3105 and 2816, 1741–964, 2640 (a single point baseline), 3116–3041, 960–256 and 3440–2501, respectively.

3. Results and discussion

3.1. FT-Raman spectrum of artificial sweeteners

Fig. 1 shows the FT-Raman spectra of sodium saccharin, sodium cyclamate and glucose monohydrate standards diluted with sodium chloride and those of the commercial table top sweetener samples analysed.

The most intense bands present at the sodium saccharin spectra are those concerning the aromatic CH stretching band at 3075 cm^{-1}, that of 1594 cm^{-1} due to the C=C stretching, those at 1292, 1166 and 1144 cm^{-1} corresponding to the asymmetric and symmetric (two bands) SO_2 stretching, respectively, and the bands at 1019 and 708 cm^{-1}, which correspond to ring vibration and CS stretching, respectively [11]. From these bands it can be seen that the band located at 1592 cm^{-1} is isolated and seems appropriate to be employed in the external calibration.

For sodium cyclamate, the most intense bands are located between 2960 and 2850 cm^{-1} due to CH_2 stretching. Other less intense bands were at 1445, 1264 and 806 cm^{-1} due to CH_2 deformation, ring "breathing" in cyclohexane "boat" conformation and in "chair" conformation, respectively. Bands at 1058 and 1033 cm^{-1} correspond to the S=O stretching [11]. Different bands appear not overlapped (806, 1475, 1264, 988 cm^{-1}) with other component in sweetener

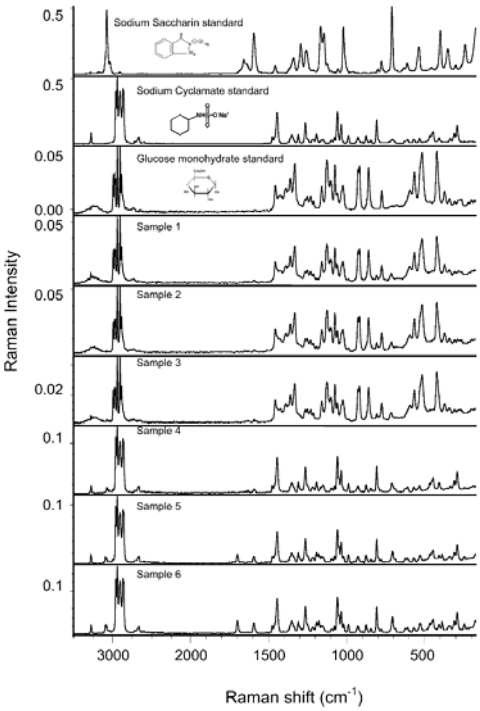

Fig. 1. FT-Raman spectra of pure sodium saccharin, sodium cyclamate and glucose monohydrate and six commercial table top sweetener formulations. Spectra are the average of 64 accumulated scans using a nominal resolution of 4 cm^{-1} and a laser power of 250 mW.

formulation and thus, could be suitable for sodium cyclamate determination by external calibration.

Glucose monohydrate, which is an additive used in three of the sample assayed (group A) shows an important number of bands in the region between 1800 and 250 cm^{-1} and can affect seriously the FT-Raman determination of sodium saccharin and sodium cyclamate by using both, external calibration and PLS approach. So, this compound was also considered in modelling FT-Raman spectra.

3.2. Effect of FT-Raman measurement conditions on sweeteners determination

The effect of the number of accumulated scans and the laser power employed for data acquisition were tested in order to improve the measurement conditions. The number of accumulated scans was modified from 36 to 121 and the laser power varied from 125 to 1250 mW.

Fig. 2 shows the signal to noise ratio (S/N) variation as a function of both, laser power and number of scans. The

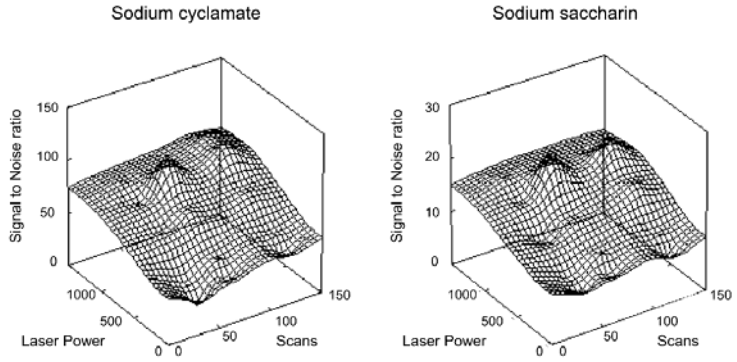

Fig. 2. Effect of the number of accumulated scans and laser power on signal to noise ratio, established from the ratio between peak height measurements at 1592 cm^{-1} (corrected with a single point baseline located at 1975 cm^{-1}) for sodium saccharin and at 806 cm^{-1} (baseline at 1800 cm^{-1}) for sodium cyclamate, and the noise measured as root mean square in the region between 2200 and 2000 cm^{-1} on the sample 1 and employing a nominal resolution of 4 cm^{-1}.

best signal to noise ratio, obtained as a ratio of the peak height signal at 1592 and 806 cm^{-1}, for sodium saccharin and sodium cyclamate, respectively, and the noise measured as root mean square in the region between 2200 and 2000 cm^{-1}, was achieved when a laser power of 1000 mW and 64 accumulated scans per spectra were used. However, on employing these conditions the linear range achieved for sodium cyclamate was lower than 10% w/w. Because of this, samples of group B should be previously diluted below this value and in these conditions, the concentration of sodium saccharin in diluted samples becomes lower than the limit of detection. To avoid that, a laser power of 250 mW was selected, despite of the lower S/N obtained for sodium cyclamate, because the linear range obtained was upper than 25% w/w thus making possible the simultaneous determination of both sweeteners in samples with a small concentration of sodium saccharin.

In order to ensure a compromise between sampling throughput and precision 64 scans per spectra were selected that provides a faster spectral recording than the accumulation of 121 scans.

Other instrumentals parameters tested were the zero filling factor and scan velocity. As can be seen in Fig. 3 the best S/N was obtained for a zero filling factor of 2 and a scan velocity of 2.2 kHz.

3.3. Selection of bands for FT-Raman determination

As it is indicated in Table 1 different bands were tested for the determination of sodium saccharin and sodium cyclamate in commercial table top sweeteners. Peak height and area values employing different baseline correction were assayed for FT-Raman analysis.

The use of the band at 1592 cm^{-1} with a single point baseline fixed at 1975 cm^{-1} provided for sodium saccharin determination an excellent linearity, a repeatability, measured as relative standard deviation, of the order of 0.8% and a limit of detection of 0.2% w/w.

On the other hand, as can be seen in Table 1, the most appropriate condition for sodium cyclamate determination

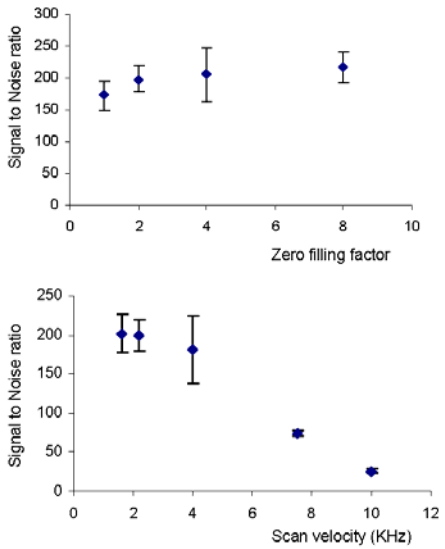

Fig. 3. Effect of the zero filling factor and scan velocity on the signal to noise ratio for sodium cyclamate, in sample 1, measured in the same conditions described in Fig. 2. Experimental conditions: 4 cm^{-1} nominal resolution and 64 accumulated scans per spectra. Values indicated are the average of three measurements and error bars correspond to the standard deviation.

Table 1
Analytical features of the FT-Raman determination of sodium saccharin and sodium cyclamate using different bands and baseline criteria

Sweetener	Measurement mode	Band	Baseline	Sweetener calibration curve ($y = a + bC$ (g g^{-1}))					
				$a \pm s_a$	$b \pm s_b$	R^2	% RSD[a]	LOD (% w/w)[b]	% Mean E_r[c]
Sodium saccharin	Height	1592	1975	0.00030 ± 0.00003	0.001199 ± 0.000005	0.9997	0.8	0.2	5.7
	Area	1597–1587		0.003 ± 0.001	0.0709 ± 0.0004	0.998	0.7	0.7	27
Sodium cyclamate	Height	806	1800	0.00083 ± 0.00013	0.001117 ± 0.000008	0.9993	1.2	0.8	1.1
	Area	811–801		0.021 ± 0.003	0.0082 ± 0.0002	0.992	1.9	1.2	27
	Height	1475	1550	0.00022 ± 0.00010	0.000301 ± 0.000006	0.994	1.9	3	11
	Area	1480–1470		0.0010 ± 0.0009	0.00237 ± 0.00006	0.992	5	3	14
	Height	1264	1550	0.0010 ± 0.0003	0.00094 ± 0.00002	0.996	0.4	1.1	13
	Area	1269–1259		0.008 ± 0.003	0.0086 ± 0.0002	0.993	0.4	1.7	23
	Height	988	1550	0.0007 ± 0.0002	0.000379 ± 0.000014	0.98	1.1	2	26
	Area	993–983		0.0045 ± 0.0016	0.00346 ± 0.00011	0.99	0.5	0.7	12

[a] Relative standard deviation obtained for five independent measurements carried out.
[b] Limit of detection established for six independent measurements of sodium chloride blank and a probability level of 99.6% ($k = 3$).
[c] Mean accuracy error expressed in % w/w obtained from the analysis of six samples.

were the use of the band at 806 cm^{-1} with a horizontal baseline fixed at 1800 cm^{-1}. It provides a repeatability of 1.2% and a limit of detection of the order of 0.8% w/w, adequate to carry out the sweetener determination in table top samples.

The mean relative accuracy error obtained for sodium saccharin and sodium cyclamate determination in all the samples, employing the best conditions assayed, were 5.7 and 1.1% w/w, respectively, as compared the results found with those obtained by HPLC.

3.4. PLS determination of sweeteners in table top samples

The possibility of a multivariate calibration technique such as the partial least squares (PLS) treatment of the FT-Raman data was evaluated based on the use of a classical design of 2^2 standards for the two analytes, sodium saccharin and sodium cyclamate, at two concentration levels.

Table 2 shows the analytical features of the use of a PLS/FT-Raman model for the determination of sodium saccharin and sodium cyclamate as a function of the use of different spectral regions and baseline criteria. It has been indicated the number of factors required for prediction of each analyte concentration with the minimum predicted residual error sum of squares (PRESS), the R^2 of the calibration model, the root mean square error of calibration (RMSEC) and the mean accuracy errors found as compared with HPLC data.

As can be seen, in the best conditions mean accuracy errors of the order of 2.2 and 2.4% w/w were obtained for sodium saccharin and sodium cyclamate, respectively, in

Table 2
Analytical features of PLS/FT-Raman determination of sodium saccharin and sodium cyclamate using a calibration model based on the use of four standards containing both analytes at two concentration levels

Data employed (cm^{-1})		Component	Factors[a]	Analytical characteristics found				
Region	Baseline			R^2[b]	RMSEC[c]	Mean accuracy error[d] (%)		
						Total	Group A	Group B
3305–169	3460–3400[e]	Sodium saccharin	3	0.9998	0.043	262	359	67
		Sodium cyclamate	1	0.9998	0.624	45	63	11
3305–2621	3460–3400[e]	Sodium saccharin	3	0.9994	0.093	28	38	8
1700–1520	1952–1800[e]	Sodium cyclamate	1	0.9997	0.679	26	36	7
822–795	1886							
3313–3006	3460–3400[e]	Sodium saccharin	6	1.0000	0.002	10	13	2.2
1618–1564	1961–1820[e]	Sodium cyclamate	2	0.9997	0.658	13	18	2.4
999–970	1003–966							
813–796	1969–1817[e]							

[a] The number of factors were chosen in order to obtain the minimum press.
[b] R^2 is the correlation coefficient of the regression line between predicted and actual values of analyte concentration in the calibration set.
[c] Root mean square error of calibration for a cross-validation expressed in % w/w.
[d] Mean accuracy error (%) found from the comparison with results obtained by HPLC.
[e] Baseline was established as the average measurement in the indicated range.

Table 3
Analytical features obtained for the PLS/FT-Raman determination of sodium saccharin and sodium cyclamate using a model which incorporates glucose monohydrate

Data employed (cm^{-1})		Component		Factors[a]	Analytical characteristics found				
Region	Baseline				R^{2b}	RMSEC[c]	Mean accuracy error[d] (%)		
							Total	Group A	Group B
R1: 3500–100	–	Sodium saccharin	R1	3	0.96	0.70	171.5	29.6	281.9
		Sodium cyclamate	R1	5	0.998	1.54	53.2	13.1	84.4
		Glucose	R1	2	0.992	3.9	5.3	5.3	–
R1: 3299–2815	3463–2468	Sodium saccharin	R1, R2	8	0.99996	0.022	48.4	7.1	80.4
R2: 1653–214	1961	Sodium cyclamate	R1, R2	3	0.991	3.7	39.9	22.9	53.2
		Glucose	R1, R2	3	0.997	2.3	4.6	4.6	–
R1: 3002–2815	3104–2815	Sodium saccharin	R1–R4	8	0.99996	0.023	4.9	2.2	6.9
R2: 1492–963	1741–964	Sodium cyclamate	R1–R4	7	0.99992	0.35	6.6	6.1	6.9
R3: 3112–3045	3116–3041	Glucose	R1–R4	2	0.996	2.6	4.3	4.3	–
R4: 954–259	960–256								
R1: 3002–2815	3104–2815	Sodium saccharin	R1–R5	8	0.99995	0.024	12.5	6.5	23.2
R2: 1492–269	1741–260	Sodium cyclamate	R1–R5	7	0.990	3.9	20.1	15.3	19.4
R3: 2692–2642	2640	Glucose	R1–R5	2	0.997	2.3	4.1	4.1	–
R4: 3112–3045	3116–3041								
R5: 3291–3255	3440–2501								
R1: 3002–2815	3104–2815	Sodium saccharin	R1–R5	9	0.99999	0.0084	4.1	1.7	5.9
R2: 1492–963	1741–964	Sodium cyclamate	R1–R5	9	1.00000	0.062	2.1	2.3	1.9
R3: 3112–3045	3116–3041	Glucose	R1–R5	2	0.996	2.7	4.3	4.3	–
R4: 954–259	960–256								
R5: 3291–3255	3440–2501								
R1: 3002–2815	3104–2815	Sodium saccharin	R1–R6	9	1.00000	0.0064	1.1	1.2	1.1
R2: 1492–963	1741–964	Sodium cyclamate	R1–R3—R5, R6	7	0.99992	0.060	1.9	1.9	1.8
R3: 2692–2642	2640	Glucose	R1, R2—R4, R5	2	0.996	2.7	4.3	4.3	–
R4: 3112–3045	3116–3041								
R5: 954–259	960–256								
R6: 3291–3255	3440–2501								

Ri: regions identified in each conditions were employed for the modelling and prediction of each analyte in order to minimize the RMSEC.
[a] The number of factors were chosen in order to obtain the minimum press.
[b] R^2 is the correlation coefficient of the regression line between predicted and actual values of analyte concentration in the calibration set.
[c] Root mean square error of calibration for a cross-validation expressed in % w/w.
[d] Mean accuracy error (%) found from the comparison with results obtained by HPLC.

samples of group B. However errors higher than 13% w/w were found for samples of group A.

The aforementioned data clearly show that the presence of glucose monohydrate in actual samples strongly affect the prediction capability of the PLS model, due to the spectral overlapping of the bands provided by the latter compound (see Fig. 1). So, an alternative PLS/FT-Raman model, based on the consideration of glucose monohydrate additionally than the two analytes at two concentration levels (2^3 standards) was used.

On using the extended PLS calibration model (Table 3) it can be seen that mean accuracy errors lower than 1.9% w/w could be found for both analytes in all the samples, those including glucose monohydrate (group A) and samples of group B.

Additionally, the extended model provides a predicted concentration of glucose monohydrate which compares well with the concentration level provided by the manufacturers with average absolute differences of 4.3% w/w.

4. Comparison between different methodologies assayed

Table 4 shows that the FT-Raman and HPLC provide comparable data for sodium saccharin and sodium cyclamate in table top sweetener samples by using both external calibration and PLS/FT-Raman data treatment, but it is clear that the accuracy errors found by using PLS are lower than those obtained by external monoparametric calibration.

When concentrations found by PLS/FT-Raman using the extended model were represented in front of those obtained by HPLC and adjusted by a linear function, the fitted equations were $C_{\text{FT-Raman}} = (-0.017 \pm 0.027) + (0.998 \pm 0.006)C_{\text{HPLC}}$ with an $R^2 = 0.9995$, for sodium saccharin and $C_{\text{FT-Raman}} = (-0.1 \pm 0.4) + (1.001 \pm 0.009)C_{\text{HPLC}}$ with an $R^2 = 0.999$ for sodium cyclamate. In these equations the intercept and slope values were statistically comparable to 0 and 1, respectively, for a probability level of 95%, thus indicating that the developed procedures

Table 4
Determination of sodium saccharin and sodium cyclamate in different table top sweetener samples by PLS/FT-Raman using the extended model and HPLC-UV

Sample	HPLC	FT-Raman	% E_r[a]	PLS/FT-Raman	% E_r[a]
Sodium saccharin					
1	1.21 ± 0.02	1.24 ± 0.10	2.5	1.21 ± 0.01	0.3
2	2.21 ± 0.07	1.9 ± 0.3	−14	2.18 ± 0.03	−1.4
3	1.81 ± 0.03	1.74 ± 0.08	−3.8	1.77 ± 0.04	−2.5
4	5.74 ± 0.11	5.5 ± 0.4	−5.3	5.65 ± 0.01	−1.5
5	6.42 ± 0.04	6.3 ± 0.5	−2.5	6.36 ± 0.03	−1.0
6	6.31 ± 0.01	6.9 ± 0.3	7.9	6.36 ± 0.02	0.8
Sodium cyclamate					
1	10.1 ± 0.2	9.8 ± 0.3	−2.7	10.09 ± 0.04	−0.1
2	7.71 ± 0.18	7.8 ± 0.2	0.8	7.4 ± 0.1	−4.1
3	8.70 ± 0.09	8.8 ± 0.6	0.7	8.6 ± 0.3	−1.4
4	62.0 ± 0.2	61.2 ± 0.5	−1.2	63.36 ± 0.06	2.2
5	64.2 ± 0.5	63.9 ± 0.7	−0.5	62.9 ± 0.4	−2.1
6	67.5 ± 0.3	67.9 ± 0.8	−0.6	67.4 ± 0.7	−0.1

[a] Accuracy relative error obtained from the comparison with the HPLC values.

provide an accuracy comparable with that of the HPLC method.

On the other hand, the developed FT-Raman provides a fast alternative to the chromatographic method (12 samples per hour in front of the 4 samples per hour), and on comparing the reagent consumption and waste generation, it can be seen that the FT-Raman procedure is an environmentally friendly methodology which eliminates the use of solvents and avoids waste generation. Moreover, the FT-Raman measurements using standard glass vials allow the storage and conservation of samples after their analysis, being a non-destructive technique.

However, FT-Raman spectrometry is a low sensitivity technique which provides a limit of detection of 0.2% for sodium saccharin and 0.8% for sodium cyclamate, clearly worse than those obtained by HPLC (0.0005 and 0.07% w/w, respectively) but appropriate for the determination of sodium saccharin and sodium cyclamate in table top sweeteners. The use of highly energetic excitation laser (operating at wavelengths i.e. 785, 515, 488 nm, etc.) and effective back scattering optics (like those employed in Raman microscopy), would provide lower detection limits than those reported in this study. Additionally, the use of thin wall glass vials or the direct powder measurement without using glass vial could contribute to reduce the loss of the back scattering light and also to enhance the sensitivity of Raman measurements.

Acknowledgements

Authors acknowledge the financial support of the Generalitat Valenciana (Agència Valenciana de Ciència i Tecnologia) to the Project Grupos 03/118, and the grant provided by the Laboratorio de Higiene Laboral y Ambiental of the Universitat de València to carry out this study. S. Armenta acknowledges the FPU Grant of the Ministerio de Educación, Cultura y Deporte (Ref. AP2002-1874).

References

[1] International Sweeteners Association, Brussels.http://www.isabru.org/
[2] M. Calull, R.M. Marce, G. Sanchez, F. Borrull, J. Chromatogr. 607 (1992) 339.
[3] Macherey-Hagel, Application Note A-1835, 2000, p. 2.
[4] Q.C. Chen, S.F. Mou, K.N. Liu, Z.Y. Yang, Z.M. Ni, J. Chromatrogr. A 771 (1997) 135.
[5] M.C. Boyce, J. Chromatrogr. A 847 (1999) 369.
[6] D.P. Nikolelis, S. Pantoulias, Electroanalysis 12 (2000) 786.
[7] C. Cabero, J. Taurina, S. Hernandez-Cassou, Anal. Chim. Acta 381 (1999) 307.
[8] R.V.S. Alfaya, A.A.S. Alfaya, Y. Gushikem, S. Rath, F.G.R. Reyes, Anal. Lett. 33 (2000) 2859.
[9] S. Armenta, G. Quintas, S. Garrigues, M. de la Guardia, Anal. Chim. Acta, doi:10.1016/j.aca.2004.02.063.
[10] S.G. Skoulika, C.A. Georgiou, Appl. Spectrosc. 55 (2001) 1259.
[11] D. Lin-Vien, N.B. Colthup, W.G. Fateley, J.G. Grasselli, Infrared and Raman Characteristic Frequencies of Organic Molecules, Academic Press, London, 1991.

Solid-phase FT-Raman determination of caffeine in energy drinks

Sergio Armenta, Salvador Garrigues and Miguel de la Guardia
[a]*Department of Analytical Chemistry, Universitat de València. Edifici Jeroni Muñoz, 50th Dr Moliner, 46100 Burjassot, Valencia, Spain.*

Analytical Chimica Acta 547 (2005) 197-203.

Impact factor of this journal (2004): 2.588
Source: Journal citation reports ISI Web of Knowledge, 2004.

Available online at www.sciencedirect.com
SCIENCE DIRECT®
Analytica Chimica Acta 547 (2005) 197–203
ANALYTICA CHIMICA ACTA
www.elsevier.com/locate/aca

Solid-phase FT-Raman determination of caffeine in energy drinks

Sergio Armenta, Salvador Garrigues*, Miguel de la Guardia

Department of Analytical Chemistry, Universitat de València, Edifici Jeroni Muñoz, 50th Dr. Moliner, 46100 Burjassot, Valencia, Spain

Received 21 February 2005; received in revised form 12 May 2005; accepted 13 May 2005
Available online 9 June 2005

Abstract

A solid-phase vibrational spectrometry-based methodology (solid-phase Fourier transform-Raman spectrometry, SP-FT-Raman) has been developed for caffeine determination in commercial energy drink samples. The Raman spectra of caffeine, fixed on a C18 solid phase packed into a glass tube of 5 mm i.d., was obtained directly between 3500 and 70 cm^{-1}. In order to quantify caffeine, Raman intensity between 573 and 542 cm^{-1} corrected using a baseline defined between 580 and 540 cm^{-1} was used. A repeatability of 3%, as relative standard deviation of five analysis of a 200 $mg\,l^{-1}$ concentration, and a limit of detection of 18 $mg\,l^{-1}$ were obtained. The SP-FT-Raman procedure provides a sampling frequency of 13.3 h^{-1}, higher than that of liquid chromatography (LC), which was 7.0 h^{-1}. The use of FT-Raman reduces the reagent consumption and waste generation, also minimizing the sample handling. Results obtained by the developed procedure were statistically comparable with those found by a reference LC method.

Keywords: Caffeine; Energy drink; FT-Raman; Solid phase

1. Introduction

Caffeine, 1,3,7-trimethylxanthine, is an alkaloid found in natural products like tea, coffee, guarana, cola nuts, cocoa beans, mate and other plants. It is also present in many painkillers and antimigraine pharmaceuticals. Caffeine is a powerful stimulant of the central nervous system and also stimulates the cardiac muscle. However, high amounts of this alkaloid have noticeable irritation of gastrointestinal tract as well causes many unwanted effects [1].

With the recent reemergence of medicinal herbs as a major player in the global dietary supplement market, new products-containing caffeine has been introduced. Of these, dry extracts of caffeine-containing herbs and carbonated beverages, known as power or energy drinks, enriched with pure caffeine or caffeine extracts are becoming popular. Therefore, determination of caffeine in soft energy drinks is nowadays an important chemical analysis.

Caffeine has been determined in drinks by different analytical techniques, such as UV–vis spectrophotometry [2], potentiometry [3] or amperometry [4] and most frequently by using separation methods like liquid chromatography (LC) [5], ion chromatography [6], high performance thin layer chromatography (HPTLC) [7], capillary electrophoresis [8], micellar capillary electrophoresis [9] as well as gas chromatography [10] and solid-phase microextraction gas chromatography [11].

Caffeine can be also determined in beverages by the use of Fourier transform infrared spectrometry (FTIR) after extraction in chlorinated solvents [12,13] and directly by employing attenuated total reflectance [14].

The AOAC International official method of analysis of caffeine in non-alcoholic beverages is based on spectroscopic measurements after a complex and time consuming treatment of the sample with acid and basic Celite columns [15].

On the other hand, the combination of solid phase (SP) and molecular spectrometry has been successfully applied since 1976 [16]. The flow injection-solid phase spectrometry is nowadays a well-established technique based on the measurement of the analyte retained on an active solid support placed in an appropriate flow cell of a non-destructive detector. Solid-phase spectrophotometry has been applied to the determination of ciprofloxacin [17], acetylsalicylic

* Corresponding author. Tel.: +34 354 3158; fax: +34 354 4838.
E-mail address: salvador.garrigues@uv.es (S. Garrigues).

0003-2670/$ – see front matter © 2005 Elsevier B.V. All rights reserved.
doi:10.1016/j.aca.2005.05.032

acid [18], ascorbic acid and paracetamol [19] and caffeine, dimenhydrinate and acetaminophen [20] in drug formulations, using SP-UV spectrometry and for the determination of 1-naphthylamine through solid phase near infrared spectrometry (SP-NIR) [21].

The main object of this work has been the development of a solid-phase Fourier transform-Raman spectrometry (SP-FT-Raman) procedure for the simple, fast and reagent free caffeine determination in energy drinks.

2. Experimental

2.1. Apparatus and reagents

A Bruker RFS 100/S (Bremen, Germany) Fourier transform-Raman spectrometer equipped with a 2 W maximum power Nd:YAG laser that emits at 1064 nm, was employed to obtain Raman spectra of solid samples in the back scattering mode, using a glass tube of 5 mm i.d. as sample cell. Spectra treatment and data manipulation were carried out using Omnic 2.1 and Omnic Macros 2.1 (Thermo Nicolet Corp., Madison, WI, USA).

The set-up employed for FT-Raman determination of caffeine was based on the on-line retention of the alkaloid in the measurement cell. A Gilson Minipuls P2 (Villiers-le-Bel, France) peristaltic pump and 1 mm i.d. tygon pump tube and PTFE 0.8 mm i.d. connecting tubes were used to introduce the sample into the manifold. C18 bonded silica and an anionic LC-SAX solid phase both from Supelco (Madrid, Spain) with average particle sizes of 55–105 and 50–70 μm, respectively, were used as solid support. Glass wool from Panreac (Barcelona, Spain) was placed at the inlet and outlet of the glass tube, to avoid removal of the solid phase by the carrier stream, and also between the two solid phases.

A Dionex P680 Liquid Chromatograph (Sunny Vale, CA, USA), equipped with a C18 reversed phase (Kromasil) column (250 mm × 4.6 mm i.d. and 5 μm particle diameter) and an UVD 170U variable wavelength UV–vis detector was also employed for the determination of caffeine in energy drinks, being used this methodology as a reference procedure for the validation of solid-phase FT-Raman measurements.

A J.P. Selecta ultrasonic water bath (Barcelona, Spain) was employed to degassing the samples previously to their analysis.

Caffeine standard was obtained from Fluka (Buchs, Switzerland). HPLC grade methanol and KH_2PO_4, used as mobile phase, were purchased from Panreac (Barcelona, Spain). Commercial energy drink samples were obtained directly from the Spanish market.

2.2. Reference procedure

One to two grams of degassed sample was weighted inside a 10 ml volumetric flask and diluted to the volume with water. This solution was filtered through a 0.22 μm nylon filter and 20 μl were directly injected in a methanol:KH_2PO_4 2 mM (pH 3.2) (55:45) mobile phase using 1 ml min^{-1} carrier flow. Caffeine was determined in the isocratic mode by absorbance measurements at 275 nm. Area values of the chromatographic peaks obtained at a retention time of 3.50 min were interpolated in an external calibration line established from the measurement of six standard solutions of caffeine from 15.3 to 44.8 mg l^{-1}.

A typical calibration line obtained in the aforementioned conditions was $A = (-0.03 \pm 0.14) + (1.274 \pm 0.005)C_{caf}$ with a $r^2 = 0.9998$ ($n = 6$), being A peak area values and C_{caf} the concentration in mg l^{-1}. The repeatability, established as the relative standard deviation, for five independent injections of a 15.3 mg l^{-1} caffeine was of 0.09% and a limit of detection of 0.05 mg l^{-1} was achieved by this procedure.

2.3. Solid-phase FT-Raman determination of caffeine

A 5 mm i.d. glass cartridge was filled up with 300 mg LC-SAX and 300 mg C18 solid phase separated by glass wool. It was activated with 2 ml methanol and 2 ml water. Ten milliliters of degassed sample were passed through the activated cartridge with a carrier flow rate of 7.5 ml min^{-1}. After that, the cartridge was washed with 20 ml distilled water and dried with N_2 stream. The glass cartridge was placed on the sample holder and the FT-Raman spectra were recorded directly in the solid-phase focusing the laser beam at 10 mm from the top of the C18 phase and using a 4 cm^{-1} nominal resolution and accumulating 50 scans per spectrum. The Nd:YAG laser power employed was fixed at 1500 mW. A Blackman–Harris 4 apodization function, a scan velocity of 0 (1.4 kHz), a zero filling factor of 2 and an aperture of 10 mm were also employed for spectra acquisition.

A calibration curve was established loading the cartridge with 10 ml of different caffeine standard solutions, from 100 to 600 mg l^{-1}, which were adsorbed in the solid phase using the same conditions employed for samples.

For quantitative purposes peak area values between 573 and 542 cm^{-1} shift of the Raman spectra, corrected using a two points baseline defined between 580 and 540 cm^{-1} were used.

Caffeine was completely removed from the solid phase after each measurement by employing 3 ml methanol and washing with 5 ml water.

3. Results and discussion

3.1. FT-Raman spectrum of caffeine in solid phase

Fig. 1 shows the FT-Raman spectra of a C18 blank cartridge, a cartridge loaded with 10 ml of a 400 mg l^{-1} caffeine standard solution and those of different samples retained in the solid phase.

The most intense bands of the caffeine spectra are those concerning the C–N stretching band at 1300 and that of

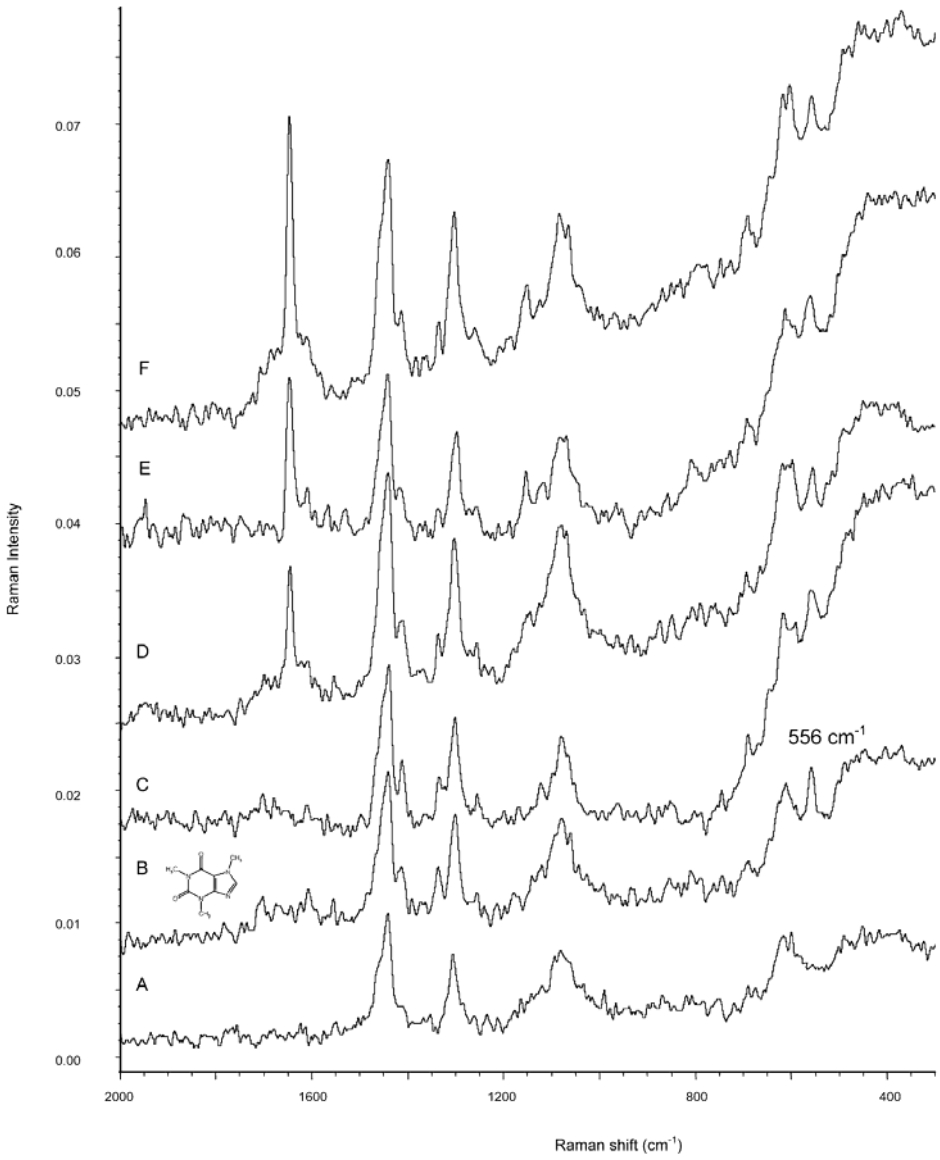

Fig. 1. FT-Raman spectra of (A) a C18 blank cartridge, (B) a cartridge loaded with 10 ml of a 400 mg l^{-1} caffeine standard solution and (C–F) 10 ml of different samples retained in the solid phase. *Note:* spectra were shift in the emission scattering intensity axe for clarity purposes.

556 cm^{-1} due to the C–N–CH_3 deformation. Other less intense bands are those located at 1600, 1550 and 1241 cm^{-1} due to C=C stretching, C=O symmetric stretching and C–N stretching, respectively [22].

On the other hand, it must be also noticed that the solid-phase bands are located between 3000 and 2828 cm^{-1} due to CH_2 aliphatic stretching. Other less intense bands were at 1440, 1305, 1077 and 614 cm^{-1} due to CH_2 and CH_3 deformation, Si–O–Si symmetrical stretching and asymmetrical Si–O–Si stretching, respectively [23].

On comparing the spectra of the caffeine standard retained and the blank cartridge, it can conclude that the bands located at 1335 and 556 cm^{-1} are well-isolated and seem appropriate to be employed in the solid-phase FT-Raman determination of caffeine in energy drinks. On the other hand, in sample spectra, the typical bands of caffeine are also well-resolved and apparently free from matrix interferences.

3.2. Effect of experimental conditions on caffeine determination

3.2.1. Variables of the retention-detection unit

Preliminary studies made on actual samples evidenced (see Fig. 2) that the direct retention of samples in a C18 cartridge provides a poor baseline under 1200 cm^{-1}, which affects dramatically the Raman shift measurement range and is probably due to the retention of matrix components additionally than caffeine. In order to avoid matrix effects and to improve the selectivity of the Raman measurements, it was assayed the use of an additional anionic solid phase (LC-SAX) located before the C18, which could clean the samples by retaining matrix components without reducing the amount of caffeine finally retained in the measurement cell, being obtained well-defined Raman spectra.

On the other hand, the retention capacity of the solid phase was tested. The retention process of analytes on a solid support depends on the volume and concentration of analyte solution and the mass of sorbent. Three hundred milligrams of C18 was used because it was the necessary amount to fill the appropriate height of the glass tube and to facilitate the handling of samples and cartridges. Different amounts of caffeine from 1 to 10 mg corresponding to 2–20 ml of a solution of 500 mg l^{-1} caffeine, were retained on the solid support using a loading carrier flow of 7.50 ml min^{-1}. As can be seen in the inset of Fig. 2, 7 mg of caffeine was the maximum amount retained quantitatively in 300 mg of the adsorbent, corresponding this value to a 2.3% (w/w) final concentration in the solid support.

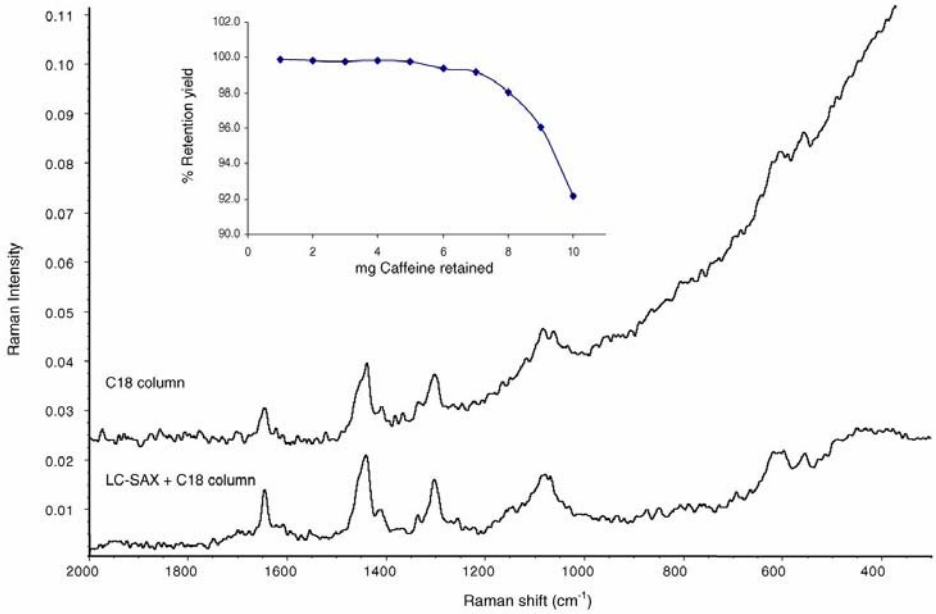

Fig. 2. Raman spectra of a sample retained on a C18 column and on the same column with a previous LC-SAX load. Inset: retention capacity of C18 solid phase. Different amounts of caffeine from 1 to 10 mg (corresponding to 2–20 ml of a solution of 500 mg l^{-1}) were retained on 300 mg of the solid support using a loading flow rate of 7.50 ml min^{-1}.

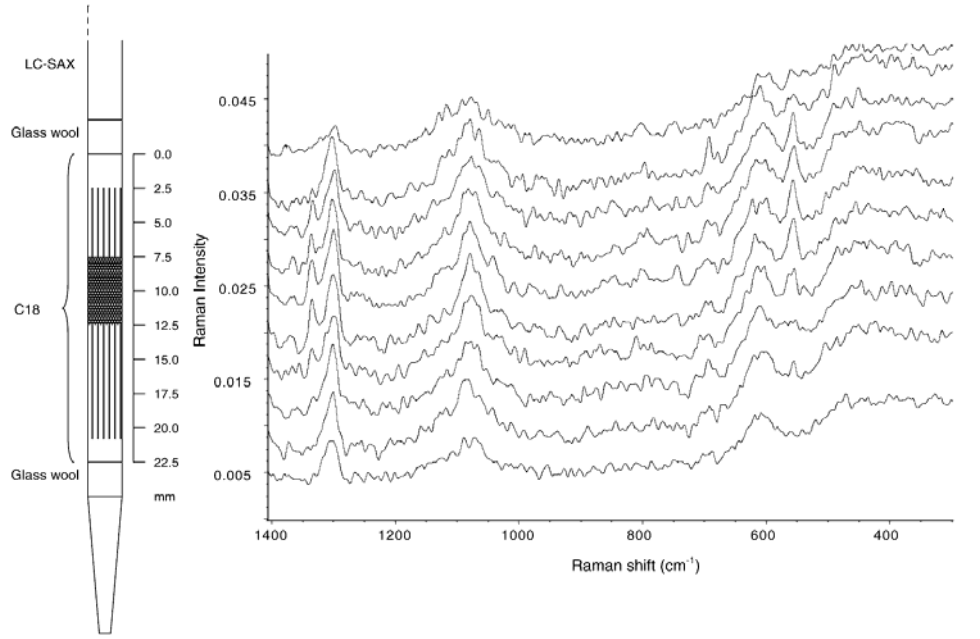

Fig. 3. Distribution of caffeine through a C18 solid support packed on a glass tube of 5 mm i.d. filled with 300 mg solid phase and an upper load of LC-SAX. *Note:* Raman spectra correspond to a 10 ml solution of 400 mg l^{-1} caffeine retained and measured from the cell top (0 mm) to the bottom (22.5 mm). *Note:* spectra were shift in the emission scattering intensity axe for clarity purposes.

In flow-systems, the adsorbed analyte provides a longitudinally distributed concentration gradient (see Fig. 3). So, the influence of the measurement height on the solid support loaded with caffeine was measured from the cell top to the bottom (from 0 to 22.5 mm) in order to improve the experimental conditions. Raman spectra of 10 ml of a 400 mg l^{-1} caffeine standard solution retained into a glass tube of 5 mm of i.d. filled with 300 mg C18 were obtained at different height position. As can be seen in Fig. 3, the analytical signal was strongly dependent on the measurement height, being obtained the maximum signal between 7.5 and 12.5 mm. Therefore, 10 mm was chosen for the following experiments.

In order to evaluate the effect of horizontal sample positioning changes and possible glass tube variations on the precision of measurements, 10 ml aliquots of a caffeine standard solution of 400 mg l^{-1} retained into C18 solid phase were measured using three different glass tubes and changing the horizontal position randomly three times. A relative standard deviation of 1.4% was found for measurements carried out on the same tube and 5.0% for different glass tubes, thus showing that the direct SP-FT-Raman measurements provides an appropriate repeatability to carry out the caffeine determination in commercially available energy drinks.

3.2.2. *FIA variables*

The effect of flow rate was studied in order to assess a quantitative retention of caffeine in the solid phase. A change in loading flow rate from 1.62 to 7.50 ml min^{-1} did not affect the alkaloid retention. Therefore, a flow-rate value of 7.50 ml min^{-1} was selected in order to achieve the maximum sample throughput.

3.3. *Selection of bands for SP-FT-Raman determination of caffeine*

In order to select the best measurement conditions for SP-FT-Raman caffeine determination, for the two bands at 556 and 1335 cm^{-1}, different measurement modes (peak height and peak area values) were assayed using an univariate calibration in all cases and evaluating the results in terms of sensitivity, repeatability and limit of detection. Table 1 shows the main figures of merit of different external calibration lines obtained from caffeine retained in C18 and using bands in the spectral region from 2000 to 70 cm^{-1}.

In all the cases assayed, the limit of detection found was of the order of 18–42 mg l^{-1}. The use of the peak area measurement between 573 and 542 cm^{-1} corrected using a baseline defined between 580 and 540 cm^{-1} was selected because it

Table 1
Analytical features of the SP-FT-Raman determination of caffeine using different bands and measurement modes

Measurement mode	Raman shift (cm^{-1})	Baseline correction	$I = a + bC_{mg}$		r^2 ($n = 5$)	R.S.D. (%)	LOD ($mg\,l^{-1}$)
			$a \pm s_a$	$b \pm s_b$			
Height	556	580–540	0.0002 ± 0.0009	0.0016 ± 0.0008	0.994	8	42
Area	573–542	580–540	−0.0003 ± 0.0007	0.0232 ± 0.0002	0.9990	3	18
Height	1335	1354–1323	−0.000 ± 0.003	0.0016 ± 0.0002	0.990	9	42
Area	1354–1325	1354–1323	0.001 ± 0.002	0.010 ± 0.001	0.990	6	25

Note: calibration lines were established as a function of the caffeine (mg) retained in the solid phase.

provided the best sensitivity, a limit of detection of 18 $mg\,l^{-1}$, estimated as the ratio between three times the standard deviation of a 100 $mg\,l^{-1}$ caffeine standard solution signal and the slope of the calibration curve, and a repeatability of 3% for five independent measurements of caffeine Raman intensities at a concentration level of 200 $mg\,l^{-1}$.

3.4. Analytical figures of merit

The calibration graph was obtained according to the procedure described above using 10 ml of different standards solutions ranging from 100 to 600 $mg\,l^{-1}$. The calibration equation obtained was $A = (-0.0003 \pm 0.0007) + (0.0232 \pm 0.0002)C_{Caf}$ with a $r^2 = 0.9990$ ($n = 5$), being A the peak area values and C_{Caf} the milligram of caffeine retained on 300 mg of C18 solid support.

The aforementioned calibration line corresponds to an equation of $A = -0.0003 + 0.000232C_{Caf}$, being C_{Caf} the concentration of caffeine in the retained solution expressed in $mg\,l^{-1}$, which is 31 times higher than that obtained $A = -0.0052 + 0.0000074C_{Caf}$ for aqueous caffeine solutions directly measured by FT-Raman.

In order to evaluate the proposed SP-FT-Raman method, a recovery study was carried out on sample spiked with known amounts of caffeine from 98 to 283 $mg\,l^{-1}$. The mean recovery value found was 99 ± 3%, thus indicating the absence of systematic errors in the developed procedure, as can be seen in data of Table 2.

The sampling frequency was also evaluated, obtaining a value of 13.3 h^{-1}.

Table 2
Recovery studies on caffeine added to commercially available energy drink samples by using SP-FT-Raman spectrometry

Caffeine added ($mg\,l^{-1}$)	Caffeine found ($mg\,l^{-1}$)	Recovery (%)	Mean recovery
98	95	97	99 ± 3
	97	99	
	99	101	
140	141	100	
	146	104	
	134	96	
259	244	94	
	256	99	
	265	102	
272	284	104	
	265	97	
	278	102	
283	275	97	
	283	99	
	279	98	

Sample content: 221 $mg\,l^{-1}$.

4. Analysis of samples

A series of commercially available energy drink samples were analysed by solid-phase FT-Raman spectrometry and by a liquid chromatography (LC-UV) reference procedure. Data found are summarized in Table 3. From these results, it can be seen that the developed procedure provided statistically comparable results in all the cases with those found by the LC reference method using a Student's t-test of paired results for a probability level of 95% (see Table 3).

When concentrations found by solid-phase FT-Raman were represented in front of those obtained by LC and adjusted by a linear function, the fitted equation was $C_{SP\text{-}FT\text{-}Raman} = (0 \pm 4) + (1.00 \pm 0.02)C_{LC}$ with a regression coefficient $r^2 = 0.997$ ($n = 12$). In that equation, the intercept and slope values were statistically comparable to 0 and 1, respectively, for a probability level of 95%, thus indicating that the developed procedure provide accuracy comparable with that of the LC method.

Table 3
Results obtained in the analysis of commercial samples of energy drinks

Sample	LC-UV (caffeine $mg\,l^{-1}$)	SP-FT-Raman (caffeine $mg\,l^{-1}$)	t_{exp}
Burn	225.6 ± 0.5	221 ± 7	1.466
Burn (sugar free)	224.8 ± 0.6	230 ± 8	1.444
Red bull	235.5 ± 1.0	235 ± 6	0.180
Red bull (sugar free)	240.7 ± 0.3	238 ± 6	1.005
Mountain dew	308.7 ± 1.5	305 ± 6	1.338
Hacendado	106.4 ± 0.9	108 ± 6	0.590
Carrefour	243.7 ± 0.2	247 ± 6	1.229
Big puma	241.0 ± 1.4	239 ± 4	1.055
Non-stop (orange)	111.4 ± 0.5	110 ± 4	0.780
Non-stop (lemon)	109.4 ± 0.5	106 ± 5	1.513
Locura	197.2 ± 0.5	198 ± 7	0.255
Locura (sugar free)	213.91 ± 0.06	218 ± 6	1.370

$t_{tab} = 1.812$ with a probability level of 95% and 10 d.f. Concentration values are the average of two-independent analyses measured in triplicate ± S.D. of the six values found.

5. Conclusion

The synergistic combination of FT-Raman and solid-phase retention provides a sensing methodology, which clearly enhances the sensitivity of direct Raman measurements of caffeine by a factor of 31 and offers a methodology, which could be used for the determination of caffeine in commercially available energy drinks.

The adequate selection and combined use of different solid phases permits to carry out in one step the sample clean-up and analyte preconcentration reducing the matrix effects and also increasing the selectivity of the Raman measurements, thus facilitating the direct analyte determination without the need of using of multivariate calibration techniques.

The developed SP-FT-Raman methodology provides a fast alternative to the chromatographic method (13.3 samples/h in front of 7.0 samples/h), with a reduced reagent consumption and waste generation, thus being an environmentally friendly methodology, which eliminates the use of organic solvents except the 3 ml of methanol per sample required to elute caffeine and reduces the waste generation to 41.9 ml of methanolic solutions of caffeine per hour.

Acknowledgements

The authors acknowledge the financial support of the Direcció General d' Investigació i Transferència Tecnològica de la Conselleria d'Empresa, Universitat i Ciència de la Generalitat Valenciana (Project GV04B/247 and Grupos 03-118) and the University of Valencia (Projecte UV-AE-20050203). S. Armenta also acknowledges the FPU Grant of the MECD (Ref. AP2002-1874).

References

[1] H. Ashihara, A. Crozier, Trends Plant Sci. 6 (2001) 407.
[2] J.L.F.C. Lima, C. Delerue-Matos, H.P.A. Nouws, M.C.V.F. Vaz, Food. Addit. Contam. 15 (1998) 265.
[3] A.M.S. Abdennabi, S.M. Sultan, Electroanalysis 5 (1993) 709.
[4] P. Deng, H. Li, A. Lu, Y. Dai, Shipin Kexue 98 (1988) 51.
[5] L.F. Xu, Fenxi Shiyanshi 21 (2002) 36.
[6] Q.C. Chen, S.F. Mou, X.P. Hou, Z.M. Ni, Anal. Chim. Acta 371 (1998) 287.
[7] E.A. Abourashed, J.S. Mossa, J. Pharm. Biomed. Anal. 36 (2004) 617.
[8] J.C. Walker, S.E. Zaugg, E.B. Walker, J. Chromatogr. A 781 (1997) 481.
[9] H. Okamoto, T. Nakajima, Y. Ito, J. Pharm. Biomed. Anal. 30 (2002) 815.
[10] H.J. Lin, M.L. Wang, C.W. Chen, B.S. Hwang, M.H. Lee, Y.M. Choong, Yaowu Shipin Fenxi 8 (2000) 180.
[11] S.B. Hawthorne, D.J. Miller, J. Pawliszyn, C.L. Arthur, J. Chromatogr. A 603 (1992) 185.
[12] Y. Daghbouche, S. Garrigues, M.T. Vidal, M. de la Guardia, Anal. Chem. 69 (1997) 1086.
[13] M.M. Paradkar, J. Irudayaraj, J. Food. Sci. 67 (2002) 2507.
[14] M.M. Paradkar, J. Irudayaraj, Food Chem. 78 (2002) 261.
[15] AOAC Official Method 967.11, Official Methods of Analysis of AOAC International, 17th ed., Gaithersburg, MD, 2002.
[16] K. Yoshimura, H. Waki, S. Ohashi, Talanta 23 (1976) 449.
[17] M.I. Pascual-Reguera, G. Pérez-Parras, A. Molina-Díaz, Microchem. J. 77 (2004) 79.
[18] A. Ruiz-Medina, M.L. Fernández-de Córdova, P. Ortega-Barrales, A. Molina-Díaz, Int. J. Pharm. 216 (2001) 95.
[19] A. Ruiz-Medina, M.L. Fernández-de Córdova, M.J. Ayora-Cañada, M.I. Pascual-Reguera, A. Molina-Díaz, Anal. Chim. Acta 404 (2000) 131.
[20] M.J. Ayora Cañada, M.I. Pascual Reguera, A. Molina Díaz, L.F. Capitán-Vallvey, Talanta 49 (1999) 691.
[21] P. Ortega-Barrales, M.J. Ayora-Canada, A. Molina-Diaz, S. Garrigues, M. de la Guardia, Analyst 124 (1999) 579.
[22] S. Gunasekaran, G. Sankari, S. Ponnusamy, Spectrochim. Acta A 61 (2005) 117.
[23] M. Ostroumov, E. Faulques, E. Lounejeva, C.R. Geosci. 334 (2002) 21.

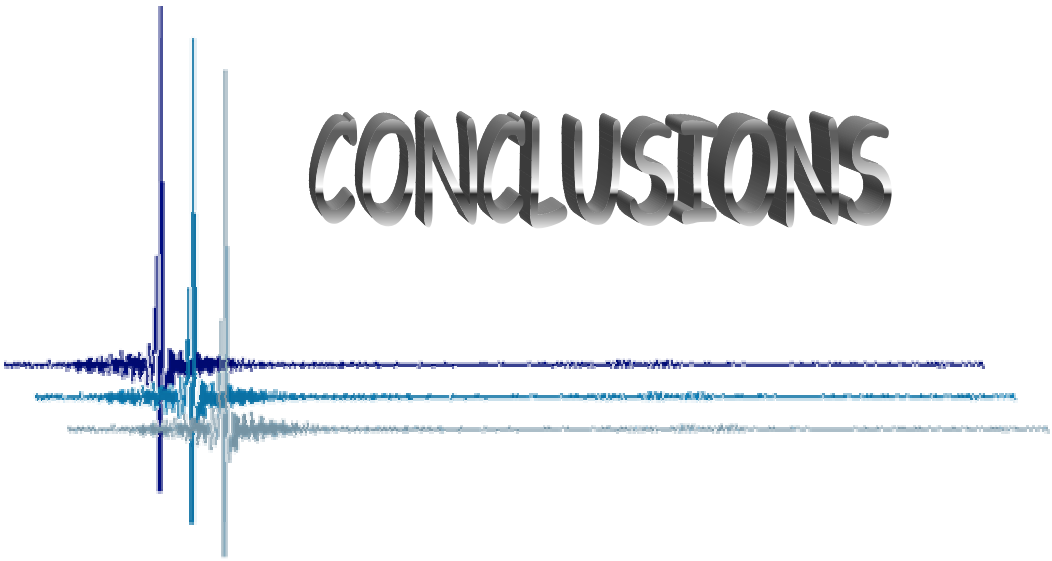

CONCLUSIONS

Additionally than the specific conclusions derived from each one of the publications compiled in this Memory, it can be concluded that, in general, the papers developed through this PhD Thesis have demonstrated that vibrational spectrometry is a very useful tool for the quality control of manufactured products and can be used in different industrial sectors. Raman and infrared spectrometries are powerful analytical techniques in the modern laboratory which offer the following advantages:

- Manufactured products with different physical and chemical properties have been successfully analysed using vibrational spectrometry based procedures. As it can be seen, transmission spectroscopy methodologies have been developed in the mid and near range for the quality control of organic molecules, such as pesticides or sweeteners, after an extraction of the target molecule with an appropriate organic solvent (preferably non-chlorinated).
  Direct quantitative analysis on solid samples have been performed by transmittance measurements using the KBr pellet technique, diffuse reflectance in the near infrared range, photoacoustic in the MIR region and Raman spectrometries. Proposed procedures have been developed in most of the cases in combination with chemometric analysis, providing an environmentally friendly alternative to reference procedures that avoid the consume of reagents and reduce the waste generation.
  Attenuated total reflectance has been the technique selected for monitoring of processes in aqueous media demonstrating its capability for the analysis of this kind of samples.
  Moreover, several compounds have been determined simultaneously by vibrational techniques using different calibration methods, such as partial least squares (PLS) or univariate linear regression.

- Regarding the environmental side effect of the developed procedures, one of the features of the methods is their ability to carry out quantitative determinations with a little or no sample preparation, reducing or eliminating the amount of reagents and

solvents employed. Non-chlorinated and mixtures of chlorinated and non-chlorinated solvents have been successfully applied for the determination of different analytes by transmittance measurements in the MIR range, reducing the toxicity and environmental impact of these measurements. In this way, flow systems, in which the analyte is extracted with the minimum amount of solvent, and direct measurements on solid samples avoids the contact of the operator with toxic substances enhancing the safety and hygiene in the laboratory environment. Because of that, these methodologies are highly appropriate to be used for routine quality control assays.
Moreover, the non-destructive nature of the vibrational techniques allows a possible storage of the solid samples and/or standards for additionally analysis.

- The proposed methodologies are very simple and fast, reducing considerably the time of analysis compared with the commonly used reference procedures based on chromatography.

- Methods developed have been validated in terms of accuracy, precision and limit of detection:

  The results obtained by the developed vibrational procedures were in all the cases comparables with those obtained by reference procedures (mainly a chromatographic method), demonstrating the accuracy of vibrational methodologies. Furthermore, the mean recovery percentages obtained on spiked samples were, in all the cases within the ranges proposed by the CIPAC.

  The precision in terms of variation coefficient, provided in all the cases RSD values lower than that obtained by the modified Horwitz equation [$RSD<2^{(1-0.5\ \log C)}\ 0.67$] (proposed by CIPAC for the acceptance of an analytical method for pesticide determination in agrochemicals). The good repeatability achieved was due to the advances in the instrumentation and the minimum treatment of the

samples being in all the cases acceptable for the quality control of manufactured products.

The limit of detection values, established as the IUPAC method were in all the cases acceptable for the analysis of commercial formulations. In the case of Raman spectrometry, the limit of detection value for caffeine has been improved through the retention of the analyte in a solid phase and direct measurement of the cartridge expanding the range of concentrations to be determined till parts per million (ppm) levels. Moreover, the selectivity of the methodology has been also improved and problems of sample fluorescence were avoided.

Regarding the applicability of the developed studies, it has been evidenced in this Thesis, that vibrational spectrometry is definitely one of the fastest, reliable and suitable techniques for monitoring processes and quality control purposes in industrial fields, such as agrochemical or food sector.

On the other hand, as well as these general conclusions, in which different solutions have been applied to specific problems, it could be emphasized the methodological contributions of some of the enclosed studies.

The sequential and automated extraction of several analytes in a same sample, in a closed system, employing solvents with different properties, provides an integrated methodology, which reduces the mutual interferences of sample components, the time of analysis and the contact of the operator with toxic substances.

The evaluation of different functions to be optimized in a NIR-based analytical method for iprodione determination in agrochemicals has evidenced that the optimum conditions of a procedure depend clearly on the criterion selected and it must be chosen based on the priority of the

analyst, which is not always the maximum sensitivity nor the best precision, or simply accuracy or productivity, but, in general a combination of all the analytical features.

Finally, the development of a sensor based on the combination of solid phase (SP) retention and Raman spectrometry is the first precedent published on this field and permits the determination of analytes in samples at parts per million level. Additionally, the combination of solid phases with different nature reduces interferences of other compounds and avoids the possible fluorescence of these molecules.


CONCLUSIONES


ALEXANDER PP VI

Además de las conclusiones específicas que se extraen de cada una de las publicaciones recopiladas en esta memoria, se puede concluir de forma general que las publicaciones desarrolladas en esta Tesis Doctoral han demostrado que la espectrometría vibracional es una herramienta muy útil para el control de calidad de productos manufacturados y puede ser empleada en diferentes sectores industriales. La espectrometría Raman e infrarroja son técnicas analíticas potentes en los laboratorios modernos que ofrecen las siguientes ventajas:

- Se han analizado con éxito productos manufacturados con diferentes propiedades físico-químicas empleando métodos basados en técnicas vibracionales. Como puede observarse, se han desarrollado procedimientos que emplean medidas de transmisión en la región del infrarrojo medio y próximo para el control de calidad de moléculas orgánicas, como pesticidas o edulcorantes, tras su extracción con un disolvente orgánico apropiado (preferiblemente un disolvente no-clorado).

  Se han llevado acabo análisis directos sobre muestras sólidas mediante medidas de transmitancia utilizando la técnica de las pastillas de KBr, de reflectancia difusa en la región del infrarrojo próximo, fotoacústicas en la región MIR y mediante espectroscopia Raman. Estos procedimientos han sido desarrollados, en la mayoría de los casos, en combinación con métodos quimiométricos de análisis, proporcionando alternativas medioambientalmente sostenibles a los métodos de referencia, que eliminan el consumo de reactivos y reducen la generación de residuos.

  La reflectancia total atenuada ha sido la técnica seleccionada para realizar la monitorización de procesos en medios acuosos demostrando su validez para dichos análisis en este tipo de muestras.

  Adicionalmente, se han determinado varios compuestos de forma simultánea mediante técnicas vibracionales empleando diferentes métodos de calibración, como son el de los mínimos cuadrados parciales (PLS) o la calibración lineal univariada.

- En lo correspondiente al impacto medioambiental de los procedimientos desarrollados, una de las características de los métodos descritos es la posibilidad de llevar a cabo determinaciones cuantitativas con una mínima o inexistente preparación de la muestra, reduciendo o eliminando, de esta forma, la cantidad de reactivos y disolventes empleados. Se han utilizado disolventes no halogenados o mezclas de disolventes halogenados y no halogenados para la extracción y determinación de diferentes analitos mediante medidas de transmitancia en la región MIR, reduciendo la toxicidad y el impacto negativo en el medioambiente de estas metodologías. En este sentido, se han empleado sistemas en flujo, en los que el analito se extrae con la mínima cantidad de disolvente y medidas directas sobre muestras sólidas que evitan el contacto del operador con sustancias tóxicas, mejorando la seguridad y la higiene del ambiente laboral. Debido a todo ello, las metodologías desarrolladas son muy apropiadas para ser empleadas en análisis rutinarios de control de calidad.
  Adicionalmente, la naturaleza no destructiva de las técnicas vibracionales permite un posible almacenamiento de las muestras y/o los estándares para posteriores análisis.

- Las metodologías propuestas son muy simples y rápidas, reduciendo de forma considerable el tiempo de análisis comparado con los métodos de referencia basados en separaciones cromatográficas empleados habitualmente.

- Los métodos desarrollados han sido validados en terminos de exactitud, precisión y límites de detección:

  Los resultados obtenidos por los métodos vibracionales desarrollados en esta Tesis fueron, en todos los casos, comparables con los encontrados mediante procedimientos de referencia (principalmente métodos cromatográficos), demostrando la exactitud de las metodologías vibracionales. Además, las recuperaciones medias obtenidas sobre muestras adicionadas

estuvieron, en todos los casos, dentro de los rangos propuestos por CIPAC.

La precisión, en términos de coeficiente de variación, proporcionó en todos los casos valores de RSD menores que los obtenidos mediante la ecuación modificada de Horwitz [$RSD<2^{(1-0.5\ logC)}\ 0.67$] (propuesta por CIPAC para aceptar un método analítico para el análisis de agroquímicos). La buena repetibilidad obtenida se debe a los avances obtenidos en la instrumentación y al mínimo tratamiento de las muestras y en todos los procedimientos fue aceptable para el control de calidad de productos manufacturados.

Los valores de límite de detección, establecidos según el criterio IUPAC, fueron en todos los casos adecuados para el análisis de formulaciones comerciales. En el caso de la espectrometría Raman, el límite de detección para el análisis de cafeína fue mejorado, mediante la retención del analito en una fase sólida y posterior medida directa del cartucho de retención, incrementando el rango de concentraciones que pueden ser determinadas hasta niveles de partes por millón (ppm). Además se mejoró la selectividad de la metodología y se solucionaron problemas de fluorescencia en la muestra.

En relación a la aplicabilidad de los estudios realizados, se ha evidenciado en esta Tesis Doctoral, que la espectrometría vibracional es definitivamente una de las técnicas más rápidas, fiables y apropiadas para realizar la monitorización de procesos y para análisis rutinarios de control de calidad en diferentes sectores industriales, como el agroquímico o el alimentario.

Por otra parte, además de las conclusiones generales, en las que se han aplicado diferentes soluciones a problemas específicos, pueden subrallarse algunas contribuciones metodológicas de los estudios anexos.

La extracción secuencial y mecanizada de varios analitos en una misma muestra, empleando disolventes con diferentes propiedades, proporciona una metodología integrada, la cual reduce las interferencias mutuas de los componentes de la muestra, el tiempo de análisis y el contacto del operador con sustancias tóxicas.

La evaluación de diferentes funciones para ser utilizadas como respuesta en la optimización de un método basado en medidas de transmitancia en la región NIR para la determinación de iprodiona en formulados comerciales evidencia que las condiciones óptimas de un procedimiento dependen claramente del criterio seleccionado y éste debe ser escogido en función de las necesidades del analista, no siendo siempre la máxima sensibilidad ni la mejor precisión, o simplemente exactitud o productividad, sino en general una combinación de todas estas características analíticas.

Finalmente, el desarrollo de un sensor basado en la combinación de retención en fase sólida (SP) y espectrometría Raman es el primer precedente publicado en este campo y permite la determinación de analitos que están presentes en muestras a niveles de partes por millón (ppm). Además, la combinación de fases sólidas con distinta naturaleza reduce la interferencia de otros compuestos y evita la posible fluorescencia de estas moléculas.

BIBLIOGRAFÍA

[Almond y Knowles, 1999] *Almond M.J.; Knowles, S.J.* **Quantitative analysis of agrochemical formulations by multivariate spectroscopic techniques** *Applied Spectrosopy 53 (1999) 1128-1137.*

[Armaroli et al. 2004] *Armaroli, T.; Bécue, T.; Gautier, S.* **Diffuse reflection infrared spectroscopy [DRIFTS]: Application to the in situ analysis of catalysts** *Oil & Gas Science and Technology, Rev. IFP 59 (2004) 215-237.*

[*Armenta et al.,* 2005] *Armenta, S.; Garrigues, S.; de la Guardia, M.* **Quantitative vibrational spectrometry in the 21st century: a scientometric evaluation** *Spectroscopy Letters 38 (2005) 665-675.*

[AOAC] Official Methods of Analysis of AOAC INTERNATIONAL [OMA], *Gaithersburg, MD, USA (2002).*

[Bell, 1881] *Bell, A.G.* **Upon the Production of Sound by Radiant Energy** *Philosophical Magazine 11 (1881) 510-528.*

[Bell et al., 2002] *Bell, S.E.J.; Boyd, A.R.* **Raman Spectroscopy – An Overview of its Application and Potential for Life Sciences** *WMRC, Business Briefing, Life Sciences Technology (2002).*

[Blanco et al., 1998] *Blanco, M.; Coello, J.; Iturriaga, H.; Maspoch, S.; de la Pezuela, C.* **Near-infrared spectroscopy in the pharmaceutical industry** *Analyst 123 (1998) 135R-150R.*

[Cadet y de la Guardia, 2000] *Cadet, F.; de la Guardia, M.* **Quantitative analysis, Infrared** Encyclopedia of Analytical Chemistry, *Ed. R.A. Meyers John Wiley & Sons, New York, NY, USA (2000).*

[Cassella et al., 2000] *Cassella, A.R .; Jorgensen-Cassella, R.; Garrigues, S.; Santelli, R.E.; de Campos R.C.; de la Guardia, M.* **Flow injection-FTIR determination of dithiocarbamate pesticides** *Analyst 125 (2000) 1829-1833.*

[Cassella et al., 2001] *Cassella, A.R .; Garrigues, S.; de Campos R.C.; de la Guardia, M.* **Fourier transform infrared spectrometric determination of Ziram** *Talanta 54 (2001) 1087-1094.*

[*CIPAC Guidelines]* CIPAC Guidelines, Collaborative International Pesticides Analytical Council Improved version of document CIPAC 3807, *Abingdon, England.*

[*CIPAC Methods]* CIPAC Methods, Collaborative International Pesticides Analytical Council, *Abingdon, England.*

[Corley, 2003] *Corley, J.* **Best practices in establishing detection and quantification limits for pesticide residues in foods** *Handbook of residue analytical methods for agrochemicals, John Wiley & Sons, New York, NY, USA (2003).*

[Corti et al., 1999] *Corti, P.; Ceramelli, G.; Dreassi, E. ; Mattii, S.* **Near infrared transmittance analysis for the assay of solid pharmaceutical dosage forms** *Analyst 124 (1999) 755-758.*

[Downey, 1998] *Downey, G.* **Food and food ingredient authentication by mid-infrared spectroscopy and chemometrics** *TrAC-trends in analytical chemistry 17 (1998) 418-424.*

[Eilert y Wetzel, 2002] *Eilert, A.J.; Wetzel, D.L.* **Optics and sample handling for near-infrared diffuse reflection** Handbook of vibrational spectroscopy *Ed. J.M. Chalmers and P.R. Griffiths, John Wiley & Sons, New York, NY, USA (2002).*

[Estienne et al., 2000] *Estienne, F.; Massart, D.L.; Zanier-Szydlowski, N.; Marteau, P.* **Multivariate calibration with Raman spectroscopic data: a case study** *Analytica Chimica Acta 424 (2000) 185-201.*

[Farenfort, 1961] *Fahrenfort, J.* **Attenuated Total Reflection: A new principle for the production of useful infrared reflection spectra of organic compound** *Spectrochimica Acta 17 (1961) 698-709.*

[Fitzpatrick y Reffner, 2002] *Fitzpatrick, J.; Reffner, J.A.* **Macro and micro internal reflection accessories** Handbook of vibrational spectroscopy *Ed. J.M. Chalmers and P.R. Griffiths, John Wiley & Sons, New York, NY, USA (2002).*

[Fleischmann et al. 1974] *Fleischmann, M.; Hendra, P.J.; Mcquillan, A.J.* **Raman spectra of pyridine adsorbed at a silver electrode** *Chemical Physics Letters 26 (1974) 163-166.*

[Fletcher y Van Staden], 2003] *Fletcher, P.J.; van-Staden, J.F.* **Determination of ethanol in distilled liquors using sequential injection analysis with spectrophotometric detection** *Analytica Chimica Acta 499 (2003) 123-128.*

[Gallignani et al., 1993] *Gallignani, M.; Garrigues, S.; Martínez-Vado, A.; de la Guardia, M.* **Determination of Carbaryl in pesticide formulations by Fourier transform infrared spectroscopy with flow injection** *Analyst 118 (1993) 1043-1048.*

[Garrigues y de la Guardia, 2002] *Garrigues, S.; de la Guardia, M.* **Flow injection análisis-Fourier transform infrared spectrometry [FIA/FTIR]**, *Handbook of vibrational spectroscopy Ed. J.M. Chalmers and P.R. Griffiths, John Wiley & Sons, New York, NY, USA (2002).*

[Geladi, 2003] *Geladi, P.* **Chemometrics in spectroscopy. Part 1. Classical chemometrics** *Spectrochimica Acta Part B 58 (2003) 767-782.*

[Griffiths y Olinger, 2002] *Griffiths, P.R. Olinger, J.M.* **Continuum theories of diffuse reflection**, Handbook of vibrational spectroscopy *Ed. J.M. Chalmers and P.R. Griffiths, John Wiley & Sons, New York, NY, USA (2002).*

[Gupta et al., 1996] *Gupta, S.; Sharma K.K.; Handa, S.K.* **Fourier transform infrared spectroscopic determination of Fenvalerate in emulsifiable concentrate formulation** *Journal of AOAC International 76 (1996) 1260-1262.*

[Hannah, 2002] *Hannah, R.W.* **Standard sampling techniques for infrared spectroscopy**, Handbook of vibrational spectroscopy *Ed. J.M. Chalmers and P.R. Griffiths, John Wiley & Sons, New York, NY, USA (2002).*

[Harrick, 1960] *Harrick, N.J.* **Surface chemistry from spectral analysis of totally internally reflected radiation**. *Journal of Physical Chemistry 64 (1960) 1110-1114.*

[Haykin, 1999] *Haykin, S.* **Neural Networks: A Comprehensive Foundation**, *Prentice-Hall, New Jersey, USA (1999).*

[Herschel, 1800] *Herschel, W.* **Investigation of the powers of the prismatic colours to heat and illuminate objects** *Philosophical Transactions 90 (1800) 255-283.*

[Hind et al., 2001] *Hind, A.R.; Bhargava, S.K.; McKinnon, A.* **At the solid/liquid interface: FTIR/ATR-the tool of choice** *Advances in colloid and interface science 93 (2001) 91-114.*

[Hidajat y Chong, 2000] *Hidajat, K.; Chong, S.M.* **Quality characterisation of crude oils by partial least square calibration of NIR spectral profiles** *Journal of near infrared spectroscopy 8 (2000) 53-59.*

[Huggett y Nixon, 1957] *Huggett, A.St.G.; Nixon, D.A.* **Use of glucose oxidase, peroxidase, and o-dianisidine in determination of blood and urinary glucose** *The Lancet 270 (1957) 368-370.*

[Kubelka y Munk, 1931] *Kubelka, P.; Munk, F.* **Ein Beitrag zur Optik der Far-. banstriche** *Zeitschrift fr Technishen Physik 12 (1931) 593–601.*

[Lendl et al., 1997] *Lendl, B.; Schindler, R.; Frank, J.; Kellner, R.* **Fourier Transform infrared detection in miniaturized total analysis systems for sucrose analysis** *Analytical Chemistry 69 (1997) 2877-2881.*

[Liu et al., 1994] *Liu, B.Y.; Tian, H.J.; Cui, J.; Song, ZJ.* **Determination of artemisinin in formulations by IR spectrometry** *Yaowu-Fenxi-Zazhi 14 (1994) 47-48*.

[Lo et al., 1996] *Lo, C.C.; Ho, M.H.; Hung, M.D.* **Use of high-performance liquid-chromatographic and atomic-absorption methods to distinguish propineb, zineb, maneb, and mancozeb fungicides** *Journal of Agricultural and Food Chemistry 44 (1996) 2720-2723.*

[Mark, 1989] *Mark, H.* **Chemometrics in near-infrared spectroscopy** *Analytica Chimica Acta 223 (1989) 75-93.*

[Martens y Naes, 1991] *Martens, H. Naes, T.* **Multivariate Calibration**, *Ed. John Wiley & Sons, New York, NY, USA (1991).*

[McClelland et al., 2002] *McClelland, J.F.; Jones, R.W.; Luo, S.; Seaverson, L.M.* FT-IR **Photoacoustic Spectroscopy**, Handbook of vibrational spectroscopy *Ed. J.M. Chalmers and P.R. Griffiths, John Wiley & Sons, New York, NY, USA (2002).*

[McClure, 1994] *McClure, W.F.* **Near-infra-red spectroscopy. The giant is running strong** *Analytical Chemistry 66 (1994) 43A-53A.*

[Merck, 2001] *Merck index, 13th Edition, Merck & Co. Inc. New Jersey, USA (2001).*

[Michaelian, 2003] *Michaelian K.H.* **Photoacoustic Infrared Spectroscopy**, *Ed. John Wiley & Sons, New York, NY, USA (2003).*

[Mirabella, 2002] *Mirabella, F.M.* **Principles, Theory and Practice of internal reflection spectroscopy**, Handbook of vibrational spectroscopy *Ed. J.M. Chalmers and P.R. Griffiths, John Wiley & Sons, New York, NY, USA (2002).*

[Milosevic y Berets, 2002] *Milosevic, M:; Berets, S.L.* **Accessories and sample handling for mid-infrared diffuse reflection spectroscopy**, Handbook of vibrational spectroscopy *Ed. J.M. Chalmers and P.R. Griffiths, John Wiley & Sons, New York, NY, USA (2002).*

[MTEC, 2005] *MTEC, MTEC Model 300,* **Photoacoustic detector operating instructions** *MTEC Photoacoustics, Inc., Iowa, USA (2005).*

[*Nordon et al.,* 2005*]* *Nordon, A.; Mills, A.; Burn, R.T.; Cusick, F.M.; Littlejohn, D.* **Comparison of non-invasive NIR and Raman spectrometries for determination of alcohol content of spirits** *Analytica Chimica Acta 548 (2005) 148-158.*

[*Olinga y Siesler*, 2000] *Olinga, A.; Siesler, H.W.* **Quality control and process monitoring by vibrational spectroscopy** Nir-news 11 (2000) 9-11, 13.

[ONU, 1999] *ONU, Organización Naciones Unidas,* Programa de las Naciones Unidas para el Medio Ambiente, Protocolo de Montreal relativo a las sustancias que agotan la capa de ozono, *Beijing (1999).*

[Ozaki and Berry, 2002] *Ozaki, Y.; Berry, R.J.* **Sampling techniques in near-infrared transmisión spectroscopy**, Handbook of vibrational spectroscopy *Ed. J.M. Chalmers and P.R. Griffiths, John Wiley & Sons, New York, NY, USA (2002).*

[Quintás et al., 2002] *Quintás, G.; Morales-Noé, A.; Parrilla, C.; S.; Garrigues, S.; de la Guardia, M.* **Fourier transform infrared**

determination of Fluometuron in pesticide formulations, *Vibrational Spectroscopy 31 (2002) 63-69.*

[Quintás et al.[a], 2003] *Quintás, G.; Morales-Noé, A.; Armenta, S.; Garrigues, S.; de la Guardia, M.* **An infrared method, with reduced solvent consumption, for the determination of Chlorsulfuron in pesticide formulations** *Spectroscopy Letters 36 (2003) 515-529.*

[Quintás et al.[b], 2003] *Quintás, G.; Armenta, S.; Garrigues, S.; de la Guardia, M.,* **A simple and fast procedure for Fenoxycarb determination in pesticide formulations based on infrared spectrometry** *Ciencia 11 (2003) 319-327.*

[Quintás et al.[c], 2003] *Quintás, G.; Armenta, S.; Morales-Noé, A.; Garrigues, S.; de la Guardia, M.* **Simultaneous determination of Folpet and Metalaxyl in pesticide formulations by flow injection Fourier transform infrared spectrometry** *Analytica Chimica Acta 480 (2003) 11-21.*

[Quintás et al.[d], 2003] *Quintás, G.; Garrigues, S.; de la Guardia, M.* **FT-Raman determination of Malathion in pesticide formulations** *Talanta 63 (2003) 345-350.*

[Quintás et al., 2004(a)] *Quintás, G.; Armenta, S.; Garrigues, S.; de la Guardia, M.* **Fourier transform infrared determination of Imidacloprid in pesticide formulations** *Journal of Brazilian Chemical Society 15 (2004) 307-312.*

[Quintás et al., 2004(b)] *Quintás, G.; Morales-Noé, A.; Armenta, S.; Garrigues, S.; de la Guardia, M.* **Fourier transform infrared spectrometric determination of Malathion in pesticide formulations** *Analytica Chimica Acta 502 (2004) 213-220.*

[Quintás et al., 2004(c)] *Quintás, G.; Garrigues, S.; Pastor, A.; de la Guardia, M.* **FT-Raman determination of Mepiquat chloride in agrochemical products** *Vibrational Spectroscopy 36 (2004) 41-46.*

[Quintás et al., 2005] *Quintás, G.; Moros, J.; Armenta, S.; Garrigues, S.; de la Guardia, M.* **Stopped-flow method for FTIR determination of Pirimicarb and Endosulfan in commercial pesticide formulation**s *Journal of AOAC International 88 (2005) 399-405.*

[Raman y Krishnan, 1928] *Raman, C.V.; Krishnan, K.S.* **A New Type of Secondary Radiation** *Nature 121 (1928) 501-502.*

[Reeves y Zapf, 1998] Reeves, J.B.; Zapf, C.M. **Mid-infrared diffuse reflectance spectroscopy for discriminant analysis of food ingredients** *Journal of Agricultural and Food Chemistry 46 (1998) 3614-3622.*

[*Rosencwaig et al*., 1976] Rosencwaig, A. Gersho, A. **Theory of the Photoacoustic. Effect in Solids** *Journal of Applied Physics 47 (1976) 64–69.*

[Sato-Berru et al.] *Sato-Berrú, R.Y.; Medina-Valtierra, J.; Medina-Gutiérrez, C.; Frausto-Reyes C.* Quantitative **NIR–Raman analysis of methyl-parathion pesticide microdroplets on aluminum substrates** *Spectrochimica Acta Part A: Molecular and Biomolecular Spectroscopy 60 (2004) 2231-2234.*

[Sharma et al., 1997] *Sharma, K.K.; Gupta S.; Handa, S.K.* **Fourier-transform infrared spectroscopic determination of Cypermethrin and Deltamethrin in emulsifiable concentrate formulations** *Talanta 44 (1997) 2075-2079.*

[Skoog et al., 2003] *Skoog, D.A.; Holler, F.J., Nieman T.A.* **Principios de Análisis Instrumental** [5ª Edición]. *Mc Graw-Hill, Madrid, España (2003).*

[Skoulika et al., 1999] *Skoulika, S.G.; Georgiou, C.A.; Polissiou, M.G.* **Quantitative determination of Fenthion in pesticide formulations by FT-Raman** *Applied Spectroscopy 53 (1999) 1470-1474.*

[Skoulika et al., 2000(a)] *Skoulika, S.G.; Georgiou, C.A.; Polissiou, M.G.* **FT-Raman spectroscopy – analytical tool for routine analysis of Diazinon pesticide formulations** *Talanta 51 (2000) 599-604.*

[Skoulika y Georgiou, 2000(b)] *Skoulika, S.G.; Georgiou*, *C.A.* **Univariate and multivariate calibration for the quantitative determination of Methyl-parathion in pesticide formulations by FT-Raman** *Applied Spectroscopy* 54 (2000) 747-752.

[*Skoulika y Georgiou,* 2003*]* *Skoulika, S.G.; Georgiou, C.A.* **Rapid, noninvasive quantitative determination of acyclovir in pharmaceutical solid dosage forms through their poly[vinyl chloride] blister package by solid-state Fourier transform Raman spectroscopy** Applied spectroscopy 57 (2003) 407-412.

[Smith, 1979] *Smith, A.L.* **Applied infrared spectroscopy: Fundamentals, techniques and analytical problem-solving** *Chemical Analysis, vol. 54. Ed. John Wiley & Sons, New York, NY, USA (1979).*

[Smith, 1996] *Smith, B.C.* **Fundamentals of Fourier transform infrared spectroscopy** *Ed. CRC Press, Boca Raton, FL, USA (1996).*

[Sherman, 1997] *Sherman, C.P.* **Infrared Spectroscopy**, Chapter 15, Handbook of instrumental techniques for analytical chemistry, *Ed. Frank Settle, Prentice Hall, Upper Saddle River, NJ, USA (1997).*

[Thermo Spectra-Tech, 2001] *Thermo Nicolet Corp.,* **Users guide***, Madison, USA, (2002).*

[Termo Nicolet Corp., 2002] *Thermo Spectra-Tech.,* **Crystal reference guide**, *Thermo Nicolet Corp., Madison, USA, (2001).*

[Wang y McCreery, 1989] *Wang, Y.; McCreery, R.L.* **Evaluation of a diode laser/charge coupled device spectrometer for near-infrared Raman spectroscopy** *Analytical Chemistry 61 (1989) 2647-2651.*

[Wilson y Tapp, 1999] *Wilson, R.H.; Tapp, H.S.* **Mid-infrared spectroscopy for food analysis: recent new applications and relevant developments in sample presentation methods** *TrAC-trends in analytical chemistry 18 (1999) 85-93.*

[Zeisel et al., 1998] *Zeisel, D.; Deckert, V.; Zenobi, R.; Vo-Dinh, T.* **Near-field surface-enhanced Raman spectroscopy of dye molecules adsorbed on silver island films** *Chemical Physics Letters 283 (1998) 381-385.*